

UNIVERSITY OF NOTTINGHAM  
DEPARTMENT OF CIVIL ENGINEERING

ENDURANCE TESTING OF BRIDGE DECK EXPANSION JOINTS

by

Kwok-Ching Sham, B.Sc. (Hons)

Thesis submitted to the University of Nottingham  
for the degree of Doctor of Philosophy

April 1990



CONTENTS		PAGES
	ABSTRACT	i
	ACKNOWLEDGEMENT	v
CHAPTER 1	INTRODUCTION	1
1.1	Expansion Joint Types.	2
1.1.1	Open Joints.	2
1.1.2	Closed Joints.	3
1.2	Practical Observations from Manufacturers and Engineers.	5
1.2.1	Contacts Made with Manufacturers.	5
1.2.2	Discussions with County Engineers.	7
1.3	Outline of the Research.	8
CHAPTER 2	LITERATURE REVIEW	11
2.1	Introduction.	11
2.2	Mechanical Properties of Bituminous Materials.	12
2.3	Fatigue Tests on Bituminous Materials.	14
2.3.1	Conventional Fatigue Tests.	14
2.3.2	Test Control Modes.	15
2.3.3	Miner's Hypothesis.	18
2.3.4	Effects of Rest Periods.	19

2.4	Simulative Testing on Pavement Structures.	19
2.5	Laboratory Testing on Expansion Joints.	21
2.5.1	Model Joint Machines.	21
2.5.2	Tests on Asphaltic Plug Joints.	22
2.6	Machine Designs for Expansion Joint Testing.	23
2.6.1	Design Proposed by Agreement Board.	23
2.6.2	Machines Designed in Austria.	24
2.7	Site Investigation of In-service Expansion Joints.	25
2.7.1	TRRL Investigations.	25
2.7.2	Research in Belgium.	27
2.8	Summary.	29
CHAPTER 3	DETAILS OF THE TEST EQUIPMENT	32
3.1	Introduction.	32
3.2	Mechanical Details of the Expansion Joint Simulator (EJS).	34
3.3	The Actuators and the Hydraulic Power Supply System.	35
3.4	The Control System.	36
3.5	Details of the Mould.	38
3.6	Temperature Controlled Room.	40

CHAPTER 4	COMMISSIONING AND MODIFICATION OF THE EQUIPMENT	41
4.1	Commissioning of the EJS.	41
4.1.1	Performance Test on the Hydraulic Pump and Actuators.	42
4.1.2	Coupling of the Horizontal Actuator.	42
4.1.3	Trial Tests with Joint Specimens.	43
4.2	Modifications to the Test Facilities.	46
4.2.1	The EJS.	46
4.2.2	The Mould.	48
4.3	Improvements to the Dartec System.	49
4.3.1	Monitoring of System Signals.	49
4.3.2	Trip Facilities.	50
4.3.3	New Annexe Attached to the Temperature Controlled Room.	51
4.4	Newly Developed Compaction Rig.	52
4.5	Choice of Measuring Devices and Instrumentation.	54
4.5.1	Introduction.	54
4.5.2	Instruments for Measuring Displacements.	55
4.5.3	Instrumentation of the Specimens.	58
4.6	Development of the Data Acquisition System.	60
4.6.1	Introduction.	60
4.6.2	Dartec Data Processing Boards and Software.	62
4.6.3	Independent Data Acquisition System.	63

CHAPTER 5	FORMULATION OF TEST PROGRAMMES	67
5.1	Introduction.	67
5.2	Test Methods.	68
5.2.1	Methods of Accelerating Test Rate.	68
5.2.2	Test Control Mode.	70
5.2.3	Suitable Types of Accelerated Test Methods.	71
5.3	Test Specimen.	72
5.3.1	Choice of the Joint Type for Testing.	72
5.3.2	Details of Buried Joint and Test Specimen.	73
5.3.3	Mix Design.	74
5.4	Selection of Test Parameters.	74
5.4.1	Thermal Movements.	78
5.4.2	Traffic Induced Movements.	78
5.4.3	Test Loading Frequency and Waveform.	79
5.4.4	Test Temperature.	80
5.4.5	Initial Stress Conditions.	81
CHAPTER 6	PRELIMINARY TESTING	83
6.1	Introduction.	83
6.2	Preliminary Test Procedures.	83
6.2.1	Initial Stiffness measurement.	84
6.2.2	Initial Stress Conditioning.	85
6.2.3	Horizontal Traffic Associated Cycling.	86
6.2.4	Thermal Movement Cycling.	87

6.3	Preliminary Tests.	88
6.3.1	Specimen Test No. 1.	90
6.3.2	Specimen Test No. 2.	91
6.3.3	Specimen Test No. 3.	92
6.3.4	Specimen Test No. 4.	94
6.4	Discussion.	95
6.4.1	Method of Making Specimens.	95
6.4.2	Test Control.	98
6.4.3	Failure Pattern of the Specimens.	99
6.4.4	Stiffness Measurement.	100
6.4.5	Preconditioning Process.	104
CHAPTER 7	THE MAIN TEST PROGRAMME AND RESULTS	105
7.1	Introduction.	105
7.2	The Test Programme.	105
7.3	Results of the Traffic Induced Horizontal Movement Tests.	108
7.3.1	Test Observations on Group 1 Specimens.	110
7.3.2	Discussion on Test Data.	112
7.3.3	Fatigue Lives of the Joint Specimens.	116
7.4	Long-term (Thermal) Horizontal Movement Tests.	122
7.4.1	Details of the Tests.	122
7.4.2	Load Histories of the Specimen Tests.	124
7.4.3	Definition of Specimen Failure.	125

CHAPTER 8	APPLICATION OF THE TEST RESULTS	129
8.1	Introduction.	129
8.2	Application of Test Results.	129
8.2.1	Grading and Selection of Joint Systems.	129
8.2.2	Comparative Testing.	130
8.2.3	Use of Test Results to Improve Joint Design.	131
8.2.4	Direct Prediction of Joint Life.	132
8.3	Use of Laboratory Test and Site Investigation Results to Estimate the Lives of Working Buried Joints.	133
8.3.1	Introduction.	133
8.3.2	Use of Experimental Results.	133
8.3.3	Estimated Joint Damage Caused by Thermal Movements.	135
8.3.4	Life Estimation of Working Joints.	139
8.3.5	Examples.	140
8.3.6	Discussion.	144
CHAPTER 9	FURTHER JOINT SPECIMEN TESTING.	146
9.1	Introduction.	146
9.2	Vertical Movement Tests.	149
9.2.1	Coupling of the Vertical Actuator.	149
9.2.2	Instrumentation.	149



9.2.3	Test Details and Results.	150
9.3	Rotational Movement Tests.	152
9.3.1	Modification to the Expansion Joint Simulator (EJS).	152
9.3.2	Test Details and Results.	153
CHAPTER 10	CONCLUSIONS AND RECOMMENDATIONS FOR FUTURE WORK.	155
10.1	Conclusions.	155
10.2	Proposals for Future Work and Recommendations.	159
REFERENCES		164
APPENDICES		
A.	ELECTRONIC BOARDS OF THE DARTEC 9500 SYSTEM.	174
B.	STANDARD SOFTWARE OF THE DARTEC 9500 SYSTEM.	179
C.	PROPOSAL FOR FIELD MEASUREMENTS ON BRIDGE DECK EXPANSION JOINTS. (PREPARED FOR TRRL BRIDGE DIVISION: MAY 1988)	182



## ABSTRACT

The primary aim of this research was to develop a testing facility, known as an expansion joint simulator (EJS) (Brodrick et al 1986, Sham et al 1988 and Sham and Brown 1989), which allows bituminous expansion joint systems for bridge decks to be tested in the laboratory at an accelerated rate to assess their field potential performance. This performance is affected by a variety and combination of factors, such as workmanship, joint design and the bridge deck movements at the joint gap (Price 1982 (a) & (b) and 1983). The last of these factors is of prime importance. The principal deck movements are the long-term horizontal movements due to temperature variations and the short-term horizontal, vertical and rotational movements induced by the moving traffic. The EJS is capable of generating such deck movements in a controlled laboratory environment.

A review of the literature on expansion joints, bridge deck movements and simulative methods used in testing pavement and expansion joint materials is presented. Conventional methods used for fatigue testing on bituminous materials are discussed and new equipment designs for expansion joint testing and experimental techniques are also included.

As part of the development of the EJS, a series of tests on buried type joint specimens was conducted with the facility under computer control to replace the more conventional analogue control systems. Although some standard software (appendix B) was supplied by the manufacturer, special software was developed as part of the project.

A technique for the production of test specimens with consistent quality was developed in the laboratory. The test specimens were fully instrumented and all data was collected by a computer controlled data acquisition system which used software developed during the period of this research.

Trial tests, which involved three specimens, were used to commission the EJS and its control systems. As a result, appropriate modifications were carried out on the equipment. Four more specimens were used in a preliminary test programme before the main programme was started. These test results provided useful information for the improvement of the instrumentation and method of testing.

The main test programme consisted of a series of tests on buried joint specimens subjected to different types of horizontal joint gap movements. The first part of the test programme was designed to investigate the effects of short-term horizontal movements, which simulated the effects of moving traffic, on the fatigue lives of buried joints. Based on the results of these tests, the

relationship between the gap movements and the joint lives was established and four joint life curves were produced. These results indicated that a power law of the order 3 to 4 could be applied to joint damage effects caused by different amounts of traffic induced horizontal movements when conventional hot rolled asphalt paving materials were used.

Results from these tests were used to estimate service lives of buried joints. There was a good agreement between the calculated joint lives and those obtained from TRRL (Transport and Roads Research Laboratory) field studies (Price 1982 (a)). It could, therefore, be concluded that it is feasible to test buried joints and other similar joint types off the road using the EJS. However, further development of the joint life estimating technique requires more precise calibration of the existing model. This will involve more laboratory testing and the collection of additional site performance data by means of a specially designed research programme.

The second part of the main test programme involved four specimens which were used to investigate the effects of long-term horizontal movements on joint lives. Although the results from these tests were inconclusive, they provided a means to identify the regions of stress concentrations inside a buried joint. Thus, useful information was obtained for the improvement of joint design.

Due to the encouraging results obtained from the main tests, an extension of 6 months was granted by the TRRL to carry out a

short series of new tests. These tests helped to further develop the EJS and were designed to investigate how short-term traffic induced vertical and bending deck movements could affect joint lives.

### ACKNOWLEDGEMENTS

The author wishes to thank all those who have given help and advice in this research project. In particular, thanks are due to Professor P.S. Pell, Head of the Department, for providing the excellent facilities in the department, and Professor S.F. Brown for his invaluable supervision, guidance and encouragement throughout the whole project.

Practical advice and support from Dr. Janet Brunton and Mr. Keith Cooper are very much appreciated. Special thanks are due to Mr. Barry Brodrick for the initial effort he had put into the design of the joint simulator. Mr. Barry Brodrick and Dr. Janet Brunton had also kindly read this thesis and made useful comments. Thanks are also due to Mr. Andy Leyko and Mr. Dennis Lockyer for their technical assistance in making test specimens, construction and maintenance of the apparatus. Assistance from all other members of staff in the department is also very much appreciated.

Excellent cooperation was received from the engineers of Nottingham and Leicester County Councils in providing information about practical problems related to bridge deck expansion joints and in the arrangement of site visits for joint inspection.

Furthermore, the author would like to thank a number of outside organisations for providing technical information and the materials necessary to produce test specimens. These include Dartec Ltd., CIL Microsystem Ltd., Associated Asphalt Co. Ltd, Avon Industrial Polymers Ltd, Bardon Hill Quarries, Expandite Limited and Zebraflex Sealants Ltd.

Special thanks are due to my wife, Judy. Apart from her daily work in her office, she also took care of our children and all domestic affairs when I was working away from our home during the past three and a half years.

Final acknowledgement must go to Dr. D. Cullington and Mr. R. Eyre of the Transport and Road Research Laboratory for their enthusiastic support and efforts to provide financial sponsorship, without which this research would not have been possible.



## CHAPTER ONE

### INTRODUCTION.

Over the years, premature failure of bridge deck expansion joints has caused serious maintenance problems for engineers in the U.K. and abroad. This frequently required maintenance is expensive and the hidden costs to the community, due to traffic interruption, are considerable. Failed joints also contribute a great deal to the deterioration of bridge structures, and subsequent damage could be costly and difficult to rectify.

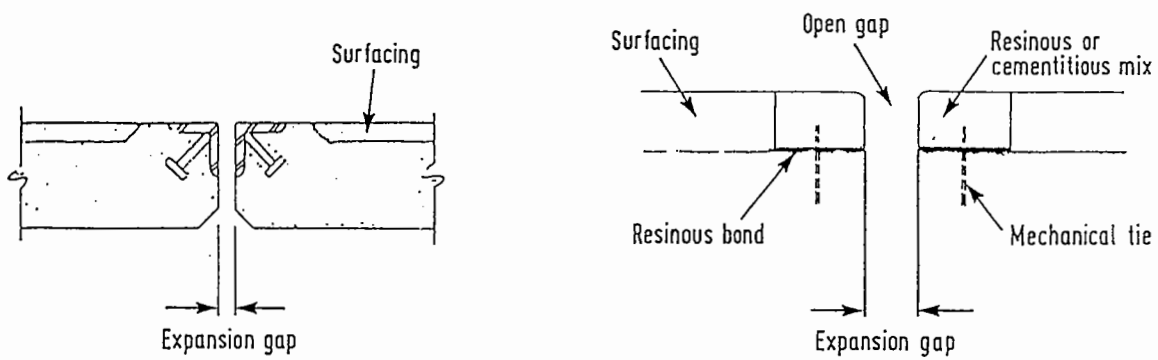
The main function of expansion joints (Day 1981) is to divide a bridge deck into sections and allow them to move in response to traffic loadings and temperature changes without causing unacceptable stresses in the joint and the bridge structure. Before the 1950's, the majority of highway bridges in the U.K. had spans less than 15 m (Black et al 1976). The deck movement of these bridges was usually too small to cause concern and expansion joints were not always provided. During the intensive road improvement programme in the 1950's, the number of bridges of 30 m to 60 m span increased making expansion joints one of the essential components of a bridge structure.

## 1.1 EXPANSION JOINT TYPES.

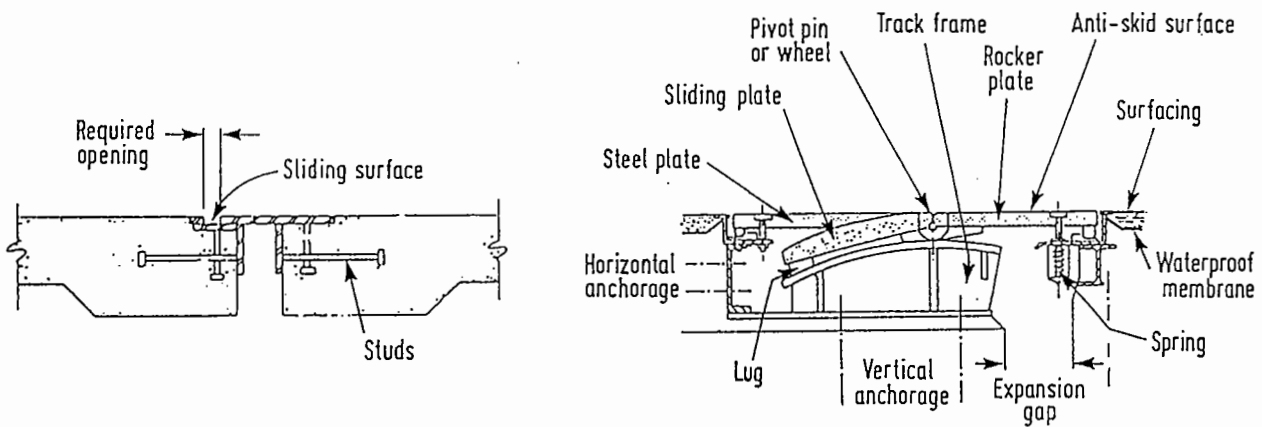
### 1.1.1 Open Joints.

When bridge expansion joints were first introduced, open joints were commonly used for bridges with longitudinal deck movements greater than 20 mm. There are mainly three types (Purvis and Berger 1983) of open joints, namely, butt joints, plate bearing joints and tooth joints (Fig. 1.1 (a) to (c)). Butt joints are used for bridges with a thermal movement of up to 25 mm and plate bearing joints are for movements from 25 mm to 75 mm (a specially designed plate bearing joint can be used for joints with a movement up to 1500 mm (Price 1984)) while tooth joints are used for modern bridges which have an end movement greater than 75 mm. (for the finger type, movement can be up to 900 mm (Price 1984)).

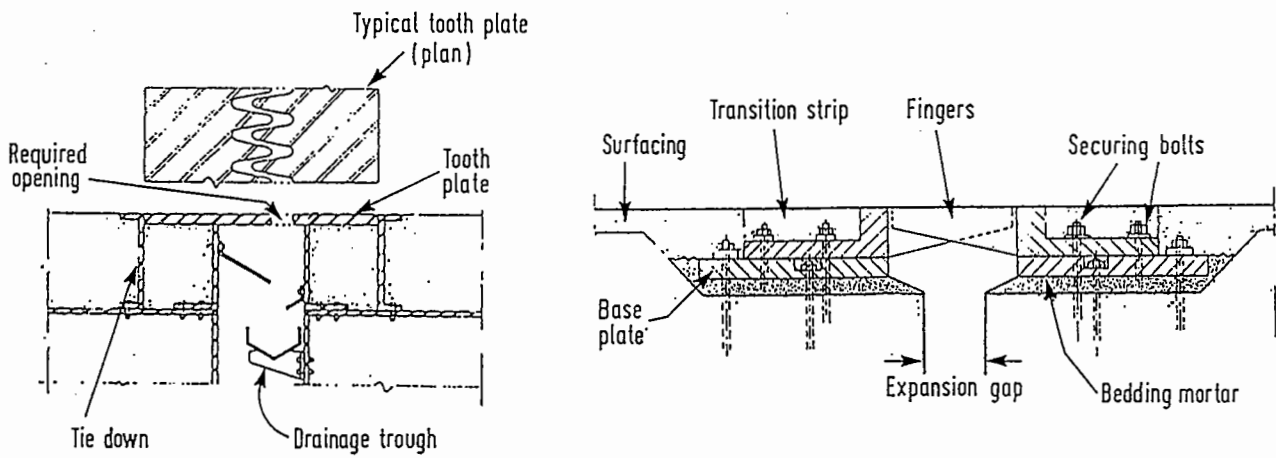
Open joints performed well when properly maintained (Manning and Witecki 1981). However, the increase in use of deicing salt in recent years caused new problems. This corrosive substance dissolved in the thawing snow, went through the joint gap and attacked the bridge structure underneath. Consequently, deterioration of structures due to salt attack became a serious problem in bridge maintenance. One of the solutions to overcome this problem was to construct a drainage system to discharge the contaminated water away from the structure. Unfortunately, open joints allowed road debris to reach the trough and soon blocked up the whole drainage system. A limited space between the joint and the supporting structure meant that cleaning of the system



a) BUTT JOINTS



b) PLATE JOINTS



c) TOOTH AND FINGER JOINTS

FIGURE 1.1 OPEN JOINTS

was not always possible. Incompressible substances trapped inside the joint gap could even prevent deck movement and sometimes caused serious damage to the bridge structures. As a result, a watertight closed joint system was in demand.

#### 1.1.2 Closed Joints.

Closed joint systems consist of filled joints, compression seal joints, buried joints, asphaltic plug joints and elastomeric joints. Typical details of these joint types are shown in Figs. 1.2 to 1.6.

A filled joint is similar to the open butt joint except that the opening is filled with a suitable sealant which is normally poured in-situ. Filled joints are used for bridges with movements up to 12 mm. Failure of this type of joint is often caused by the sealant debonding from the nosing material, and as this separation propagates, it will be finally pulled out of the joint gap by the passing traffic. Debonding of the nosing material from the adjacent deck surfacing and the underlying concrete is another common failure mode of this joint type.

Compression seals are generally made from neoprene compound and are available in different sizes and cross-sections to suit different joint widths. In application, these extruded seals are inserted into joint openings in a compression state and remain the same throughout their service life. Compression seal joints

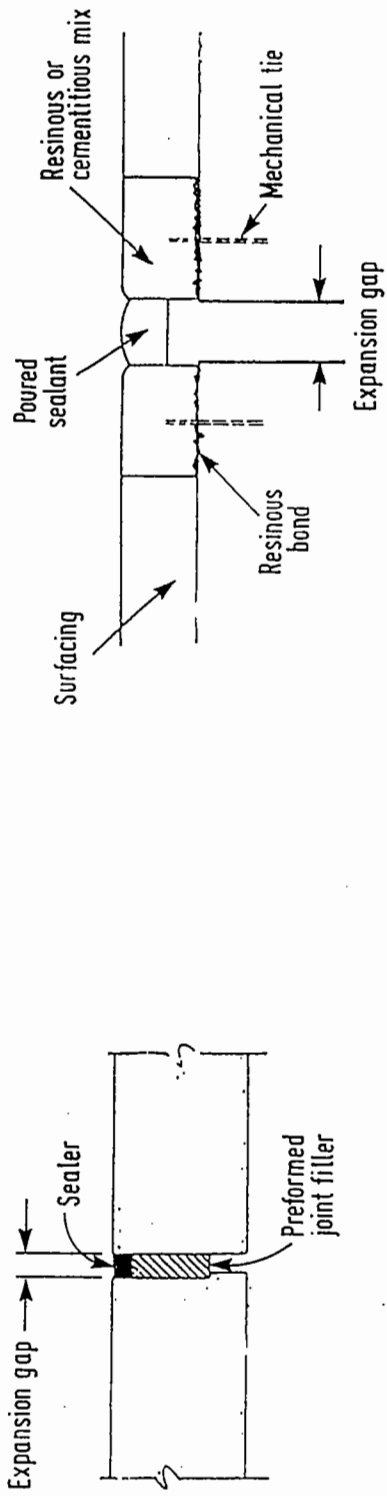


FIGURE 1.2 FILLED JOINTS

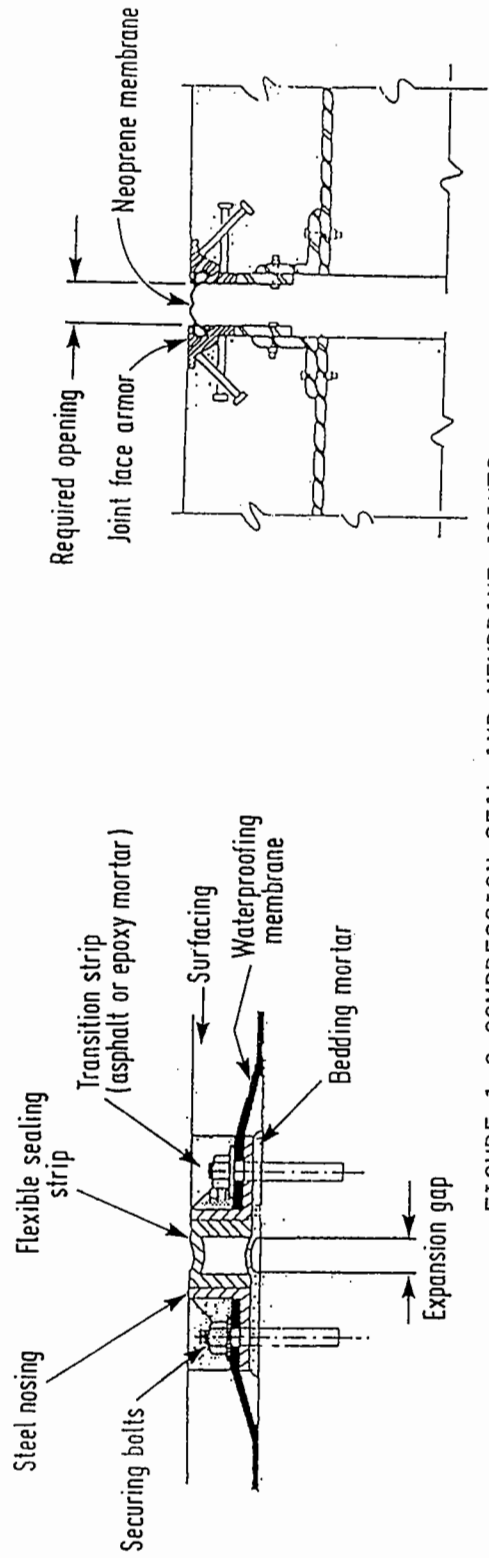


FIGURE 1.3 COMPRESSION SEAL AND MEMBRANE JOINTS

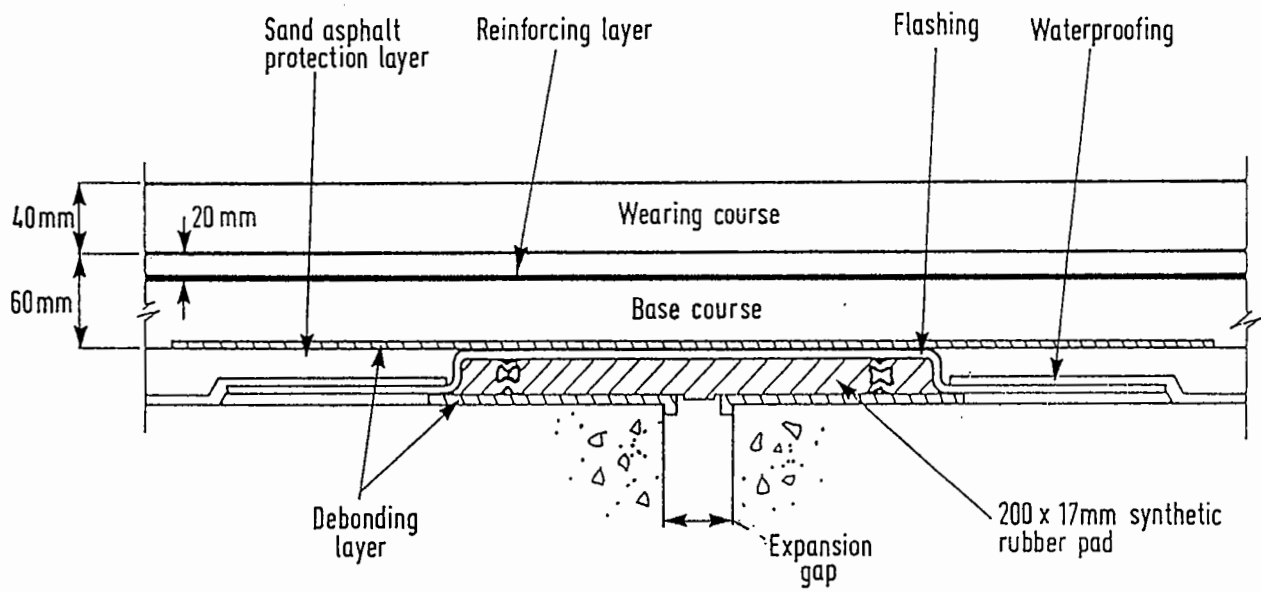


FIGURE 1.4 BURIED JOINT

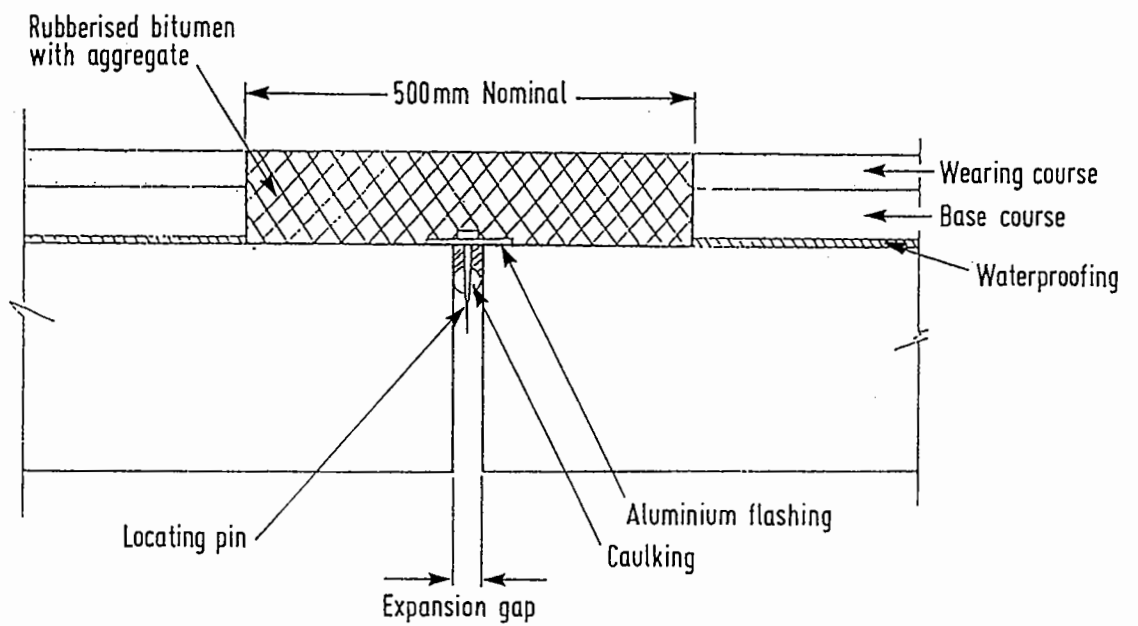
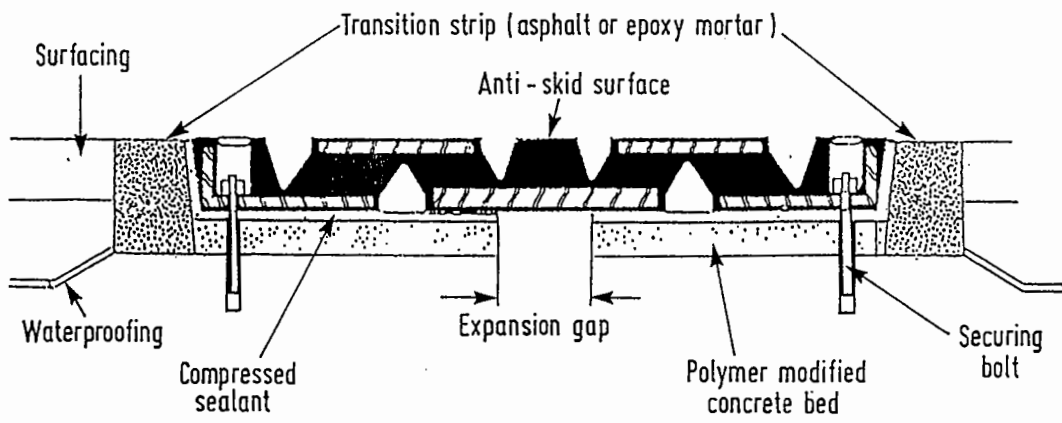
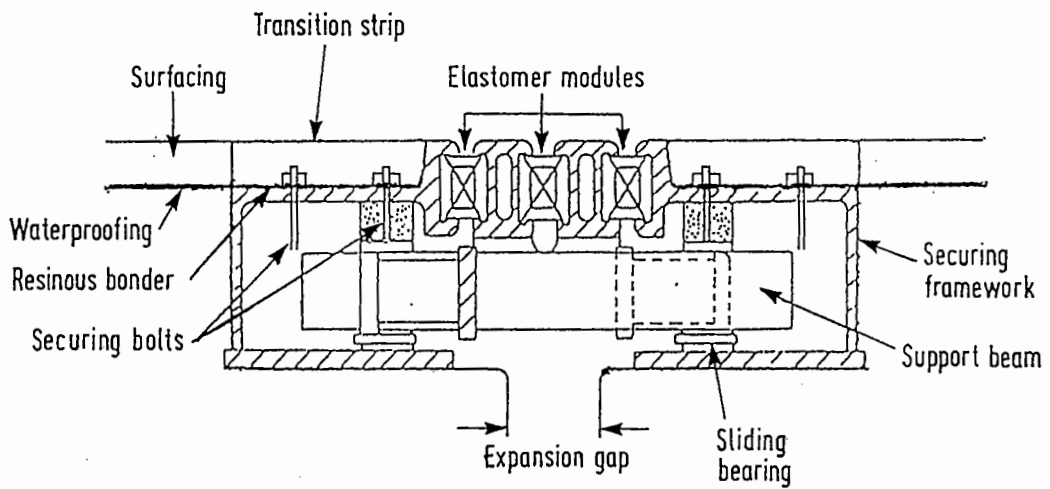


FIGURE 1.5 ASPHALTIC PLUG JOINT



REINFORCED ELASTOMERIC PAD TYPE



ELASTOMER MODULE TYPE

FIGURE 1.6 ELASTOMERIC JOINTS

are used for bridges with deck movements up to 40 mm. This type of joint is widely used in the U.S.A. (Puccio 1981) and has a very good performance record.

Buried and asphaltic plug joints are widely used in the U.K. They provide excellent riding quality and are easy to replace in the event of joint failure or pavement resurfacing. These joints are suitable for bridges with deck movements up to 20 mm and 40 mm respectively. Buried joints are more sensitive to traffic associated movements than other types of joints (Price 1982 (a)). Failure normally starts in the form of fatigue cracks which appear in the surfacing above the joint gap. It then propagates to the full width of the carriageway, followed by multiple cracks which appear on both sides of the principal crack. Spalling then starts and the joint material will eventually be dislodged under the impacts from passing traffic (Price 1984, 1982 (a) & (b)).

An elastomeric joint consists of a rubber pad, which is usually reinforced with aluminium plates to increase its ability to span across the joint gap. It relies on the elastic properties of the rubber pad to accommodate bridge deck movements which can be up to 500 mm. Although failure of anchorage bolts occurs in some cases, joint problems are mainly caused by the transition strip which tends to debond from the adjacent asphalt and eventually becomes dislodged.



## 1.2 PRACTICAL OBSERVATIONS FROM MANUFACTURERS AND ENGINEERS.

### 1.2.1 Contacts Made with Manufacturers.

It is important to know the types of expansion joint systems which are available and their popularity in the market at present, their technical specifications, construction details, installation procedures and important points relevant to the design and installation processes. Contacts were, therefore, made with some leading bridge deck expansion joint manufacturers. The names of these manufacturers are listed in Table 1.1.

Through these contacts, it is understood that manufacturers are aware of bridge deck expansion joint problems. They are willing to improve their products and make them more competitive. Some companies have developed their own material testing rigs, as they are interested in proving their products comply with their clients' standard and perform better than rival products. However, due to a large amount of time and money required in carrying out such tests properly, no manufacturers could afford to undertake a long term research project to develop a sophisticated test apparatus or a proper method for bridge deck expansion joint testing. Manufacturers had difficulty in ensuring consistent quality for their products especially those supplied by other organisations, e.g. binders from oil companies, but, they are endeavouring to further improve quality control. Manufacturers often complained they had no control over site conditions and, with a tight construction schedule, they were

Table 1.1. Joint Manufacturers.

Manufacturer	Product name	Joint type
Redland Prismo Ltd Associated Asphalt Co Ltd * Zebraflex Sealants Ltd Advance Sealants Ltd	Thorma Joint Asphapol Zebrajoint Hotfalt	Asphaltic plug
Avon Industrial Polymers Ltd	Avon Buried Joint	Buried Joint
Industrial Flooring Service Ltd ICI Speciality Chemicals Ltd Britflex Resin Systems Ltd *	Monojoint HAC Strelax, RN Britflex	In-situ Nosings
Expandite Ltd *  Servicised Ltd	Transflex / B7  Waboflex	Elastomeric

\* Manufacturers who had been met.

often under pressure to install joints even under adverse weather conditions. This eventually affected the performance of the joints in service. It was the manufacturers' opinion that bridge designers were often unable to provide a correctly estimated amount of joint movement for their bridges at the design stage. As a result, manufacturers were unable to produce an optimum design for their joints.

#### 1.2.2 Discussions with County Engineers.

A meeting was held with Leicester County Council bridge engineers on 3rd July 1986 to discuss expansion joint problems and a site visit to inspect some local bridge structures was arranged for the afternoon. It was the county council engineers' experience that manufacturers' products often failed to perform as they claimed. However, the engineers had no means to verify the durability of a newly designed joint system other than install it on a bridge and observe its performance in service. The engineers considered the manufacturers were using their bridges as a testing ground for the products. This has highlighted the need to develop a laboratory test facility which allows joint systems to be tested off the road and in a relatively short time prior to acceptance.

On 16th July 1986, a visit was arranged by Nottingham County Council to observe the on-site operations of installing Britflex asphaltic plug joints in the Crow Park Railway Bridge near

Carlton on Trent.

### 1.3 OUTLINE OF THE RESEARCH.

The research described in the thesis was commissioned in response to the recommendation of the working paper prepared by R Eyre and D W Cullington of the TRRL, in conjunction with A J Pretlove of the University of Reading, 1984. The main objective of the project was to design, build and develop an Expansion Joint Simulator (EJS) which could carry out accelerated tests on flexible bridge deck expansion joints, with thermal movements ranging up to 50 mm, under laboratory conditions. It was intended to simulate different types of bridge deck movements in the laboratory using the EJS. These movements included long-term horizontal movements due to diurnal or seasonal changes of temperature and short-term horizontal, vertical and rotational movements due to traffic.

The expansion joint simulator was built in the University of Nottingham during the first 14 months of the contract. This work was carried out by the Senior Experimental Officer with technician assistance. The author was then appointed to commission and develop the EJS. During the machine development, a series of tests on buried joints were carried out.

Although some changes have been made in the emphasis of the project during the period of the research, the primary aims of

the research can be catagorised under the following headings:

1. Design and build the Expansion Joint Simulator (EJS).
2. Conduct a literature review of joints and testing facilities.
3. Further develop the EJS and carry out any modifications as found necessary during the commissioning of the machine.
4. Develop a computer controlled data acquisition system including software and instrumentation.
5. Establish procedures for specimen production in the laboratory and carry out joint tests using the EJS.
6. Develop an appropriate method for analysis and presentation of test results and establish a method to estimate joint lives based on laboratory results.
7. Investigate the possibility of improving joint design using the knowlege gained from a series of tests using the EJS.
8. Set down a direction for future research.

It was important to develop the test facility (EJS) in such a way that it could isolate the various movements that occur at bridge deck joints. Although in service these are combined, certain types of movements might cause more distress in a joint and should be studied individually. However, it was also considered

essential that, eventually, the movements should be combined in the simulator as development continued. An important aspect of this research was to demonstrate the possibility of building laboratory equipment to test bridge deck expansion joints off the road. A model could then be established to estimate in-service joint lives based on the test results. The knowledge gained from the experimental work might also be used to improve joint design. Although the buried joint was the only joint type to be investigated in this research, the EJS was designed for testing similar closed joint systems capable of movements up to 50 mm.

## CHAPTER TWO

### LITERATURE REVIEW.

#### 2.1 INTRODUCTION.

Historically, the importance of maintenance on bridge deck expansion joints had been widely overlooked. It is only recently that the endurance of bridge deck expansion joints has become a widely recognised problem in many countries. Engineers started to realise the serious consequences of many years of neglect and often found that the number of failed joints grew faster than the number they could manage to repair.

Little research has been conducted on the endurance of bridge deck expansion joints, so there is not a great deal of information directly related to the present project. Price (1984) observed that failure of buried joints was mainly caused by fatigue cracking developed in the standard bituminous surfacing layers laid over the joints and this was supported by Jones (1982). Therefore, this literature review also includes studies of the basic mechanical properties and conventional fatigue testing methods used for bituminous materials and testing on pavements. Existing laboratory facilities used for bridge deck

expansion joint testing are also investigated. Subsequently, appropriate theory and experimental techniques developed with the aid of this review are adopted for the research work. Various designs of joint testing machines proposed by different researchers are described and site investigations on the in-service performance of buried-type joints are also reviewed.

## 2.2 MECHANICAL PROPERTIES OF BITUMINOUS MATERIALS.

For an elastic material, there is a constant stress-strain relation, called Young's modulus (E), which is defined as a ratio between stress and strain. However, for a visco-elastic material like bitumen, this ratio is both temperature and loading time dependent. Van der Poel introduced the concept of stiffness modulus (S) for a bituminous material and defined it as:

$$(S)_{T,t} = \left( \frac{\text{stress}}{\text{strain}} \right)_{T,t}$$

Based on this concept and an enormous amount of experimental data, Van der Poel produced a nomograph for predicting the stiffness of a bitumen (S<sub>b</sub>) for any particular combination of temperature (T) and loading time (t) for which the stress is applied (Van der Poel 1954).

Van der Poel extended this concept to asphalt mixes and found



that the stiffness of an asphalt mix is primarily dependent on the bitumen stiffness and the void content of the mix. Van Draat and Sommer (1955) and Heukelom and Klomp (1964) extended Van der Poel's work and derived a set of equations for calculating the stiffness of asphalt mixes. A correction was also suggested which should be applied for mixes with a void content more than 3%. The Shell organisation extended these studies and produced a new nomograph for predicting the dynamic stiffness of bituminous materials (Bonnaure et al 1977) in 1977. It is widely accepted that bituminous materials behave elastically when subjected to dynamic loadings, such as moving traffic. Based on earlier work by the Shell Laboratory (Van Draat 1955 and Heukelom and Klomp 1964), Brown (1978 (b)) established the following equation to determine the elastic stiffness of a mix,  $S_m$ , when the void content and binder stiffness are greater than 3% and 5 MPa respectively.

$$S_m = S_b \left[ 1 + \frac{257.5 - 2.5 \text{ VMA}}{n ( \text{VMA} - 3 )} \right]^n$$

where  $S_b$  = binder stiffness (MPa)

VMA = Void in mixed aggregate (in percentage)

$$n = 0.83 \log \left[ \frac{4 \times 10^4}{S_b} \right]$$

The above equation can also be presented in a graphical form as shown in Fig. 2.1.

### 2.3 FATIGUE TESTS ON BITUMINOUS MATERIALS

Excessive permanent deformation and fatigue cracking are the two general modes which cause failure of bituminous materials in pavements. Failures for buried joints are mainly caused by fatigue. This is due to the inability of the surfacing material to withstand the repeated or fluctuating thermal and traffic induced stresses which generally have a value less than the static loading capacity of the material.

#### 2.3.1 Conventional Fatigue Tests.

Fatigue properties of bituminous materials have been studied since the early 1950's. In the laboratory, different types of apparatus and specimen shapes have been used in simple fatigue tests. Deacon and Monismith tested rectangular specimens as simply supported beams by 3 or 4 point bending (Epps and Monismith 1970 and Deacon and Monismith 1967), and cylindrical specimens with a gradually reducing cross-section to mid-height (waisted) were used in the rotating bending fatigue test by Pell (1967) and Taylor (1968). Trapezoidal shaped specimens were also tested as

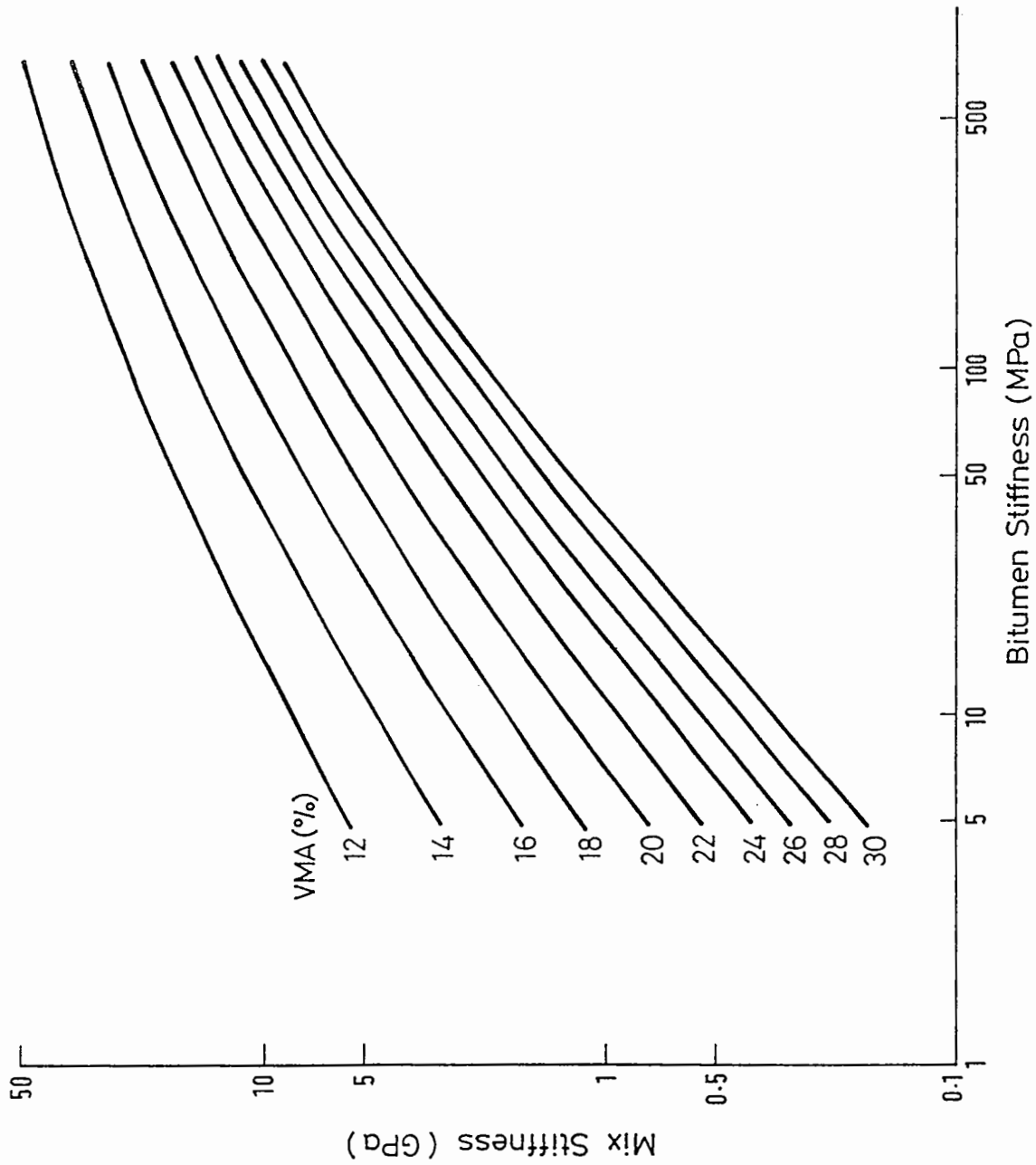


FIG. 2.1 THE RELATIONSHIP BETWEEN MIX STIFFNESS, BINDER STIFFNESS AND VMA IN THE ELASTIC REGION, AFTER BROWN

vertical cantilevers by Van Dijk et al (1972). Later, at the University of Nottingham, Cooper (1976) used cylindrical specimens, 100 mm in diameter and 225 mm long, to carry out fatigue tests under uniaxial tensile and compressive loads. Identical specimens can be used for stiffness testing using the same machine and this allows fatigue life and stiffness of the material to be compared on the same basis. Sawn specimens of 75 mm square x 220 mm long were used by TRRL (Raithby and Sterling 1972) in a similar test. Cylindrical specimens can also be tested under more realistic stress conditions using a triaxial apparatus.

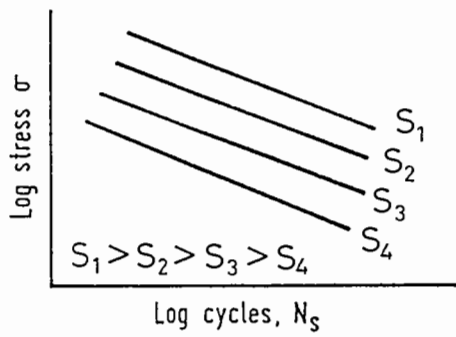
### 2.3.2 Test Control Modes

Fatigue tests can be performed under controlled stress or controlled strain conditions. In a controlled stress fatigue test, a cyclic stress of constant amplitude is applied to the test specimen. Although the applied stress is often sinusoidal, stress with other regular waveforms may be used. Different stress levels are used in separate tests until results covering a wide range of stress conditions are obtained. In the controlled strain fatigue test, a cyclic strain is used. When specimens of different stiffnesses are tested under controlled stress, the results are plotted on a log-log scale with stress against number of cycles to fail, the mean fatigue life for each stiffness can be represented by a series of parallel straight lines as shown in Fig. 2.2(a). However, if these results are replotted in terms of

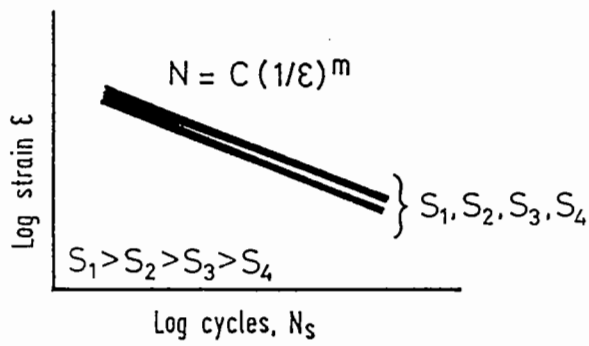
initial strain, using the stress-strain relationship (elastic stiffness), the lines will coincide as shown in Fig. 2.2(b). This demonstrates that the initial strain and the fatigue life of a bituminous material have a unique relationship which is independent of the temperature and loading time (Pell 1973). This is known as the strain criterion of fatigue testing for bituminous materials and remains true for a wide range of test temperatures up to about 25 °C. If identical specimens are tested in controlled strain, the final plot will be as shown in Fig. 2.2(c). In this case, only the lines of high stiffness are coincident.

The failure modes of these two tests are in fact different. In the controlled stress test, the formation of a crack causes stress concentration at the crack tip. This accelerates the crack propagation and fracture of the specimen is rapid. In the controlled strain test, once a crack starts, the stress in the specimen decreases and this slows down the crack propagation rate. It is believed that (Deacon 1973), under pavement service conditions, bituminous materials are likely to be subjected to a type of loading which is intermediate between these two modes. Fig. 2.3 shows the stress and strain conditions during tests using different control modes.

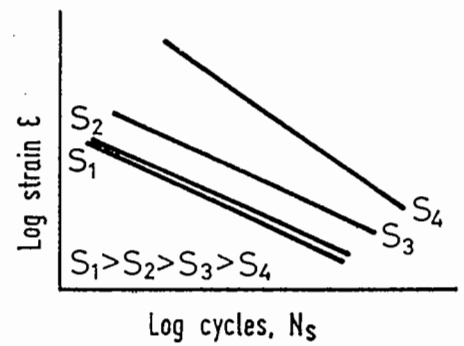
The fatigue life of a bituminous material is dependent on the control mode used in the test. Monismith and Deacon (1969) defined the control modes in a more quantitative way by



(a) Controlled stress fatigue tests at different stiffnesses  $S_1, S_2$  etc.

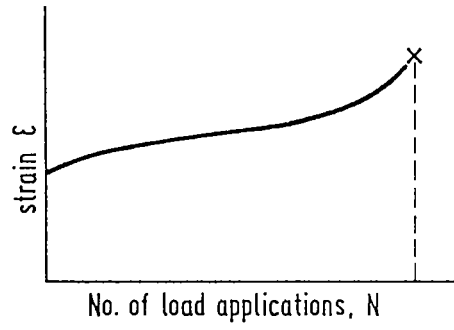
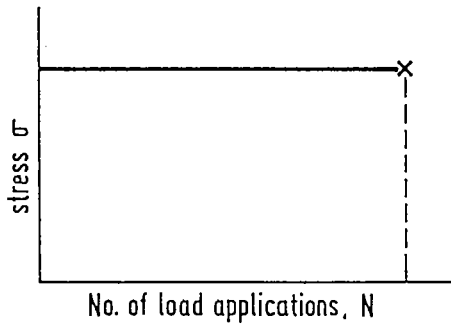


(b) Controlled stress fatigue tests

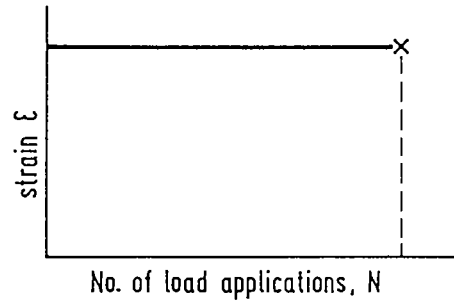
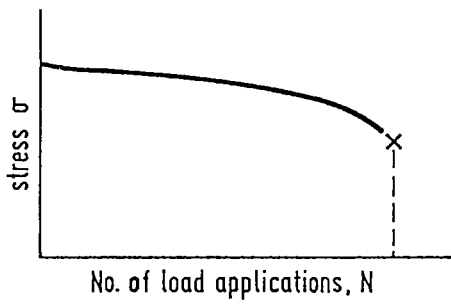


(c) Controlled strain fatigue tests

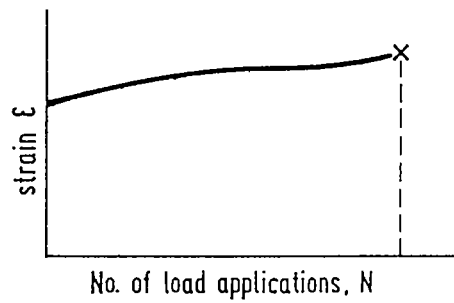
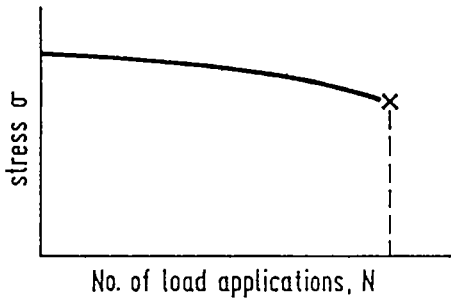
FIGURE 2.2 EFFECT OF STIFFNESS ON FATIGUE LIFE UNDER DIFFERENT MODE OF LOADING, AFTER PELL



CONTROLLED - STRESS MODE



CONTROLLED - STRAIN MODE



INTERMEDIATE MODE

FIGURE 2.3 TYPES OF FATIGUE TESTS, AFTER PELL

introducing a parameter called mode factor as shown below:

$$\text{Mode factor} = \frac{|A| - |B|}{|A| + |B|}$$

Where  $|A|$  and  $|B|$  are the percentage changes stress and strain respectively for a defined percentage reduction in stiffness.

Typical results of fatigue tests with different mode factors are shown in Fig. 2.4. A controlled stress test has a mode factor of -1 while the value changes to +1 in a controlled strain test. For an intermediate controlled test, the mode factor has a value between -1 and +1.

Fig. 2.5 shows that the mode factor decreases as the stiffness and thickness of the bituminous layer increase. Therefore, it was suggested (Pell 1973) that controlled stress testing should be used for bituminous layers with a thickness of 150 mm or more and controlled strain to layers with a thickness of 50 mm or less. For the intermediate thickness, a control between the two modes would be suitable.



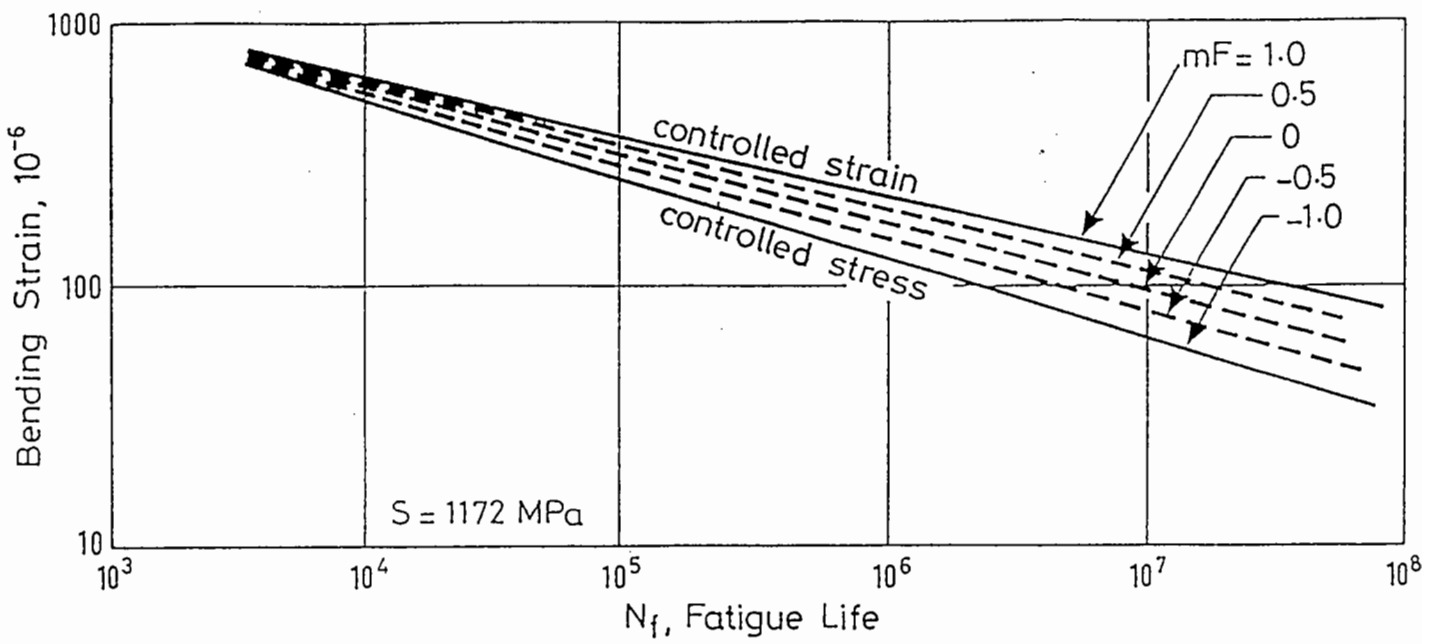


FIG.2.4 FATIGUE CURVES FOR SERIES OF MODES OF LOADING, AFTER SHELL LAB

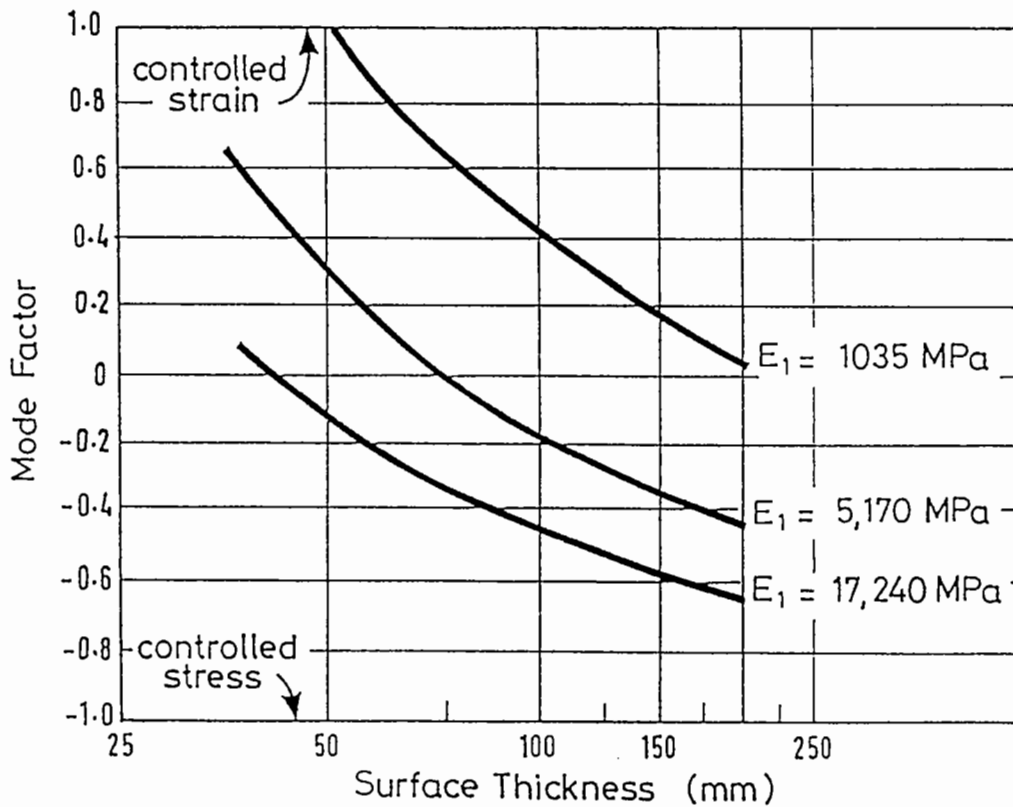


FIG.2.5 VARIATION OF MODE FACTOR WITH SURFACE THICKNESS, AFTER SHELL LAB

### 2.3.3 Miner's Hypothesis.

Traffic loading conditions and temperature change continually in service, so the stress and strain in the surfacing materials also change. It has been shown (Deacon 1965 and McElvaney 1972) that the cumulative fatigue damage to bituminous materials in service can be evaluated by means of a linear hypothesis such as Miner's rule which is given below:-

$$\sum_{i=1}^j \frac{n_i}{N_i}$$

where  $n_i$  = number of applications at strain level  $e_i$ .

$N_i$  = number of applications to failure at constant strain level  $e_i$ .

$j$  = number of different strain levels.

In 1965 Deacon (1965) provided experimental evidence to justify the use of Miner's rule. This was later supported by the experimental findings at the University of Nottingham (McElvaney 1972) and by O'Neil (1970). The application of Miner's rule is illustrated in section 7.3.3.

#### 2.3.4 Effects of Rest Periods.

Under normal traffic conditions, an expansion joint will be subjected to a succession of traffic load pulses separated by quiet intervals. The duration of these rest periods varies with the change in traffic intensity throughout the day. The important effects of these rest periods between load pulses on fatigue performance of bituminous materials have been investigated by several researchers (Van Dijk 1972, Raithby and Sterling 1970 & 1972 and McElvaney and Pell 1973.). Raithby and Sterling suggested that when a specimen is tested with continuous sinusoidal cyclic loading, a life factor (the ratio of fatigue life with rest period to life without) ranging from 5 to 25 should be used to account for the omission of rest periods during laboratory testing. It was also found that when the rest periods were over 0.5 second the life factor became constant. With temperatures between 10 and 25 C, test results showed that the life factor would range from 15 to 25. In the U. K., the average annual pavement temperature is about 15 C and the rest periods between loads are normally greater than 0.5 second, therefore, a life factor between 15 and 25 would be appropriate for general application.

#### 2.4 SIMULATIVE TESTS ON PAVEMENT STRUCTURES.

The uniaxial fatigue tests using samples of various regular

shapes, like those discussed in section 2.3 allow the relative fatigue lives of different materials to be compared using a relatively simple test. However, these tests fail to reproduce the in-service stress and strain conditions to which a real structure is likely to be subjected.

Attempts have been made by researchers to simulate in-situ traffic loading conditions in the laboratory. At the University of Nottingham, pavement sections 4.8 m x 2.5 m x 1.5 m deep were tested with a semi full scale facility, the "Pavement Test Facility" (Brown and Brodrick 1981 (a) & (b)), using a moving loaded wheel. Full scale wheel tracking tests on pavement were conducted by TRRL with The "Road Pavement Testing Facility" (TRRL 1983). Van Dijk (1975) developed a less complex but effective wheel tracking machine which was capable of fatigue testing a pair of 950 mm x 440 mm x 40 mm thick slabs with a rolling wheel. This machine provided Van Dijk with a means to monitor the progression of crack formation in a pavement surfacing layer in a quantitative way. Fig. 2.6 shows the relationship between crack development and measured strain. Three fatigue stages were identified by monitoring the strain changes at the underside of the slabs. The first stage  $N_1$  represents the time when cracks were initiated and strain started to increase. It is usually at this point that a complete fracture of an elemental test specimen occurs which is the limit of the conventional controlled stress fatigue test. At the second stage,  $N_2$ , the measured strain reached its highest point and started to decrease quickly. It was

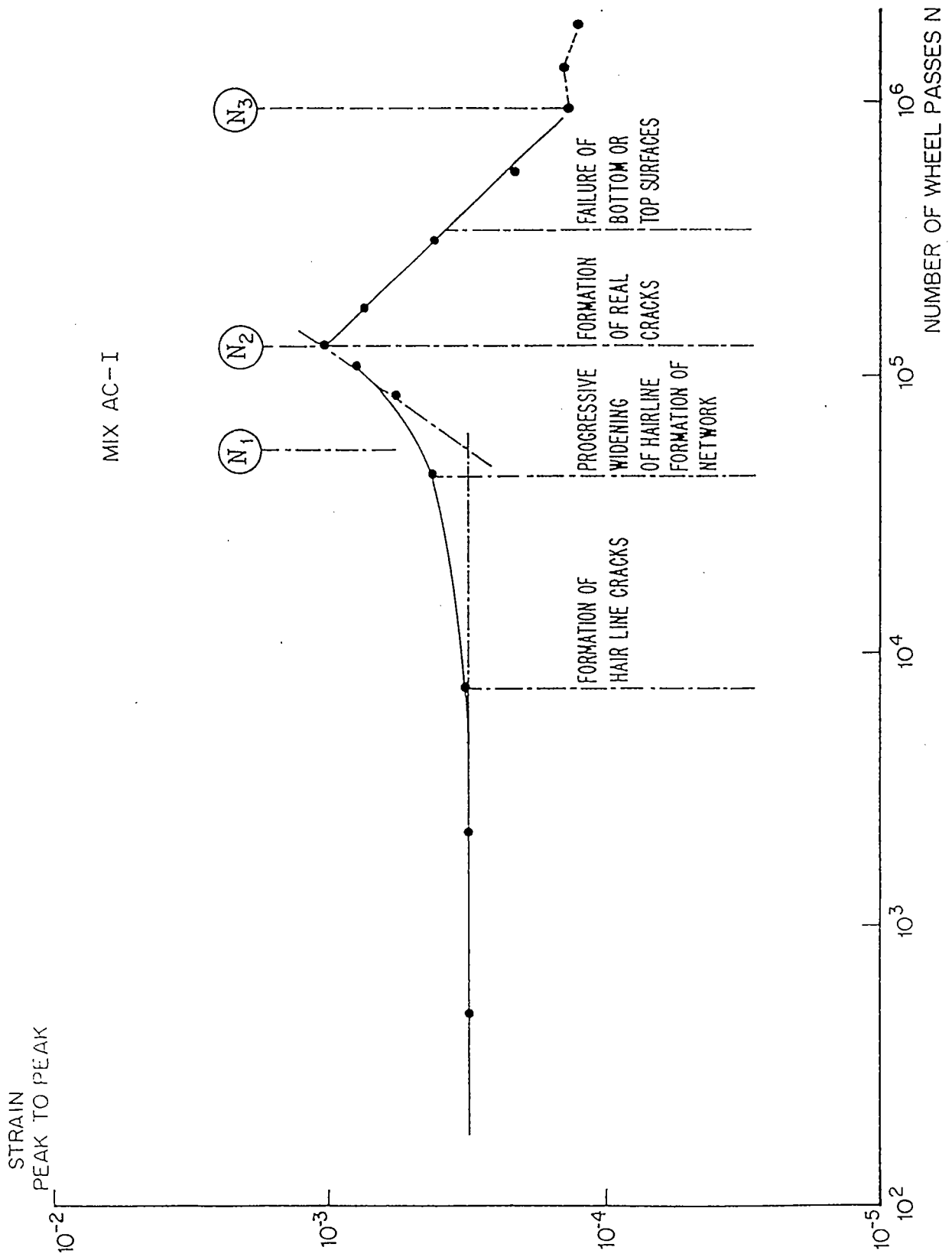


FIG. 2.6 CRACK DEVELOPMENT AS A FUNCTION OF STRAIN READINGS AT EQUIVALENT NUMBER OF WHEEL PASSES, AFTER VAN DIJK.

at this point that a real crack was developed. At the third stage,  $N_3$ , the strain came to its lowest point and remained unchanged. This was mainly due to the total fracture of the pavement which ceased to act as a continuous body. The point  $N_3$  also corresponded to the total failure point of an in-service pavement. A slab testing facility, similar to that developed by Van Dijk, had also been used in the University of Nottingham to study the improved performance of polymer grid reinforced asphalt pavements (Brown et al 1985 and 1986).

## 2.5 LABORATORY TESTING ON EXPANSION JOINTS.

### 2.5.1 Model Joint Machines.

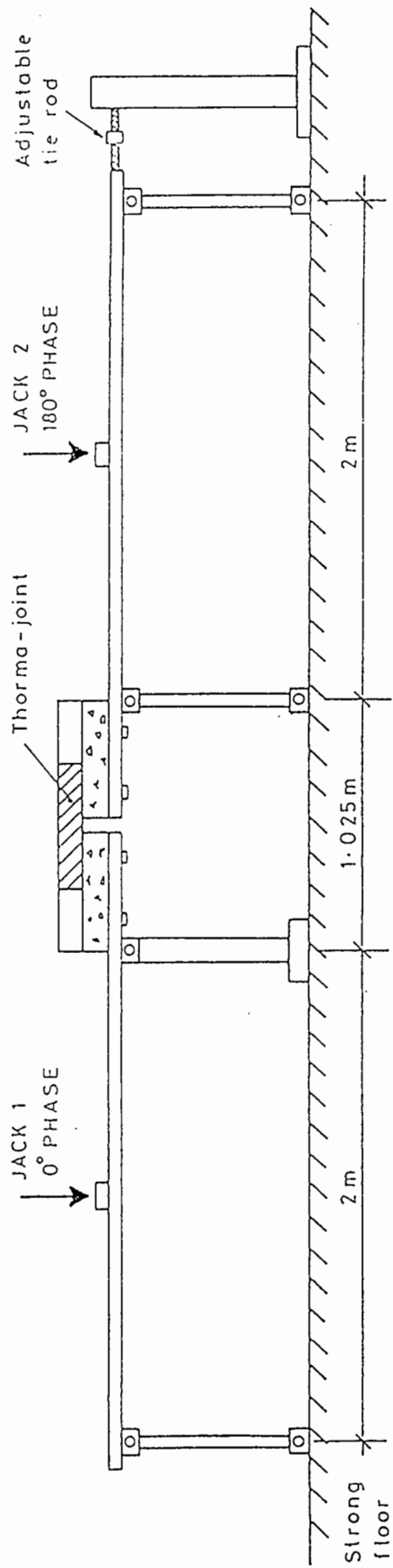
Kozlov (1981) developed simple "Model Joint Machines" for testing preformed elastomeric compression seals under in-service environmental conditions. The machines were driven by temperature activated devices called "bellow-assembly thermostatic motors". Continuous thermal movements, ranging from 11.4 mm to 48.3 mm, could be simulated in response to the changes of ambient temperature. In total, sixteen machines were built and nineteen joint specimens were tested with the previously mentioned simulated thermal movements. All machines were placed outdoors to allow the specimens to be exposed to natural environmental conditions. No attempt was made by Kozlov to accelerate the rate of his testing. The loss of resilience of the compression seals was measured periodically throughout the tests. Based on the test

data, a method for determining the life expectancy of the compression seals was developed. Kozlov concluded that the quality of similar preformed elastomeric compression seals varied significantly, and because of this, it was recommended that the compression seal manufacturers and rubber specialists should improve their quality control before a method of identifying adequate preformed compression seals could be established.

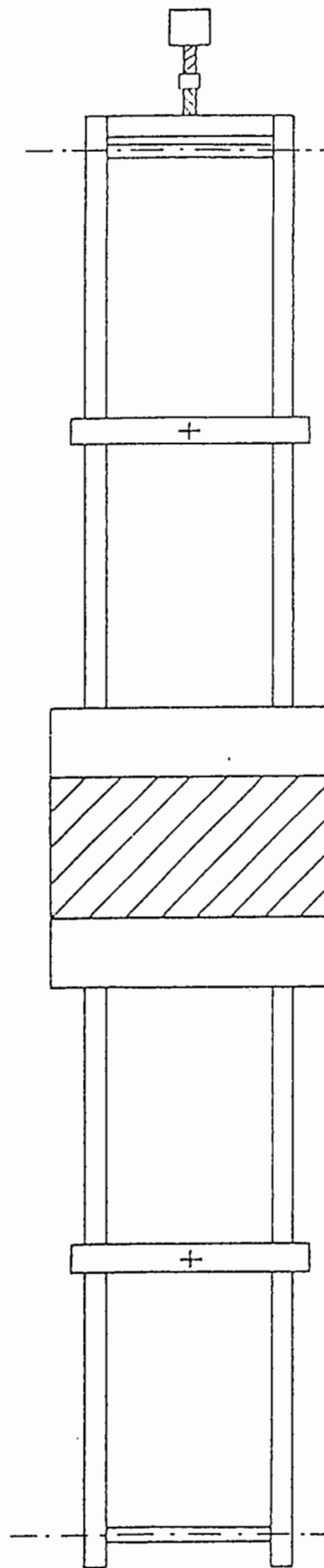
#### 2.5.2 Tests on Asphaltic Plug Joints.

Commercial tests on asphaltic plug joints were carried out by Hobbs (1982), at an accelerated rate and a controlled temperature, using 1 m square slab specimens. Fig. 2.7 shows the details of the test rig used by Hobbs. The specimens were subjected to two million cycles of lift and tilt movements with a value of 0.09 mm and  $1.8 \times 10^{-04}$  radian respectively. The simulated movements were generated by a pair of hydraulic jacks capable of applying a load of 25 kN and 110 mm stroke. The jacks were operated  $180^\circ$  out of phase to reproduce the effects of a passing lorry on a bridge structure as illustrated in Fig. 2.8. Thermal movements of  $\pm 7.5$  mm were applied to the initial joint gap of 37.5 mm by means of operating a threaded tie rod mechanism manually. No details of instrumentation has been reported. Due to certain limitations of this machine, precise controls of the induced movements were not possible.

A successful method for comparing the durability of different



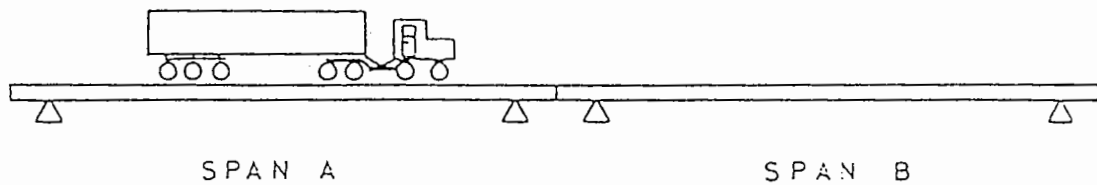
ELEVATION



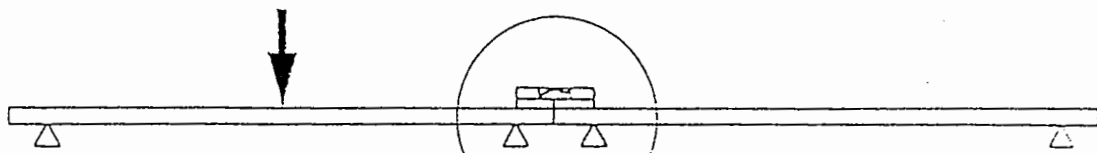
PLAN

FIGURE 2.7 THORMA-JOINT TEST RIG - SCHEMATIC, AFTER HOBBS



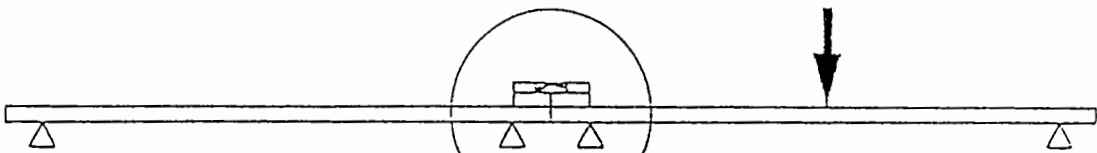
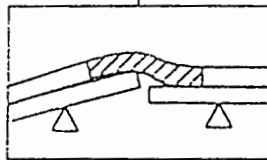


PROTOTYPE



MODEL:  $0^\circ$  Phase angle

SPAN A LOADED



MODEL:  $180^\circ$  Phase angle

SPAN B LOADED

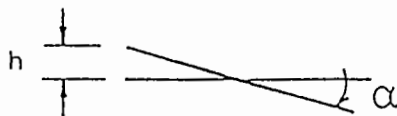
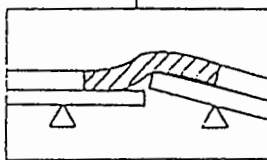


FIGURE 2.8 SIMULATION OF VEHICLE CROSSING TWO SPAN VIADUCT, AFTER HOBBS

asphaltic plug joint designs was reported by Huband and Wood (1986). This involved finite element analysis and computer modelling of a standard in-service asphaltic joint.

## 2.6 MACHINE DESIGNS FOR EXPANSION JOINT TESTING.

### 2.6.1 Design Proposed by Agreement Board.

A more complex machine, the "Test Rig for Motorway Jointings", was designed by Stevenson (1976). The test rig consisted of a base plate and four sub-assemblies, as shown in Fig. 2.9, and was capable of producing simulative bridge deck movements along three mutually perpendicular axes. Along the longitudinal axes, horizontal movements of  $\pm 2$  mm and  $\pm 100$  mm, representing traffic induced and thermal movements respectively, could be generated. Horizontal movements along the lateral axes, ranging from 0 mm to 50 mm, could also be produced as required. Vertical movements could vary from 0 mm to  $\pm 6$  mm. All movements could be generated, by means of four electro-mechanical motors with adjustable cams, at the frequencies indicated in Fig. 2.9. The rig could accommodate joint specimens with a maximum size of 2 m x 1 m. Various types of joints, such as buried joints, compression seals and mechanical joints, could be tested in a temperature controlled environment. The actual performance of this proposed machine has not yet been reported.

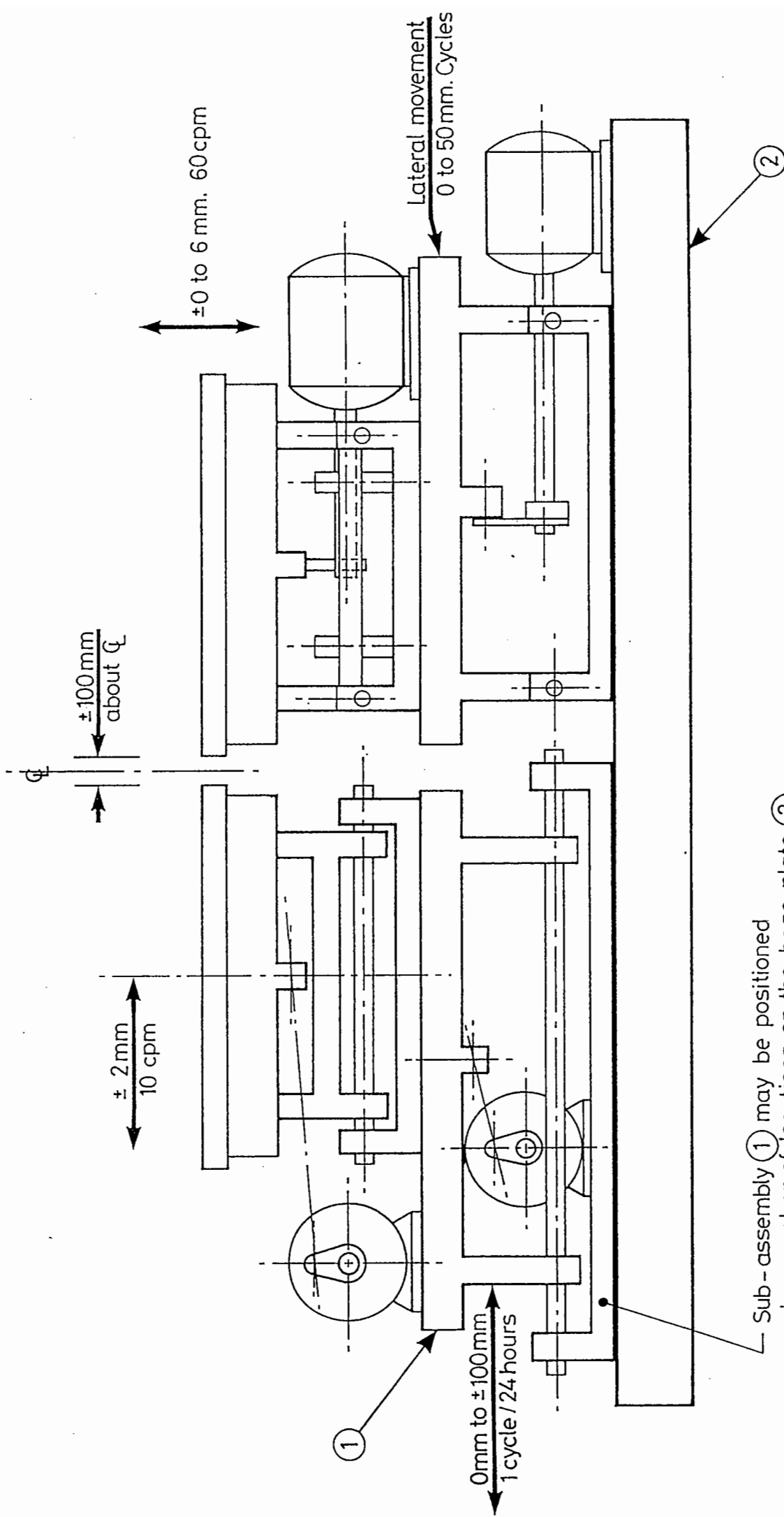


FIG. 2.9 TEST RIG FOR MOTORWAY JOINTINGS, AFTER STEVENSON

### 2.6.2 Machines Designed in Austria.

Wicke et al (Eyre 1987) designed a set of four machines, together with a proposed test programme (Fig. 2.10), for testing elastomeric and flexible neoprene sealant expansion joints. The first machine (test unit no. 1) could be used to study the response of joint materials to horizontal joint movements at different temperatures by measuring the restoring forces of the joint materials after each full stretch of the joint system. The second proposed machine (test unit no. 2) was a rotary tracking system. The machine would have four single wheels mounting on four steel arms. The wheel would run on a 7.5 m diameter track with a maximum speed of 30 km/h. Four joint specimens could be tested simultaneously under a rolling load of 87.5 kN. In total, 6 million loading cycles was proposed for each test and no joint damage should be expected after the test. Dynamic loading tests could be carried out using the third machine called a hydropulse system (test unit no. 3). The machine consisted of a loading frame and a hydraulic jack capable of producing a load and stroke of 250 kN and 100 mm respectively. Joint specimens with a size of 4 m x 2.5 m could be tested under a dynamic loading of 122.5 kN for 6 million cycles. The specimen would be placed on a slope of 16 % to the horizontal to allow horizontal and vertical load components to be generated by a single jack. The final machine (test unit no. 4) consisted of a base frame made of heavy steel girders. Joint specimens could be supported by two movable tables. Slow horizontal and vertical movements were produced by

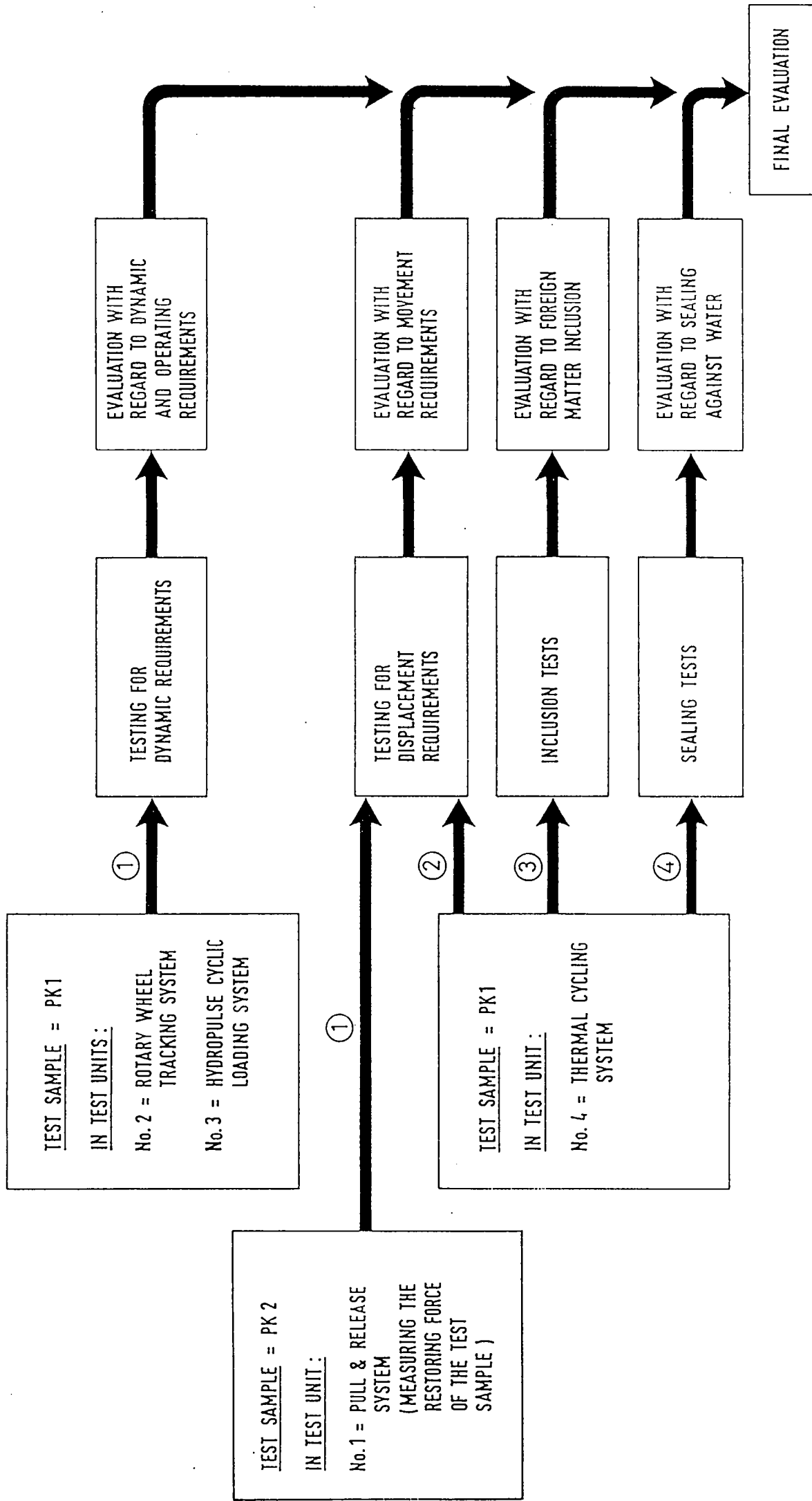


FIG. 2.10 PROGRAMME FOR TESTING BRIDGE DECK  
EXPANSION JOINT, AFTER WICKE et al.

an electric motor drive unit through push-pull and lifting spindles respectively. It was proposed that joint specimens should be subjected to each of these movements for up to 2500 cycles during testing. The same machine could also be used to investigate the effects of the inclusion of foreign materials in the joint gaps and water tightness of the joint system. Although no test results have been reported so far, it is likely that these tests would provide an objective means for assessing performance of expansion joints and help engineers to select a better joint system for a bridge at its design stage.

## 2.7 SITE INVESTIGATION ON IN-SERVICE EXPANSION JOINTS.

### 2.7.1 TRRL Investigations.

Long-term observation on the in-service performance of fifty buried type joints had been conducted by Price (1982 (a)) over a period of seven years. This involved buried joints comprising various materials and installed in different bridge structures. The key factors which affect the in-service performance of the joints were identified and graded according to their degree of influence on the deterioration of the joints. The grading of these factors, as shown in Table 2.1, was used to obtain the "Deterioration Index" of each joint. Fig. 2.11 shows the Deterioration Index and the in-service condition of the joints under investigation. Price concluded that deck movements induced by traffic and temperature changes, material used in the joint,

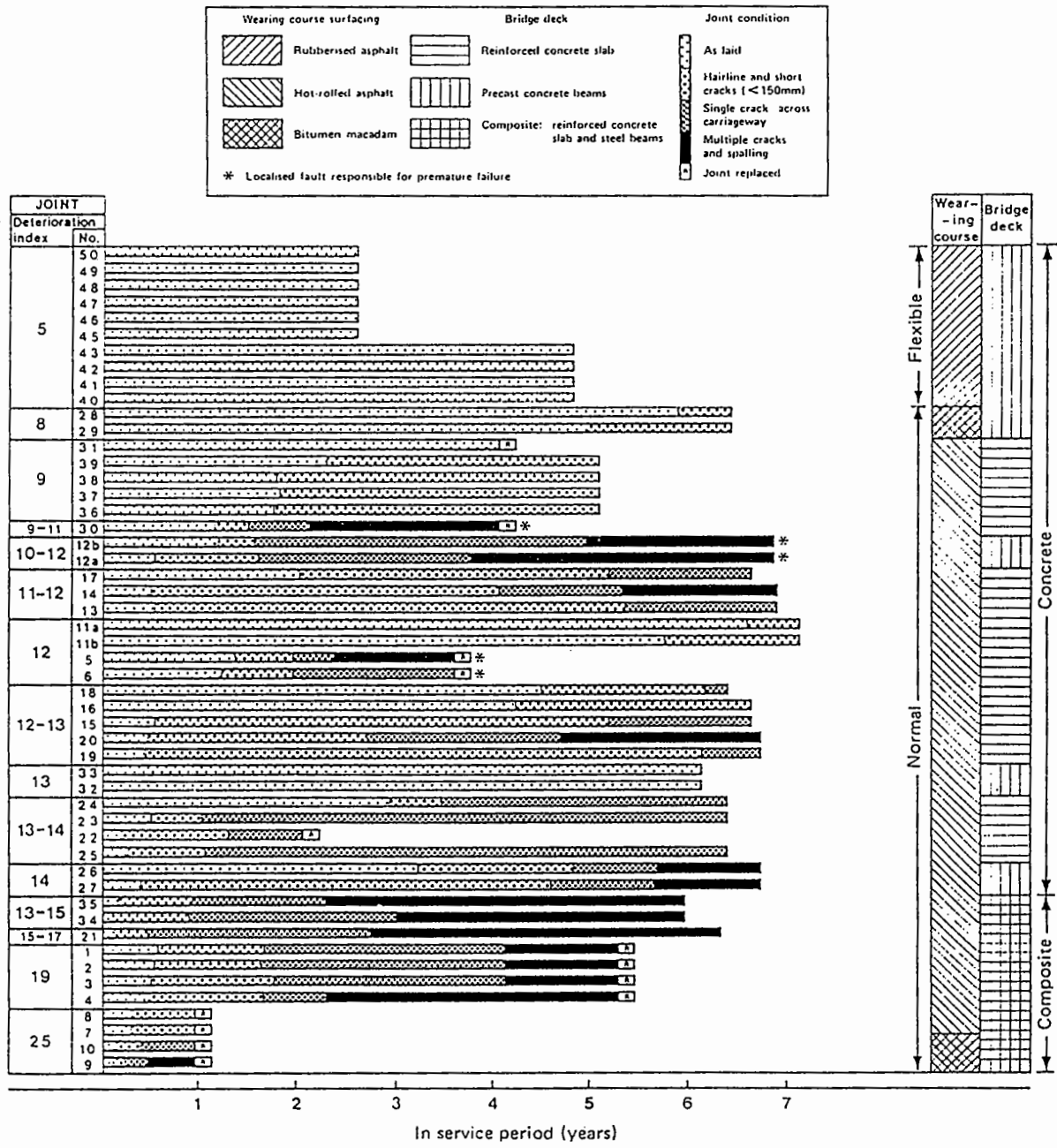


FIGURE 2.11 IN SERVICE CONDITION OF THE JOINT  
 (EXTRACT FROM TRRL REPORT SR740)

Table 2.1 Evaluation of joint performance: the contribution of the various factors  
(extract from TRRL report SR 740)

Factor	Contribution to deterioration		
	Large	Moderate	Negligible
	2*	1*	0*
Dynamic vertical displacement (mm)	> 4	2→4	< 2
Dynamic deck end rotation (radians x 10 <sup>-6</sup> )	> 400	100→200	< 100
Dynamic horizontal movement (mm)	> 0.10	0.05→0.10	< 0.05
Thermal horizontal movement (mm)	> 14	9→14	< 9
Heavy commercial traffic Frequency/lane/hour	> 50	10→50	< 10
Surfacing flexibility	Poor	Moderate	Good
Surfacing thickness (mm)	< 75	75→100	< 100
Surfacing compaction	Poor	Moderate	Good
Joint debonding layer	Omission	Single foil faced	Double foil faced
Joint reinforcing layer	Omission	Fibre matt	Expanded metal
Installation temperature °C	< 5	5→15	> 15
Workmanship	Poor	Moderate	Good
Installation weather	Wet, freezing	Damp, dusty	Dry
In-service weathering <sup>†</sup>	Long periods of icing	Short periods of icing	No icing
Function of the bearings	Poor	Moderate	Good

\* Grading given to the contribution to deterioration by the individual factors

<sup>†</sup> Applicable once cracking has commenced



site preparation and workmanship, weather and temperature during installation and in-service weathering were the factors influencing the performance of buried joints. However, it was often a complex combination of these factors which affects the final performance of a joint.

### 2.7.2 Research in Belgium.

A five-year project on bridge deck expansion joints was conducted by Clauwaert (1986) at the Belgium Road Research Centre. Traffic induced joint gap movements on different bridges were recorded by means of site instrumentation. A set of these measurements from one of the sites is presented in Fig. 2.12. The duration of the joint movements depends on the span of the structure and the speed of the vehicle and usually has a value between 1.5 and 3 seconds.

Clauwaert introduced a stress concentration factor ( $K_s$ ) for calculating the critical stress in the surfacing material of a buried joint. The factor was defined as the ratio of the strain of the joint material, measured at the underside of the surfacing above the joint gap, to the strain of a free body made of the same material and subjected to the same amount of displacement. Fig. 2.13 illustrates the definition and typical value of the stress concentration factor for a buried joint. An attempt was made to predict the service life of a buried joint using site measured horizontal joint movement spectra, calculated stress

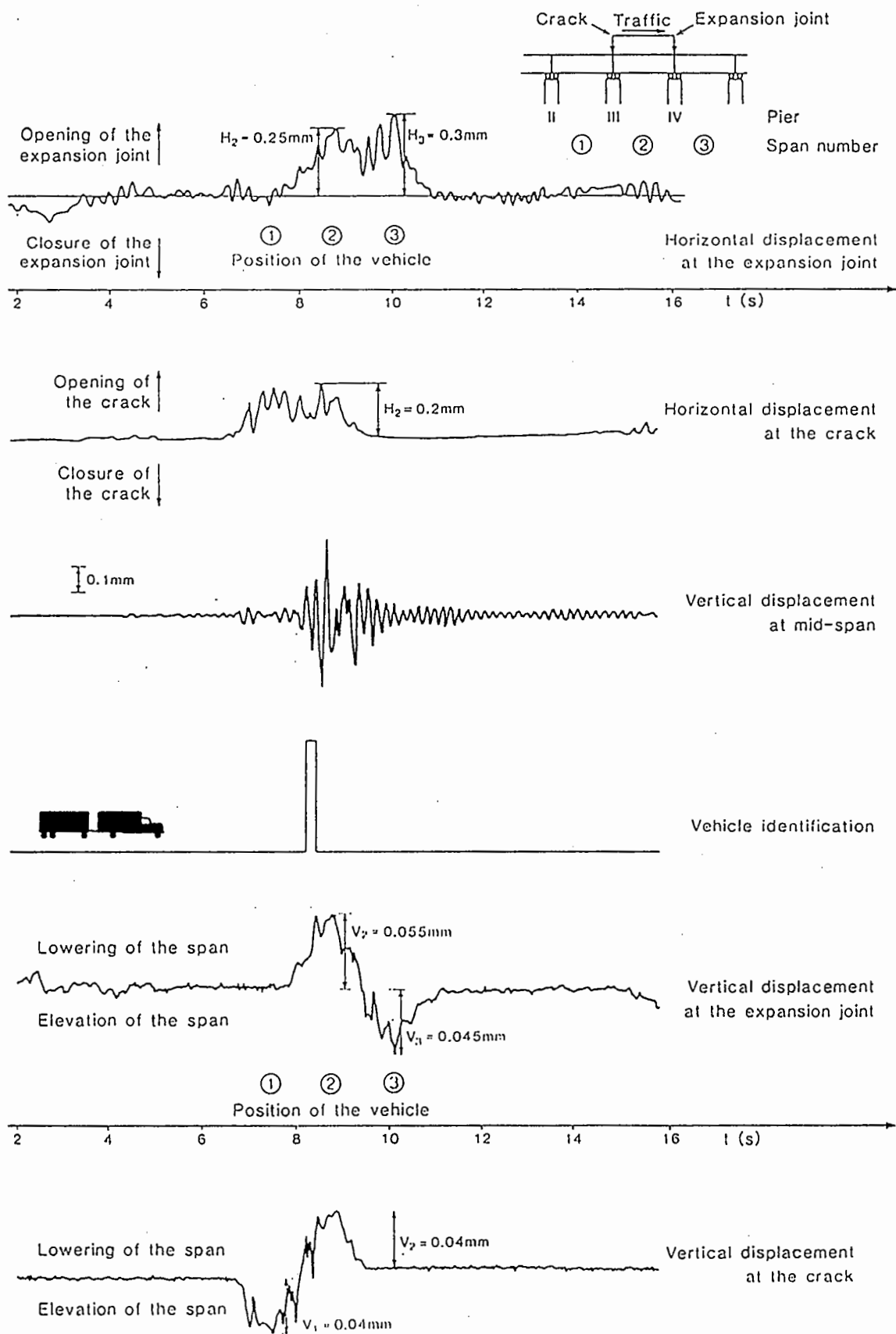
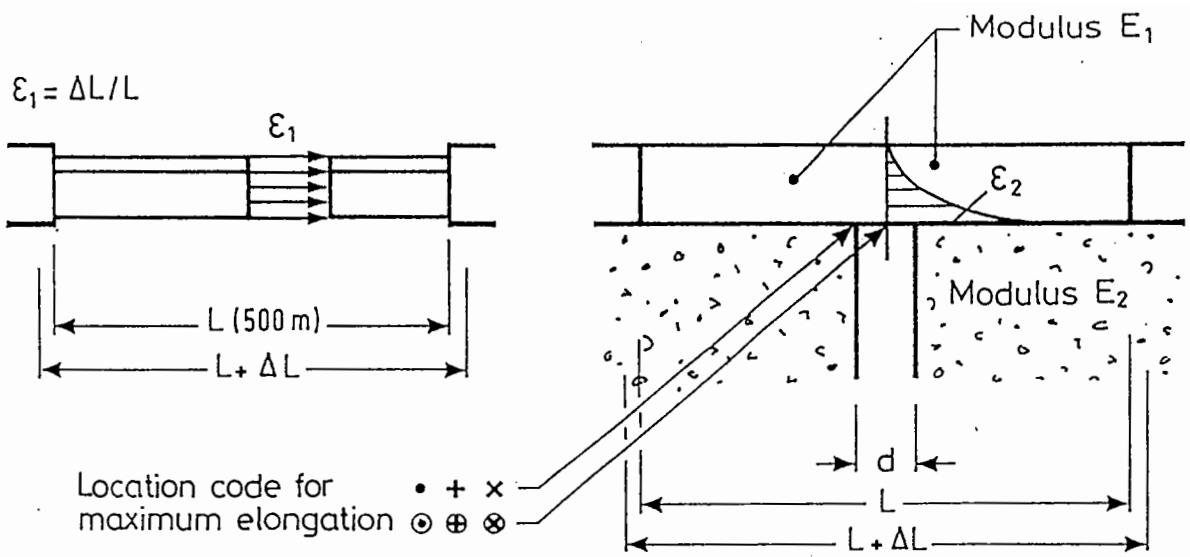


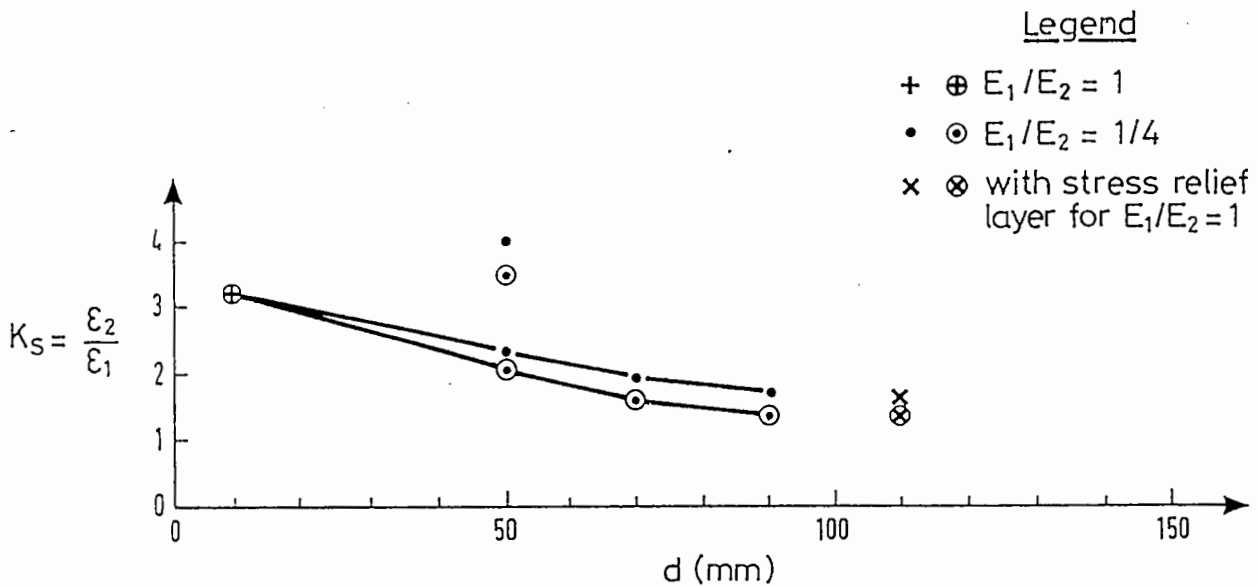
FIG. 2.12 DISPLACEMENT UNDER HEAVY TRAFFIC

AT BRIDGE JOINTS VIADUCT ON E5

LIÈGE, BELGIUM.



(a) DEFINITION OF THE STRESS CONCENTRATION FACTOR



(b) VARIATION OF  $K_s$  IN RELATION TO THE GAP WIDTH AND THE RATIO OF THE MODULI

FIG. 2.13 VARIATION OF STRESS CONCENTRATION FACTOR IN A BURIED JOINT, AFTER CLAUWAERT

concentration factor and a fatigue life curve obtained from the results of a series of simple fatigue tests on trapezoidal samples. Although this provided a method to predict the relative lives of different joints, the service lives of the joints would be greatly underestimated.

As far as buried joints are concerned, Clauwaert drew the following conclusions:

1. The stress in the joint material, created by a wheel load directly on top of the joint, had less significant effect on joint life than that caused by a traffic induced movement which had its maximum value when the wheel load was located at the mid span of a bridge structure. However, the rolling action of the wheel loads had a healing effect on slightly cracked joints, especially when temperature was high.
2. The stress concentration factor was a function of the ratio of the moduli of the joint material and the deck concrete, the thickness of the surfacing and the width of the joint gap. The value of the factor lay between 1 and 4. The  $K_s$  value would increase by as much as twice the normal value when the surfacing material was much more flexible than the deck concrete, i.e. during a hot summer. The  $K_s$  value of a particular joint could be reduced by means of increasing the joint gap or using a stress relief layer between the surfacing and the bridge deck.

## 2.8 SUMMARY.

1. While conventional uniaxial fatigue tests provide an easy and economical way of assessing the fatigue performance of a bituminous material, they use specimens of simple shapes which have no similarity to a real structure. Since a more accurate assessment of joint performance is required in bridge deck expansion joint testing, test specimens with more realistic construction details must be used.

2. The fatigue resistance of a bituminous mix is highly dependent on its void content. To ensure consistency of expansion joint test results, specimens must be produced with a relatively constant void content by means of an accurate control on the amount of compaction applied during specimen manufacture.

3. The fatigue performance of a bituminous mix will also be affected by the control mode used during testing. Under in-service conditions, buried joint materials are likely to be subjected to a type of loading which is intermediate between a stress and a strain control mode, but close to the latter.

4. It was reported that the strain criterion of fatigue testing of bituminous material would remain appropriate for test temperatures up to 25 C. Therefore, it was decided that endurance testing on buried joints should be carried out at temperatures

not exceeding 25<sup>o</sup> C.

5. It was suggested in the literature that Miner's rule could be used to calculate the cumulative fatigue damage to bituminous materials when subjected to a variety of stresses or strains. This technique was adopted to evaluate joint test results when test conditions were appropriate.

6. Test results of Van Dijk's work from wheel tracking showed that three fatigue stages (N1, N2 & N3 as shown in Fig. 2.6) could be identified from the strain measurements taken at the underside of the specimens. Graphical plots of the strain changes measured on the top surface of buried joint specimens during joint testing showed a similar pattern (Figs. 7.3 (c) & 7.5 (c)). This provided a good indication that a realistic failure mode, similar to those produced by a tracking machine, had been reproduced by the EJS.

7. Detailed review of other joint testing machines provided useful information on the design and performance of these facilities. This in turn helped to provide new ideas and avoid mistakes during development of the EJS.

8. Price's report on buried joints provided limited but important information on the in-service performance of this type of joint. The basic parameters used for testing joint specimens with the EJS were formulated using this information. To account for the rest period effects, joint test results were multiplied

by a life factor of 20, as suggested by Raithby and Sterling, before being used to compare with the site investigation results reported by Price.

9. Results from the Belgium research provided evidence that testing bridge deck expansion joints off the road would be possible but a long-term commitment would be essential for the success of this kind project.





## CHAPTER THREE.

### DETAILS OF THE TEST EQUIPMENT.

#### 3.1 INTRODUCTION

One of the main objectives of this research was to develop a facility capable of testing expansion joint systems, with simulated bridge deck movements as experienced by expansion joints during their service lives, under controlled laboratory conditions and at an accelerated rate . These include traffic induced horizontal, vertical and rotational movements and long term diurnal or seasonal thermal movements. It was important that these movements could be generated one at a time to allow their individual effects on the endurance of bridge deck expansion joints to be isolated and studied independently. However, when simulation of the in-service conditions of a working joint was required, all these movements needed to be produced simultaneously. As far as this research was concerned, the horizontal movements induced by traffic could be as small as 0.05 mm, while the thermal movements could be as large as 50 mm. The test equipment was required to generate these simulated bridge deck movements accurately over the specified range. Unwanted resonant oscillations in the mounting frame during a dynamic load test had to be prevented.

The duration of a bridge deck expansion test could vary from several hours to several weeks. In order to finish a test as soon as possible, the test would be expected to run continuously day and night. Therefore, it was desirable that the equipment should be operational with a minimum of manual supervision. Testing time could be further reduced by using a higher loading frequency during cycling. However, this would probably not exceed 10 Hz.

Due to the temperature susceptibility of bituminous materials, all specimens had to be tested in a temperature controlled environment. A suitable temperature controlled room should therefore be large enough to house the whole test equipment and the test specimen while still having enough working space for the safety of the operator. The temperature in the room should be capable of being kept constant or varied over a realistic range and the temperature control should operate automatically once all control parameters have been set.

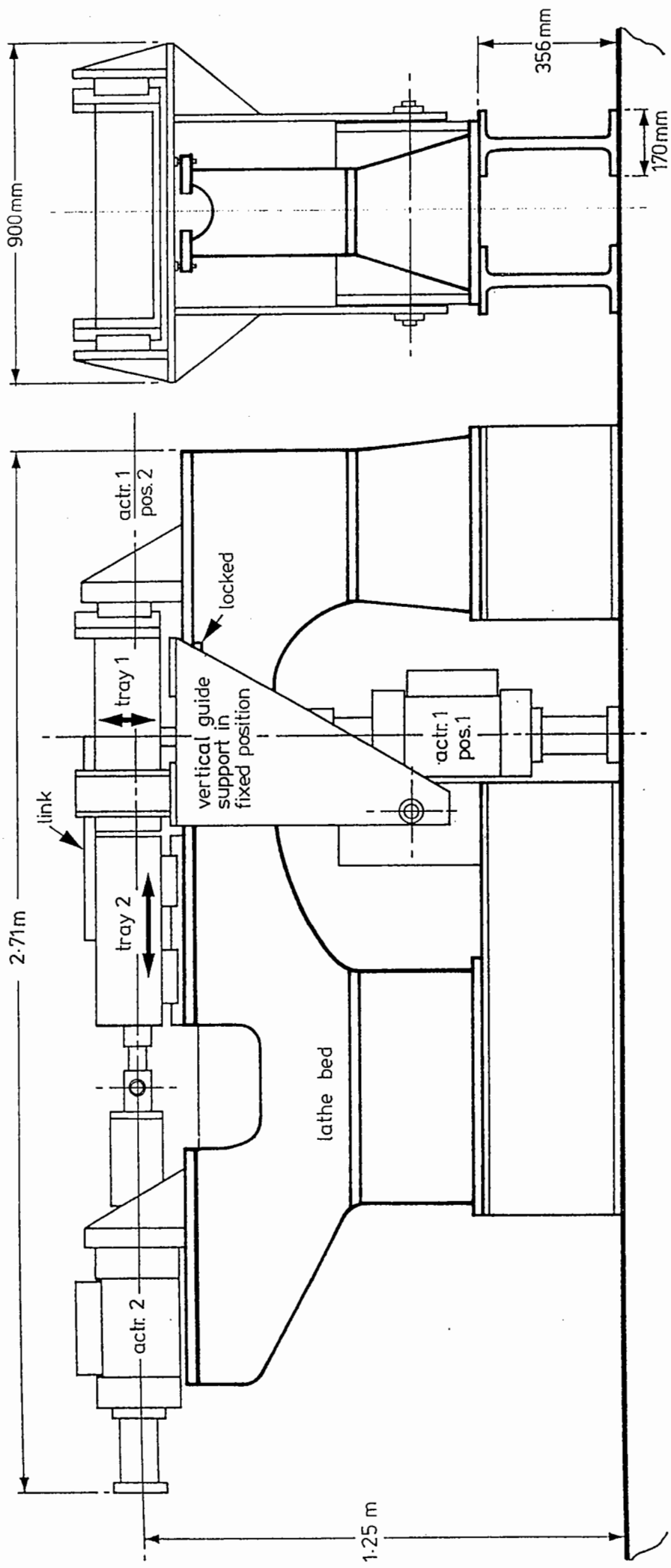
The equipment was designed and built in the first stage of this research project. Sections 3.2 to 3.6 describe the state of the equipment when the author was first appointed. Details of the subsequent changes and improvement made on the equipment are discussed in Chapter 4.

### 3.2 MECHANICAL DETAILS OF THE EXPANSION JOINT SIMULATOR (EJS)

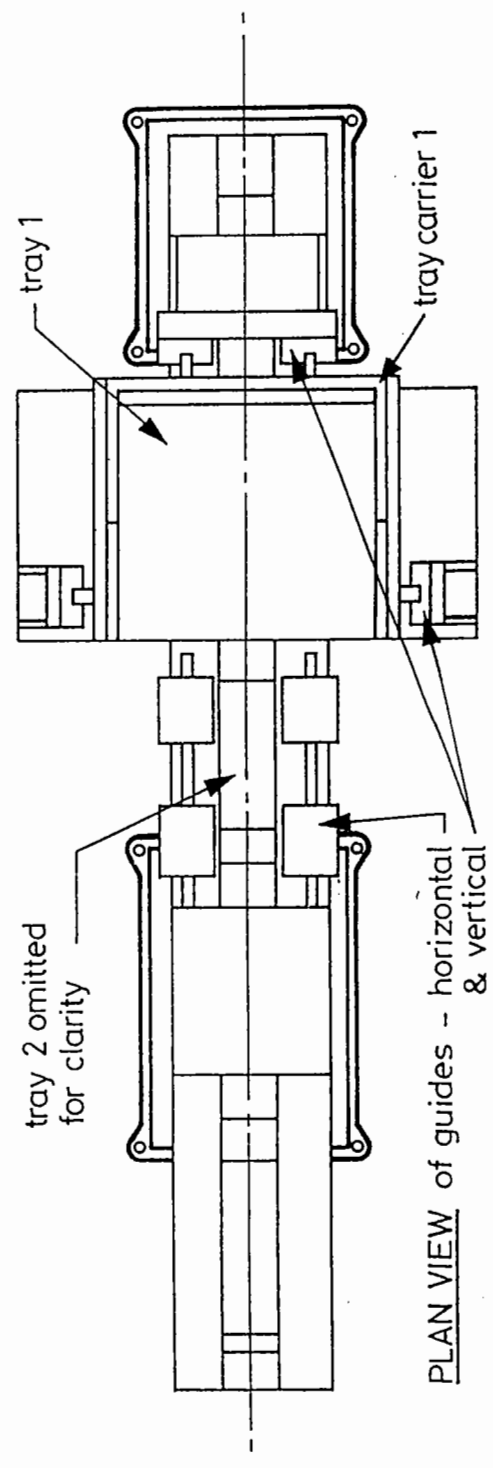
Fig. 3.1. shows the mechanical components of the Expansion Joint Simulator (EJS). A cast iron lathe bed forms the basic frame of the simulator of sufficient mass to minimise the possible resonance effects generated during a cyclic test. Two tray carriers are permanently fixed to eight linear bearing guides which are in turn mounted on the top of the lathe bed. Each bearing unit is capable of resisting a load of 32 kN in two directions at right angles to the line of the bearing motion.

The simulated bridge deck movements are generated by using two Dartec servo-hydraulic actuators each with a built-in load cell and position LVDT. The location of the actuators are shown in Fig. 3.1. The actuators are supplied by two optional oil pumps of 40 l/min. or 125 l/min capacity, the selection of which depends on stroke and frequency. Each actuator is capable of generating a maximum tensile or compressive load of 100 kN.

During the test, actuators 1 (vertical) and 2 (horizontal) are coupled to tray carriers 1 and 2 respectively. With such an arrangement, actuator 1 can move tray carrier 1 up and down the vertical bearing guides and tray carrier 2 can be reciprocated along the horizontal bearing guides by actuator 2. Thus actuator 2 can be activated to reproduce the horizontal movements of the bridge deck at the joint and actuator one the vertical movements, either individually or combined.



END VIEW  
(without actuators)



PLAN VIEW of guides - horizontal & vertical

FIG.3.1 EXPANSION JOINT SIMULATOR

Tray 1 is normally free from the triangular support system. However, if "bending" of the test specimen is required, tray 1 could be clamped to the triangular support, which is then released from its restraints. With actuator 1 working at position 2 rotation of tray 1 can be achieved.

### 3.3 THE ACTUATORS AND THE HYDRAULIC POWER SUPPLY SYSTEM.

The actuators for the EJS are the Dartec type 12D, double acting hydraulic fatigue actuators. Each actuator is fitted with an integral displacement transducer (LVDT), a load cell and a type 76 servo-valve designed for a 57 l/min oil flow.

For a standard system, hydraulic power is supplied by a Dartec hydraulic power pack. However, for economic reasons, the EJS is connected to an existing hydraulic power supply system which is available in the University. A schematic diagram of the system and its attached test equipment is shown in Fig. 3.2. The Los pump is capable of supplying two different oil flow rates of 40 and 150 l/min. The second flow rate provides a useful option when large actuator strokes are required or additional hydraulic systems are used on the same line.

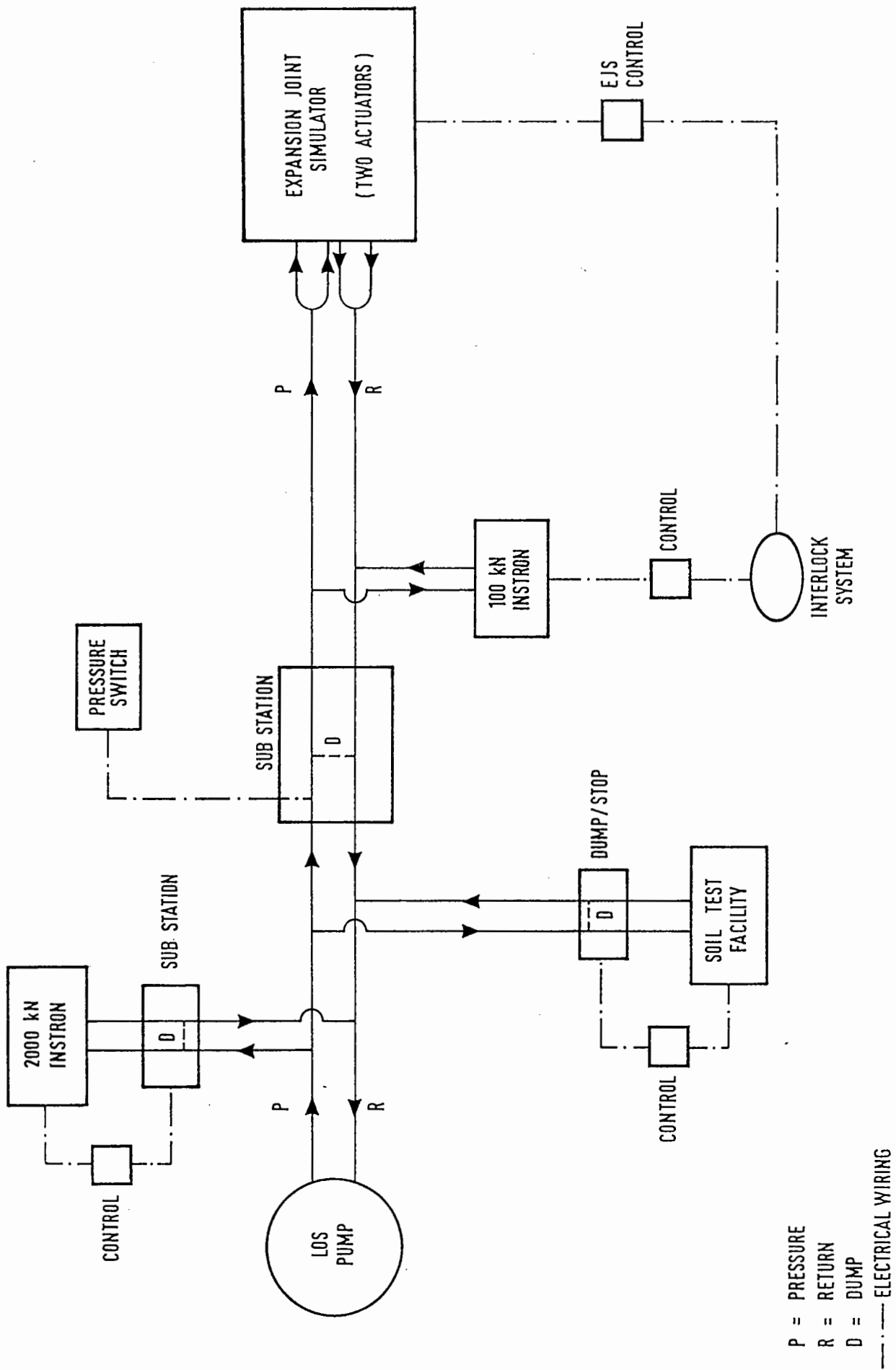


FIG.3.2 SCHEMATIC DIAGRAM OF THE HYDRAULIC SUPPLY SYSTEM

### 3.4 THE CONTROL SYSTEM

The two electronic units used to control the actuators are known as the Dartec 9500's. Each unit is built up with a different number of printed electronic circuit boards. Each board has its own 16 bit micro-processor and memory to handle all the real time functions for a test and provides instant response to different events during a test. Using this distributed processing technology, each board is allowed to execute a dedicated task within its capacity. The system can also be improved or tailored at a later stage by changing or adding different electronic boards as user requirements change. All boards in the units are linked to a supervisory computer through two RS 232C interfaces which allow communication between the operator and the control systems to be made via the computer keyboard. The micro-processor in different boards can be set through the supervisory computer using specially designed four digital codes. The computer can be any device, from a small micro to a large mainframe, with the required number of RS 232C connections. Whenever the computer becomes obsolete, it can be changed or upgraded to a different model as necessary.

A complete Dartec 9500 system consists of a supervisory computer, a 9-slot chassis and nine printed circuit boards. A minimum system designed for dynamic testing, as recommended by the manufacturer, includes the supervisory computer, the 9-slot chassis and five boards. These are a1 (Analogue to Digital), b1 (Controller), e1 (Data Processing), p1 (Function Generation) and

g2 (Computer Interface) boards. Normally, the minimum system will be further enhanced by adding a v1 (Trip) board, a data display panel and a control front panel to form a standard basic system. The v1 board provides essential trip facilities to protect the simulator from overloading and to stop the machine whenever a safety condition is not met. The front panels give a continuous display of information, such as the load and stroke (position), and make the setting up operation much easier.

In order to build the joint simulator to meet the performance specifications and to keep the costs within the original budget, the configuration of the Dartec systems used in the University of Nottingham was modified as shown in Fig. 3.3. System A consists of six boards, namely, a1, a2, b1, g2, and v1, while system B consists of a1, b1 and g2 boards only. Data processing, e1 boards, on both systems were omitted. The two control systems work as a master and a slave. They share a single p1 board and a v1 board. The signals generated by the function generator drive the actuator (vertical) of the master system A directly. These signals are then fed to the slave system B, through a supplementary A-D board (a2) to drive the horizontal actuator. The loop is closed through the position feedback and the horizontal movement becomes synchronised to that of the vertical actuator. The additional "summer" on the a2 board and an external command "summer" provided the facilities to invert and scale the slave command and also move the actuator to a different starting point with a d.c. offset. The trip board responds to the internal



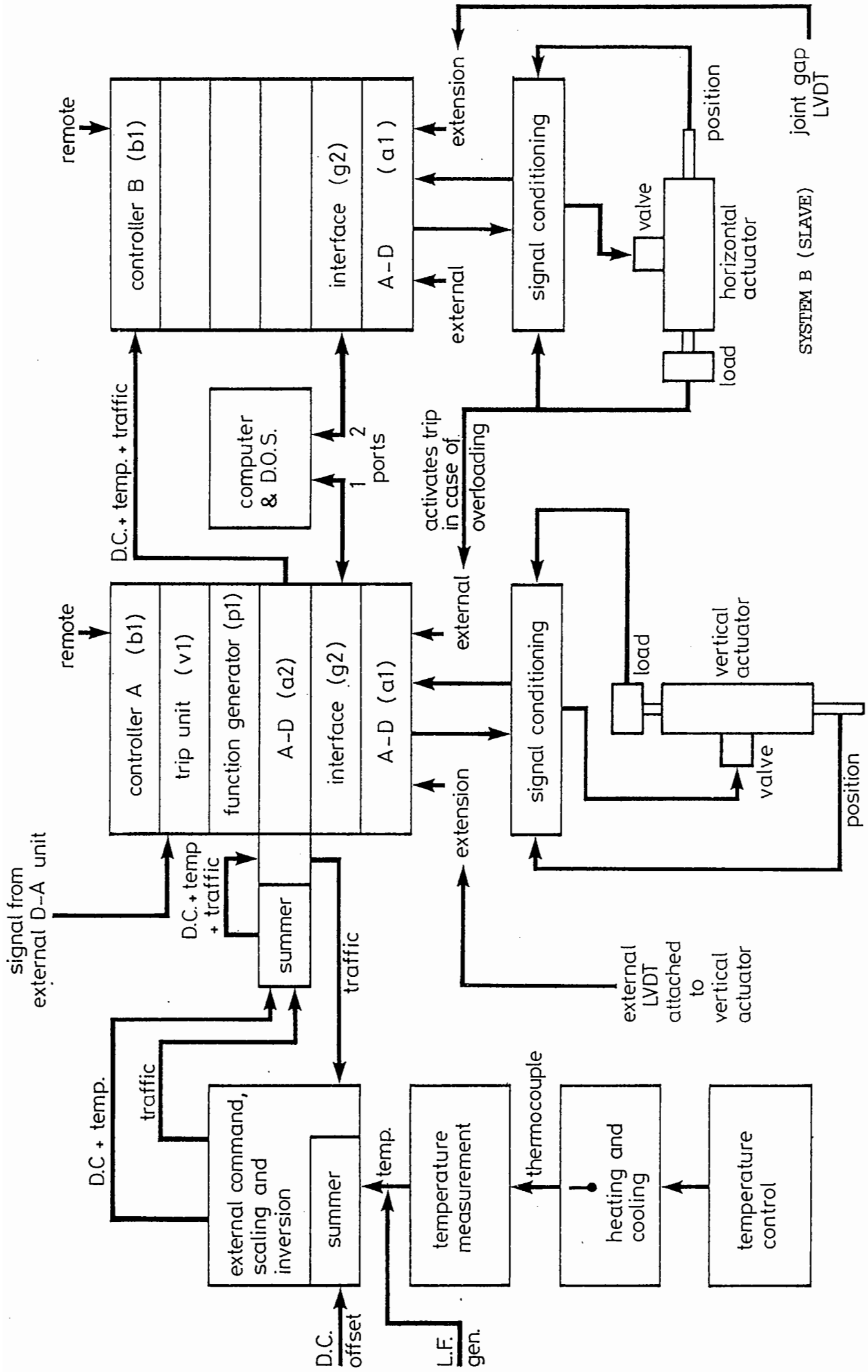


FIG. 3.3 SCHEMATIC DIAGRAM OF THE CONTROL SYSTEM USED IN NOTTINGHAM.

SYSTEM A (MASTER)

signals of the master system but not the slave. The function of each printed circuit mentioned above is described in more detail in appendix A. Table 3.1 gives a summary of the capabilities of the EJS.

### 3.5 DETAILS OF THE MOULD.

The mould used to house the specimen consists of two separate parts, called inner trays. The trays are joined together by a pair of steel links which are arranged to set a 20 mm wide gap between them. When assembled, the inner size of the mould is 1020mm long x 500 mm wide x 100mm deep.

One of the important features of the inner trays is the method of specimen connection to the base plates. Five 10 mm square x 450 mm long steel ribs were welded across each base plate at 85 mm spacing (Fig. 3.4). These ribs were intended to key the specimen firmly to the mould. Fig.3.5 shows the mould when fitted to the EJS.

The specimen was cast in-situ with the trays linked together and when the specimen was ready for testing, it was lifted up by an overhead crane and fitted into the tray carriers. Bolts were used to hold the inner trays and the tray carriers together. After the actuators were positioned and coupled up to the tray carriers, the links are removed. This released the specimen and allowed a joint gap movement to develop under the control of the

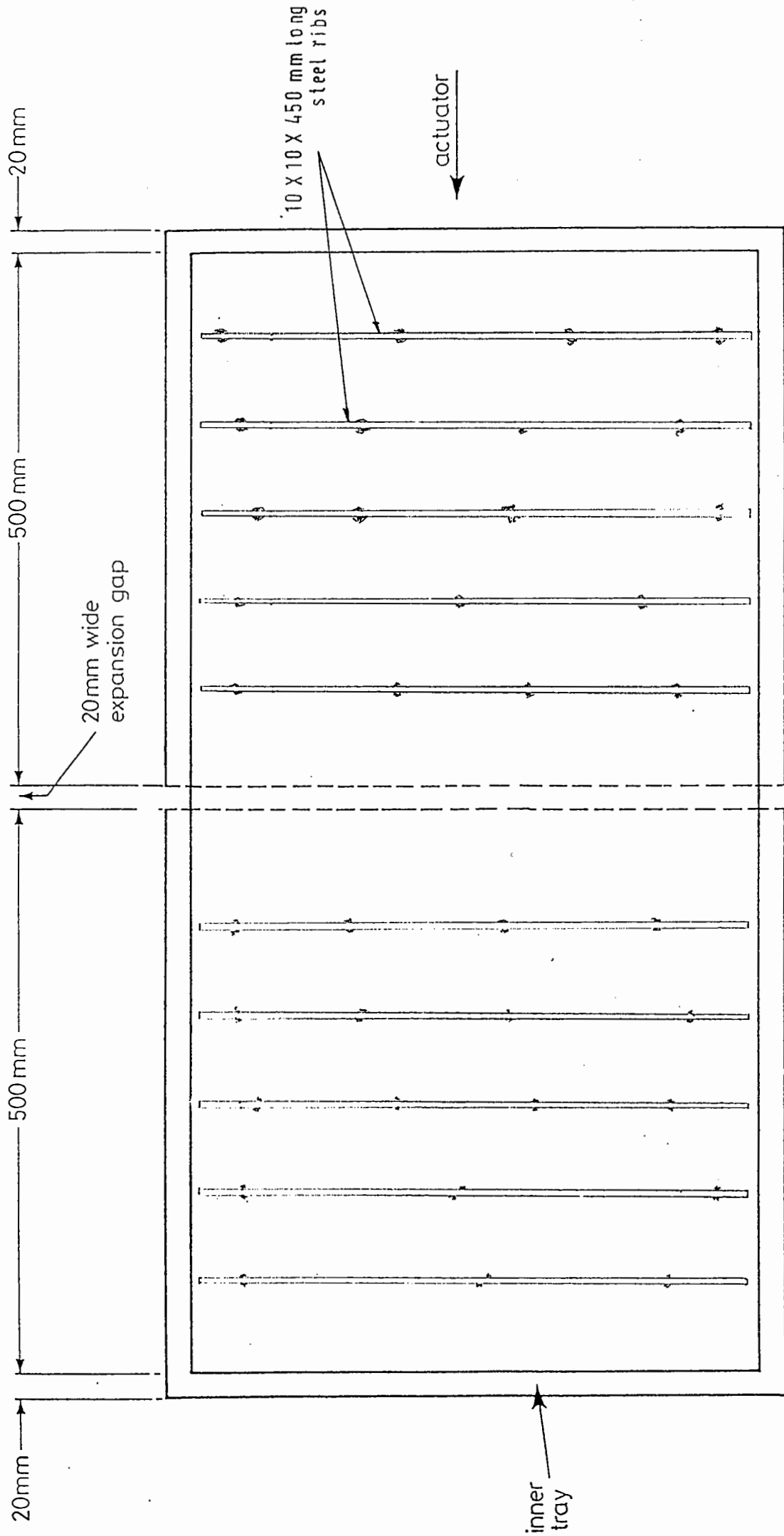


FIG. 3.4 DETAILS OF THE INNER TRAYS.  
 (Initial design)

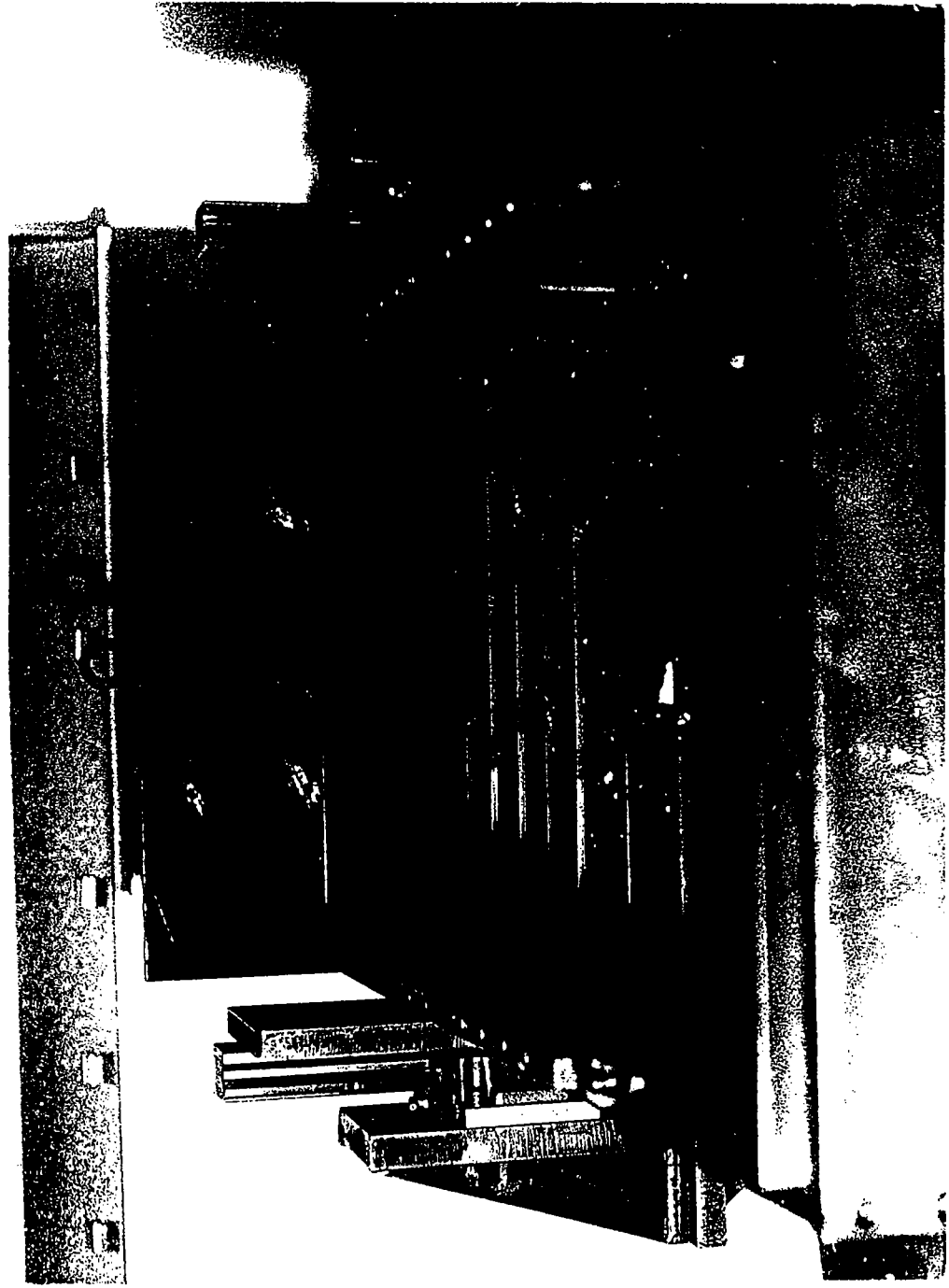


FIG. 3.5 DETAILS OF THE INNER TRAYS.  
(Initial design)

Table 3.1 Capabilities of The EJS.

<p style="text-align: center;"><u>Actuators</u></p> <p>Static Load Rating</p> <p>Dynamic Load Rating</p> <p>Total Working Stroke</p>	<p style="text-align: center;">+100 kN</p> <p style="text-align: center;">+70 kN</p> <p style="text-align: center;">100 mm</p>
<p style="text-align: center;"><u>Control System</u></p> <p>Supervising Computer</p> <p>Control Units</p>	<p style="text-align: center;">Texas Instrument PC</p> <p style="text-align: center;">2 No. of Dartec 9500s</p>
<p style="text-align: center;"><u>Wave Form Generation</u></p> <p>Wave Forms</p> <p>Frequency</p>	<p style="text-align: center;">Sine, Square and Ramp</p> <p style="text-align: center;">0 - 200 Hz.</p>
<p style="text-align: center;"><u>Sample Size</u></p> <p>Length</p> <p>Width</p> <p>Depth</p> <p>Gap Width</p>	<p style="text-align: center;">1000 mm + Gap Width</p> <p style="text-align: center;">500 mm</p> <p style="text-align: center;">1.00 mm</p> <p style="text-align: center;">20 mm (Variable)</p>
<p style="text-align: center;"><u>Temperature Control</u></p> <p>Temperature Range</p>	<p style="text-align: center;">5 °C - 40 °C</p>

Dartec actuators.

### 3.6 TEMPERATURE CONTROLLED ROOM.

The EJS was placed in a thermally insulated room (Fig. 3.6) which had an internal size of 1.9 m x 3.9 m x 2.2 m high. Directly above the EJS, a 690 mm x 1220 mm opening was provided in the roof of the room. This opening gave an easy access for unloading joint specimens onto the EJS using an overhead crane. A removable slab made of insulation material was used to cover the roof opening when it was not in use. The temperature inside the room was controlled by a combined heating and cooling system using four programmable electronic relays which were in turn controlled by a digital time clock. The design temperature range for the room was between + 5 °C and + 40 °C. With such an arrangement, the ambient temperature inside the room was kept constant or varied within these limits automatically during tests. Initially, the temperature room also accommodated the Dartec Control Systems so for safety reasons, it was planned to build a partition inside the room to separate the control system from the test area.

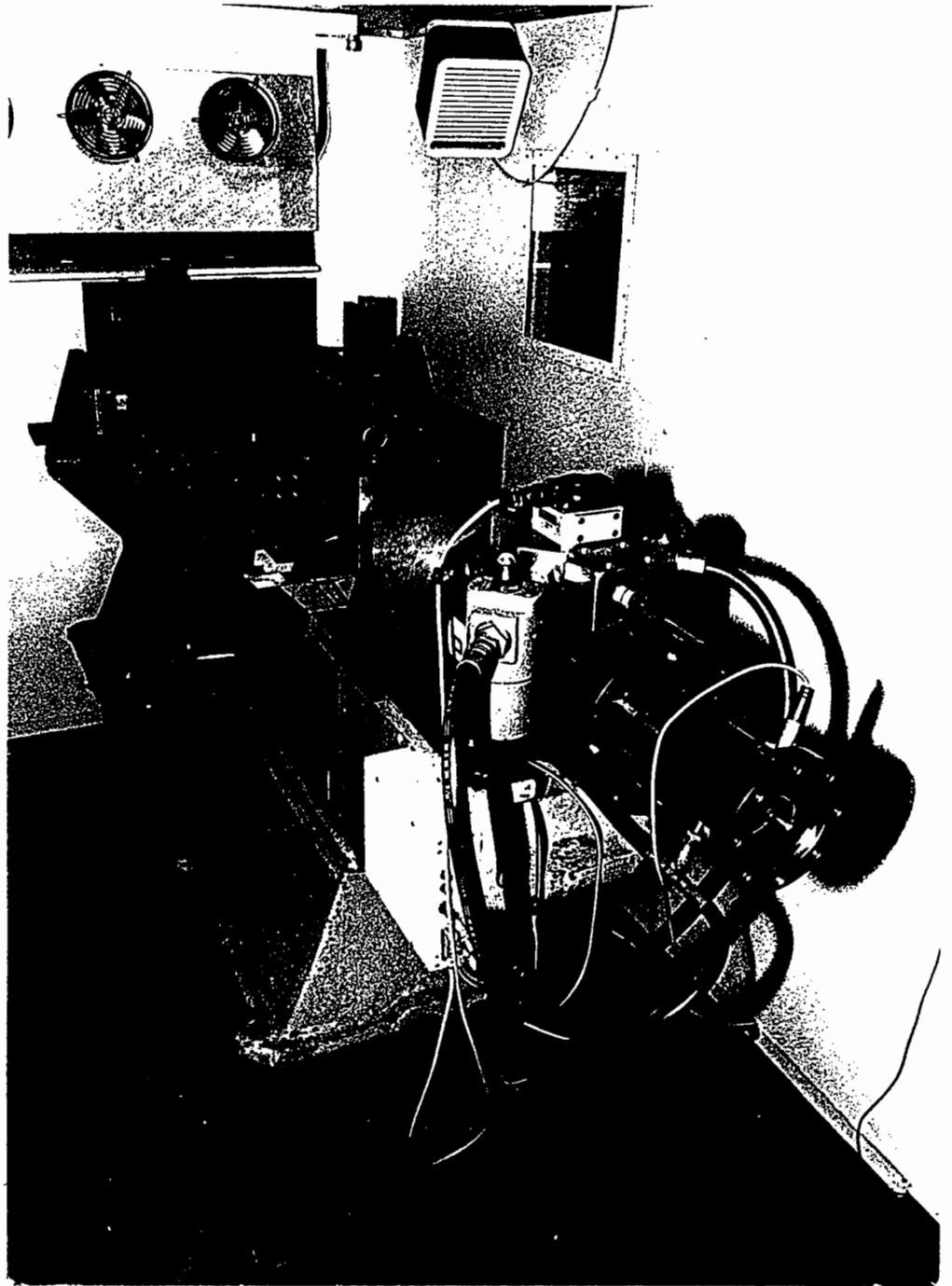


FIG. 3.6 EXPANSION JOINT SIMULATOR IN  
TEMPERATURE CONTROLLED ROOM.





## CHAPTER FOUR

### COMMISSIONING AND MODIFICATION OF THE EQUIPMENT.

#### 4.1 COMMISSIONING OF THE EJS.

Commissioning of the EJS was basically carried out in two stages. In the first stage, the performance of the hydraulic pump, which was not bought with the system, and the actuators was investigated at zero load. This test confirmed that the stroke limits of the actuators, at a specific oil flow rate, complied with the design specifications of the EJS. These simple tests also gave an opportunity to become familiar with the basic operations of the two Dartec 9500 control systems without taking any risk of damaging the machine due to accidental overloading.

The second stage of the commissioning involved three joint specimens made of recycled bituminous material. Through these tests, the techniques required for making, handling and compacting joint specimens were learnt. The response of the mechanical components of the EJS when subjected to different cyclic loadings was also studied. As a result of these tests, essential modifications and development necessary to improve the test facility were identified.

#### 4.1.1 Performance Test on the Hydraulic Pump and Actuators.

Prior to starting any test with a specimen in place, the performance of the hydraulic pump and the stroke limitations of both actuators was checked. During a series of trial tests with zero loading, it was possible to obtain stroke movements up to  $\pm 1.0$  mm at a frequency of 10 Hz on both actuators simultaneously. At this stage the flexible hoses connected to the actuators started to oscillate at an unacceptable level, so any further increase in amplitude was not explored. In the tests, the 40 l/min. pump option (125 l/min was also available) was used. In effect, a total "peak to peak" stroke of 2 mm for two actuators was achieved and this was almost equivalent to the Dartec's specifications of 5 mm at zero load for one actuator fitted with a 38 l/min valve. This was satisfactory as the EJS was designed to a specification of  $\pm 0.5$  mm tray movement at 10 Hz.

#### 4.1.2 Coupling of the Horizontal Actuator.

A coupling was required to link the horizontal actuator and the tray carrier before a test under load in this direction could be started. Details of the coupling are as shown in Figs. 4.1 & 4.2. This coupling had to be designed in such a way that it allowed three dimensional flexibility under the applied thrust of the actuator, otherwise, serious damage to the actuator and tray carrier bearing guides could occur as a result of misalignment. A

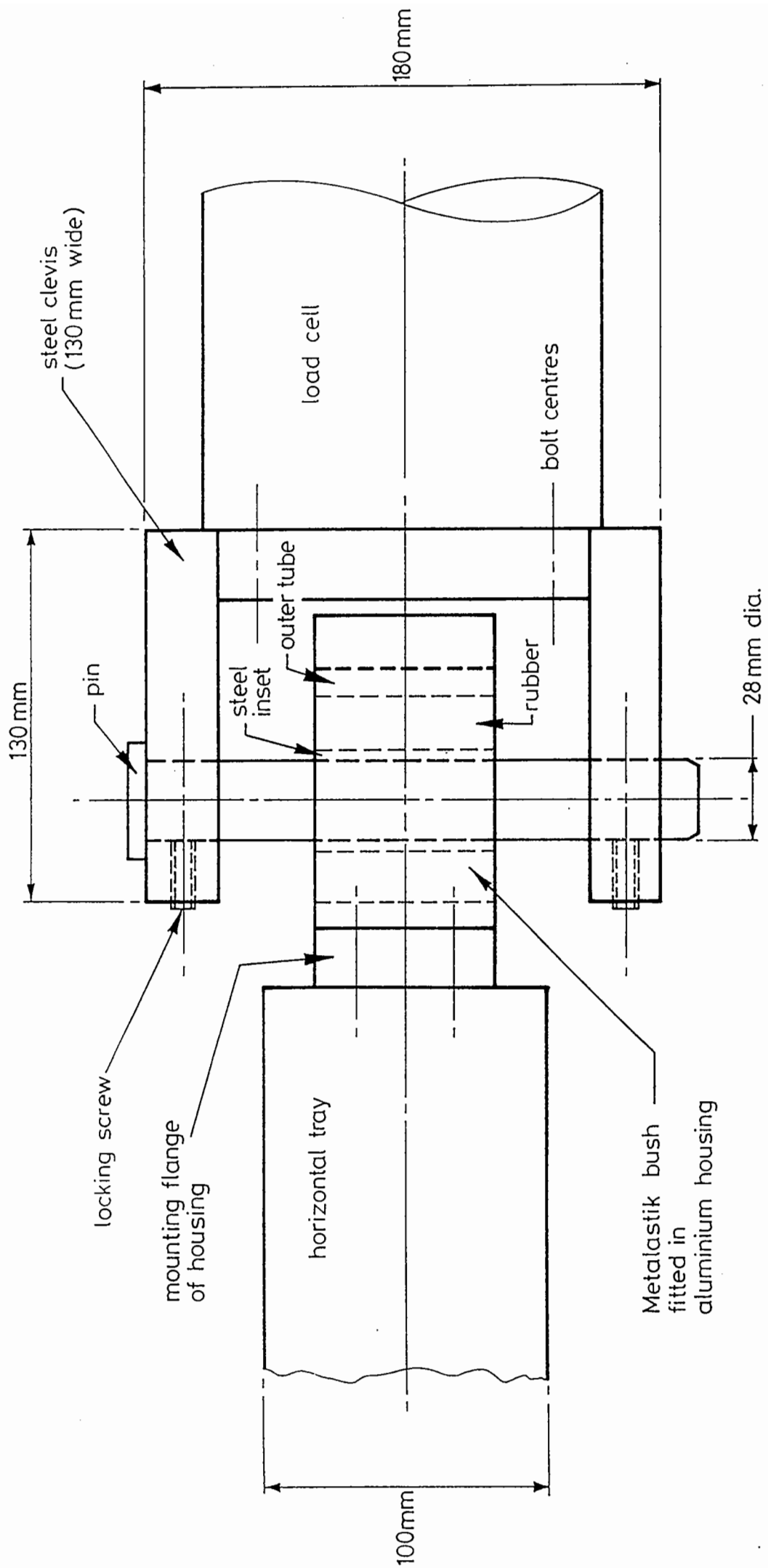


FIG.4.1 COUPLING BETWEEN ACTUATOR LOAD CELL AND HORIZONTAL TRAY

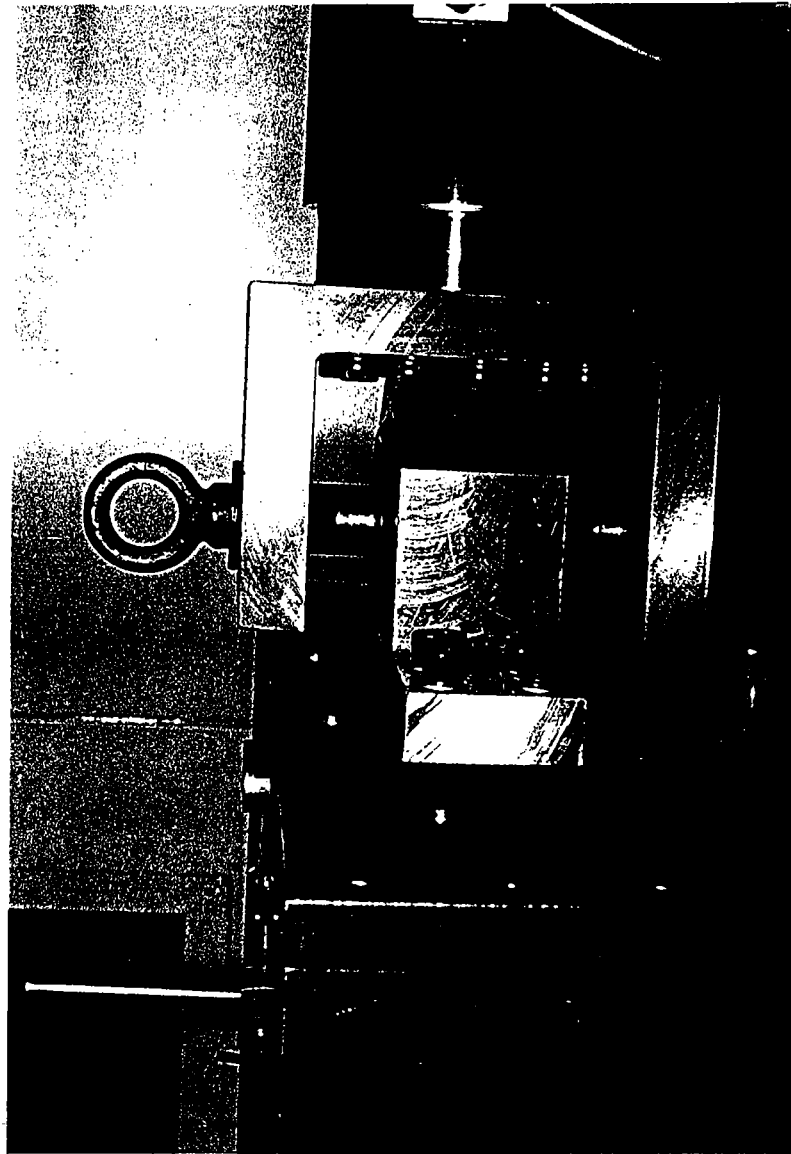


FIG. 4.2 THE HORIZONTAL COUPLING.

high load vibration isolating rubber bush produced by Metalastik was adapted. This consisted of a stiff rubber set around a hardened steel spherical insert which had a hole drilled through its centre. An aluminium housing was manufactured in the University workshop to accommodate the bush which was fixed in place with screws. The whole assembly was bolted to the end plate of the tray carrier and coupled with a "sliding fit" pin to a large steel clevis which was fixed to the actuator load cell. This arrangement allowed flexibility in all directions but remained most stiff at right angles to the pin. It provided a safe and effective way to transfer the horizontal thrust generated by the actuator to the specimen.

#### 4.1.3 Trial Tests with Joint Specimens.

In total, three joint specimens were used in these tests. Two of the specimens were buried joints made of a recycled 200 pen Dense Bitumen Macadam mix compacted into the inner trays. When the test on the second buried joint was finished, the existing DBM material was cut away for 250 mm on either side of the joint gap. Asphaltic plug joint material was then hot poured into the cavity in layers of about 20 mm thick. Preheated stones supplied by the manufacturer were compacted into each of these layers until the top of the asphaltic plug joint material was flush with the existing DBM surface. This third test specimen was also representative of an asphaltic plug joint.

All the commissioning tests were performed in the horizontal plane only and the main objectives of these trials were to:

- i) Investigate the response of the actuators and the mechanical components of the EJS when subjected to cyclic loading.
- ii) Establish a method of making specimens. This included mould handling and heating, material mixing and specimen compaction.
- iii) Investigate the effectiveness of ribs welded to the base of the inner trays as shear connectors to hold the test specimens.
- iv) Measure the amount of movement across the joint gap corresponding to a fixed value of the actuator stroke.
- v) Find the relationship between the strain in the joint material and the joint gap movement.
- vi) Establish a method to detect when and where the crack initiates.

Since the trial tests were mainly designed for the purposes of commissioning the EJS and improvement work on the machine was carried out continually throughout the test period, no complete set of test data was obtained. Detailed discussion on the test findings, major modification and development work on the equipment are reported in sections 4.2 to 4.6. Observations

resulting from the tests are briefly described as follows:

i) Excessive deflections of some mechanical components of the EJS were observed during the cyclic tests. Appropriate strengthening of the machine was carried out as described in section 4.2.1.

ii) The link across the inner trays was rigid enough to permit transportation of the specimen and the system of lowering the linked inner trays and fixing to the outer trays worked successfully. The ribs welded to the base of the inner trays worked effectively but the specimen tended to crack at the same line as the ribs. Modifications to improve the design of the mould are described in section 4.2.2.

iii) The compaction of the trial specimens was effected by using a vibrating hammer. However, this was not able to achieve an even and repeatable level of compaction and so it was decided to build a compaction rig incorporating hydraulic jacks to compact specimens by application of static pressure. Details of this rig are discussed in section 4.4.

iv) Due to the necessary compliance in the connection between the actuator and the outer tray, the movement across the joint gap was found to be different from the output stroke of the actuator and a fixed relationship between the two could not be established. Therefore, independent monitoring of the joint gap would be necessary.

v) The strains in the joint material measured during the trial tests were found to vary and depended on the position and time at which they were measured. In order to record these strain values accurately and with a time reference, better instrumentation and data collecting techniques were required and the details of this development are discussed in sections 4.5 & 4.6.

vi) Although there was no effective way to detect the initiation of a crack, there was a noticeable drop of tensile load in the joint material shortly before the specimen failed. It might be possible to detect the formation and position of a crack by monitoring the changes of the tensile load and material strain respectively. However, further investigation was required to confirm this.

## 4.2 MODIFICATIONS TO THE TEST FACILITIES.

### 4.2.1 The EJS.

During the cyclic loading tests of the EJS, the end of the horizontal actuator was seen to move up and down in response to the applied loads. This was traced to the opening and closing of the trough in the lathe bed and insufficient stiffness of the steel mounting bracket for the horizontal actuator. Two 20 mm thick steel plates were used to bridge the trough and three props, made of steel channel sections, were used to support the



overhanging body of the horizontal actuator and the end of the lathe bed. Extra steel plates were welded to strengthen the existing mounting bracket for the horizontal actuator. Further trial tests confirmed that these modifications all had the effect of reducing the end oscillation of the actuator.

When there was a gap between the end plates of the tray carriers and the inner trays, bending of the end plates on the tray carriers was observed due to the central loading of the coupling and the reaction against the rear vertical guides. The steel plates at the loading end were joined together with bolts to bridge the gaps. This eliminated the excessive bending on these plates. At the reaction end, extra bolts were used to stabilise the inner tray and the tray carriers.

The coupling of the horizontal actuator performed well during the trial tests. However, some "play" developed after several thousand load cycles at a frequency of 5 Hz. This was rectified by adding two screws to lock the fixing pin firmly in the hole of the clevis as shown in Fig. 4.1. Horizontal coupling to the actuator by means of a "sliding fit" pin required a very accurate alignment which was difficult to achieve. An alternative method was adapted which involved loosening the bolts, holding the bushing to the tray, fitting the pin and then retightening the bolts while monitoring the load. Overloading could be avoided by backing off the actuator using the manual remote control switches.

#### 4.2.2 The Mould

For the initial design of the mould (Figs. 3.4 & 3.5), 10 mm square steel ribs were welded across the base plates of the mould at 85 mm spacings. Due to stress concentration effects, the test specimen often failed with a crack formed across the slab in line with one of these ribs. To avoid this unnatural crack formation, it was decided to replace the original ribs with some shorter ones, 50 mm in length, and some randomly placed stubs.

All ribs and studs projected 10 mm above the top of the base plates. Figs. 4.3 & 4.4 show the details of the inner trays after the modifications. In order to provide a consistent effective slab thickness, two 10 mm thick metal plates were fixed to the base plates on either side of the joint gap. The steel plate also formed a debonding area where the ribs and studs were not required. The ends of the plates away from the joint were gently radiused to reduce any stress concentration in that region. When the 10 mm thick plates were in place, they provided a smooth area 420 mm long x 500 mm wide with the expansion gap as its centre line. Self adhesive aluminium tape was used to cover the plates and the joint gap to provide a realistic debonding surface which would match the in-service condition.

The length and height of the links were also increased from 505 mm and 45 mm to 1020 mm and 50 mm respectively. With the newly designed links in place, the overall depth of the mould

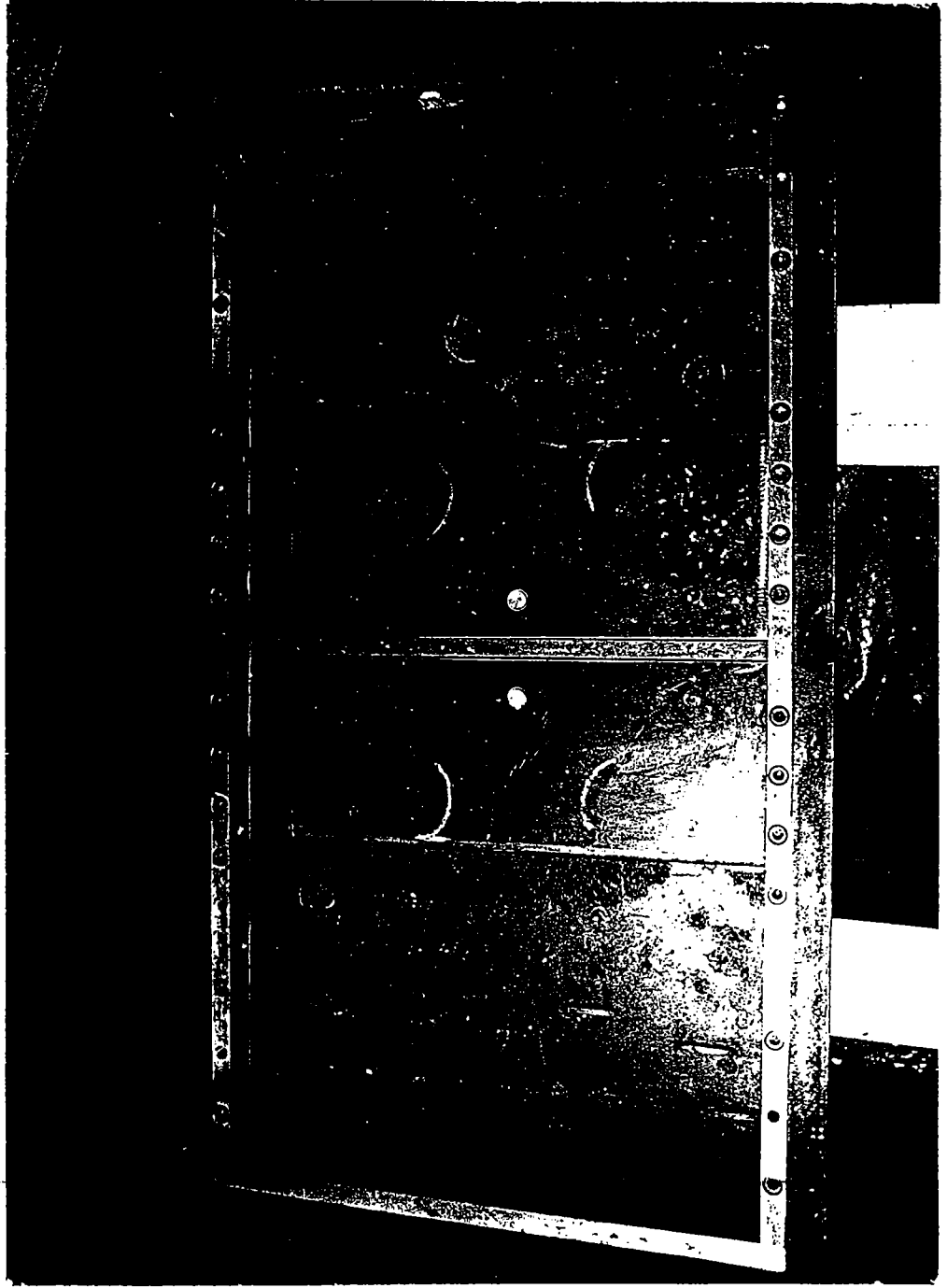


FIG. 4.3 DETAILS OF THE MODIFIED INNER TRAYS.  
(Plan)

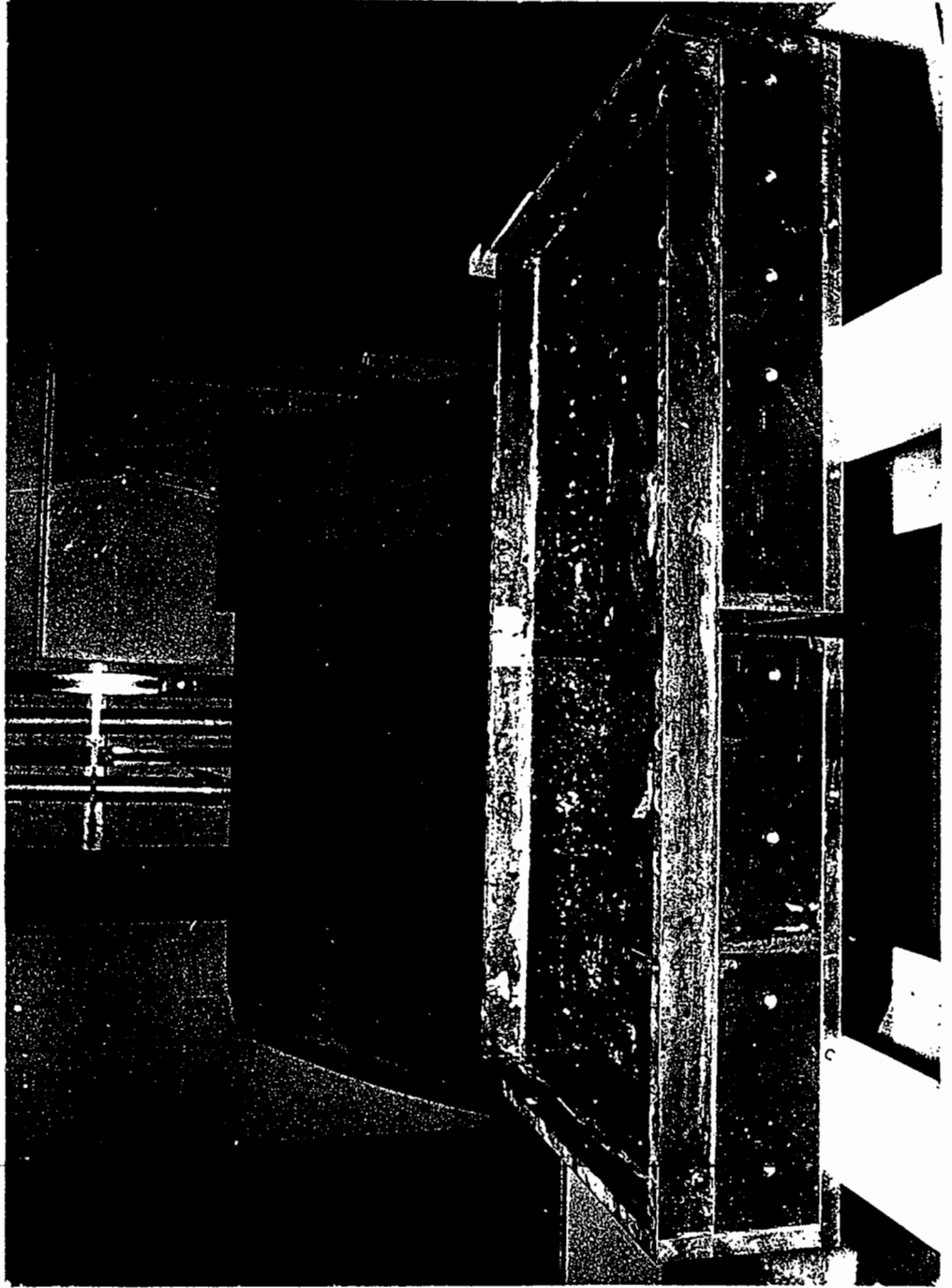


FIG. 4.4 SIDE VIEW OF THE MODIFIED INNER TRAYS.

became 150 mm, i.e. 50 mm greater than the original design. This provided sufficient depth to hold enough uncompacted bituminous mix to make a 100 mm thick specimen.

#### 4.3 IMPROVEMENT TO THE DARTEC SYSTEM.

##### 4.3.1 Monitoring of System Signals.

During the commissioning tests, the output signals from the built-in load cells and the stroke LVDT's were monitored through the monitor socket on the front panel of the actuator electronic units. The output at the socket is controlled by a five position switch and the signal for each position is described as follows:

1. Displacement signal from the built-in LVDT.
2. Built-in Load cell signal.
3. Servo-valve amp. input error signal.
4. Valves current (0.4V = 100 mA)
5. + 15 volts (30 V) supplies.

Such an arrangement allows only one output signal to be monitored at a time. Changing the channels involves turning the five position switch manually.

Based on the information given in the Dartec system manual, a 25-way Cannon socket was located at the rear of the al (Analogue to Digital) boards. This socket may be used to monitor analogue

signals from the system and for some other functions. Two monitor boxes were then made in the University and connected to the rear socket of the al boards. Each of these boxes provide two output and two input channels. The output channels allow the load cell and stroke LVDT signals from the actuators to be monitored simultaneously. and the input channels are for the feedback signals from external and extension devices. The function of these devices is discussed in the next section.

#### 4.3.2 Trip Facilities.

Although there was a Trip (v1) board installed in the control system of the EJS, it did not work initially and failed to cut off the hydraulic power supply when the system was tripped. This was because the control system was not connected to a Dartec pump and could not complete its test routine. An interface was built in the University to simulate the switching arrangements on a Dartec pump so that the trip facilities and safety routine could then be activated. Although the Trip board was only fitted in system A (the master), it was possible for system B (the slave) to share the trip available facilities. This could be done by connecting the load and stroke output signals from system B to the external and extension input channels of system A using the monitor boxes. In such an arrangement, the trip board responded to the load and stroke signals of the master system internally and the corresponding signals from the slave system externally. Because the input Extension channel on both systems were later

required for actuator control purpose (as discussed in section 6.2.3), they were not used for trip facilities. This trip sharing method worked well, but only provided limited trip facilities for system B.

Eight external input channels were also provided by the trip board. Trip actions could be initiated by external electronic signals fed through these inputs. An electronic signal of 5 - 24V represents a true state while a signal less than 1V indicates a false state. These inputs are scanned at 5 ms intervals, when one of the input signals is found to be not in the defined state, a selected trip action will be initiated. Since a 9500-VI Trip Interface Panel was not supplied, these facilities were not available initially. An interface was then made in the University and connected to the Trip board to provide these useful functions.

#### 4.3.3 New Annexe Attached to the Temperature Controlled Room.

Initially, the Dartec control system, together with the computer, were inside the temperature controlled room. It was planned to build a partition inside the room to separate the Dartec system from the test area. However, this would result in a cramped operating area in proximity to high pressure hoses. Due to practical and safety reasons, the original idea was abandoned. A small annexe was built against the main room to accommodate the control system. A 450 mm x 450 mm double glazed panel was fitted

to the insulated wall of the temperature controlled room inside the annexe. This allowed visual inspection of the specimen and the simulator when a test was in progress. Thus, the Dartec control system could be operated from the annexe in a normal room temperature environment. Fig. 4.5 shows the Dartec 9500 system inside the annexe. A new electricity supply circuit was also fixed in the annexe of the Dartec 9500 system. The quality of the power supply was enhanced by using a transient and filter socket unit which protected the Dartec system and other electronic equipment from electrical surges.

#### 4.4 NEWLY DEVELOPED COMPACTION RIG.

An accurate comparison between test results is only possible if all specimens used in the tests are of the same quality. Therefore, it is important that specimens are manufactured using repeatable procedures and in particular compaction should be well controlled. The main parameters which affect the fatigue resistance of the test specimen are the binder type and content, together with the void content of the mix after compaction. The compactability of the mix is affected also by aggregate type. If the materials are obtained from the same source every time and the mix compositions kept constant, the only remaining variable is the void content. This is highly dependent on the degree of compaction and the temperature of the mix when it is compacted. The temperature is important as during compaction the bitumen used in the mix works as a lubricant between aggregate particles





FIG. 4.5 DARTEC CONTROL SYSTEM.

to facilitate the packing process. The effectiveness of this lubricant is highly dependent on its viscosity which, in turn, depends on temperature. If the degree of compaction and the temperature of the mix could be controlled properly each time a specimen was made, the void content of the finished specimen would not vary significantly.

The specimens used in the trial tests were compacted with a vibrating hammer. After the hot mix had been placed in the mould, the hammer, with a 110 mm x 110 mm compaction foot was used to apply short bursts of vibration evenly to the specimen at overlapping locations. Then a piece of 200 mm x 300 mm marine plywood was placed between the vibrating hammer and the top of the specimen to provide additional compaction and a level surface finish. The plywood was then moved to the next section of the specimen and the compaction process repeated until the whole specimen has been covered. Despite these efforts, the density measurements of the finished specimen were so low that this method of compaction was considered to be unsatisfactory.

On site, rollers of different types and capacities are used for compacting bituminous materials. The contact pressure produced by these rollers can be as high as 630 kPa. Due to the small size of the specimen, compaction with even the smallest roller would not be possible without carrying out time-consuming modifications to the mould. Furthermore, hiring a roller each time would be expensive due to the number of specimens required.

Instead, a compaction structure was built for a trial. Basically, it consisted of two steel frames which enclosed the mould. The hot mix was placed into the heated mould and covered with four 20 mm thick preheated metal plates. Four 20 t jacks were then positioned between two load spreading beams on top of the plates and the top members of the two frames as shown in Fig. 4.6. It was estimated that only two-thirds of the jack capacity would be utilised to produce the required level of pressure. The resultant contact pressure exerted on the specimen was estimated to be 1050 kPa approximately. A high static contact pressure was necessary in order to simulate the high effective pressure produced dynamically by a roller. Compaction trials using the frame were carried out later in the project and their results are discussed in section 6.4.1.

#### 4.5 CHOICE OF MEASURING DEVICES AND INSTRUMENTATION.

##### 4.5.1 Introduction.

It is always important to decide which measurements should be taken and what measuring instruments should be used during a laboratory experiment, particularly when a new facility has been developed and specimen behaviour is somewhat unknown. Primary measurements taken during investigations on in-service bridge deck expansion joints often include the amount of movement across the joint gap, the magnitude and frequencies of the traffic loading and the temperature. Similar measurements need to be

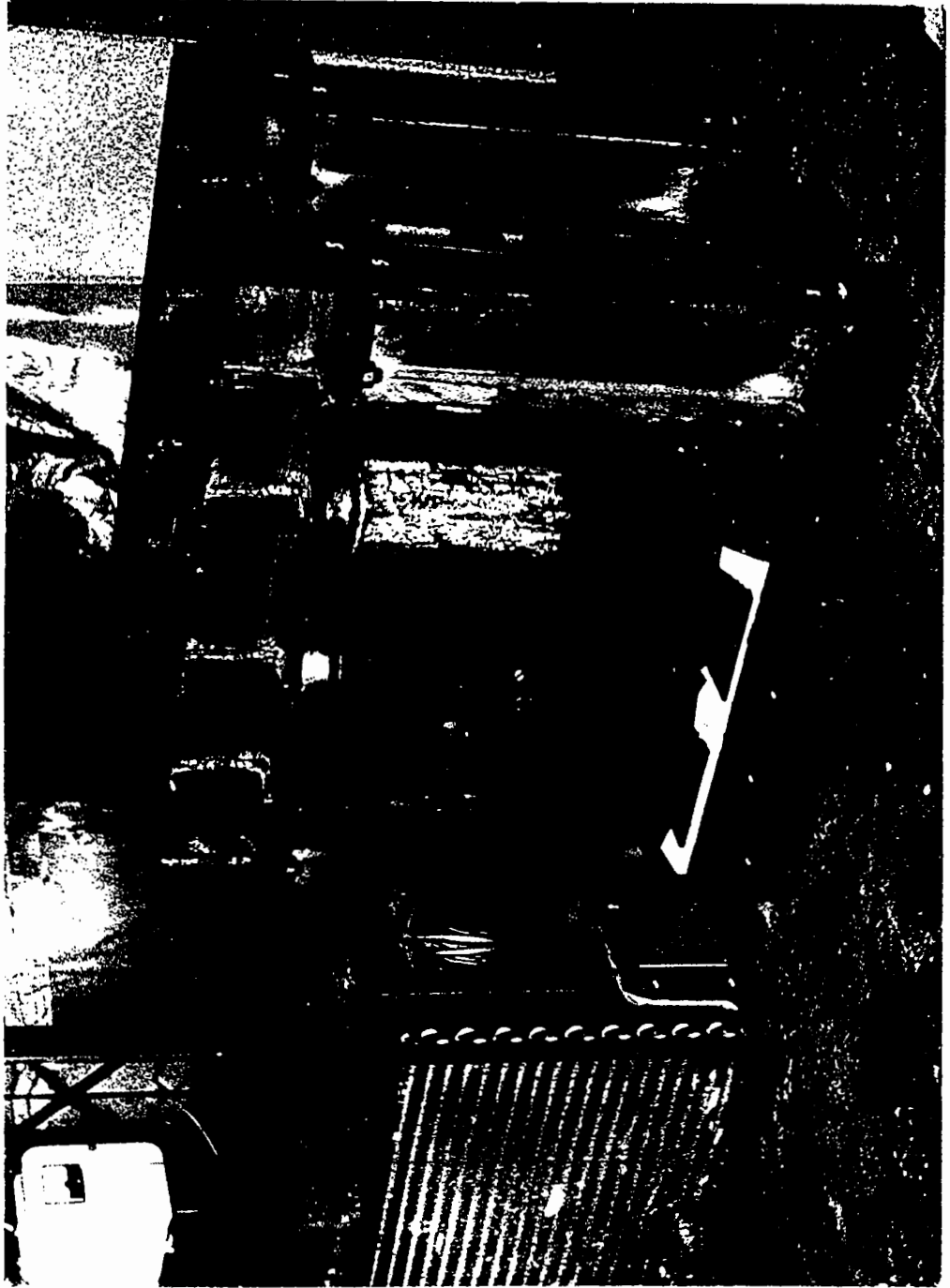


FIG. 4.6 COMPACTION OF SPECIMEN USING  
STEEL FRAMES AND JACKS.

taken during the laboratory tests for possible comparison with data obtained on site at a later stage. In addition, strains in the joint material should be measured at different positions across the joint gap. Strain measurements are important because it is known that the fatigue resistance of a bituminous material mainly depends on the level of cyclic strain which the material experiences (Pell 1973). The measurement of the distribution of strains in the joint material may help to identify the critical region at which cracks first occur.

There are many types of measuring instruments which can be used to measure displacements. The instruments used for the cyclic tests of the project, must have a flat frequency response up to 10 Hz. and be capable of measuring small movements accurately. They should be relatively inexpensive, reliable and durable and, once set up and connected to data recording equipment, no further adjustment should be required. Preferably, the maximum outputs from the instruments should be  $\pm 10V$  in order to be compatible with the Dartec system.

#### 4.5.2 Instruments for Measuring Displacements.

Displacements and strains can be measured using LVDT's (Linear Variable Differential Transformer), strain gauges, Demec gauges and inductance strain coils. The following were used during trial tests and their suitability for this research project is discussed.

(a) Demec Gauge.

In the early stage of the trial tests, demec pips were fixed on the top surface of the specimens. Displacements between each pair of pips could be measured using a demec gauge when required. Although this method of measurement is relatively simple, it is less accurate and can only be operated manually. The demec gauge was therefore only used as an inexpensive tool to study the distribution of material strains on the surface of the specimens and so help to design a suitable method of instrumentation. There was no intention to use this instrument for any major tests.

(b) Strain Coils

Strain coils have been used widely by different researchers (Brown 1978, Brown and Brodrick 1973, Selig 1974 and Paterson 1972.). They are used in pairs which consist of an excited, or "driven" coil, and a "pick-up" coil. When in operation, the coils are connected to a Bison instrument which has a power supply, oscillator, amplitude and phase balance controls, amplifier and calibration functions built in (Bison Instruction Manual).

Although strain coils were relatively inexpensive and easily installed, certain disadvantages became apparent when used on a test specimen. The Bison instrument could only monitor one pair

of coils at a time. When several pairs of strain coils were required, they needed to be scanned in turn as pairs and balanced using the phase and amplitude control manually, all of which was time consuming. The Bison instrument could be modified to include an automatic balance facility but this would increase the cost of the instrument. Furthermore, the speed of data capture for a few pairs of coils was unacceptably slow and the steel mould used to house the test specimen would cause interference to the electro-magnetic field generated around the coil and affect the instrument calibration. The amount of background noise compared with the small magnitude of the measured output signal during the trials proved to be too large. As a result, it was decided not to use strain coils.

(c) LVDT (Linear Variable Differential Transformer)

There are two types of LVDT's namely, the AC LVDT and the DC LVDT. Unlike the AC LVDT, the DC LVDT has the oscillator and the demodulator built inside the body of the transducer. the DC LVDT transducers are simple to use and cheaper to buy. Due to its low current consumption, the DC LVDT can be used in remote situations by using a battery. However, the signal generated by the DC LVDT is less stable and often drifts from its zero position. The AC LVDT transducer gives a higher order of accuracy and linearity. It has a better response to high frequency armature movements and operates over a wider temperature range which is essential for the test applications envisaged. It was, therefore, decided to use the AC LVDT transducers for displacement measurements for the

bridge joint testing programmes.

#### 4.5.3 Instrumentation of the Specimens.

In the later stage of the trial tests, demec pips were replaced by some specially made metal studs. On the top surface of each specimen, six studs were fixed along the longitudinal centre line of the specimen with a distance of 100 mm between each pair of studs. An LVDT was mounted on a pair of the studs to measure the strain in the material. It was necessary to move the LVDT to different positions each time if strain measurements at various positions were required. The movement across the joint gap on both sides of the specimen was measured by a pair of LVDT's (G1 & G2, Fig. 4.7). Load applied to the specimen and the stroke of the Dartec actuator were measured with the "built-in" load cell and displacement LVDT respectively. A thermocouple was installed to measure the temperature inside the specimen near the joint gap. An oscilloscope monitored the waveforms and amplitudes of any two outputs of these instruments and a record of the results was obtained with a u.v. recorder.

Based on the experience gained from the trial tests, some modifications to the instrumentation were found to be necessary. Fig. 4.7 shows the final version of the instrumentation for test specimens.



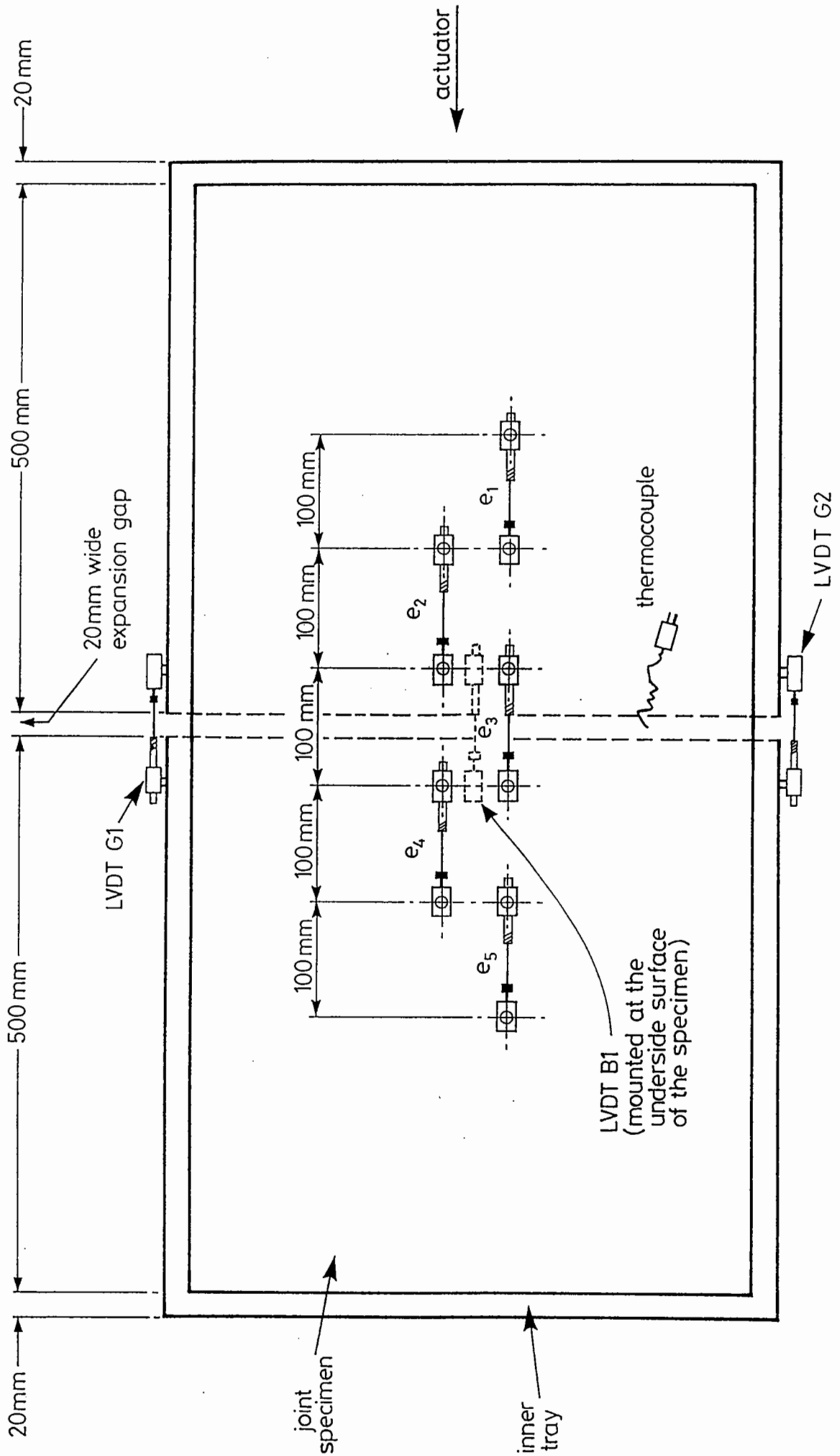


FIG. 4.7 PLAN : INSTRUMENTATION OF THE SPECIMEN

Instead of one LVDT, five LVDT's (e1 to e5) were fixed permanently on the top of the specimen. Later in the research it was decided to fix another LVDT (B1) at the underside surface of some selected specimens across the joint gap. This arrangement allowed the strain of the joint material at different positions to be measured simultaneously. In order to avoid distortion in measurement, the gap LVDT's (G1 & G2) were relocated to positions which were coincident with the line of action of the horizontal actuator. LVDT's of different measuring ranges were used for strain and gap measurements in order to optimise the resolution of the output signals. In total, there were nine different output signals needed to be monitored namely, 5 LVDT's for material strains, 2 LVDT's for joint gap movements, 1 LVDT for actuator stroke and 1 from the built-in load cell of the horizontal actuator.

Although the u.v. recorder could accommodate 12 input channels and print out data for each channel whenever necessary, it was found to be tedious to use and relied heavily on manual supervision. It was possible to connect the u.v. recorder to a time clock control so that a print-out could be produced automatically at pre-set intervals but this was considered to be unreliable, especially when the input signals were beyond the width of the recorder paper. Identifying each individual signal was difficult if overlapping of traces occurred. The output of the u.v. recorder was a trace on paper and had to be measured with a scale rule, followed by a calculation to convert this data into real values. All the converted data then had to be entered

manually into a computer before the results could be analysed. In conclusion, the instrumentation developed in the trial tests were found to work satisfactorily but the data acquisition system needed to be computerised so that tests and data collection could be carried out with greater accuracy and minimum manual supervision.

#### 4.6 DEVELOPMENT OF THE DATA ACQUISITION SYSTEM.

##### 4.6.1 Introduction.

In order to remain within the estimated costs when the simulator was built, a data acquisition facility was not included in the Dartec system. All the measuring instruments used during the preliminary tests were only available for a short time. It was therefore necessary to apply for additional funding to purchase a suitable data acquisition system.

As discussed in section 4.5.3, use of a computerised data acquisition was recommended for this research project. The computer controlled data acquisition systems available on the market are divided into two types namely, "External Bus" and "Internal Bus" systems. Fig. 4.8 shows a schematic diagram of these two types of systems. In the external bus system, the data acquisition unit is connected to the computer via a standard interface, such as RS 232 and IEEE-488, while the latter is

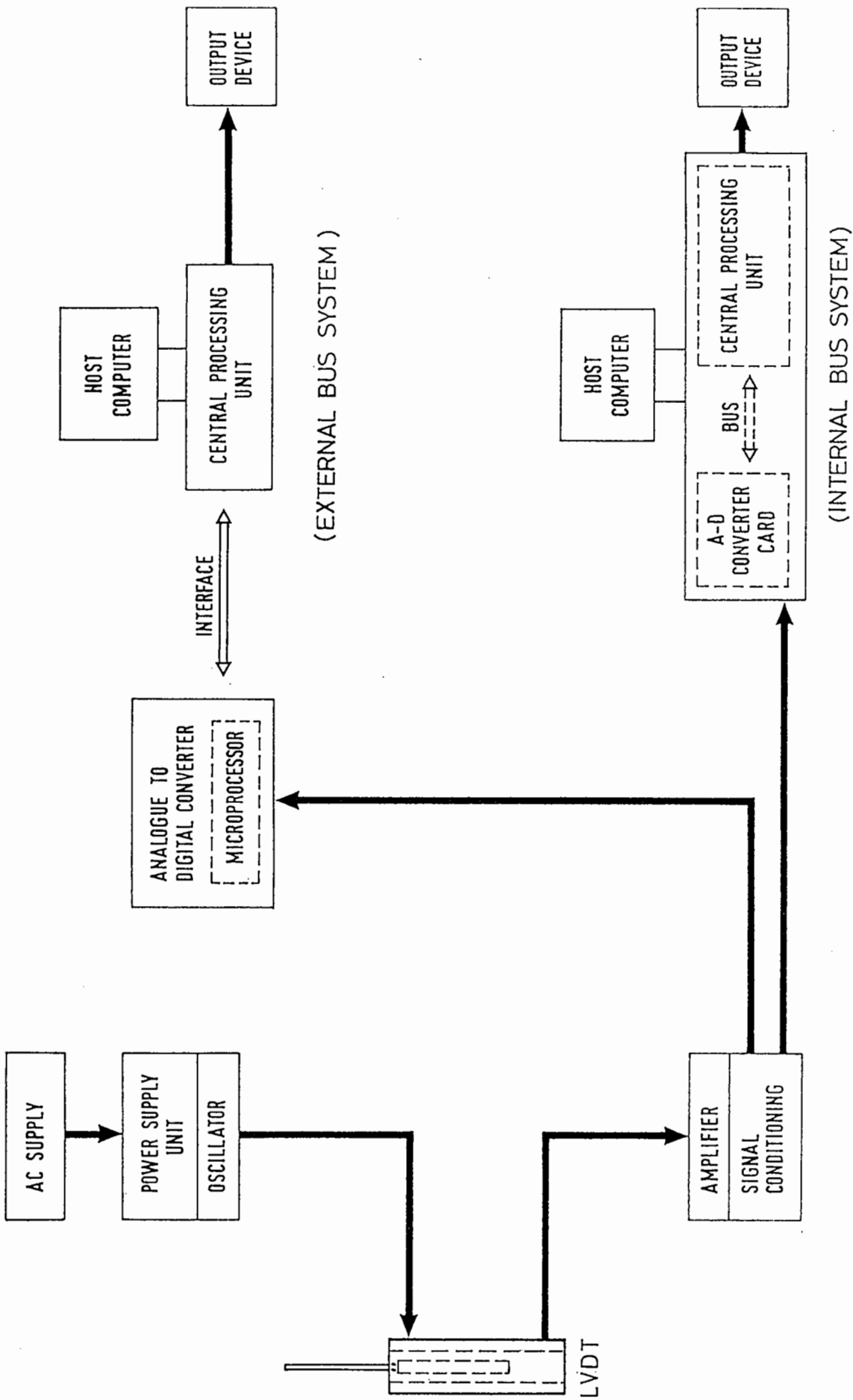


FIG.4.8 SCHEMATIC DIAGRAM OF TWO TYPES OF  
COMPUTERISED DATA ACQUISITION SYSTEMS

connected directly to the computer through an internal I/O (input and output) bus.

Each system has its own advantages which is discussed in the following:

a) External Bus System.

The Data acquisition unit of this type of system has its own internal microprocessor, power supply unit and other essential hardware. These components are housed in a single box which is independent of its host computer. Such a configuration allows the system to be operated far away from the computer and so facilitate the construction of a network of data acquisition sub-systems. Data from separate sub-systems can be interconnected via the interface and monitored by a single host computer. This type of system is extremely flexible, a system of any size can be built and alterations can be made when required.

b) Internal Bus System.

The data acquisition unit in this type of system is normally built in a form of a card which consists of all the electronic components required. This card can be directly plugged into one of the I/O ports available inside the host computer. Elimination of the relatively slow communication via an external interface results in high speed data collection. The data acquisition unit does not require its own power supply or a

separate enclosure. However, the size of these systems depends on the number of I/O ports available in the host computer.

Since the test facilities were still under development, it was unwise to fix the final configuration of the data acquisition system at that stage. Therefore, the "External Bus" system was chosen for its flexibility. There were a wide range of external bus systems produced by different manufacturers. However, the choice of many products were eliminated quickly based on the technical information given by the suppliers. A detailed investigation of two possible systems was then carried out and they are described in the following sections:

#### 4.6.2 Dartec Data Processing Boards and Software

Data acquisition can be carried out by a Dartec system with a data processing board 9500-el installed. A detailed description of the data processing board 9500-el is given in appendix A. An obvious advantage of using the 9500-el board is that it does not require an extra computer and all the data information acquired can be used by other boards of the Dartec 9500 system without modification or communication problems. Standard software for data collection could be bought "off-the -shelf" whenever necessary. However, only four channels were available for each board; load, stroke, extension and external. The load and stroke input ports are assigned for use by the built-in LVDT and load cell of the Dartec actuators respectively. This leaves only two

channels on each board for external inputs, i.e. four available inputs for a two channel system as used in this project. Two of these are occupied when the load cell signal from system B (Horizontal actuator control) is channelled to system A (vertical actuator control) for activation of trip facilities as described in section 4.3.2. Hence, this would only leave two free inputs which would be insufficient for the number of instruments on the specimen.

Further discussion with Dartec engineers confirmed that the 9500-el boards could not provide an adequate data acquisition system for the purposes of this project.

#### 4.6.3 Independent Data Acquisition System

Figs. 4.9 & 4.10 show the details of the data acquisition system developed for the project. It consisted of an IBM compatible micro computer, an A-D convertor and a D-A convertor, which were products of CIL Microsystem Ltd. An IEEE interface card completed the link between the convertor units and the computer. A matrix printer was used for data print out.

The computer used was an Amstrad PC 1512 with a 20 Mb hard disc and a single 360 k floppy disc drive. The A-D unit had 16 channels with  $\pm 15$  bit resolution and data acquisition firmware built in. The input signals ranged from  $\pm 100\text{mv}$  to  $\pm 10\text{ v}$ . The D-A convertor had 8 channels with  $\pm 15$  bit resolution and



FIG. 4.9 DATA ACQUISITION SYSTEM.



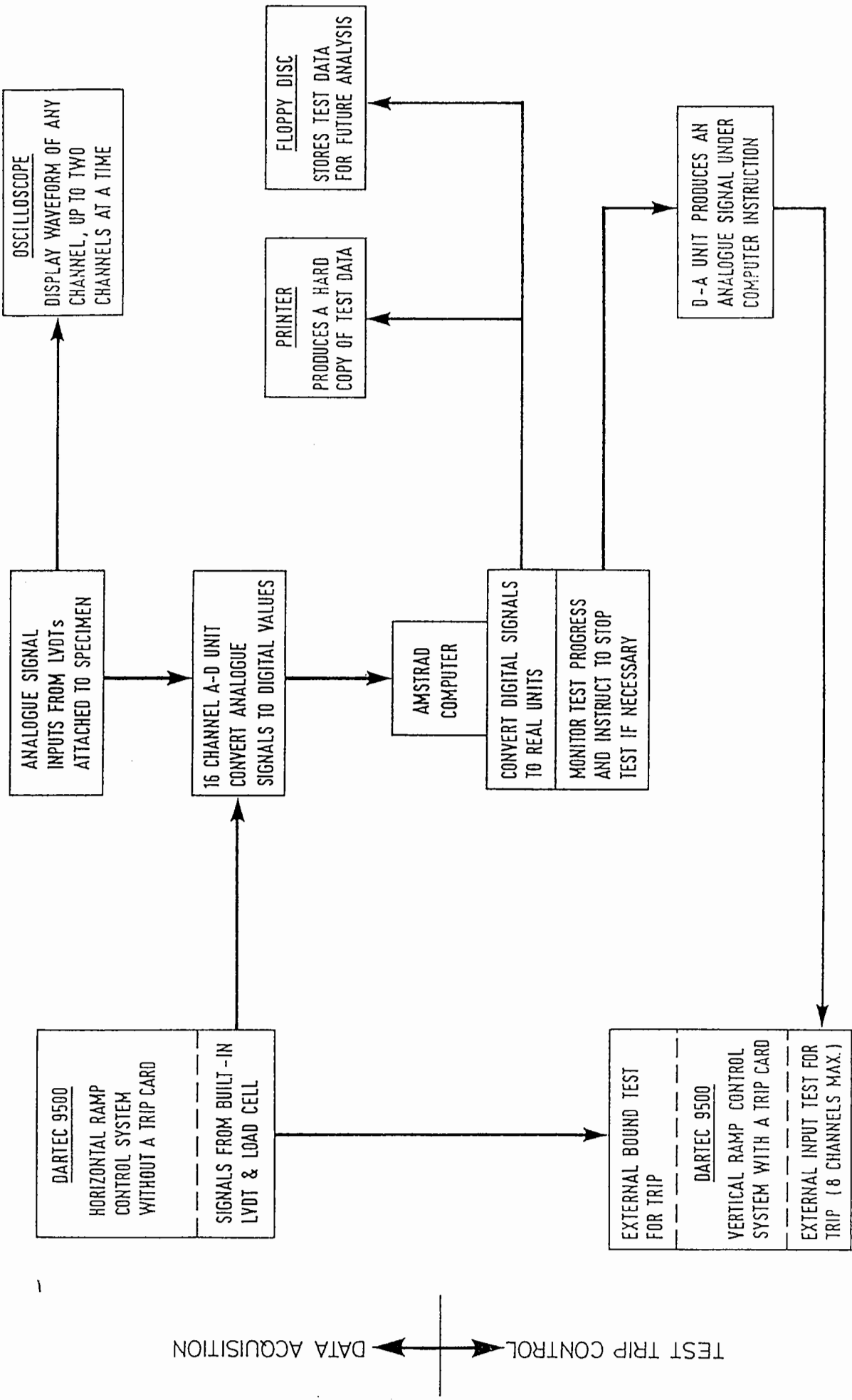


FIG. 4.10 SCHEMATIC DIAGRAM OF COMPUTER DATA ACQUISITION SYSTEM.

waveform generation firmware. The IEEE interface was specially designed for IBM compatible computers with required firmware built into the interface for data acquisition purposes. The interface card was plugged directly into an I/O slot inside the PC 1512 computer.

As mentioned in section 4.5.3, nine different instruments were required to be monitored during the laboratory trial tests. These included the built-in load cell and stroke LVDT of the horizontal actuator, the 5 LVDT's mounted on the top surface of the specimen to measure the strains in the joint material at different positions, and the 2 LVDT's mounted across the joint gap.

In application, the analogue signals from these instruments, except the stroke LVDT which was monitored with an oscilloscope, were fed into the memory of the A-D convertor. The unit then converted these analogue signals into digital values and passed the information to the computer memory. At this stage, the memory of the A-D unit was clear and ready for the next round of data acquisition. Due to the limited storage capacity of the A-D unit, data was acquired for 2 channels at a time, so four rounds of data collection were necessary for the 8 channels.

After all the data from the 8 instruments had been received, the computer started to analyse the data and calculated the maximum tensile and compressive loads, peak to peak movements measured by the LVDT's and the strain of the material near the joint gap

under the specimen. The calculated results were then stored in a floppy disc for future use. A print-out of the results was also produced in real time by using the matrix printer. The same process was repeated at 10-min intervals. During the 10 min gap, the system was used to monitor the load and the movement in the material near the joint gap. If the tensile loading decreased to a predetermined limit, which indicated the possible presence of a crack, the computer would instruct the D-A unit to send an analogue signal to the Trip Board of the Dartec System to stop the test.

After a test was finished, the data stored in the floppy disc could be analysed using standard commercial computer software. Further calculation, analysis and curve plotting of the test results could then be done by the computer without difficulty. Hard copies of the analysed results could either be printed or plotted by a matrix printer or a graphic plotter respectively.

Computer software for CIL's Data Acquisition System used in the project was developed by the author. A flow chart which shows the details of the program is presented in Fig. 4.11. Since the software was developed in the University, there was no difficulty in understanding the structure of the program, so modifications could always be done to suit the configurations of the instrumentation used in different tests. In fact, the system could even be used with other test equipment, such as the axial load elastic stiffness testing facility, standard creep test apparatus, four-point bending facility and so on. The system has

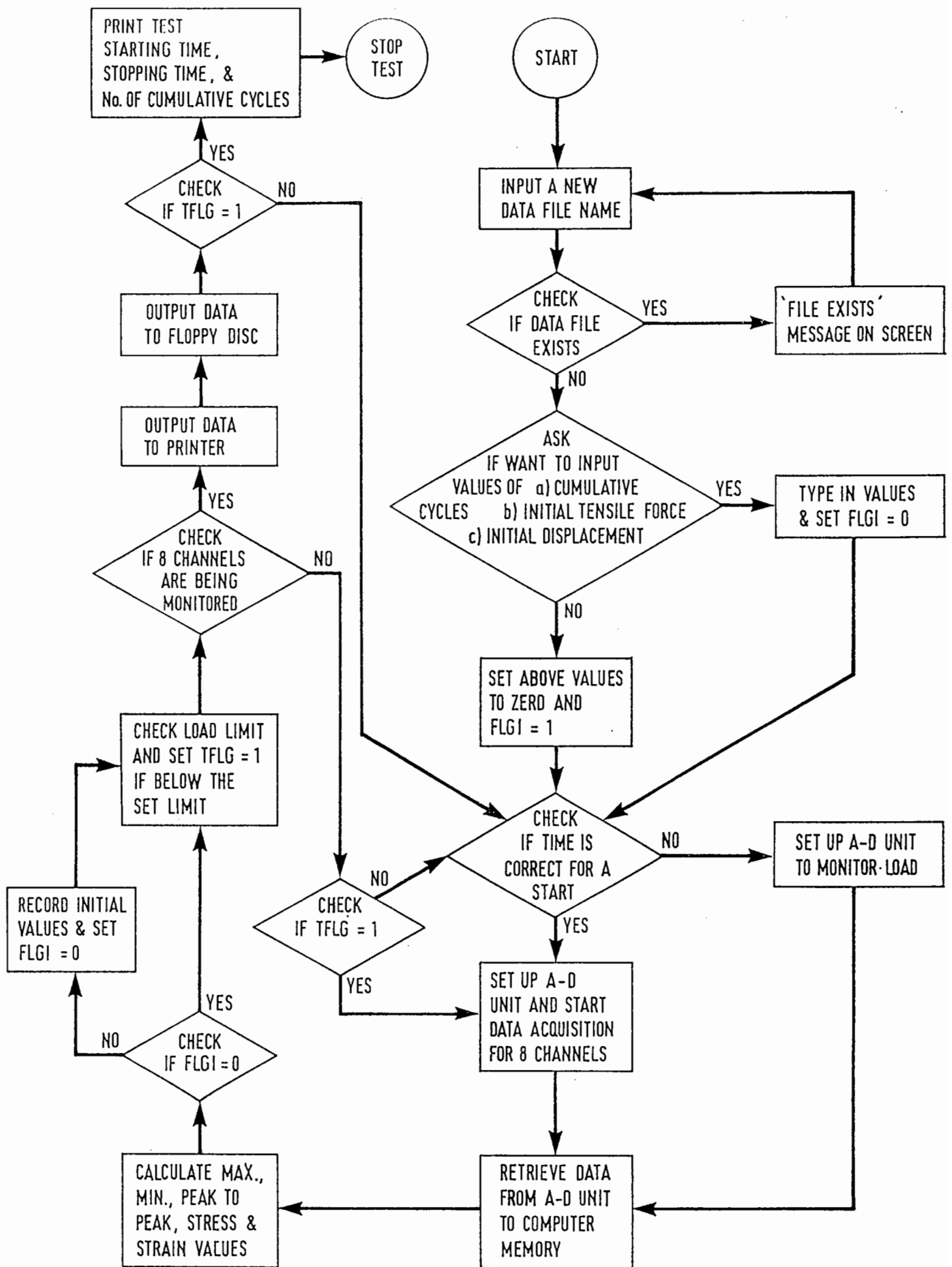


FIG. 4.11 FLOW CHART FOR THE COMPUTER DATA ACQUISITION SOFTWARE.

been used for a considerable period and has proved to be very reliable and flexible.



## CHAPTER FIVE

### FORMULATION OF TEST PROGRAMMES

#### 5.1. INTRODUCTION.

Although the primary objective of this research project was to develop a laboratory facility for testing bridge deck expansion joints, it was decided that tests on joint specimens should be conducted in parallel with the machine development. These laboratory tests could be used as a tool to obtain information on how bridge expansion joints behave when subjected to different types of deck movements. Based on the results of these tests, a simple mathematical model could then be developed for estimating the in-service lives of bridge deck expansion joints. Initially, the model would be relatively simple but its complexity could be increased as the research work continued. The reliability of the model could be verified by comparing the estimated joint lives with those obtained from site investigations on in-service joints.

The failure of bridge deck expansion joints is a complex problem as the actual causes of the failures are often not apparent. There are many factors which can affect the in-service performance of a bridge deck expansion joint, such as the design

of the joint, the material used, workmanship and deck movements. The performance of a joint system often depends on the interaction or the combined effects of these factors. It would have been extremely difficult to quantify all these effects within the time scale of the present project.

In preparing the strategy for conducting the research work, different approaches were considered. It was possible to concentrate all the attention on certain specific expansion joints and on a limited number of in-service bridge structures and study them with a series of site investigations and laboratory tests. The test parameters used, such as loading and joint gap movements, could be the exact duplicates of those measured on the structures. However, such an approach would only provide a better understanding on these specially selected joints when working under certain specific in-service conditions. It would not produce a long-term solution for general bridge deck expansion joint problems. It was decided that longer term objectives should be considered with a view to obtaining a proper understanding of the mechanics involving bridge joint failures.

## 5.2. TEST METHODS.

### 5.2.1 Methods of Accelerating Test Rate.

Bridge engineers are increasingly concerned about the accuracy of



expansion joint manufacturers' claims on the performance of their products. They would like to see a laboratory test method developed to provide objective evidence that the products will perform as claimed. Endurance testing of bridge deck expansion joints is only useful if the test can be carried out at an accelerated rate and to furnish feedback to the engineers and manufacturers in a relative short period of time.

Generally, a fatigue test can be speeded up by applying a load with a frequency which is higher than that which occurs in the service condition (Yurkowsky et al 1967 (a) & (b) and Yurkowsky and Fulton 1972).

The load frequency can be increased in two ways:

- i) Reduce the time duration of the applied load, i.e. shorten the loading time.
- ii) Reduce the time duration between each application of load, i.e. reduce or eliminate the rest periods between loads.

In the test programmes carried out, the first method was used in the tests associated with long-term (thermal) movements while both procedures were adopted for short-term traffic induced movements tests.

The testing time can also be reduced by increasing the magnitude of the applied load to cause a similar amount of damage to the

specimen in a shorter period of time. However, it is generally accepted that the relationship between stress and fatigue life is governed by a power law with an exponent between three and six (Eyre et al 1984). Such a power law must, therefore, be reasonably well established for this to be a successful method for accelerating the test.

### 5.2.2 Test Control Mode.

In conventional fatigue tests, specimens with simple shapes can be tested under controlled stress or controlled strain conditions. Due to the structural details of bridge deck expansion joints, the distribution of stress and strain in the joint materials varies both with their location and the time at which measurements are made. Therefore, it is difficult to define an appropriate reference point to monitor the applied stress or strain either on site or in the laboratory. However, the gap movements across a joint, due to traffic and temperature variations, are relatively easy to predict and measure during the periods of design and in service respectively (British Standards Institution 1980). When a specimen, which is a realistic reproduction of a working joint, is tested with a controlled gap movement, the distribution of stress and strain within the specimen will automatically be a good match to that of an in-service joint. Therefore, instead of stress or strain control, it was decided that the laboratory tests on joint specimens with the EJS would be monitored and controlled by gap movements.

### 5.2.3 Suitable Types of Accelerated Test Methods.

#### i) Constant gap movement testing.

Joint tests can be carried out by using a constant magnitude of gap movement applied at an accelerated rate. When two tests are carried out, one with an accelerated gap movement and the other at a normal rate gap movement and the results compared, a shift factor can be derived to account for the effects of rest periods. This can be used to convert the life estimates of a joint obtained from accelerated tests to the life expectancy of a similar joint when tested with gap movements applied at in-service rates. The combined effects of other working conditions, such as installation conditions and in service weathering, may also be included in this factor if appropriate. A single factor could be used for data points when similar joints are tested with different magnitudes of gap movements.

#### ii) Step gap movement testing.

Joint failure may take an excessively long time to develop when a specimen is tested with a small gap movement. In order to finish a test within a reasonable period of time, a step gap movement testing technique can be applied. A test can be started with a small gap movement as required and, at the end of a fixed number of cycles, or period of time, the gap movement can be

stepped up to a pre-determined higher level and the test continued until failure. If the life expectancy of an intact specimen, when tested with the larger gap movement, is known, the life of the similar joint, when tested solely with the smaller gap movement, can be estimated using Miner's rule as illustrated in section 7.3.3.

### 5.3 TEST SPECIMEN.

#### 5.3.1 Choice of the Joint Type for Testing.

The type of bridge deck expansion joint under investigation in the present project is the "buried joint". Buried joints have been used in the U.K. for a long time and are favoured by many of the engineers consulted (Jones 1982). Buried joints are easy to construct and have been extensively used on short span bridges. Since it allows a continuous surfacing to be laid, it provides a high riding quality. Due to their popularity in the past, there are a great number of them still in service. Buried joints generally perform satisfactorily on concrete structures. However, premature failures are observed when used on composite constructions where traffic induced movements and rotations are large. Reports on their performance have indicated variability in the degree of success or failure (Price 1982 & 1984), the reasons for which are not properly understood. The present laboratory tests on buried joints were carried out in an attempt to develop a better understanding of these problems. The test data

collected could also be used for comparison with the results obtained from investigations on site.

### 5.3.2 Details of Buried Joint and Test Specimen

A typical buried joint is a complicated laminated structure as shown in Fig. 1.4. Basically, buried joints consist of two asphaltic layers, basecourse and wearing course, laid continuously over a bridge deck and the joints. The layers are normally constructed using the same materials as those for the surfacing of a road. The materials are either HRA (Hot Rolled Asphalt) or DBM (Dense Bitumen Macadam). Although DBM has a better deformation resistance to heavy traffic, HRA gives a longer fatigue life which is more important to the performance of expansion joints. In order to spread high strain, which can be concentrated at the joint gap, a 400 mm to 500 mm wide debonding layer is provided along the underside of the basecourse. This debonding layer is placed across the joint with the gap as its centre line. Waterproofing over the joint and the rest of the bridge deck is often overlapped in order to maintain its continuity. A strip of expanded metal reinforcement is sometimes included in the basecourse above the joint to increase the spalling resistance of the material.

It is important to ensure that specimens used in the tests are representative of an in-service buried joint. A cross-sectional detail of the test specimen, which represents a full length joint

with a reduced width, is shown in Fig. 5.1. Since deterioration of buried joints normally occurs within the surfacing layers of the deck, it was decided that some less important joint components, situated below the debonding layer, could be excluded in the detail of the specimen to facilitate manufacturing.

### 5.3.3 Mix Design

Because of its higher fatigue resistance, HRA (Hot Rolled Asphalt) was used for making the test specimens. Tables 5.1 and 5.2 of this report show the details of the mix compositions. The aggregate grading curves are shown in Figs. 5.2 and 5.3. Basecourse materials to BS 594 Part 1 1985 (British Standards Institution 1985) Table 2. column 4 and wearing course materials as detailed in Table 5. column 21 in the same standard were adopted. The porphyry aggregates used were from Bardon Hill and the 50 pen bitumen was supplied by Mobil.

### 5.4 SELECTION OF TEST PARAMETERS.

The factors which affect the performance of buried joints have been reported by the TRRL (Price 1982 & 1984) and are summarised as follows:-

#### 1. Materials and Joint Type

- a) Material and joint type used.

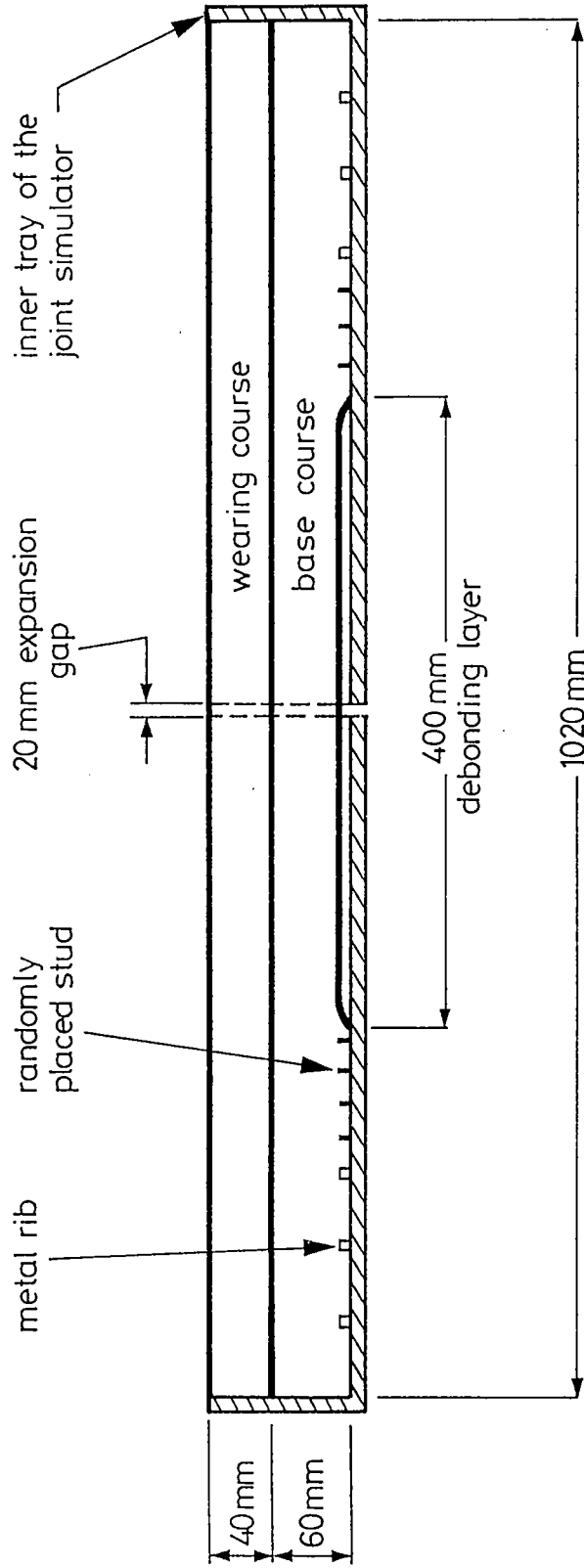


**FIG.5.1 LONGITUDINAL SECTION OF TEST SPECIMEN**

Table 5.1 Composition of basecourse mixture.

BS Test sieves	percentage by mass of total aggregate passing
28 mm	100
20 mm	90 - 100
14 mm	30 - 65
10 mm	-
6.3 mm	-
2.36 mm	30 - 40
600 $\mu$ m	10 - 44
212 $\mu$ m	3 - 25
75 $\mu$ m	2 - 8

- 1 Grade of binder: 50 pen
- 2 Binder content: 5.7%
- 3 Nominal thickness of layer: 45 mm - 80 mm



Table 5.2 Composition of recipe type F wearing course mixture.

BS test sieves	percentage by mass of total aggregate passing
28mm	-
20mm	100
14mm	85 - 100
10mm	60 - 90
6.3mm	-
2.36mm	60 - 72
600 $\mu$ m	45 - 72
212 $\mu$ m	15 - 50
75 $\mu$ m	8 - 12

- 1 Grade of binder: 50 pen
- 2 Binder content: 7.8%
- 3 Nominal thickness of layer: 40mm

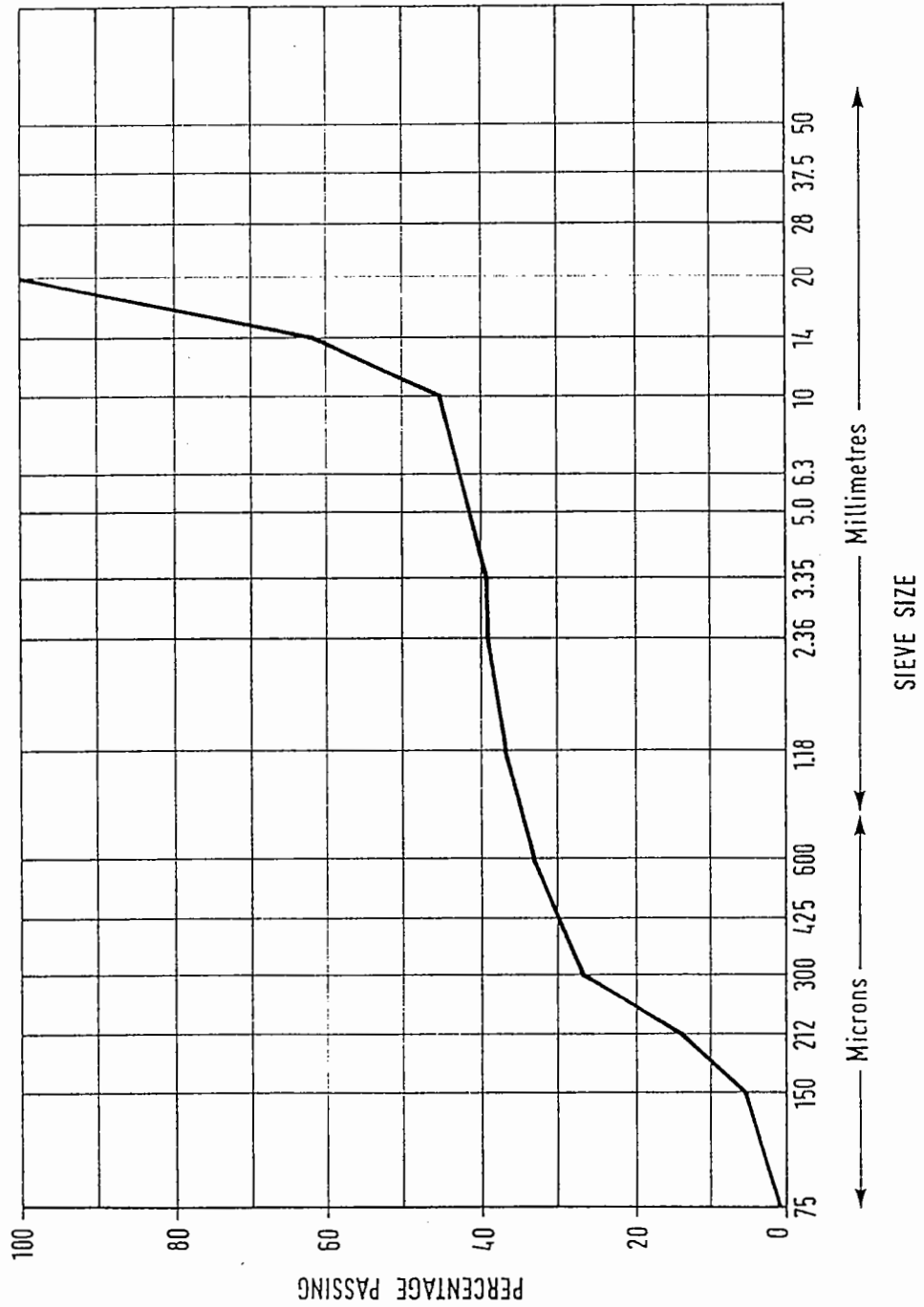


FIG. 5.2 GRADING CURVE OF HOT ROLLED ASPHALT BASE COURSE.

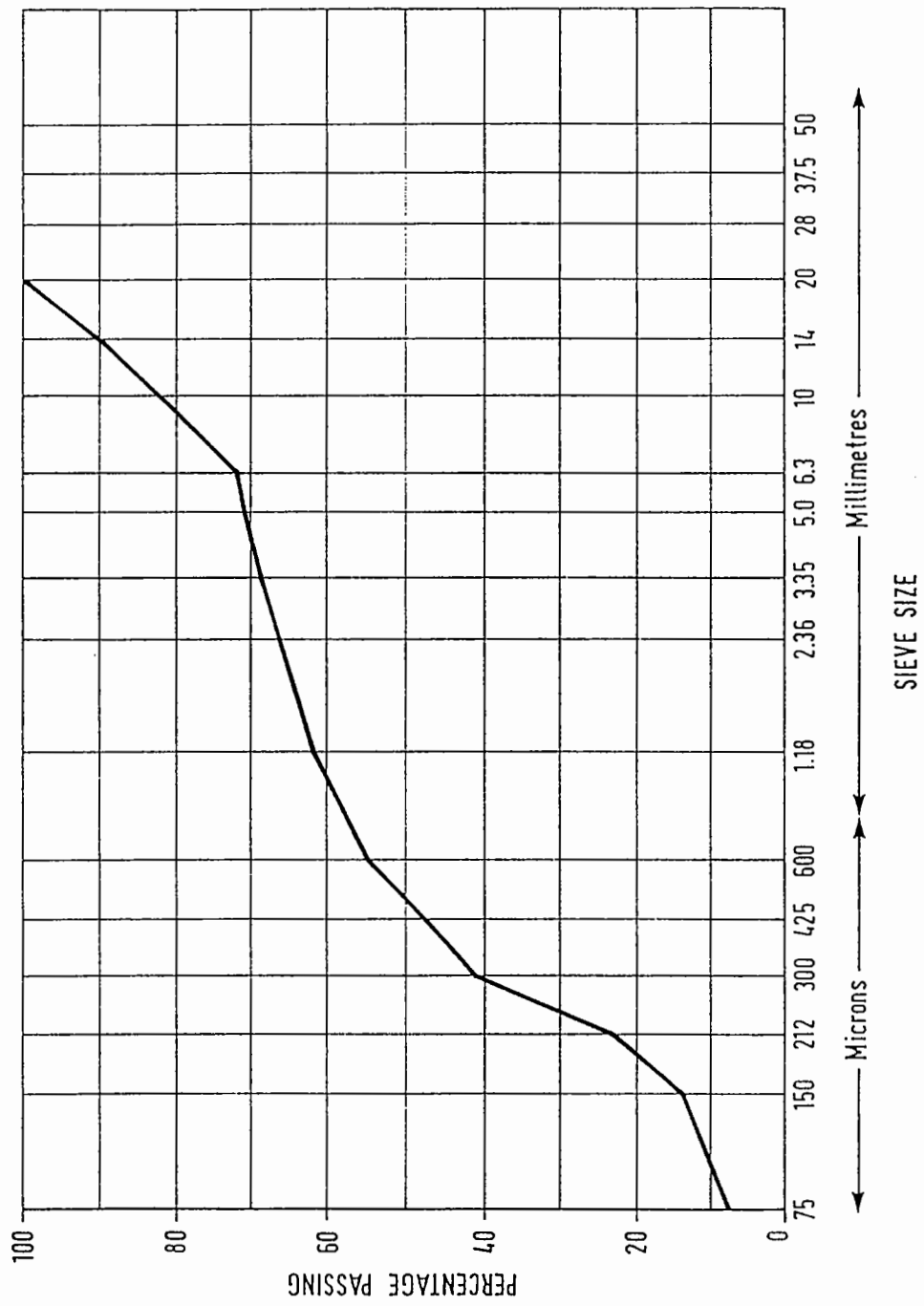


FIG. 5.3 GRADING CURVE OF HOT ROLLED ASPHALT WEARING COURSE.

b) Flexibility and thickness of the joint material.

2. Transient Movements (Horizontal, Vertical and Rotational)

a) Stiffness of the bridge deck.

b) Traffic over the joint.

c) Performance of the bearing.

3. Thermal Movements

a) Expansion length of the bridge deck.

4. Installation Conditions

a) Site preparation.

b) Workmanship.

c) Weather and temperature during installation.

5. Weathering

a) In-service weathering.

For practical reasons, it was necessary to eliminate some of these factors in the early stage of the project and concentrate on those of prime importance.

Although the normal thickness of surfacing over an in-service buried joint varies from 37 mm to 165 mm (Price 1982), the effective thickness of the test specimens was fixed at 90 mm. The effects of varying surfacing thickness on joint performance

in the tests was not investigated. Each type of joint movement was applied independently in order to study its individual effects on the performance of the joint. The effects of the directly applied wheel loads would be investigated in a separate project and the variation of in-service weathering and installation condition was not introduced in this test programme.

To keep the number of specimens at a practical level, only selected test variables were introduced, namely thermal movement, traffic induced horizontal, vertical and rotational movements, loading frequency, test temperature and stress condition of the specimen at the start of the test.

#### 5.4.1 Thermal Movements

This is the most significant type of movement which contributes to the deterioration of buried joints on concrete bridges. For bridges with a buried joint, the design maximum thermal movement is unlikely to exceed 15 mm. Although in a working environment, thermal movements are caused by temperature changes, the test temperature for the specimens was kept constant to allow the fundamental effects of the actual movement to be investigated.

#### 5.4.2 Traffic Induced Movements.

Each bridge has its own unique response even to identical

traffic loadings and it is impractical to attempt to incorporate individual bridge deck behaviour in a joint testing programme. However, traffic induced joint movements can be divided into three types, ie, horizontal, vertical and rotational. If specimens are tested with each of these in turn and at different magnitudes, the influence of each type can then be isolated. The combined effects of these movements could possibly be defined by the method of superposition. The traffic induced horizontal movement was studied in the main test programme, while the effects of vertical and rotation movements on joint performance were investigated in a series of less intensive tests.

#### 5.4.3 Test Loading Frequency and Waveform.

The normal service life of expansion joints is in terms of years, so it was necessary to compress this time scale in the laboratory tests. One of the methods of accelerating the test was to increase the cyclic frequency. During commissioning tests on trial specimens, the EJS was tested with a loading frequency of up to 10 Hz in stroke control mode. As the asphalt stiffness increased with an increase in strain rate, the resulting load transmitted to the frame caused excessive deflections of some mechanical components. The final HRA mix used in the present specimens would be stiffer than the trial specimen and would, therefore, generate even higher loads. Consequently, a frequency of 5 Hz was chosen for the tests in the main programme. This was well within the performance limits of the test instruments and

also avoided excessive heat generated by internal friction in the joint material when tested at too high a frequency. A frequency of 3 Hz was used for vertical and rotational movement tests. It was reported (Clauwaert 1986) that the duration of loading on a bridge joint was dependent on the span length and the type and speed of the vehicle passing. This resulted in a typical value ranging from 1.5 to 3 seconds. This was equivalent to a loading frequency between 0.12 and 0.24 Hz. Due to the unique relationships between fatigue life and applied tensile strain of bituminous materials, as discussed in section 2.3.2, the loading frequency was unlikely to have any significant effect on the test results. The rest period between traffic loading pulses was also omitted to further reduce the testing time.

It was reported that the fatigue life of a bituminous material varies with the shape of the waveform of the applied cyclic pulse by a factor ranging from 0.42 to 1.45 (Raithby and Sterling 1972). Since a sinusoidal waveform has a factor of 1.0, all traffic induced bridge movements were reproduced using this waveform during the laboratory tests in this research project.

#### 5.4.4 Test Temperature.

Specimens were tested at a constant temperature of 10 °C or 20 °C. Although the strain criterion indicates that temperature is unlikely to affect the fatigue life of a bituminous specimen, it was considered it was desirable to see if this was true for the

expansion joint configuration. It also provided an opportunity to commission the temperature control system of the EJS.

#### 5.4.5 Initial Stress Conditions

It is common practice to install expansion joints on site when the temperature is high and the weather is dry. This facilitates the work and improves quality control. However, as the temperature falls, the bridge deck contracts and opens up the joint. This causes tensile stresses in the joint material in addition to the stresses induced by traffic. On the other hand, if the joints are laid in winter, they will be mainly subjected to a compressive stress during their service lives. Schutz (1981) and Tons (1986) reported that this had a significant effect on the performance of joint sealants. It is of interest to see how buried joints behave under similar conditions. To simulate this stress condition, all specimens were pre-compressed or pre-tensioned before the start of horizontal cyclic movement testing. It must be emphasised that there was no intention to recreate the effect of damage due to thermal movement but only the effect of the resulting stress condition. The process must be carried out without causing any premature failure of the specimen. The joint gap under the specimen was initially set at 20 mm and by selecting gap width changes to either 17mm or 22mm a compressive or a tensile force was generated in the specimen. Cycling to simulate the horizontal movement due to traffic effects was then started relative to this new gap position. No



initial stress was applied to specimens used for vertical or rotational movement tests.



## CHAPTER SIX

### PRELIMINARY TESTING

#### 6.1. INTRODUCTION

Some preliminary tests were carried out before the main test programme was started. The main purpose of these was to collect some general data to help finalise the test procedures already formulated. The quality of laboratory made joint specimens, using the compaction frames as described in section 4.4, could be checked. These preliminary tests provided the first opportunity to observe the performance of the mechanically strengthened EJS when testing properly made specimens. Furthermore, the performance of the Dartec controls, the newly developed instrumentation and computerised data acquisition system could be studied. Computer software for control, data collection and test execution purposes could be tested and further developed during this test period. As a result, appropriate modifications could be made which would be of benefit to the future testing programme.

#### 6.2 PRELIMINARY TEST PROCEDURES

Basic test procedures were formulated to develop a specimen

testing method. The suitability of each procedure would be verified by the preliminary tests.

#### 6.2.1 Initial Stiffness Measurement

One of the methods used to check the consistency of the manufactured specimens was to compare their stiffnesses. The elastic stiffness of a bituminous material is defined as:

$$\text{Elastic Stiffness} = \text{Uniaxial Stress} / \text{Uniaxial Elastic Strain}$$

The stiffness of a joint specimen was obtained by measuring the strain of the material near and at right angles to the joint gap and the stress applied on the cross-sectional area of the specimen along the joint. The "apparent" stiffness was then calculated by dividing the applied stress by the strain. The stiffness measurements were carried out before any pre-compression or pre-tension was applied to the specimens. Trial tests indicated that it was best to cycle the specimen with a joint gap movement of  $\pm 0.05$  mm and measure the strain and stress as soon as possible. A greater gap movement could damage the specimen. On the other hand, if the movement is too small, minor errors in the displacement and load measurements became significant. If too many cycles were completed, the elastic properties of the specimen might change as fatigue damage developed. Two stiffness measurements at the same stress level

were taken at the test temperature and the mean recorded as the initial "apparent stiffness" of the specimen. Due to the geometry of the joint specimens, certain restraints were inherited and the stiffness measured was different from that obtained on a conventional unconfined cylindrical test specimen. This was because neither the stress nor the strain measured on the joint specimen was truly uniaxial. However, it may be possible to correlate this stiffness with the conventionally measured stiffness at some point in the project.

### 6.2.2 Initial Stress Conditioning

The reasons for applying initial stresses to a joint specimen before a test was started were discussed in section 5.4.5. This process could be carried out in a controlled strain mode or a controlled stress mode. When operating under controlled strain, the Dartec actuator was instructed to move a certain distance and at a certain rate. The advantage of using a controlled strain rate was that the time for completion of the operation could be calculated in advance. However, there was a danger in disregarding the stress level generated within the material. If the strain rate became too high, the stress level would increase considerably due to the material not having enough time to relax. This excessive stress level would result in serious damage to the specimen or even to the simulator itself. Although a trip facility could be set to respond to a certain stress level, the conditioning operation might be interrupted too often if a

controlled strain rate was used.

The alternative was to operate in a controlled stress mode. Computer software could be used to instruct the Dartec actuator to exert a certain amount of stress on the specimen continuously and allow the specimen to creep naturally until the required gap width was achieved. The problem with this method was that the length of time required to complete the process was unknown. However, it was safe and could be carried out automatically, without manual supervision, under the control of suitable computer software. Therefore, it was finally decided that the stress controlled method should be adopted unless proved unsuitable during testing.

### 6.2.3 Horizontal Traffic Associated Cycling

After a specimen had undergone the pre-compression or pre-tension process, it was allowed to cool down to its test temperature before application of the horizontal traffic associated cycling. In this test, the specimen was subjected to a sinusoidal horizontal gap movement generated by the Dartec actuator. The total number of cycles required to generate a predetermined length of crack across the specimen was recorded as the fatigue life of the specimen.

The test could be carried out using controlled stroke or controlled gap extension. In stroke control mode, the function

generator of the Dartec system was instructed to generate a sine wave signal with a constant programmed magnitude. The command waveform signal was then fed to the loop controller, which instructed the actuator to move accordingly (Fig. 3.3). The stroke feedback signal from the actuator was monitored by the loop controller board. If the feedback signal did not match the input command signal, the controller made a gain calculation and produces a compensation command to instruct the actuator to react until the feedback and input values were the same.

In joint gap extension control mode, the feedback signal from the actuator "built-in" LVDT was replaced by that from the external LVDT's (Fig. 4.7, G1 & G2) mounted across the joint gap. The signal from this external LVDT was fed into the Dartec system through the Extension input channel as shown in Fig. 3.3 (similar arrangement could be made for controlling the vertical actuator). When in action, the actual movement of the actuator measured by its integral LVDT was ignored and the controller commanded the actuator to continue its stroke until the gap movement reached its predetermined upper and lower limits for each cycle. Compensation command values were produced from the gap LVDT feedback signals. The final choice of the control method is discussed in section 6.4.2.

#### 6.2.4 Thermal Movement Cycling

In these tests, the specimen was extended and compressed about

its original gap position at a constant test temperature and the cycling carried out at a very low frequency. Strain rate control was used in order to simulate the damaging effects of thermal movements. The strain rate was the same for all specimens while the cyclic gap movements could be varied for each specimen. Development of computer software was necessary for test control.

### 6.3 PRELIMINARY TESTS.

Four joint specimens were used in the preliminary testing programme. No specific numbering system was applied for these specimens which were simply labelled as specimen nos. 1 to 4. Details of each test are shown in Table 6.1. Due to early difficulties experienced with the complex operation of the Dartec system, a small amount of accidental damage was done to these specimens. In addition, modifications to instrumentation, development of computer software and the use of different test controls all affected the test results. Consequently, results from these tests were not used for the final analysis.

The specimen used for test no. 4 was seriously damaged due to equipment malfunction. After discussions with Dartec, an engineer was sent to check and update the system with new electronic components which were not available at the time of the original purchase. Since then, the equipment has performed well and no further major difficulties have been encountered.



Table 6.1. Details of Preliminary tests.

Specimen No.	Control Mode	Stress condition before cycling	Horizontal Transient movement (mm)	Frequency (Hz)	Test Temp. ° ( C)
1	Stroke	Compression	$\pm 50$	5	20
2	Extension	Tension	$\pm 50$	5	20
3	Extension	Tension	$\pm 30$	5	20
4	Extension	Specimen damaged accidentally.			20

Figs. 6.1 to 6.9 show the peak to peak values of gap movement, applied load and strains in the material of each successful specimen and Figs. 6.10 shows the crack patterns of these specimens after failure. Results for test no. 4 are not included due to the accidental damage of the specimen. Observations made on each test are recorded in the following sections.

#### 6.3.1 Specimen Test No. 1

The specimen was compacted using the steel frames as discussed in section 4.4. Pre-compression was accomplished by moving the actuator with a hand held "inching" control until the applied load monitored on the screen of an oscilloscope developed a stress of approximately 60 kPa. This process took about 8 hrs to complete.

The test was carried out using the stroke control mode, details of which are described in section 6.2.3. A cyclic gap movement of  $\pm$  50 microns was introduced. The success of the test was highly dependent on the ability to control the joint gap movement accurately during the test. Fig. 6.1 shows that the control of the gap movement was reasonable during the early stage of the test. As the strength of the material reduced, the magnitude of this movement increased continuously until it reached a peak to peak value of 380 microns and the specimen suddenly failed. This final gap movement was nearly four times larger than that

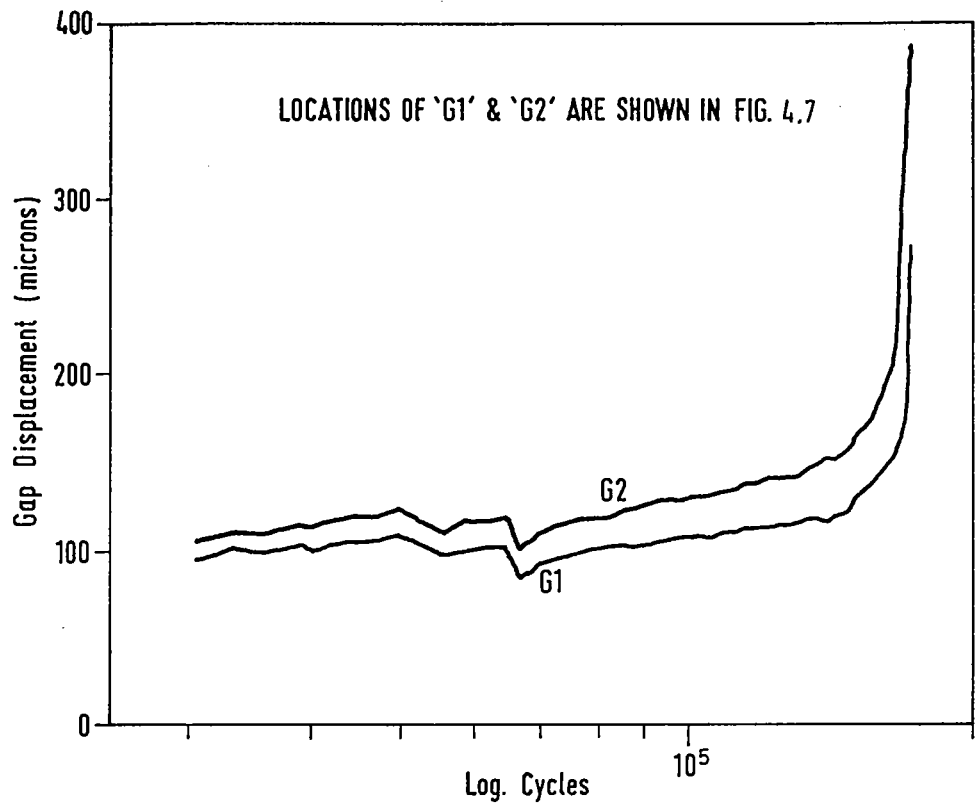


FIG. 6.1 SPECIMEN NO.1

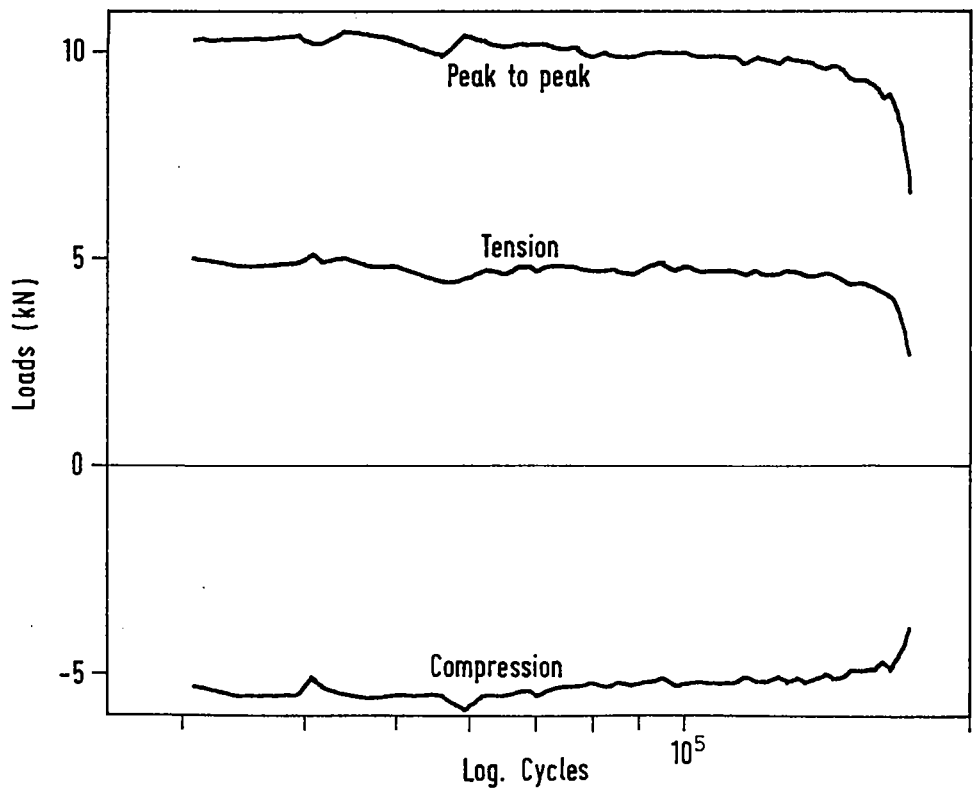


FIG. 6.2 SPECIMEN NO.1

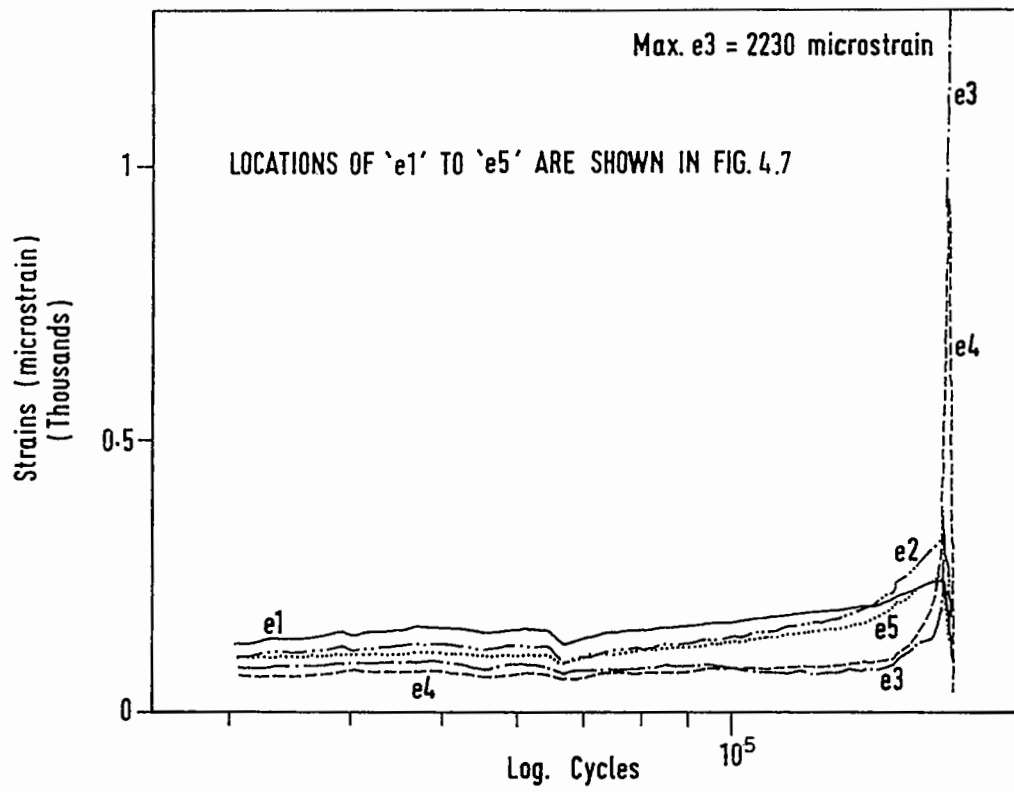


FIG. 6.3 SPECIMEN NO. 1

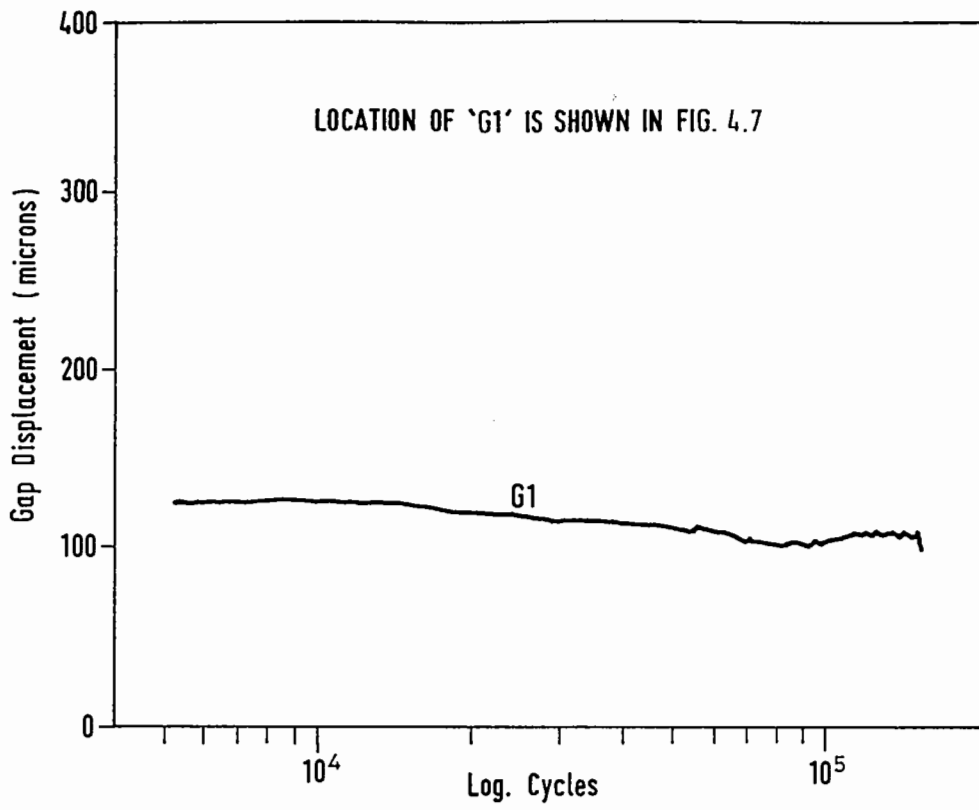


FIG. 6.4 SPECIMEN NO. 2

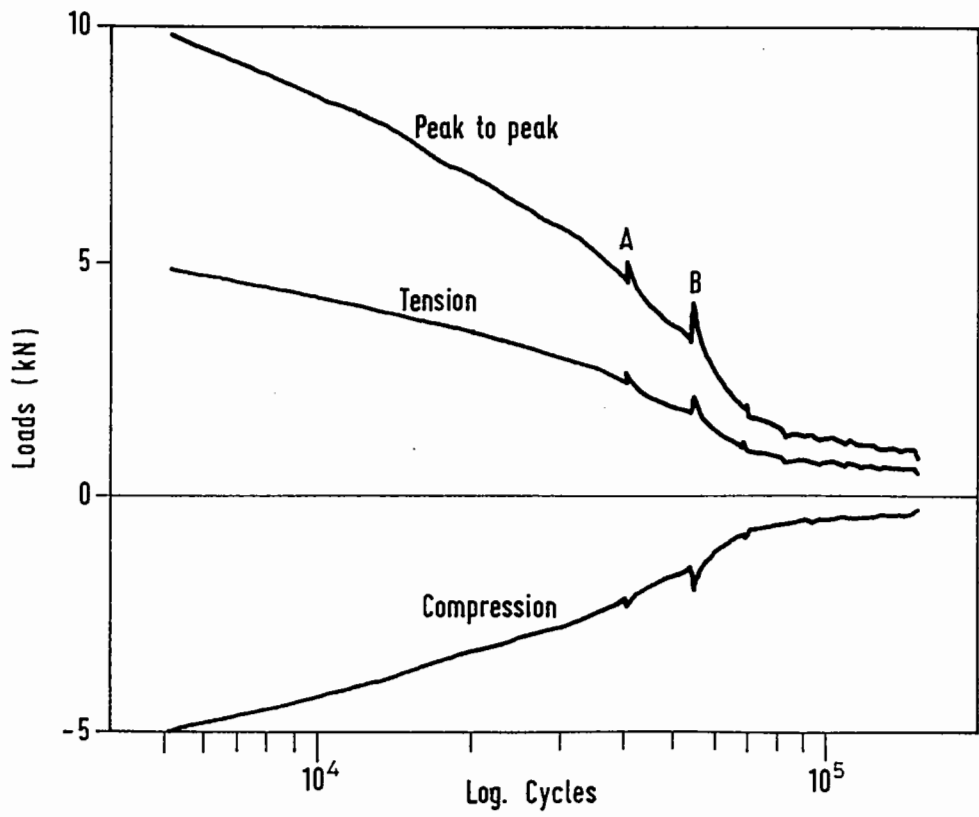


FIG. 6.5 SPECIMEN NO. 2

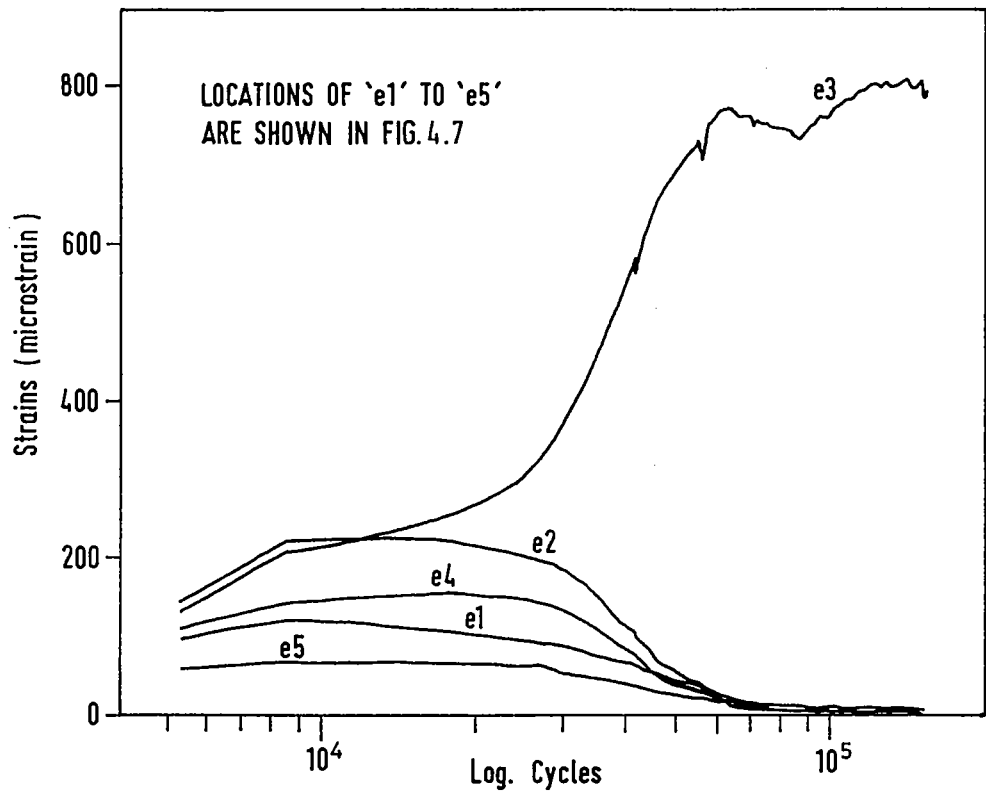


FIG. 6.6 SPECIMEN NO. 2

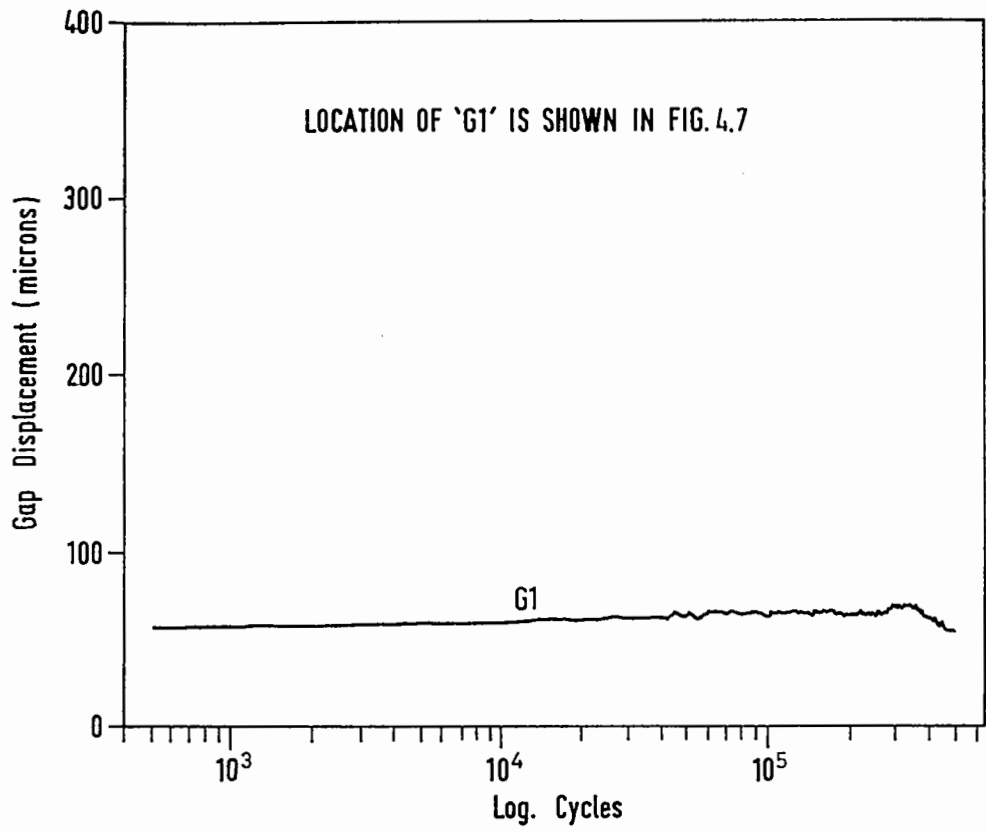


FIG. 6.7 SPECIMEN NO. 3

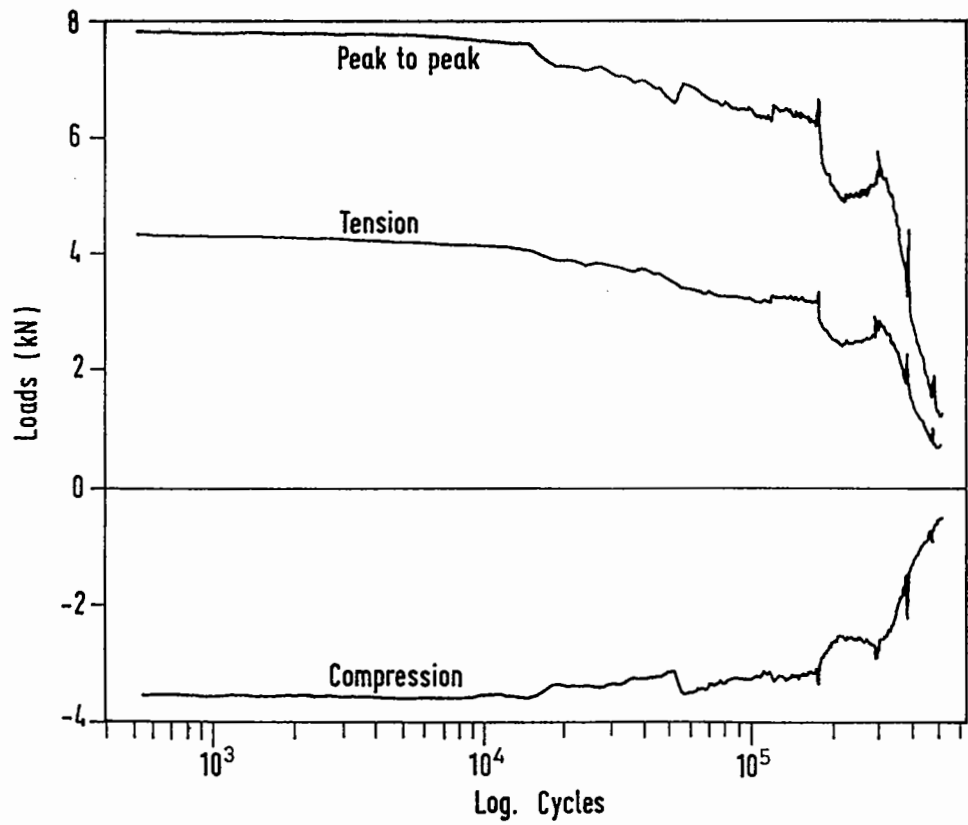


FIG. 6.8 SPECIMEN NO.3

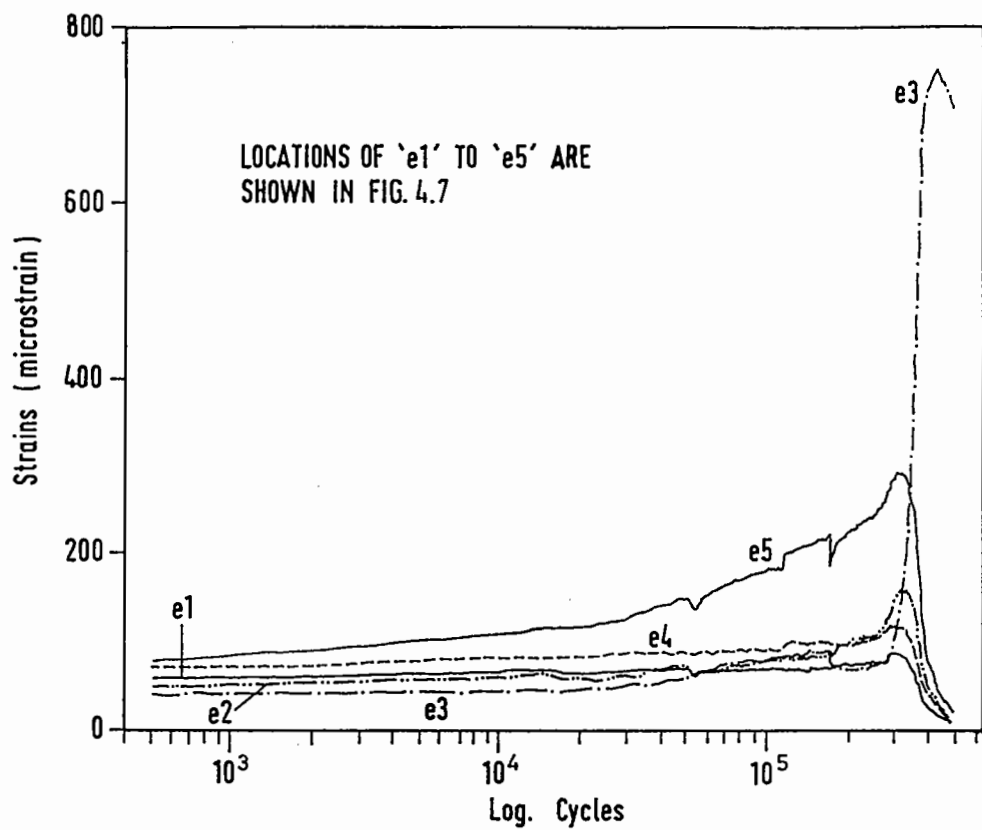


FIG. 6.9 SPECIMEN NO. 3



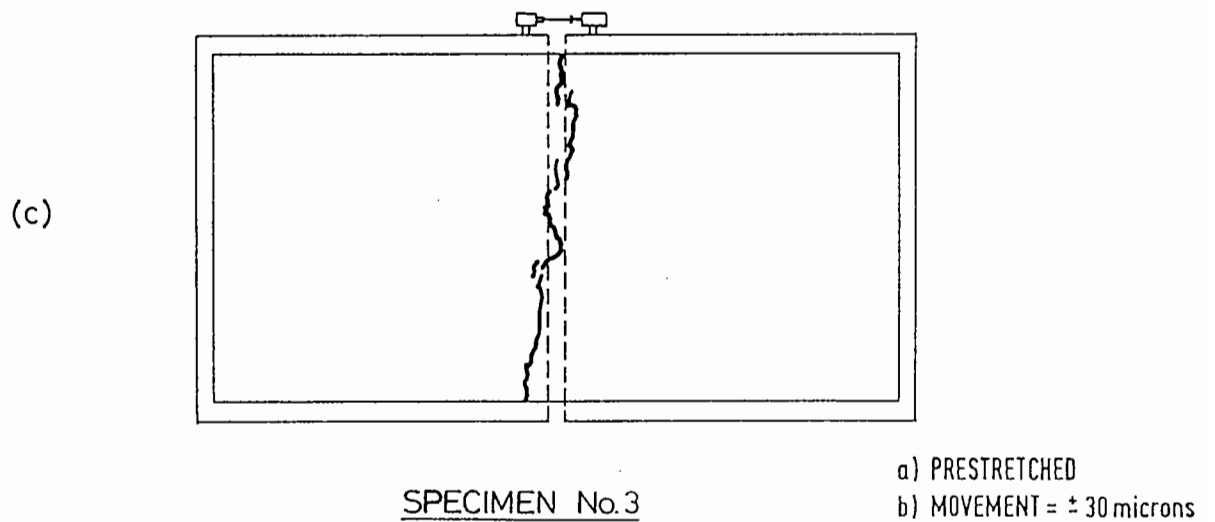
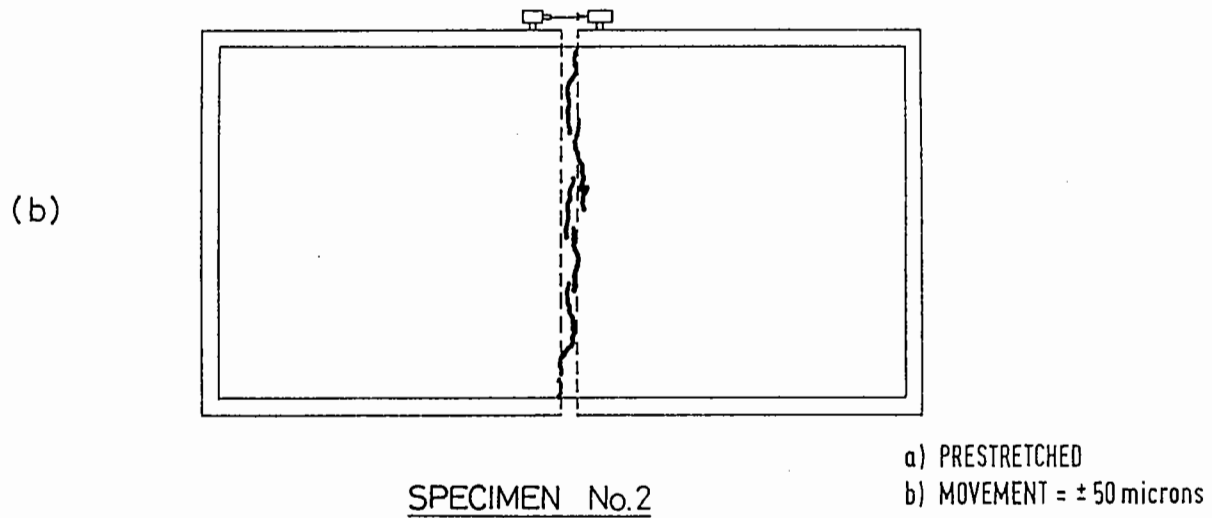
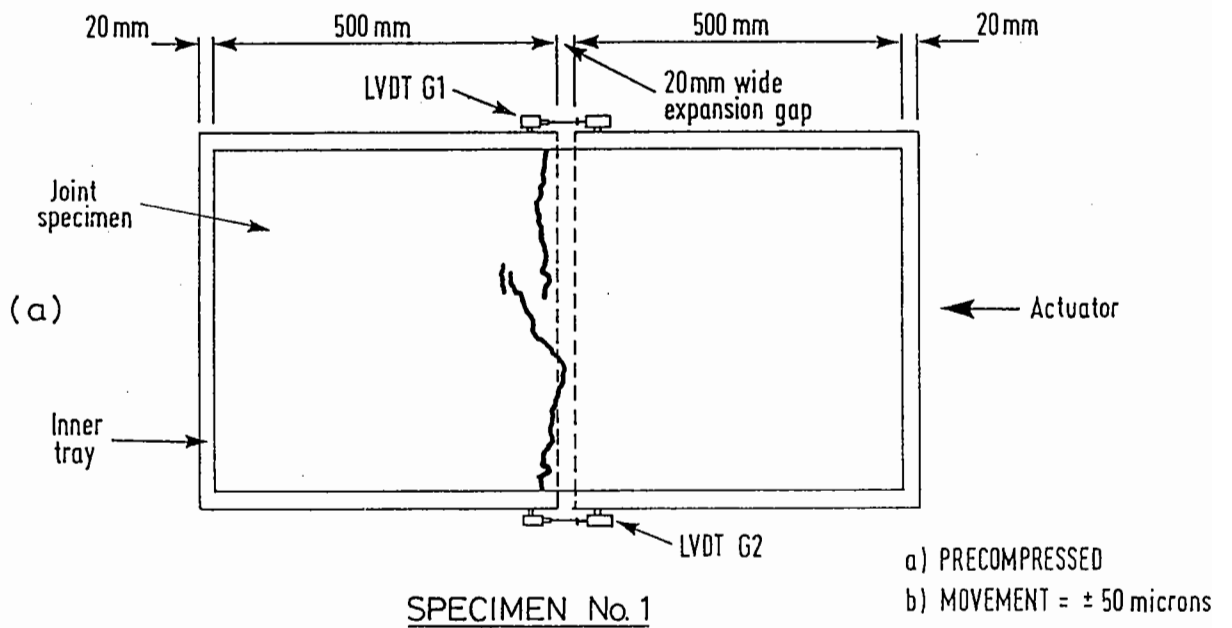


FIG. 6.10 . CRACKS INDUCED AT EXPANSION JOINT AFTER FAILURE (SLABS NO. 1 TO 3)

required. During the test, the recorded loads were almost constant (Fig. 6.2) until the failure of the specimen occurred at 166,000 cycles. This provided further evidence that the test, although under stroke control, behaved as if it were under stress control. The final crack occurred very close to the joint gap which agreed with the failure pattern noted from site observations conducted by TRRL (Price 1982 (a) & (b) and 1984). Normally, fatigue cracking will occur at a position where the initial strain is highest. However, Fig. 6.3 shows that the initial strain at the crack position was in fact the second lowest of the five strains recorded by the LVDT's positioned along the centre line of the specimen. This strain remained at the same level most of the time, and then became the highest when the crack occurred. Further testing is required to confirm that this failure pattern is repeatable.

#### 6.3.2 Specimen Test No. 2

This specimen was manufactured in the same manner as specimen no. 1, but this time pre-tensioning was applied before cyclic testing. It took about three hours to extend the specimen by 3 mm. Since the stroke control mode was unsatisfactory for accurate gap movement control, the optional extension control facility was used in this test. The details of this control method were described in section 6.2.3. Fig. 6.4 shows that the cyclic gap movement varied only slightly about a peak to peak value of 115 microns during the test and remained the same even

after the failure of the specimen. This gap movement was slightly higher than the input command value of  $\pm 50$ microns. Both compressive and tensile loads reduced rather quickly from the very beginning of the test and reached their lowest values when the specimen completely failed as shown in Fig. 6.5. The position of the crack was similar to that of specimen no 1 (Fig. 6.10). Fig. 6.6 shows that the strain measured near the joint gap started as the second largest and rapidly reached a peak after the crack was observed, while the strains in other positions started to fall. The applied gap movement for specimen no. 2 was the same as specimen no. 1, but the fatigue life was much shorter. Total failure occurred after 71,000 cycles. This may have been due to the different stress condition (in tension) of the specimen at the start of the test. Rest periods were introduced when the test was stopped overnight and the material seemed to memorise its test history, i.e. when the test was restarted, a higher material stiffness was recorded but this disappeared rapidly and the load fell sharply back to the same level as before the rest period (Fig 6.5, points A & B). A similar phenomenon was observed when a test was restarted after a rest period of several hours.

### 6.3.3 Specimen Test No. 3

Compaction and pre-tensioning was carried out in the same way as for specimen no. 2. Although it was intended to carry out the test with a cyclic gap movement of  $\pm 25$  microns, the actual

output movement was  $\pm 30$  microns which was slightly higher than the input command value (Fig. 6.7). Apart from this, the gap movement control seemed to be working correctly. The gap movement used in this test was significantly smaller than that for specimen no. 1 and the specimen took longer to fail. A complete crack occurred at 447,000 cycles. In this test, although the configuration of the instrumentation was the same as for previous tests, the positions of the LVDTs were interchanged, and changed back again, to check the accuracy of the strain measurements. The readings of the LVDT's were found to be consistent.

Fig. 6.8 shows the peak values of the loads during the test. It was interesting to see that in the first 50,000 cycles, the tensile load was consistently higher than the compressive load, this may be due to the effects of the pre-tensioning.

Fig. 6.9 shows that the strain in the joint material near the gap (e3) reached a value of 750 microstrain at one stage. This represents a displacement of 75 microns ( the LVDT had a 100 mm gauge length ) which was larger than the measured output gap movement of 60 microns. This was because only one LVDT was mounted on one side of the specimen across the gap to produce a signal for data output and feedback control. The LVDT on the other side of the gap had to be transferred to the vertical actuator, so that its position could be held, otherwise an open

loop would be created in the Dartec system when extension control was selected. Therefore, if a crack started from the side which was away from the gap LVDT and the tray was not moving perfectly parallel for the small movement involved in this test, a larger movement may be generated on that side which would not be detected by the feedback LVDT. As the crack propagated towards the middle, where the centre LVDT was located, a larger strain may have been measured. The simplest way to overcome this problem was to reposition the gap LVDT to the middle of the specimen, so that an average gap movement could always be measured. This was tried for the test on specimen no. 4 and the results are reported in the following section.

#### 6.3.4 Specimen Test No. 4

The test on specimen no. 4 was delayed as one of the controller boards was found to be faulty and a replacement had to be used. In this test, a pair of steel hollow sections was used to form a bridge so that the gap LVDT could be mounted just above the central LVDT (e3) (Fig. 4.7). Unfortunately, the new position of the gap LVDT was too high above the line of action of the horizontal actuator and a discrepancy between the magnitude of the gap movement and the measured LVDT signals was observed. This was probably due to the movement developed by the bridge about its base fixings on the trays. A successful method for obtaining an average gap movement signal was eventually developed and details of the method are described in section 7.3.2. The

slab test no. 4 was allowed to continue until forced to stop due to a fault which developed in the control system and caused serious damage to the specimen near the end of the test. The fault was diagnosed by a Dartec engineer and corrected as discussed in section 6.3.

#### 6.4 DISCUSSION.

Although many unforeseeable problems had been encountered during the preliminary testing, the purposes of the tests had been fulfilled satisfactorily. Crucial information was obtained on how the EJS and the control system responded to different test conditions. Important modifications and developments were made to the method of producing specimens, the Dartec control systems, computer software, test control method and test procedures. Some general test data were also generated. The following sections give detailed discussions on each of these developments.

##### 6.4.1 Method of Making Specimens.

All specimens used in the preliminary testing were compacted with the steel frames as discussed previously in section 4.4. Although the frames accommodated the design loading successfully during an earlier compaction trial, this method was very time consuming and was unable to produce the required pressure every time, so a repeatable level of compaction was not achieved. As a result, an alternative method was developed. This involved using the

existing 500 tons MAN hydraulic compression machine in the laboratory.

To ensure the quality control of the bituminous mixes, all materials were mixed in the laboratory at the University. Due to the amount of material required, the basecourse and wearing course mixes were divided into 16 and 10 batches respectively. Aggregates for each batch were weighed in separate trays and heated to the required mixing temperature in ovens. The heated aggregates were then put into a preheated mixer and the correct proportion of hot bitumen was added. The total mixing time consisted of two periods of one minute with a half minute stop between the two for manual stirring. The final mix was then placed back in the trays and kept hot in the ovens prior to use, while the mould (the coupled inner trays) was preheated with a propane burner. To ensure an even distribution of material within the mould, an aluminium divider was used to divide the mould into eight equal sections. Each section was filled with an equal amount of hot mix. After levelling the surface, the divider was removed and a vibrating hammer, with a 110 mm x 110 mm preheated compaction foot, was used for initial compaction. It was moved to different positions over the surface of the material and short bursts of vibration were applied. Four preheated 20 mm thick steel plates were then used to cover the initially compacted mix and the complete assembly was transferred to the MAN machine (Fig. 6.11). It was lifted by an overhead crane and placed on a heavy beam section mounted on a steel

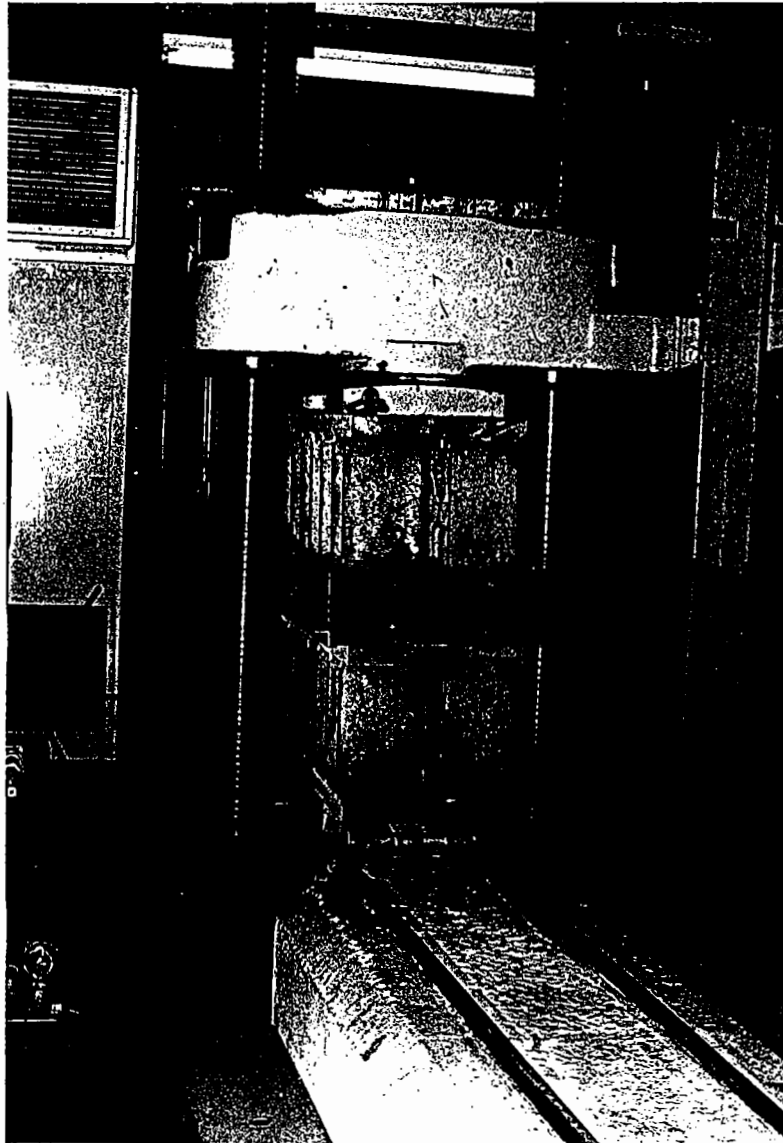


FIG. 6.11    COMPACTION OF SPECIMEN USING  
500 TONS M.A.N. MACHINE.



trolley. A similar beam section was put on top of the steel plates which covered the mix. The beams were used to spread the compaction pressure evenly over and under the specimen. The specimen, the beams and the trolley were winched along rails until the centre of the hydraulic jack in the base of the MAN machine below the trolley, was coincident with the centre of the trolley. A 400 mm x 400 mm x 60 mm thick steel compression foot attached to a screw driven crosshead was lowered and locked in a position about 10 mm above the beam on top of the specimen. The hydraulic jack was then pressurised, raising the trolley and the specimen so that the upper beam section was stopped by the metal foot. This generated a compression and the total load applied to the specimen was read off from a dial. The speed of load application could also be monitored. The load was gradually increased to 3100 kN which is equivalent to a contact pressure of 6.2MPa. The hydraulic pressure was maintained at this level for about 5 min before release. This process was repeated twice and, for the final loading, the pressure was maintained for 15 min.

The specimen was compacted in two layers. The first layer was the 60 mm thick basecourse and the second layer was the 40 mm thick wearing course. A minimum of 24 hours was allowed between the construction of these two layers. The compaction procedures used for the wearing course were similar, except that the mould was not preheated and the maximum compaction load was 2900 kN. This was equivalent to a contact pressure of 5.8 MPa. A lower pressure was used in order to avoid possible damage to the previously compacted basecourse. The manufactured specimen was

allowed to cool for at least 24 hours before testing.

Compaction could be carried out by using a small vibrating roller if the width of the mould was increased by 50 mm. This would allow test specimens to be manufactured away from the laboratory.

#### 6.4.2 Test Control.

The stroke control mode was used in preliminary test no. 1 and the result was found to be unsatisfactory. Due to the compliance of the connections between the actuator and the specimen, the generated gap movements were smaller than the output stroke of the actuators. This could be overcome by increasing the stroke command values until the cyclic gap movement reached its required level immediately after the test was started. However, as the stiffness of the material deteriorated throughout the test, the ratio between the gap and these stroke movements gradually approached and then exceeded unity. This resulted in gap movements which were larger than the required values. Effectively, the specimen failed in a manner resembling that of stress control since the gap cyclic amplitude was not constant.

For test no. 2, joint gap extension control was used and found to work satisfactorily. However, the gap movements still varied slightly throughout the test. Due to the omission of the Data Processing Board (el) in the Dartec system, the scaling of the

extension control input signal was not easily adjusted, by means of computer hardware, to suit different test requirements. Instead, a fixed scale factor of  $\pm 10$  volts input signal representing a  $\pm 100$  mm gap movement was set by computer software. This setting provided a resolution of 0.1 volt to 1 mm. However, the actual working range of the gap LVDT's was in fact  $\pm 5$  mm. By changing the scale factor, which was written in the software, to  $\pm 10$  volts representing  $\pm 5$  mm, a much improved resolution of 2 volts to 1 mm could be achieved and this considerably increased the accuracy of the extension control. Since the software package was originally developed by Dartec (appendix B), a considerable amount of time would have been required to understand the software and complete the appropriate alteration. Therefore, it was decided that specimen testing should be continued while this alteration was in progress. The modified software was introduced, eventually, after the completion of the first three specimen tests of the main test programme.

Trips were set to stop a test if the applied loading or the gap movements exceeded a certain limit to avoid accidental damage to the specimen other than that caused by normal testing.

#### 6.4.3 Failure Pattern of the Specimens.

During commissioning tests, some joint specimens failed with a crack which developed away from the gap. Since this failure mode

did not resemble what happened on site, it indicated that a realistic joint failure mechanism had not been reproduced. The problem was overcome by modifying the details of the mould as described in section 4.2.2. In working conditions, cracking in buried joints normally starts in the hard shoulder and gradually propagates along the joint gap into the carriageway. Eventually, a single continuous crack is formed across the road. Subsequently, all preliminary test specimens failed with a similar pattern (Fig. 6.10) to that observed on site.

#### 6.4.4 Stiffness Measurement.

Results showed that to measure the initial stiffness of a specimen using the method suggested in section 6.2.1 was unsatisfactory. An alternative method was used to check the consistency of the specimen quality. This involved taking four core samples from each specimen after testing as shown in Fig. 6.12. The cores were then cut horizontally to separate the basecourse and wearing course materials. As a result, eight cylindrical samples were obtained. The density and void content of these cores were measured and compared with those from other specimens. Table 6.2 shows the measured results of each specimen indicating reasonable consistency. Stiffness measurements on some of the cores were obtained using the Nottingham Asphalt Tester (NAT) at two different temperatures, 5 °C and 20 °C. The results are shown in Tables 6.3 & 6.4.

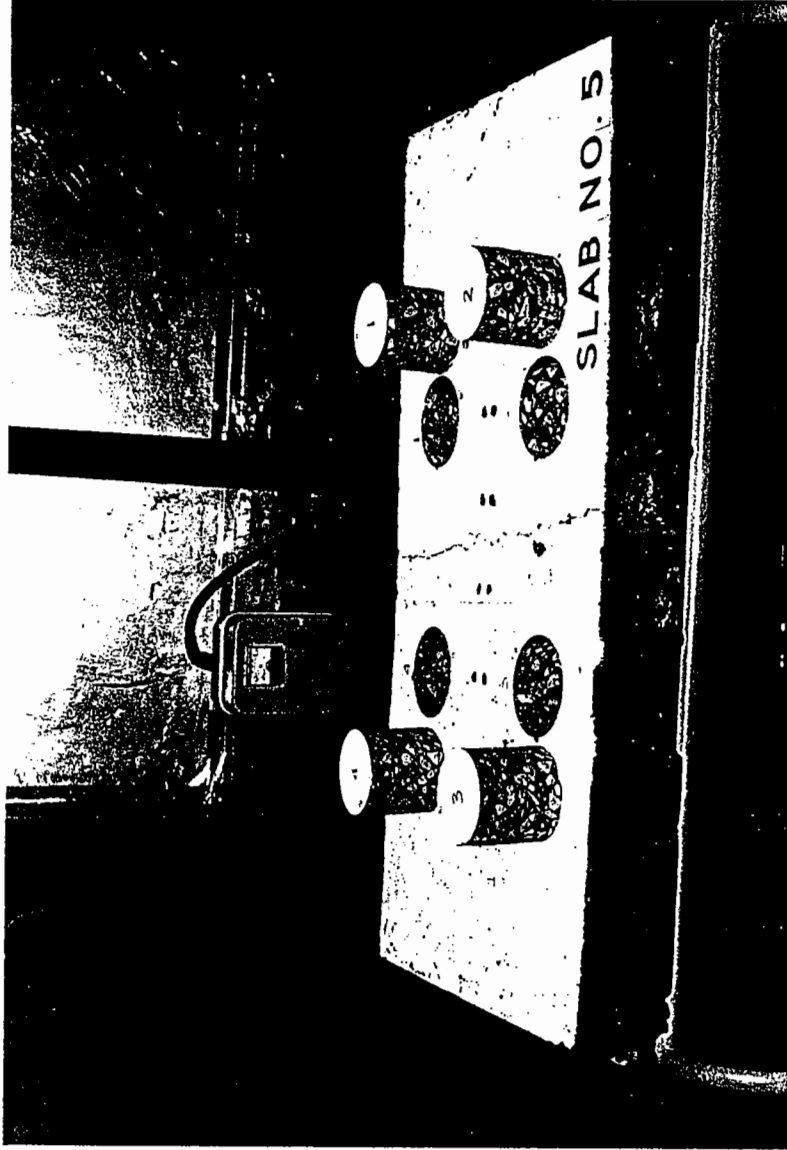


FIG. 6.12 CORES TAKEN FROM JOINT SPECIMEN  
AFTER TESTING.

Table 6.2 Measurements of Density and Void Content.

Specimen No.	Average Density (kg/m <sup>3</sup> )		Average Void Content ( % )	
	B/C	W/C	B/C	W/C
25/20C	2334	2249	6.1	6.3
50/20C	2330	2262	6.2	5.8
100/20C	2340	2310	5.8	3.8
30/20T	2336	2257	6.0	6.0
50/20T	2335	2251	6.0	6.2
100/20T	2332	2257	6.1	6.0
30/10C	2331	2260	6.2	5.9
50/10C	2321	2251	6.6	6.2
75/10C	2321	2246	6.6	6.4
25/10T	2322	2251	6.5	6.2
50/10T	2329	2281	6.2	5.0
75/10T	2339	2294	5.9	4.4
Average	2331	2264	6.2	5.7

Notes: B/C = Basecourse

W/C = Wearing course

Table 6.3 Measurements of Material Stiffness at 5 C.

Specimen No.	Average Stiffness (MPa)	
	B/C	W/C
30/10C	7023	7544
75/10C	7333	7154
25/10T	8195	7629
50/10T	7684	8733
75/10T	8408	7173
Average:	7729	7647

Notes: B/C = Basecourse

W/C = Wearing course

Table 6.4 Measurements of Material Stiffness at 20 C.

Specimen No.	Average Stiffness (MPa)	
	B/C	W/C
30/10C	1736	1892
75/10C	1661	1604
25/10T	1741	1636
50/10T	1779	1955
75/10T	1481	1948
Average:	1680	1807

Notes: B/C = Basecourse  
W/C = Wearing course



#### 6.4.5 Preconditioning Process.

Using manual control of the actuator to introduce the initial stress condition to the specimen proved to be tedious because of the very long time involved. Subsequently, special computer software was written to accomplish this process. The software instructed the Dartec actuator to compress or extend the specimen with predetermined stresses, i.e. 100 kPa for compression and 35 kPa for tension. As the specimen deformed, the actuator would respond and move to a new position to maintain the command stress level. If the specimen was overloaded for any reason, the actuator would reverse to release the excessive stress under the control of the software. When the specified amount of compression or extension was achieved, the actuator would stop automatically and hold the specimen in its final position.



## CHAPTER SEVEN

### THE MAIN TEST PROGRAMME AND RESULTS.

#### 7.1 INTRODUCTION

The main test programme was designed to investigate the effects of horizontal bridge deck movements on the performance of buried joints. The study of how buried joints responded to the traffic induced horizontal movements formed the major part of the investigation. In addition to this, a small number of tests were performed to investigate the effects of long-term horizontal deck movements. The predicted forms of joint performance curves are shown in Figs. 7.1 and 7.2.

#### 7.2 THE TEST PROGRAMME.

Details of the main test programme are presented in Table 7.1 which identifies 16 tests divided into 5 groups. The first 4 groups represented 12 successful specimen tests using traffic induced horizontal movements of different magnitudes. Groups 1 and 2 were tested at 20 C with initial stresses of compression and tension respectively. Groups 3 and 4 were tested at the same stress conditions but at a temperature of 10 C. Test 50/20T in

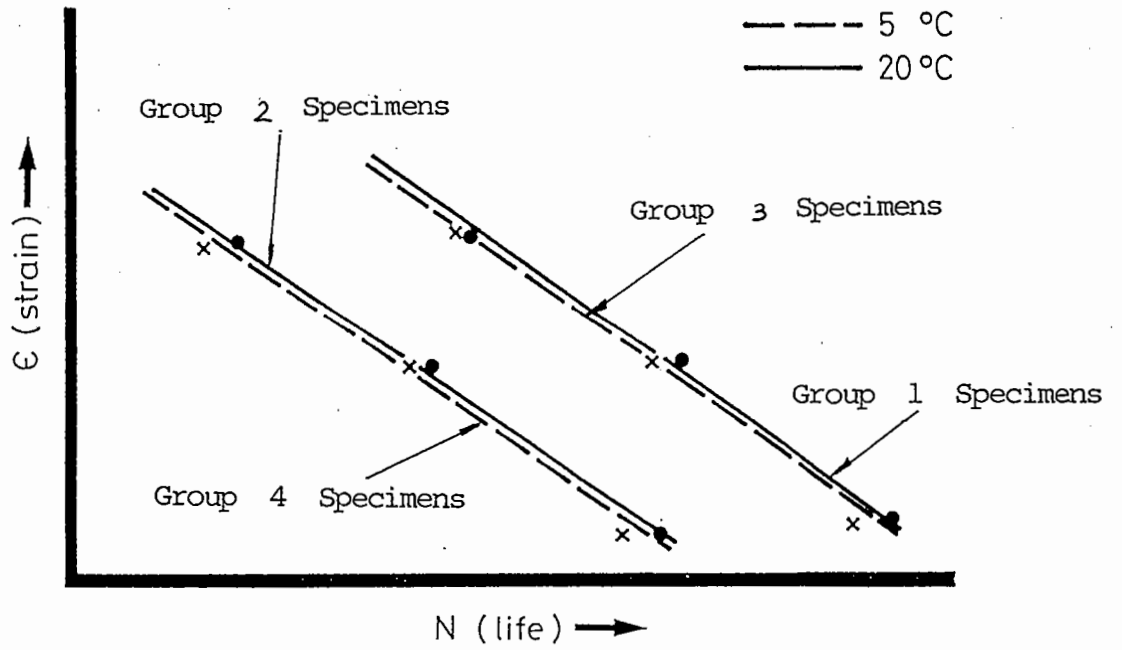


FIG. 7.1 PREDICTED TEST RESULTS OF JOINT SPECIMENS (GROUP 1 TO GROUP 4)

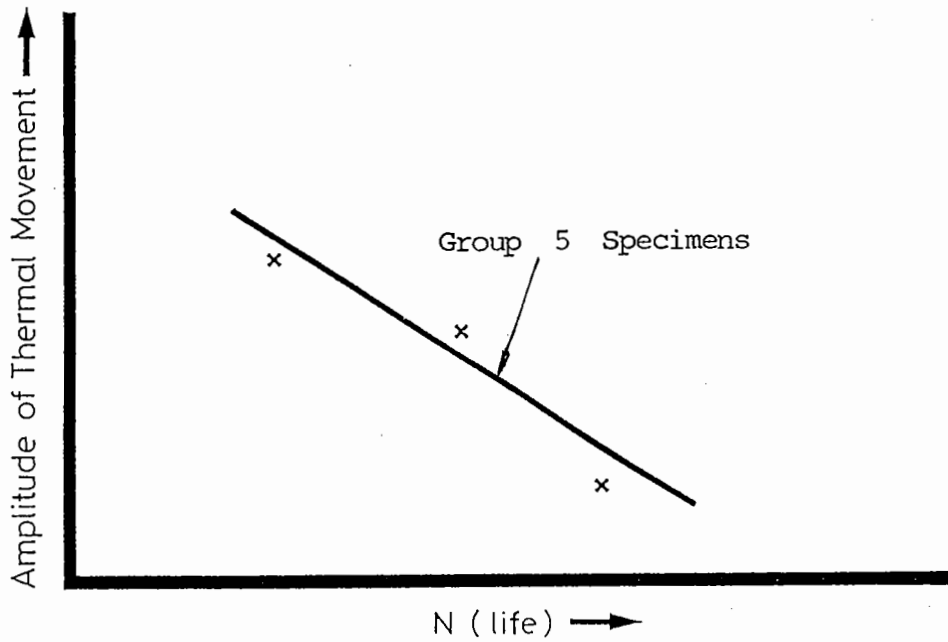


FIG. 7.2 PREDICTED TEST RESULTS OF JOINT SPECIMENS (GROUP 5)

Table 7.1 Details of the Test Programme.

Group No.	Specimen No.	Thermal movement (mm)	Horizontal movement (microns)	Frequency (Hz)	(1) Cycle per day	Test temperature (oC)	Starting joint gap (mm)
1	25/20C	-	±25	5	(120,000)	20	17
	50/20C	-	±50	5	(120,000)	20	17
	100/20C	-	±100	5	(120,000)	20	17
2	30/20T	-	±30(±25)	5	(120,000)	20	22 (23)
	50/20T	-	±50	5	(120,000)	20	22 (23)
	100/20T	-	±100	5	(120,000)	20	22 (23)
3	30/10C	-	±30(±25)	5	(120,000)	10 (5)	17
	50/10C	-	±50	5	(120,000)	10 (5)	17
	75/10C	-	±75(±100)	5	(120,000)	10 (5)	17
4	25/10T	-	±25	5	(120,000)	10 (5)	22 (23)
	50/10T	-	±50	5	(120,000)	10 (5)	22 (23)
	75/10T	-	±75(±100)	5	(120,000)	10 (5)	22 (23)
5	H/2/20C	±2(±3)	*	0.7mm/hr	till fail	20	--
	H/2/20T	±2(±5)	&	0.7mm/hr	till fail	20	--
	H/4/20T	±4(±7)	&	0.7mm/hr	till fail	20	--
	H/1.25/T	±1.25(**)	&	0.7mm/hr.	till fail	20	--

- N.B.
1. All specimens would be tested to failure.
  2. Figures in brackets are the values planned to be used originally.
  3. All specimens were manufactured with 20 mm gap.
- \* = cycle started with compression.  
 & = cycle started with tension.  
 \*\* = not included in the original test programme.

group 2 was repeated due to poor test data for the first specimen. Group 5 was the thermal movement tests. Due to the nature of this type of test, a considerable amount of time was needed for each test, so the number of test specimens was limited to four.

Although laboratory tests on expansion joint materials or systems, such as neoprene compression seals, asphaltic plug joint and site moulded sealants, had been conducted elsewhere, they provided little relevant information on how laboratory testing on buried joints should be performed. In-service joint gap movements on bridge deck with buried joints had been measured by Price (Table 2.1). He graded traffic induced horizontal movements into three classes, large ( $> 0.1$  mm), moderate ( $0.05$  mm to  $0.1$  mm) and negligible ( $< 0.05$  mm). Based on this information, the test ranges of applied traffic induced horizontal joint gap movements were set to  $\pm 0.1$  mm (large),  $\pm 0.05$  mm (moderate) and  $\pm 0.025$  mm (negligible) accordingly. The test ranges of long-term horizontal movements were originally envisaged to be  $\pm 3$  mm,  $\pm 5$  mm and  $\pm 7$  mm. Details of the selection of other test parameters are discussed in sections 5.4.3, 5.4.4 & 5.4.5. The suitability of these selected ranges was monitored carefully throughout the test period and appropriate adjustment was made when required. The test parameters appearing in brackets in Table 7.1 are the original values which were altered in the light of experience.

As it was necessary to improve the equipment in parallel with the specimen testing, modifications to the EJS, computer software and

control methods during the test period were inevitable. However, all these were kept to a minimum in order to maintain the consistency of the test results.

Table 7.2 shows the numbering system of the specimens tested for horizontal traffic induced movements. The code used to identify the test conditions for the long-term horizontal movement test specimens are explained as follows:

H	/	3	/	20	/	T or C
Long-term Horizontal Movement test		Cycling range ( <u>  </u> mm )		Test temperature ° ( C )		Cycle started with (Tension or Compression)

### 7.3 RESULTS OF THE TRAFFIC INDUCED HORIZONTAL MOVEMENT TESTS.

Test observations, similar to those in the preliminary tests, were continued on group 1 specimens and the details are discussed in section 7.3.1. Graphical presentations of test data are shown in Figs. 7.3 (a, b & c) to 7.14 (a, b & c). These figures are presented in three sets, (a), (b) and (c). Figures in set (a) show the peak to peak values of gap movements while reactive loads and strains in the specimens are shown in the sets (b) and (c) figures respectively. Discussion of the test data is given in section 7.3.2 and graphical presentation of the joint

Table 7.2 Numbering System for Joint Specimens Subjected to Horizontal Movements.

		TEST TEMPERATURES			
		10 °C		20 °C	
G A P - M I O C V R E O M N E S N - T S	+ 25 —	25/10C	25/10T	25/20C	25/20T
	+ 50 —	50/10C	50/10T	50/20C	50/20T
	+ 100 —	100/10C	100/10T	100/20C	100/50T
		Compression	Tension	Compression	Tension
INITIAL STRESS CONDITIONS					



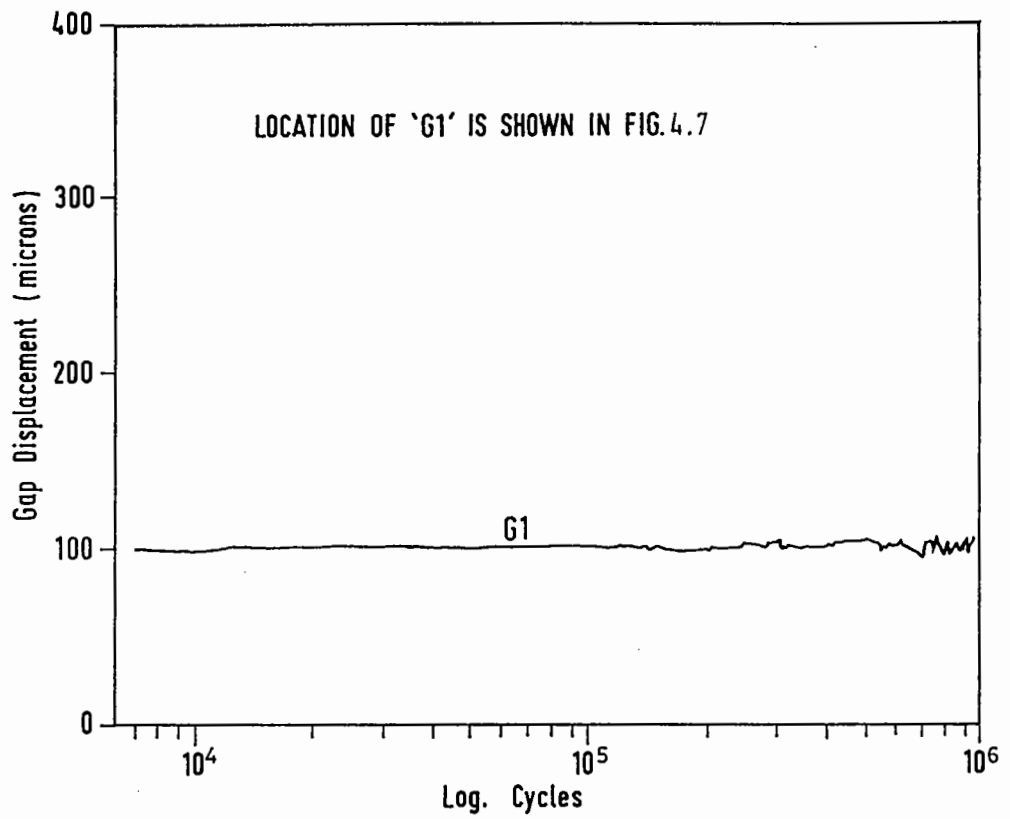


FIG. 7.3 (a) SPECIMEN NO. 25/20C

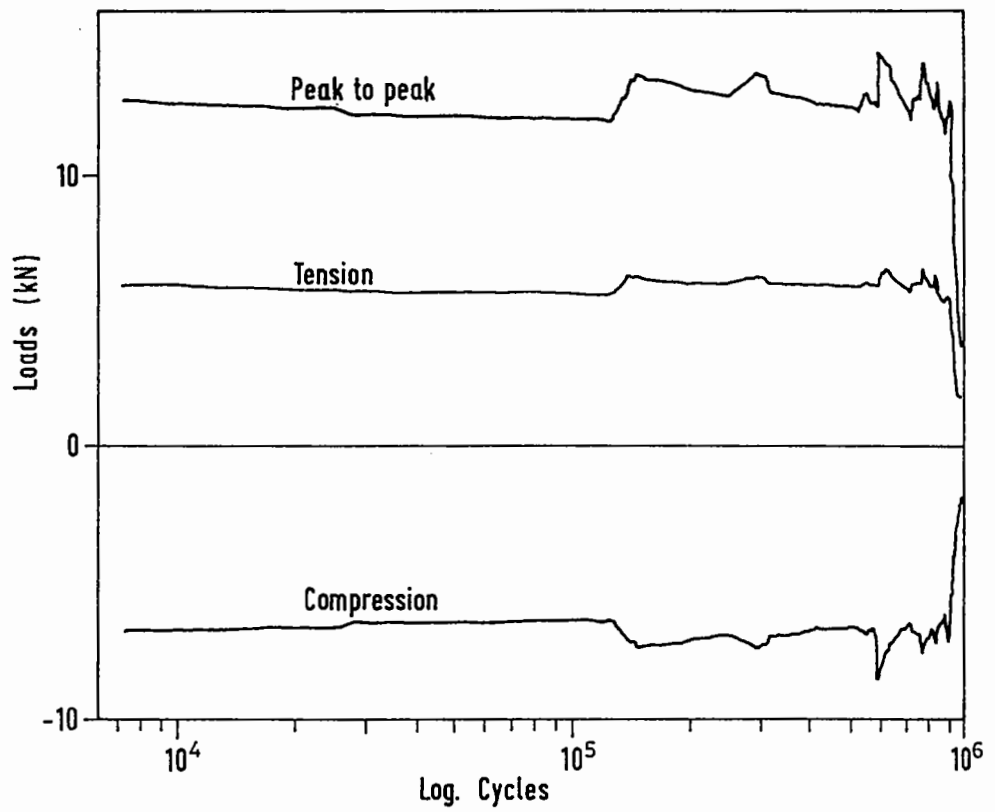


FIG. 7.3 (b) SPECIMEN NO. 25/20C

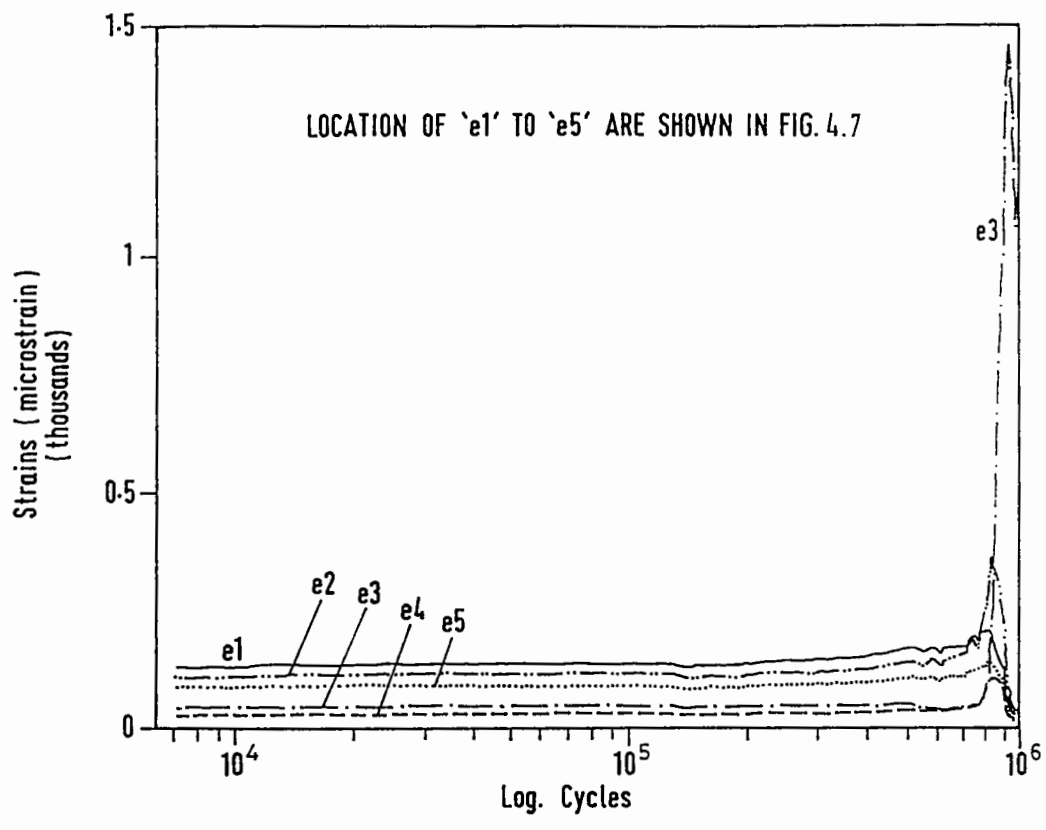


FIG. 73 (c) SPECIMEN NO. 25/20 C

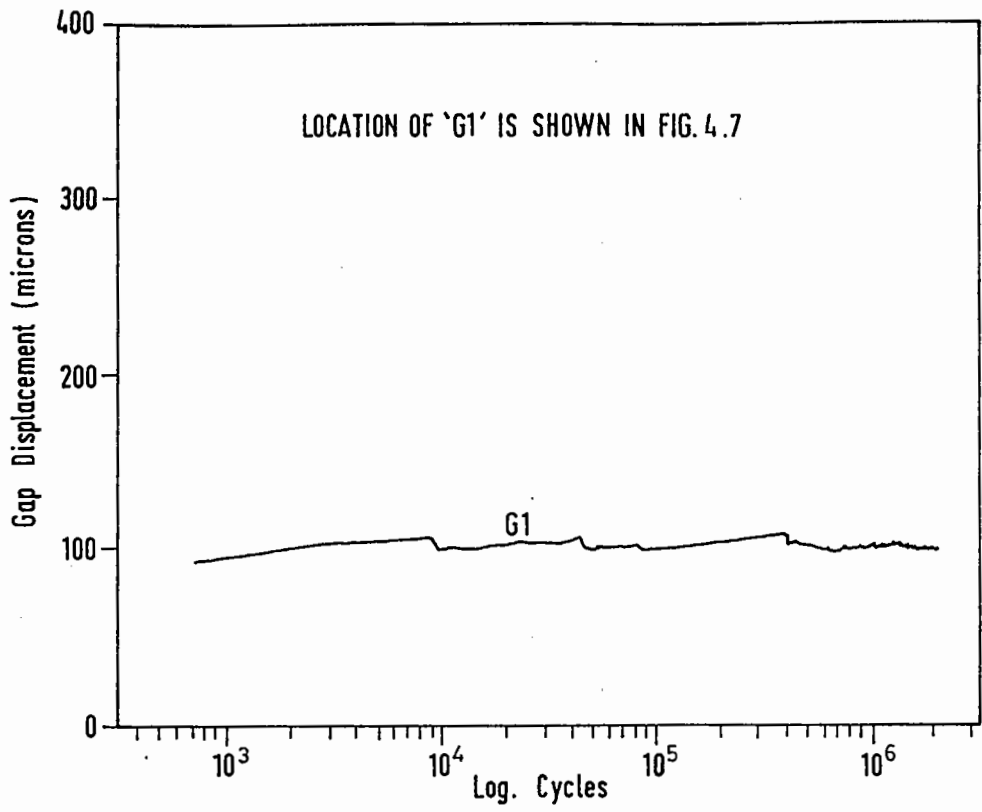


FIG. 7.4 (a) SPECIMEN NO. 50/20C

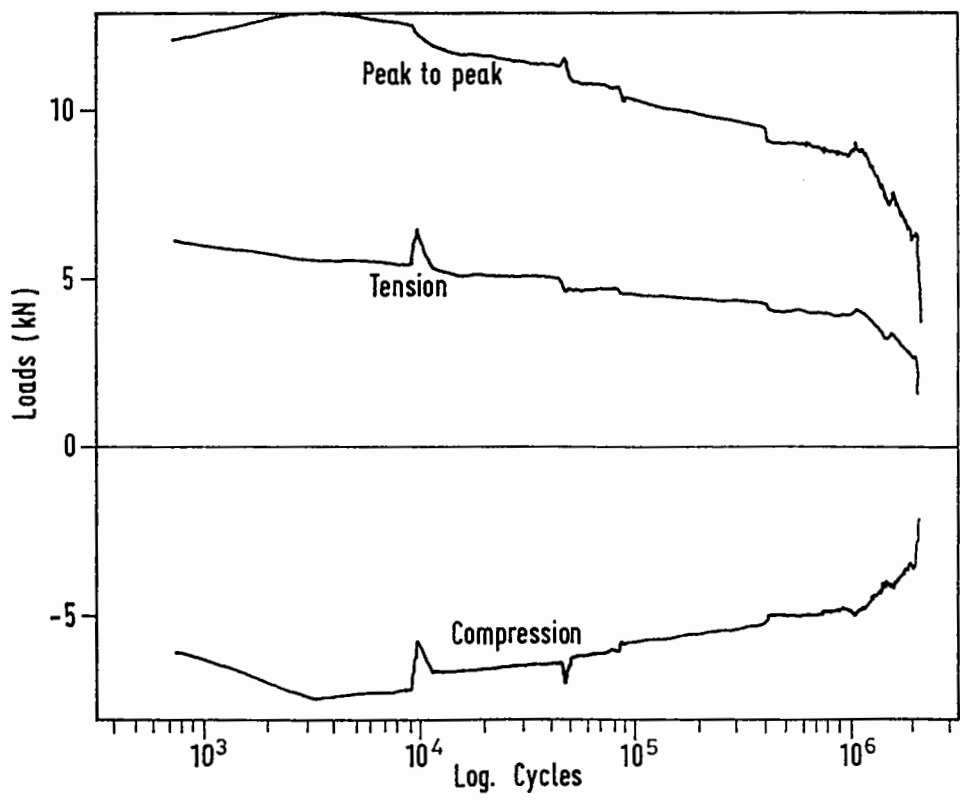


FIG. 7.4 (b) SPECIMEN NO. 50/20C

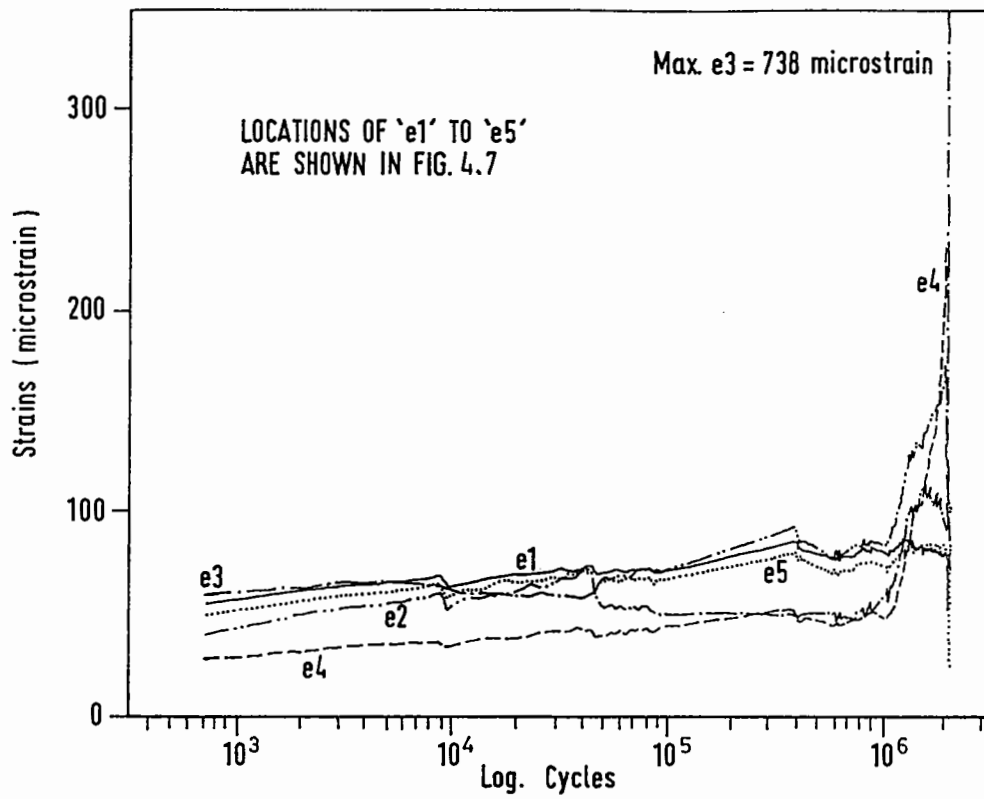


FIG. 7.4 (c) SPECIMEN NO. 50/20 C

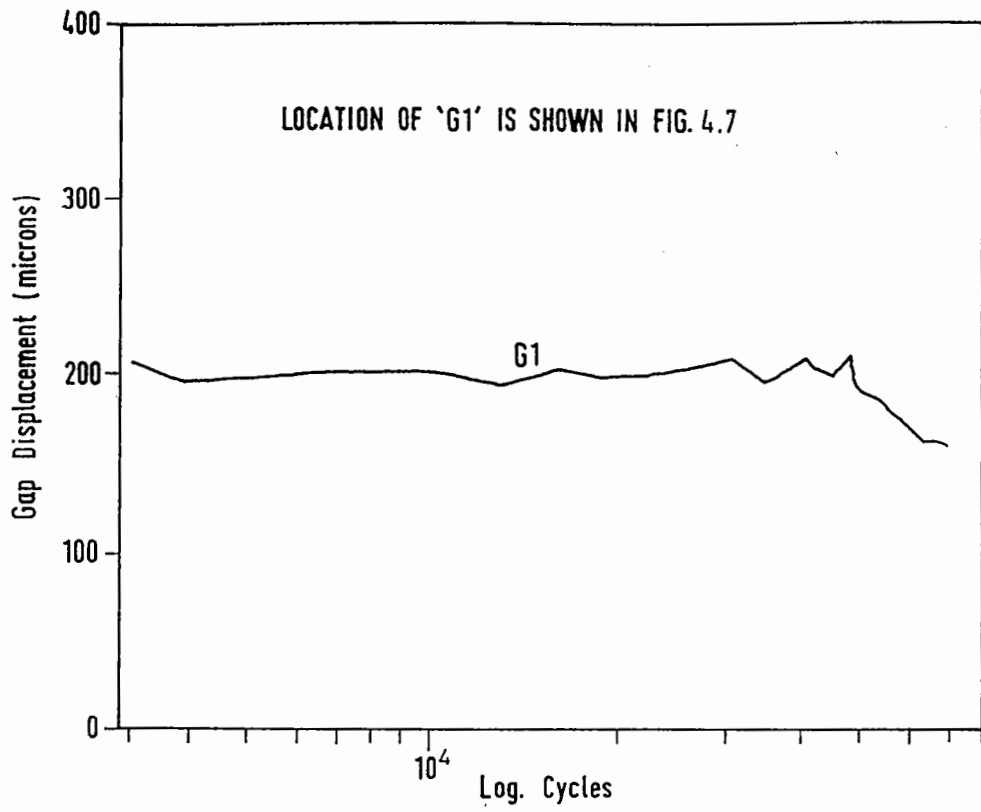


FIG. 7.5 (a) SPECIMEN NO.100/20C

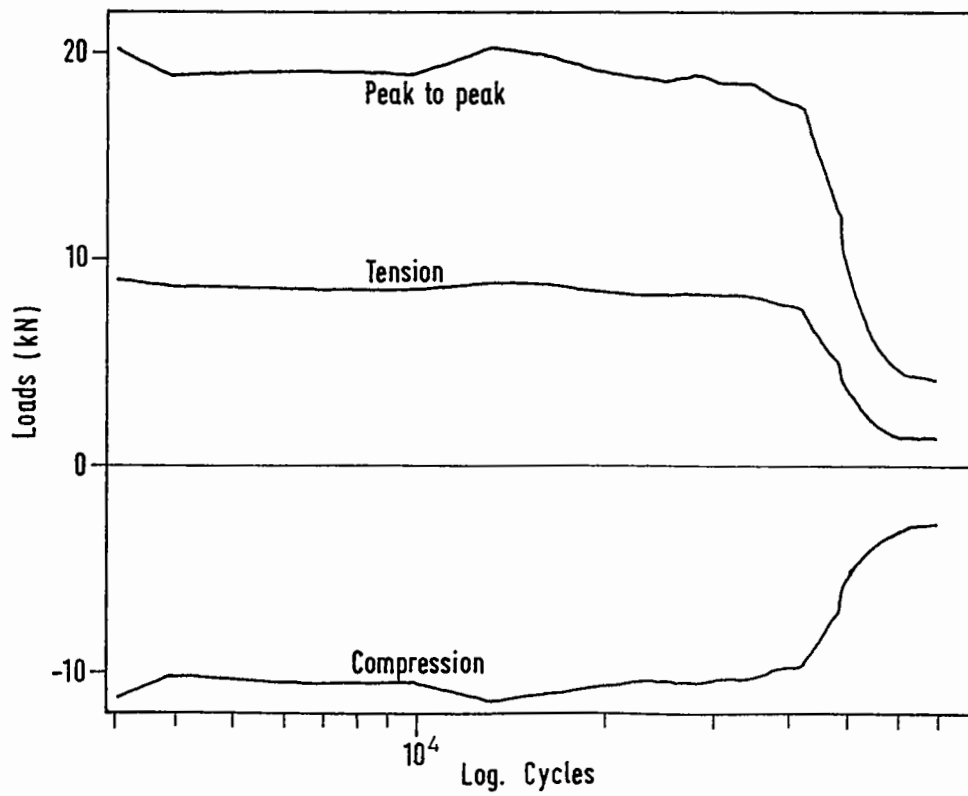


FIG. 7.5 (b) SPECIMEN NO.100/20C

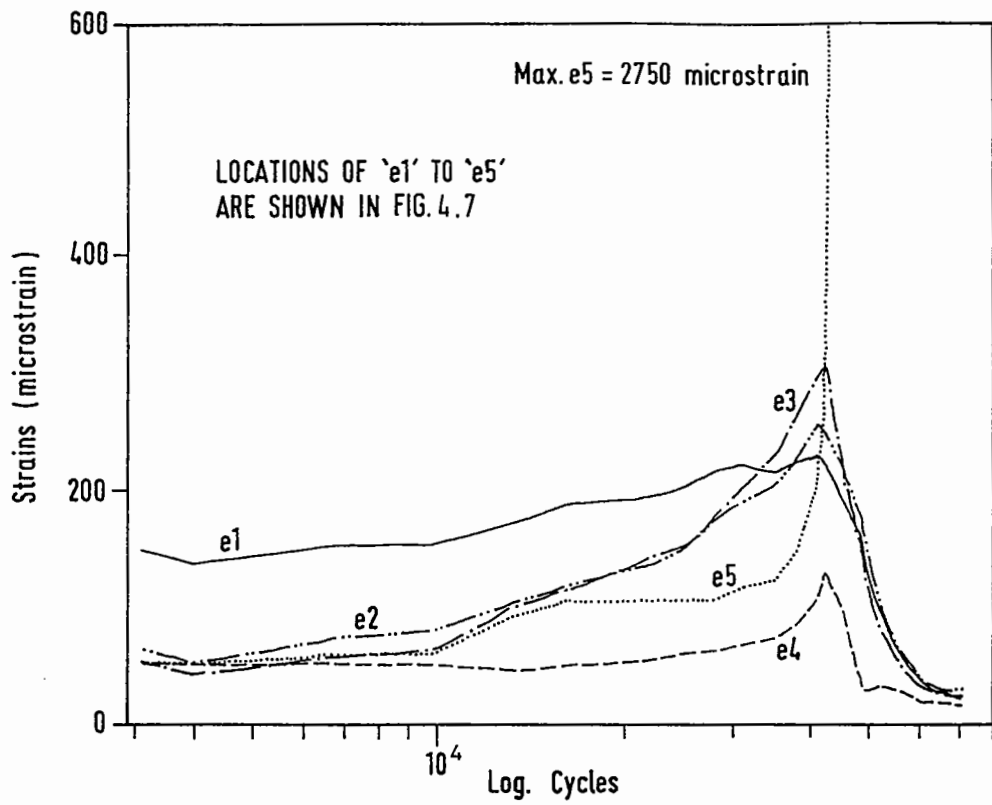


FIG. 7.5 (c) SPECIMEN NO.100/20C

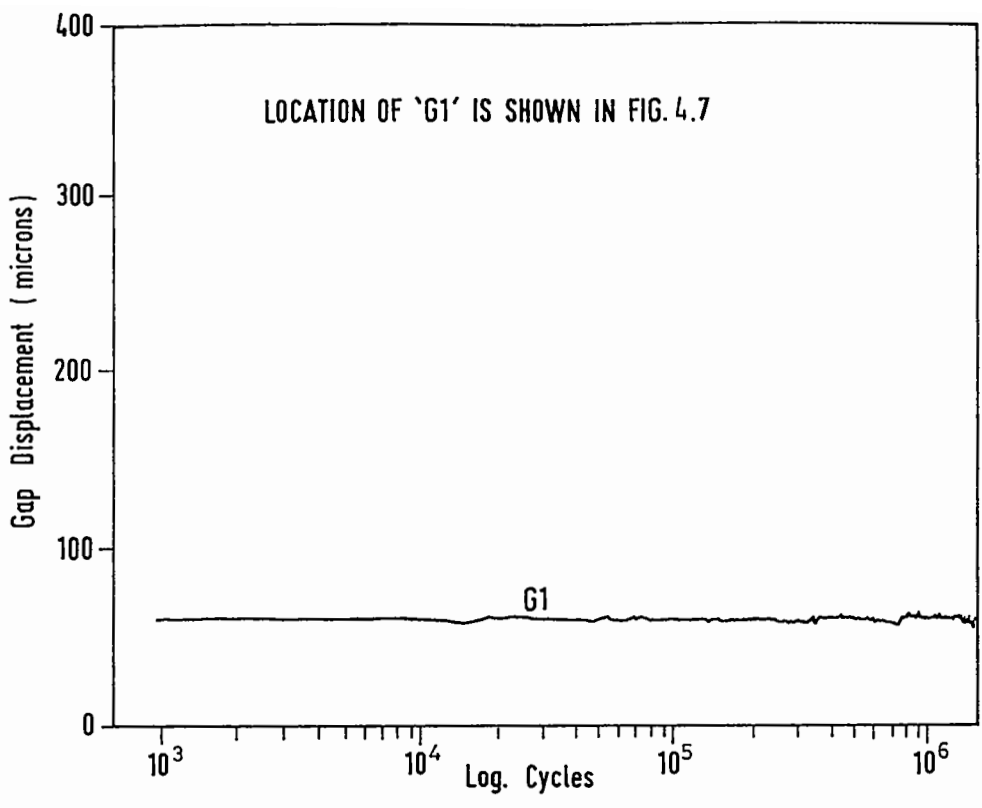


FIG. 7.6 (a) SPECIMEN NO. 30/20T

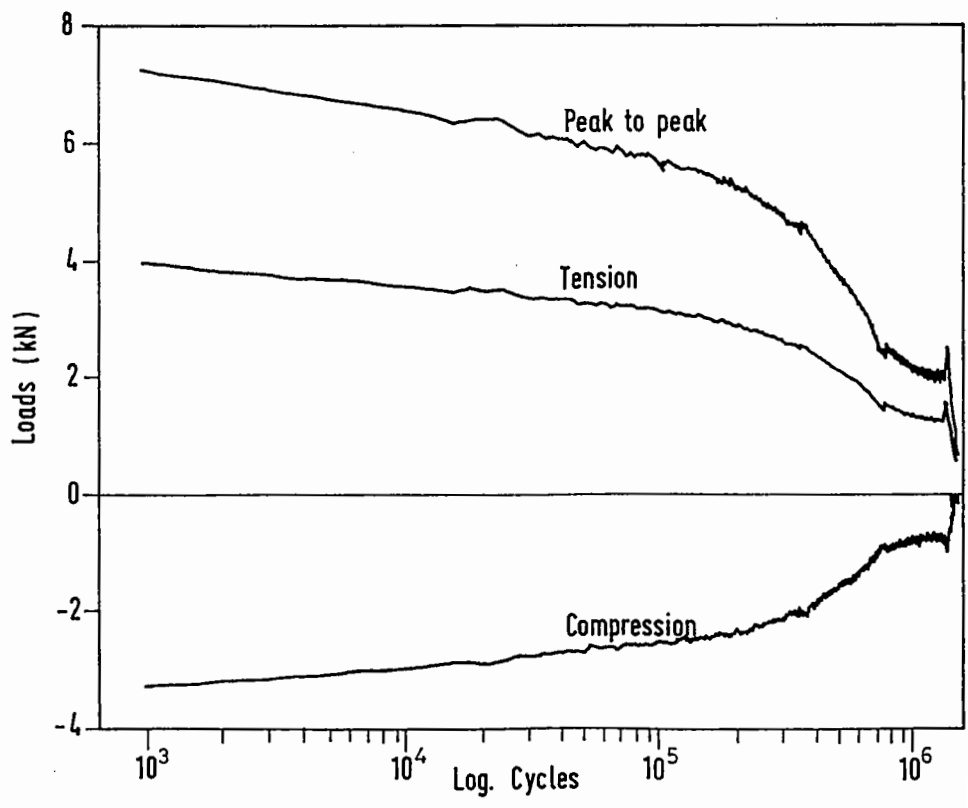


FIG. 7.6 (b) SPECIMEN NO. 30/20T

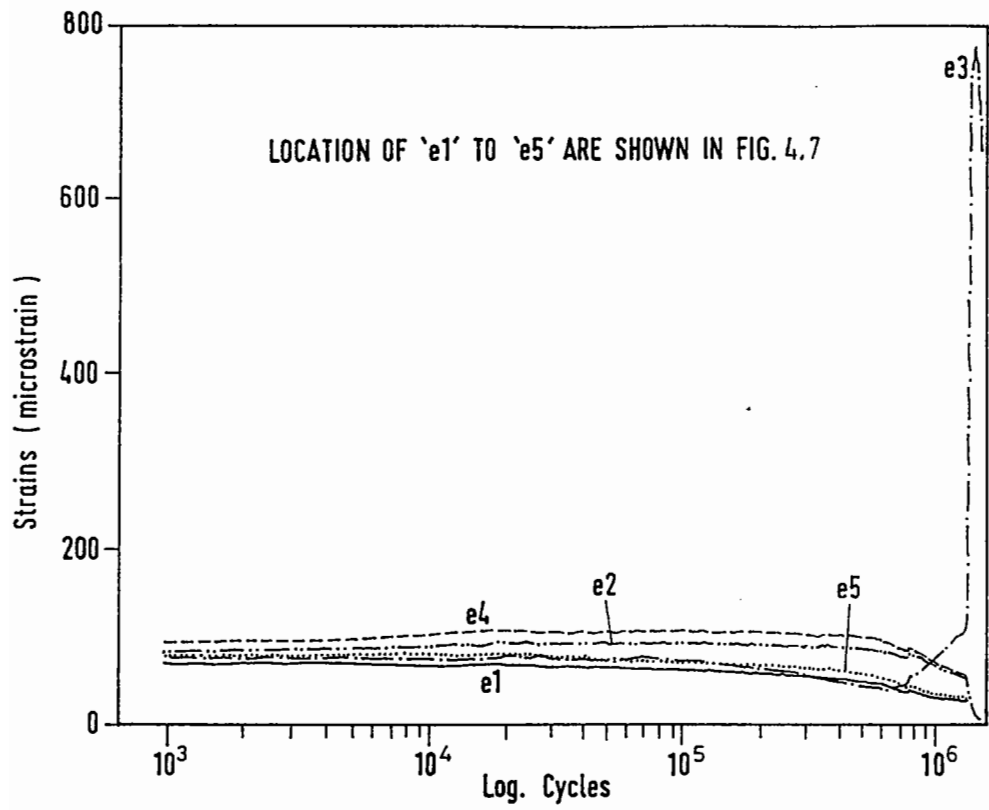


FIG. 7.6 (c) SPECIMEN NO. 30/20T



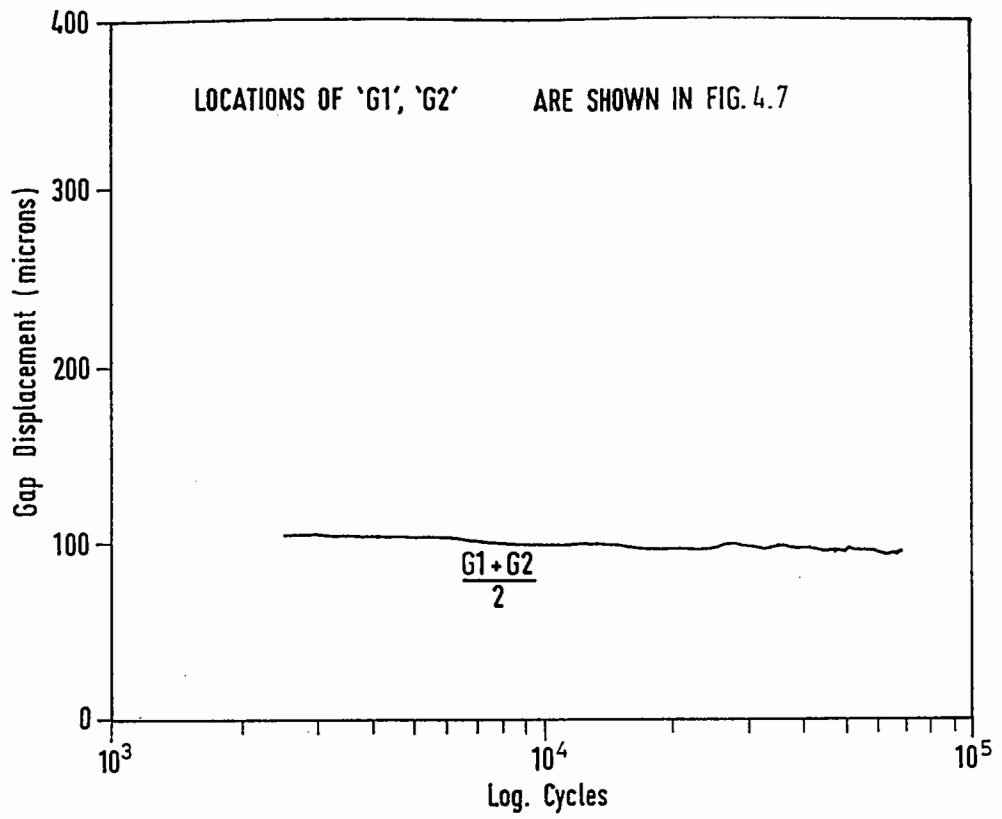


FIG. 7.7 (a) SPECIMEN NO. 50/20T

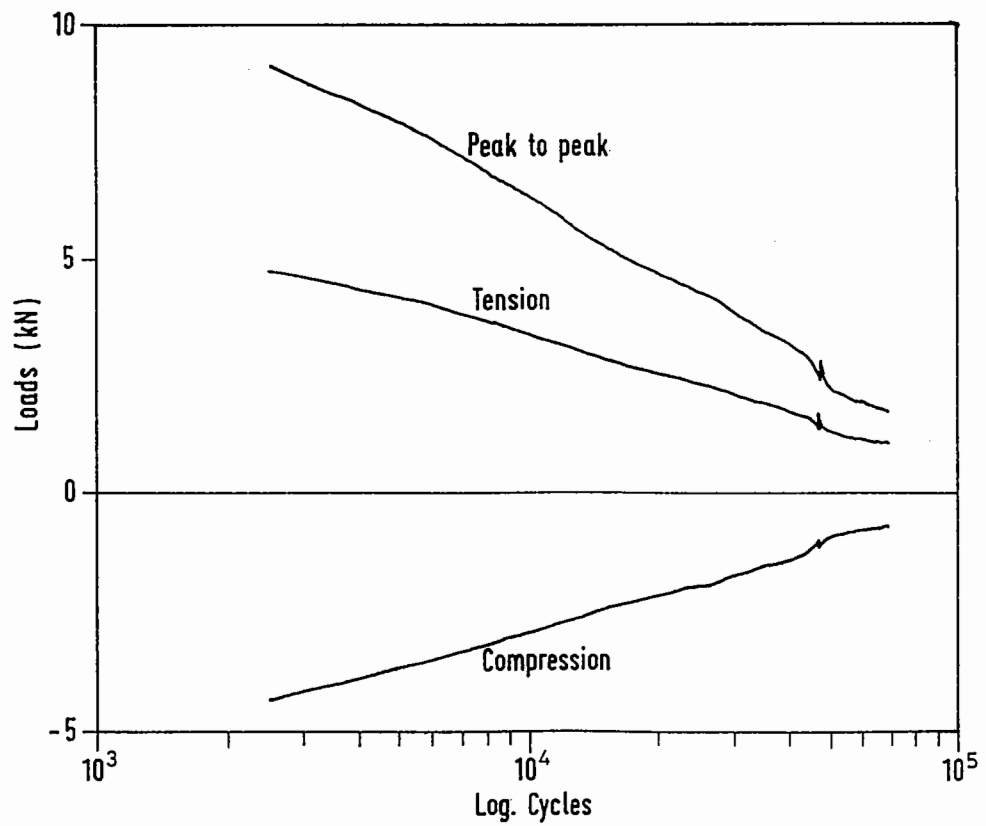


FIG. 7.7 (b) SPECIMEN NO. 50/20T

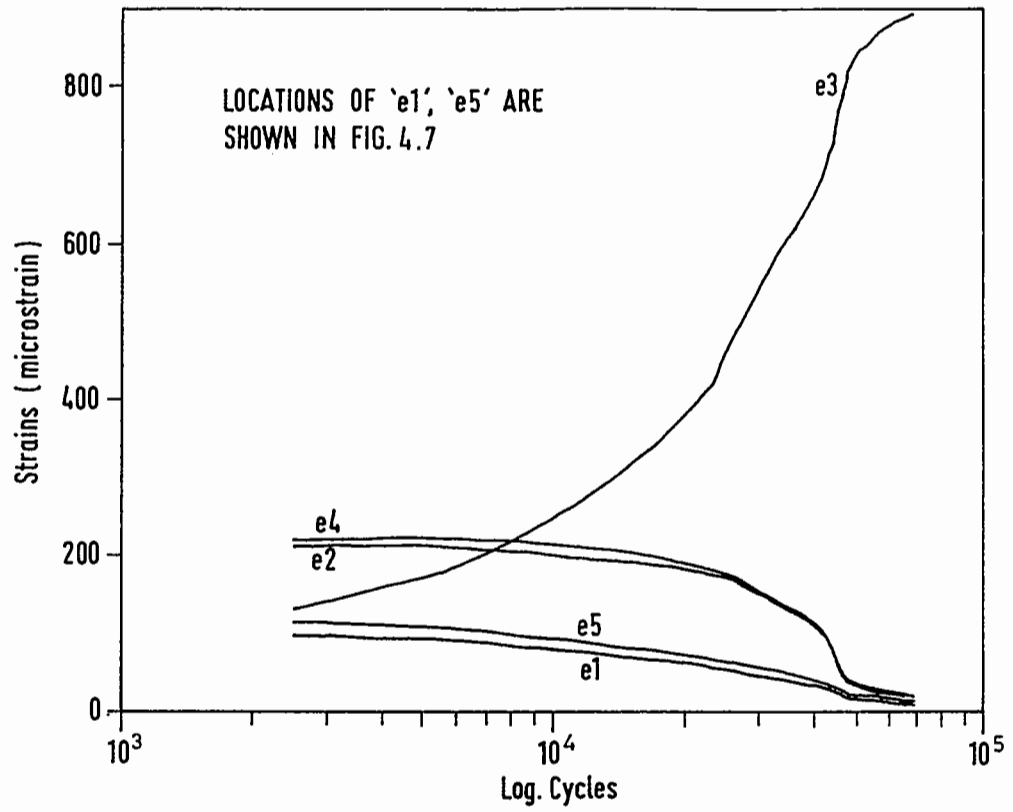


FIG. 7.7 (c) SPECIMEN NO. 50/20T

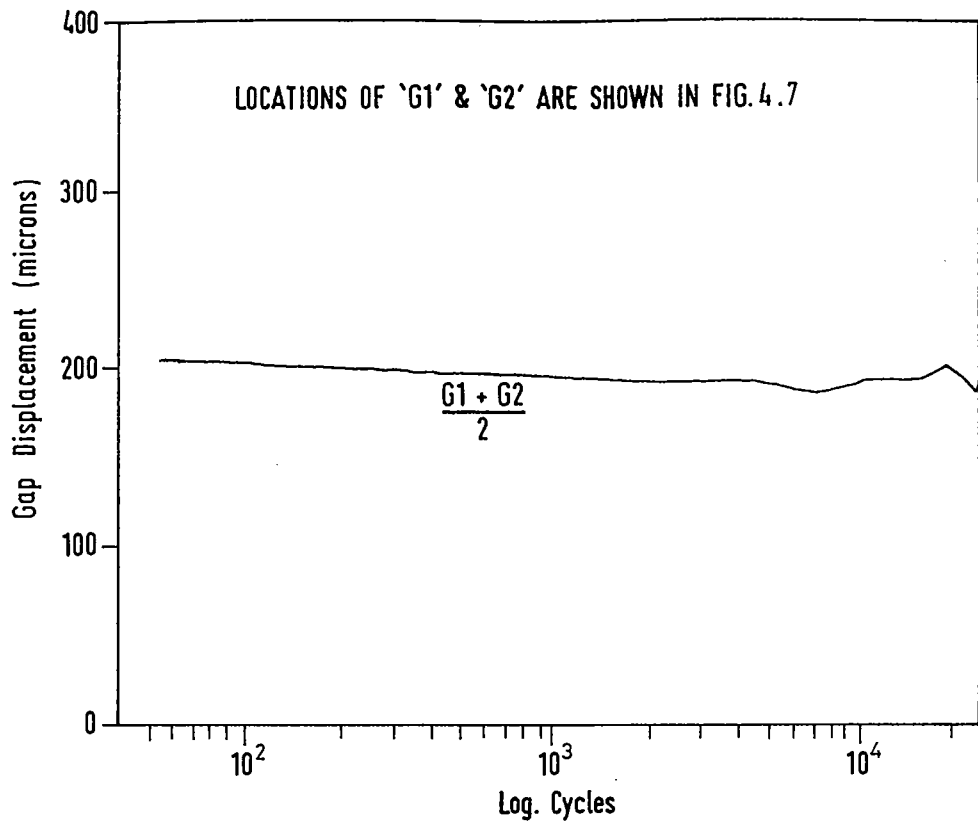


FIG. 7.8 (a) SPECIMEN NO. 100/20T

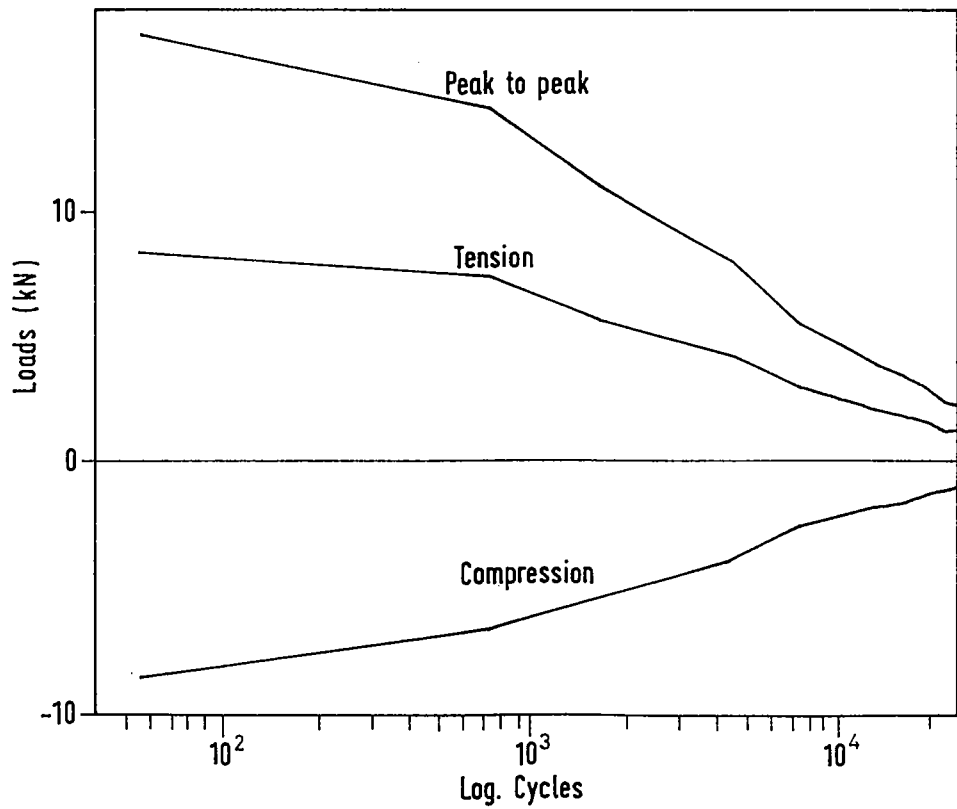


FIG. 7.8 (b) SPECIMEN NO. 100/20T

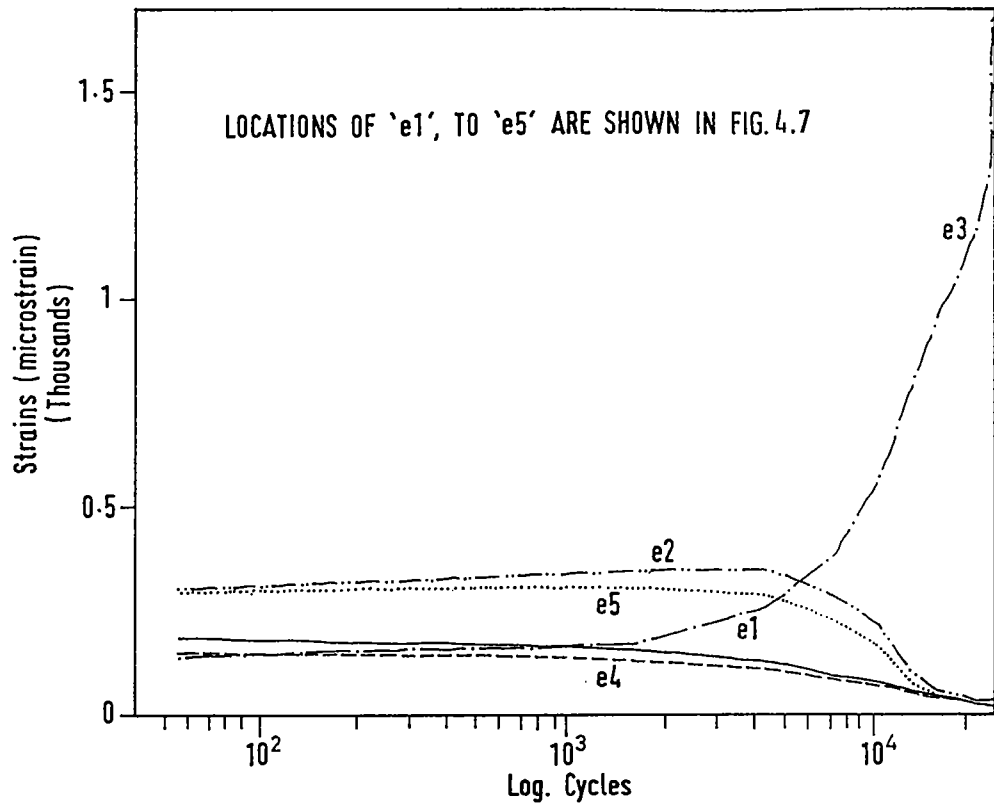


FIG. 7.8(c) SPECIMEN NO. 100/20T

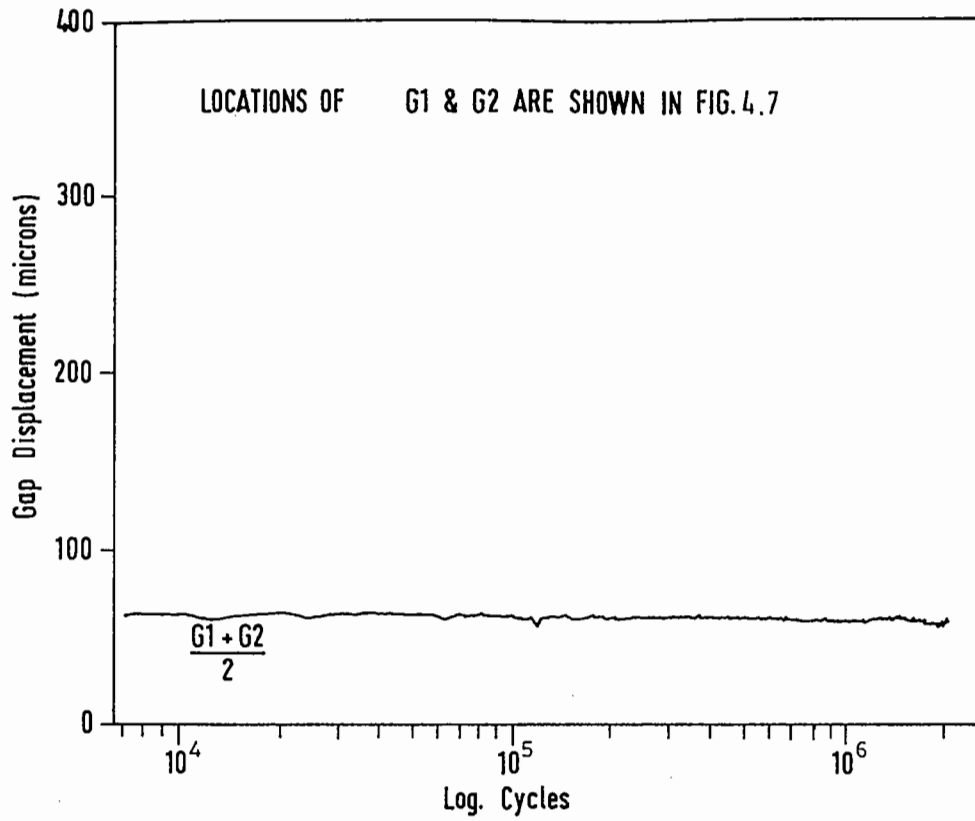


FIG. 7.9 (a) SPECIMEN NO. 30/10C

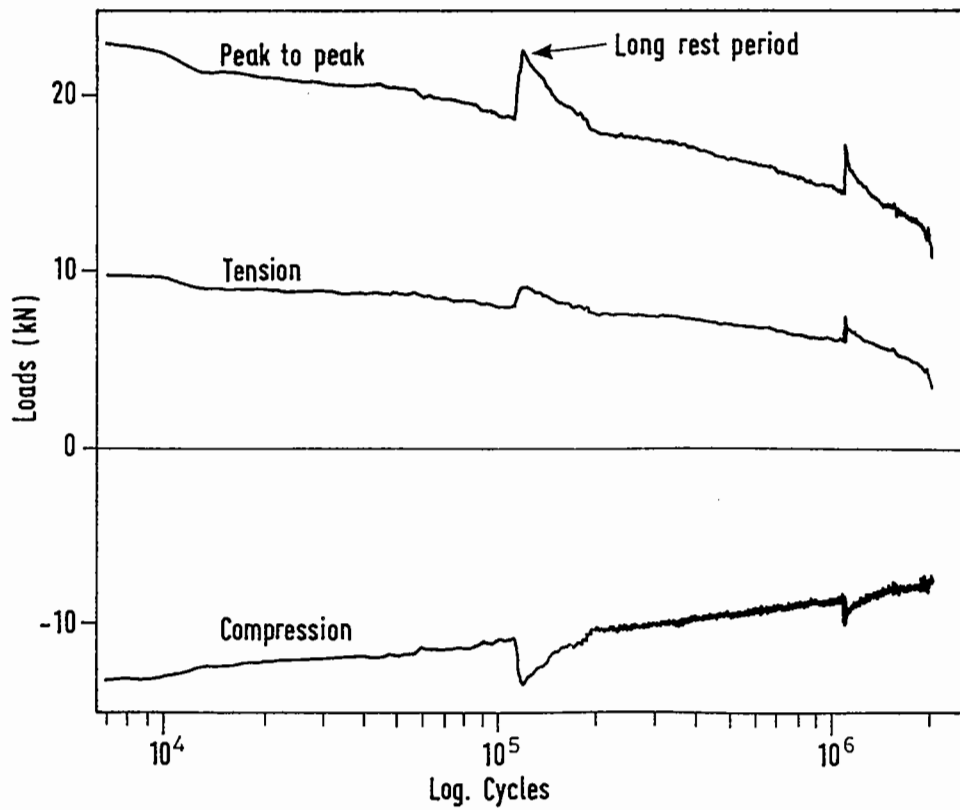


FIG. 7.9 (b) SPECIMEN NO. 30/10C

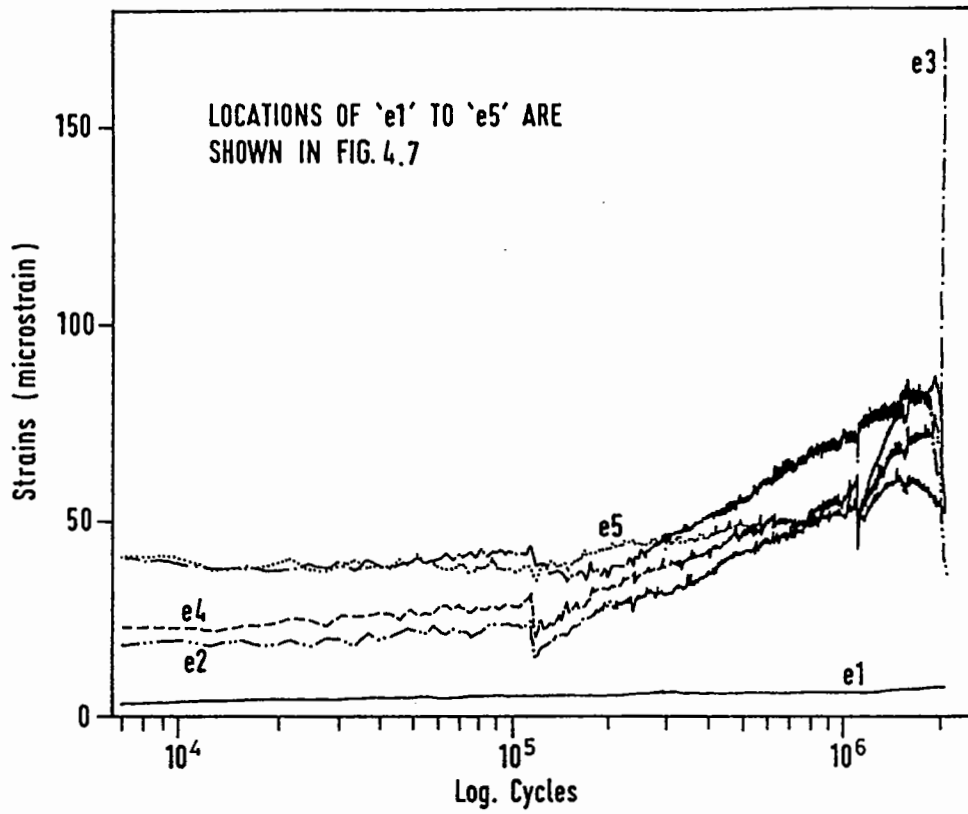


FIG. 7.9 (c) SPECIMEN NO. 30/10C

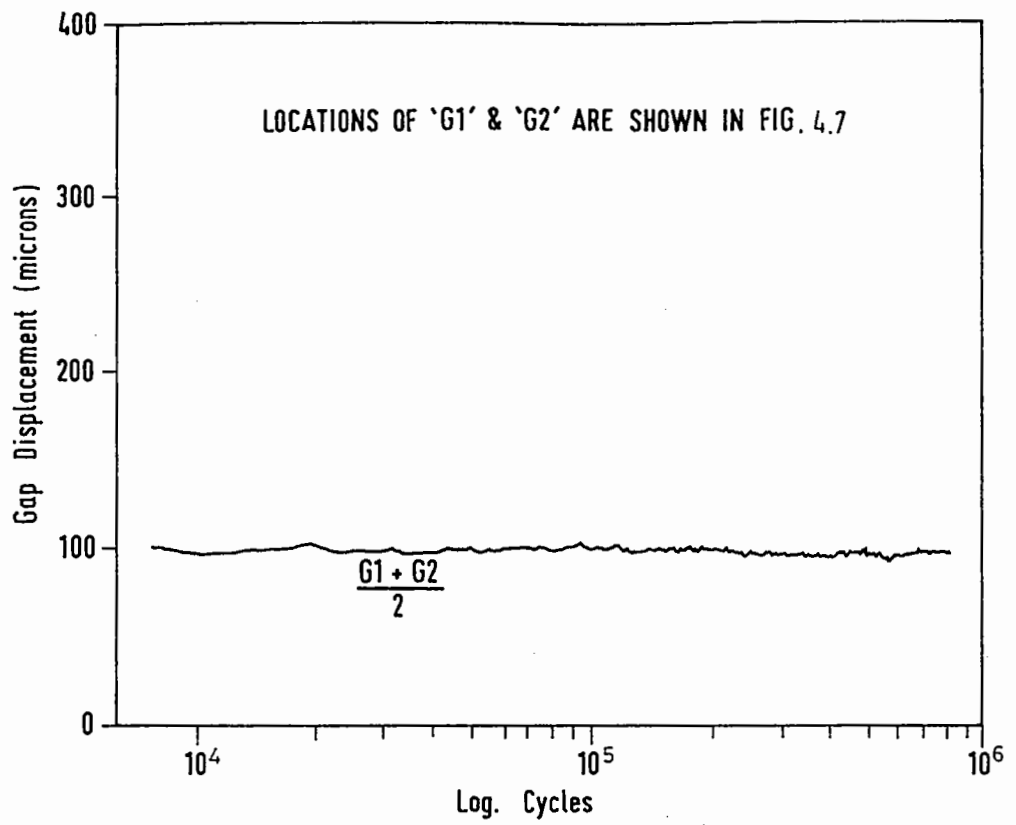


FIG. 7.10 (a) SPECIMEN NO. 50/10C

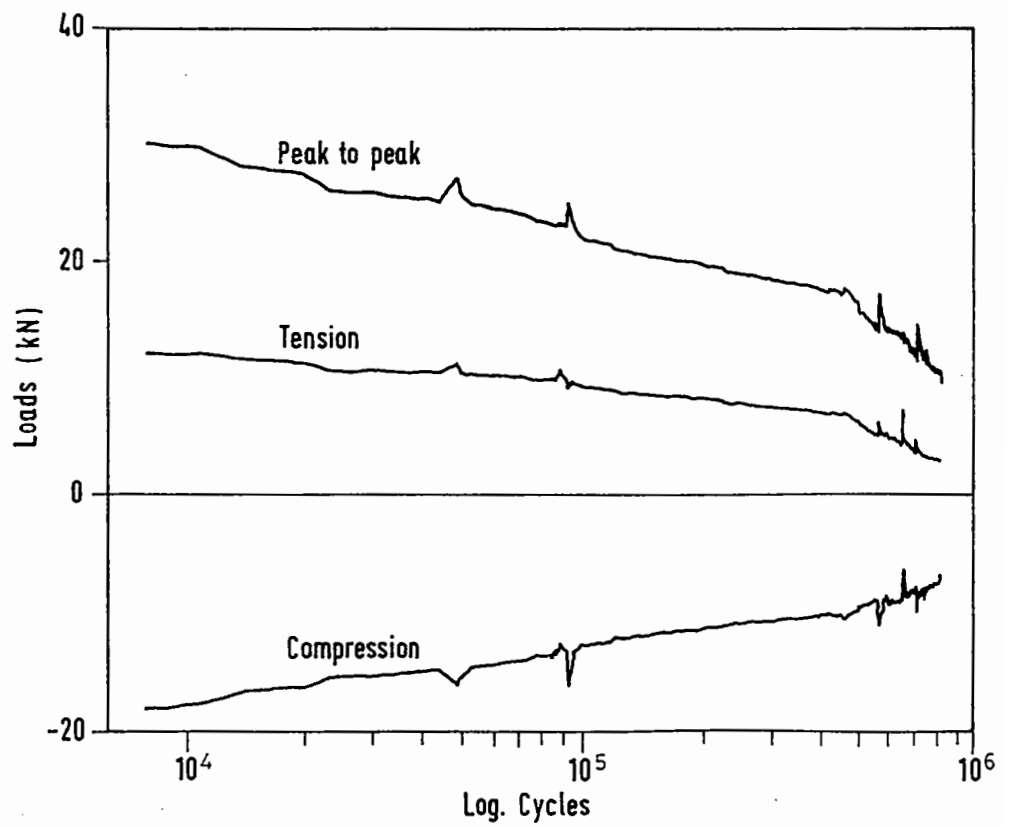


FIG. 7.10 (b) SPECIMEN NO. 50/10C

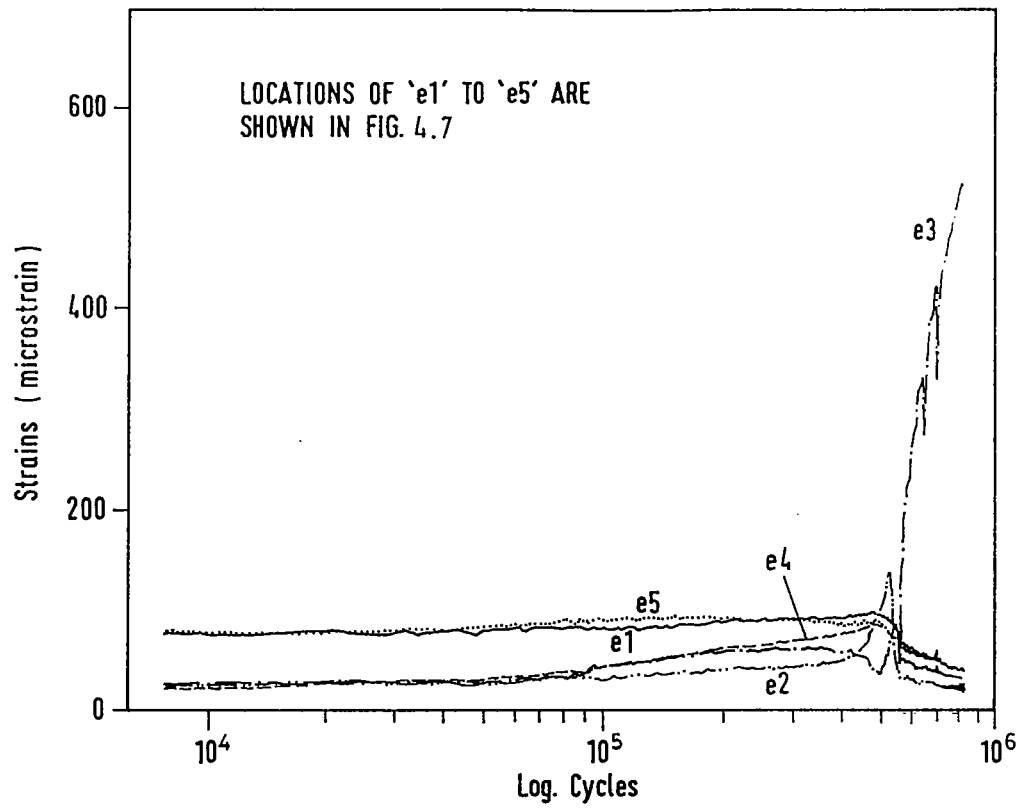


FIG. 7.10 (c) SPECIMEN NO. 50/10C



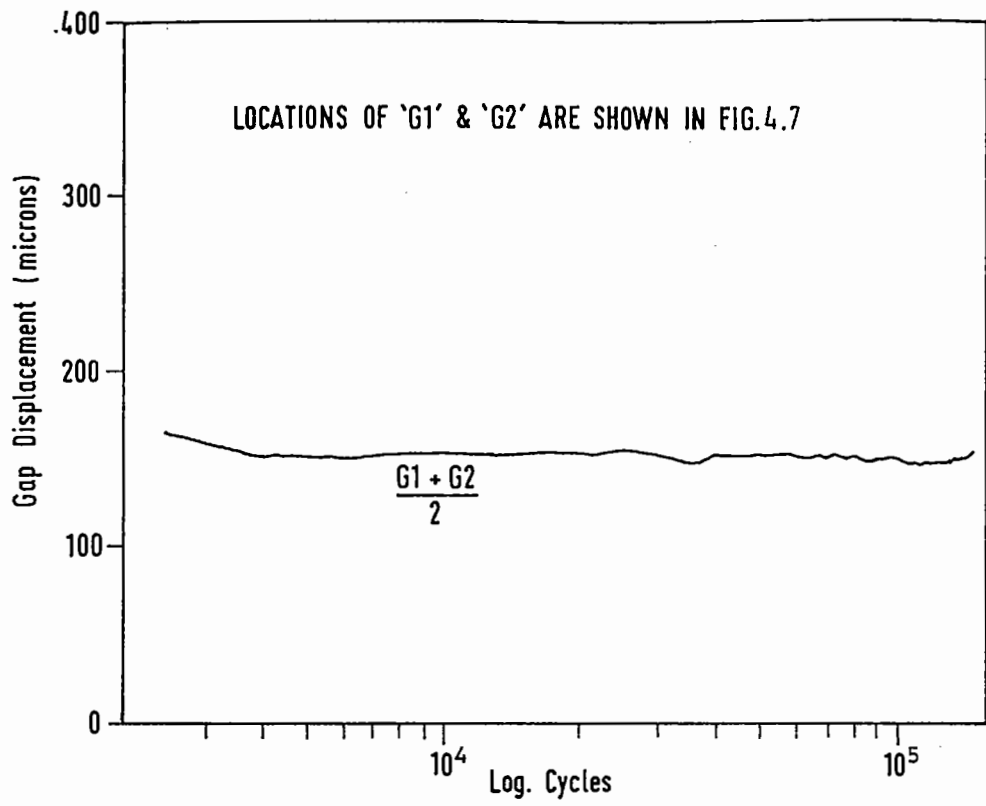


FIG. 7.11 (a) SPECIMEN NO. 75/10C

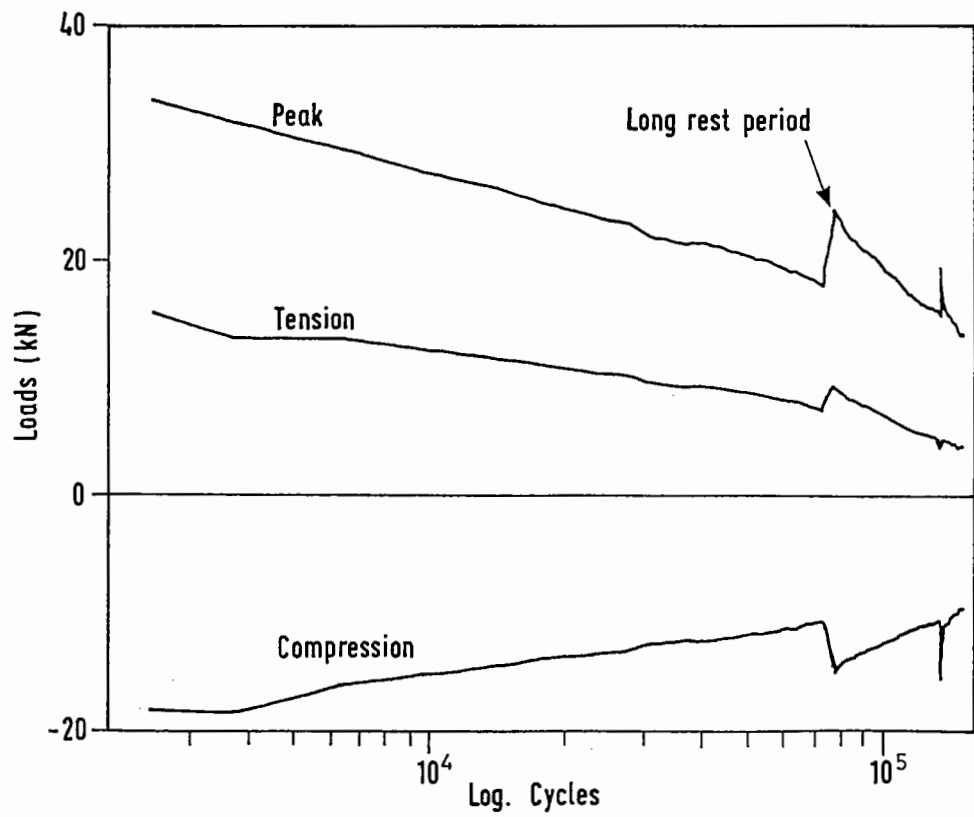


FIG. 7.11 (b) SPECIMEN NO. 75/10C

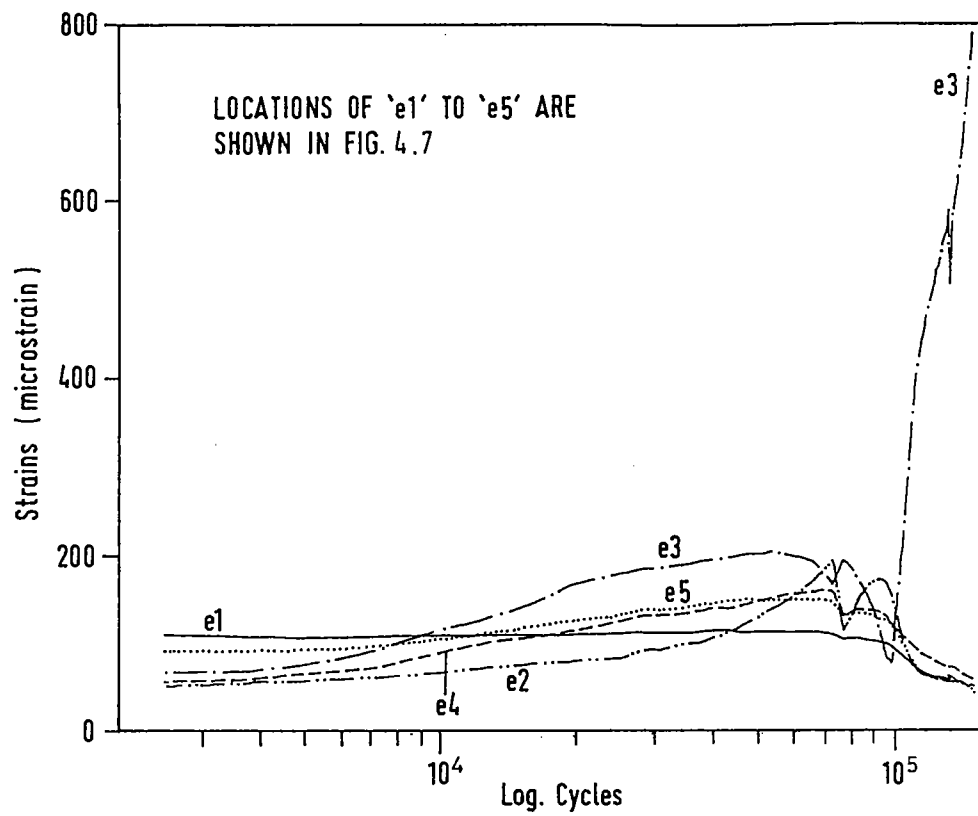


FIG. 7.11 (c) SPECIMEN NO. 75/10 C

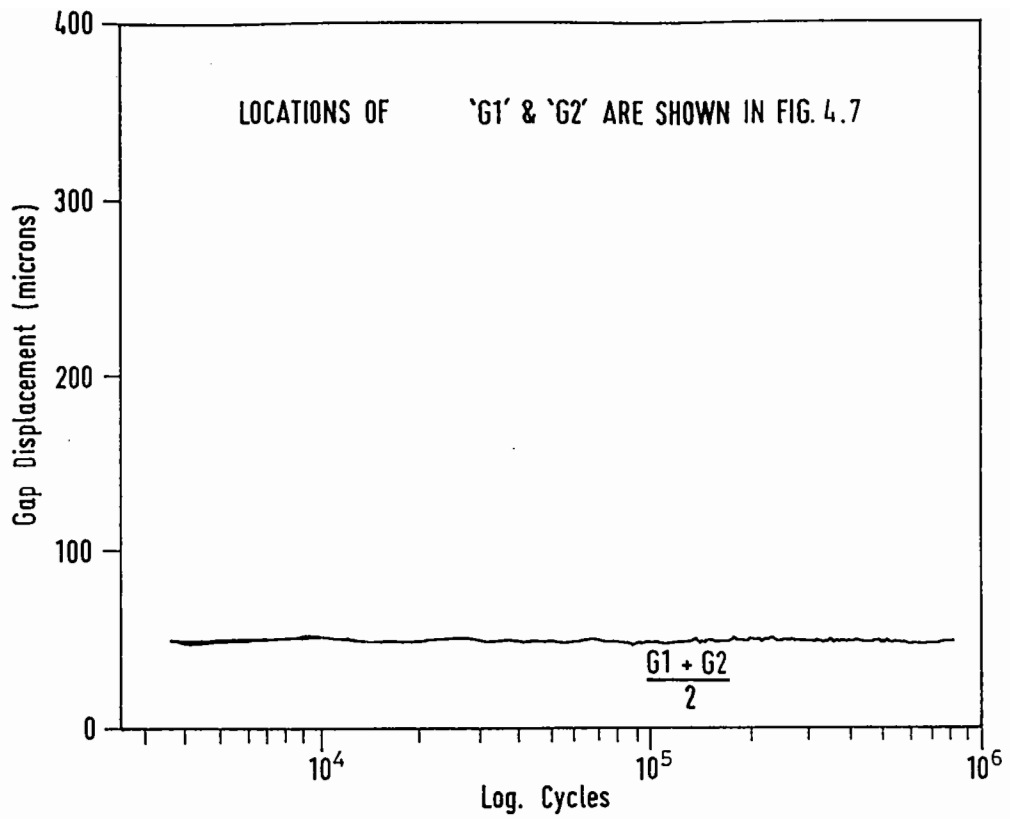


FIG. 7.12 (a) SPECIMEN NO. 25/10T

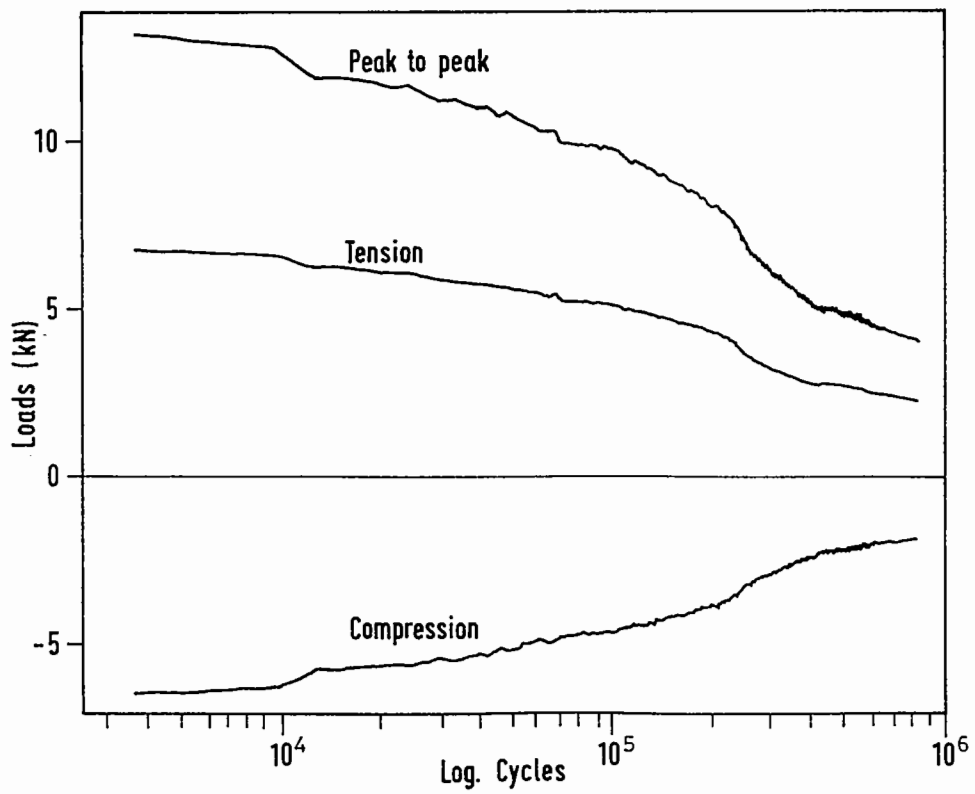


FIG. 7.12 (b) SPECIMEN NO. 25/10T

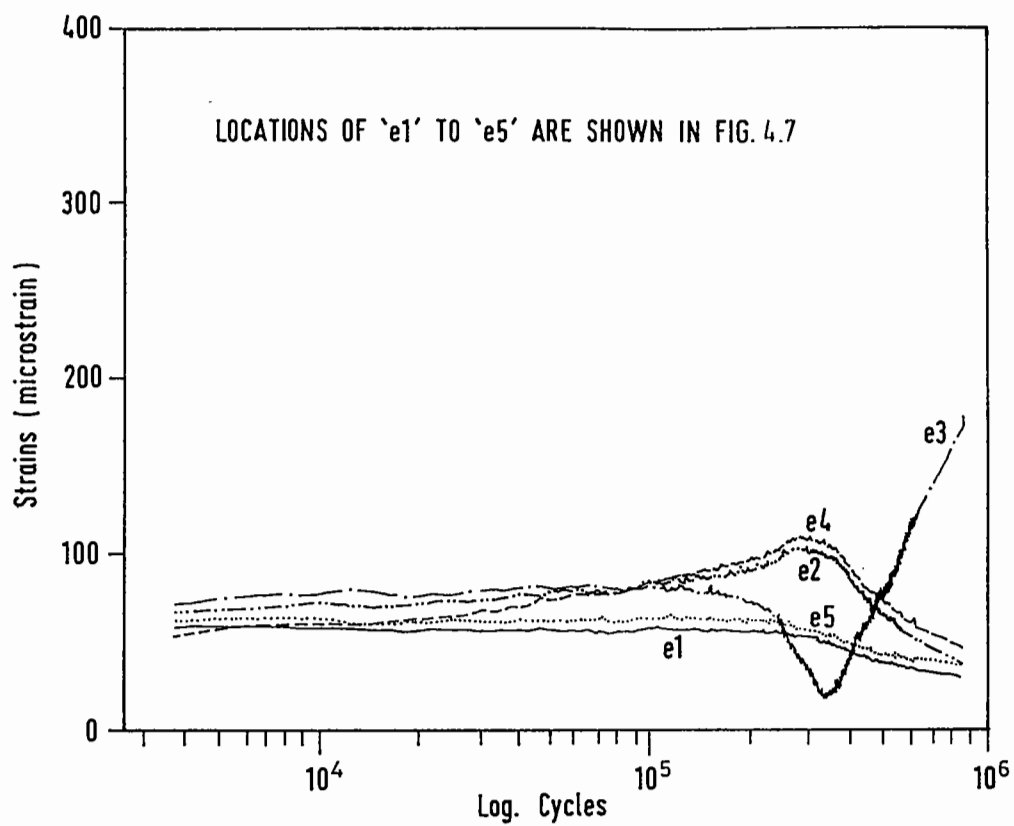


FIG. 7.12 (c) SPECIMEN NO. 25/10T

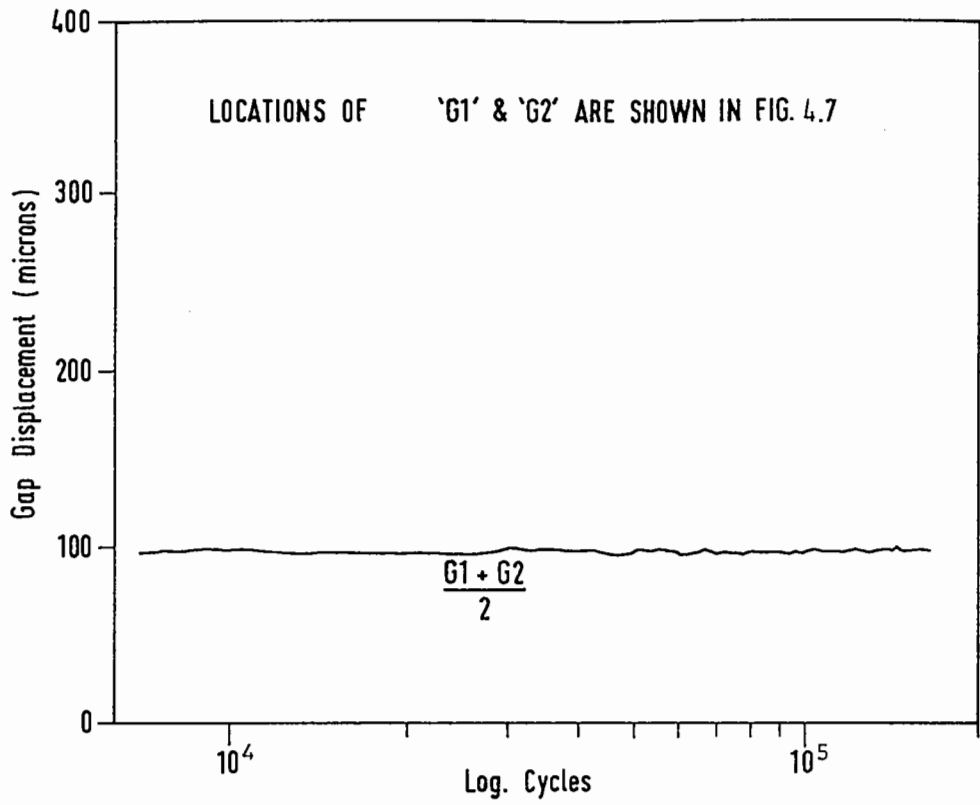


FIG. 7.13 (a) SPECIMEN NO. 50/10T

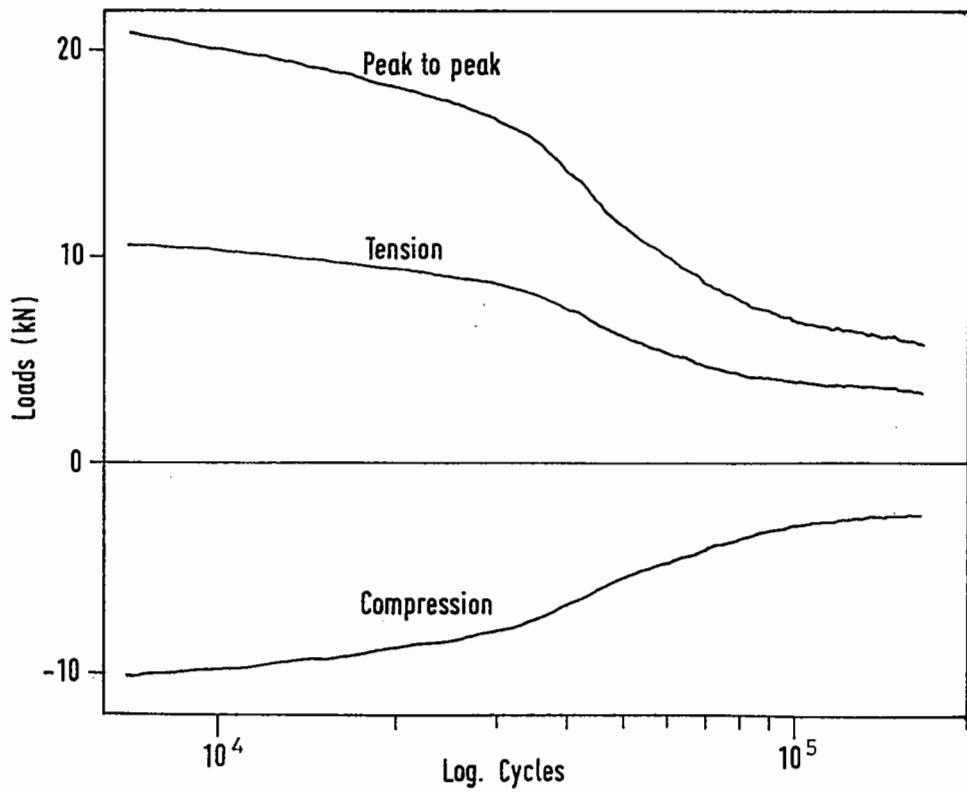


FIG. 7.13 (b) SPECIMEN NO. 50/10T

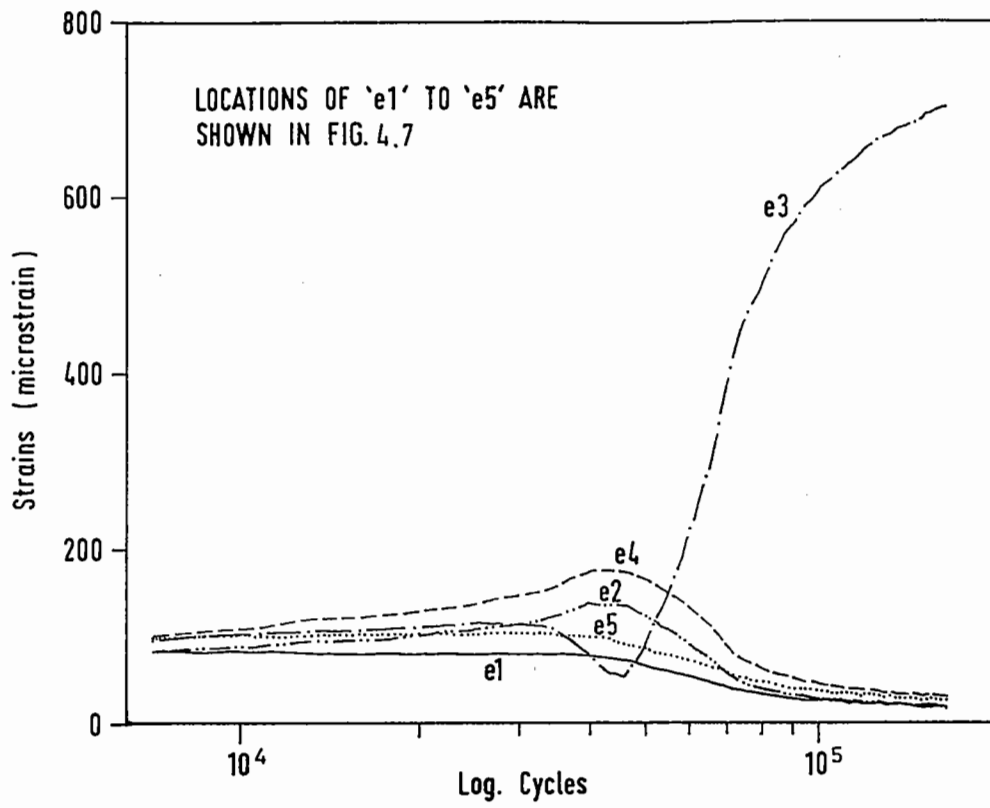


FIG. 7.13 (c) SPECIMEN NO. 50/10T

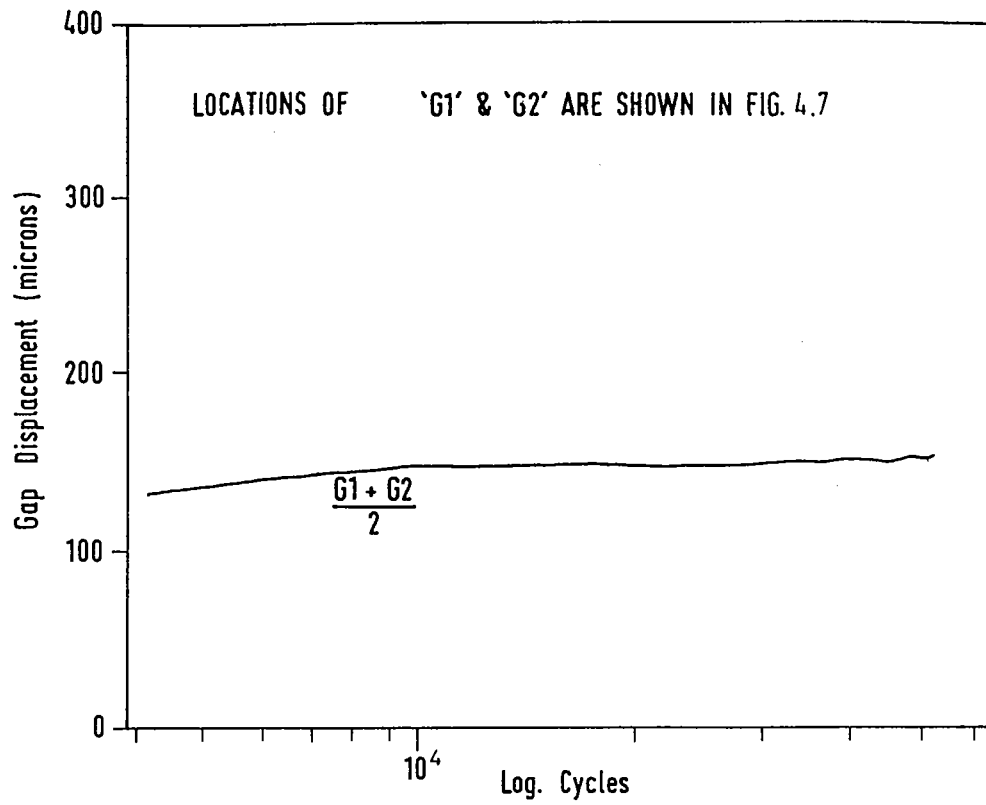


FIG. 7.14 (a) SPECIMEN NO. 75/10T

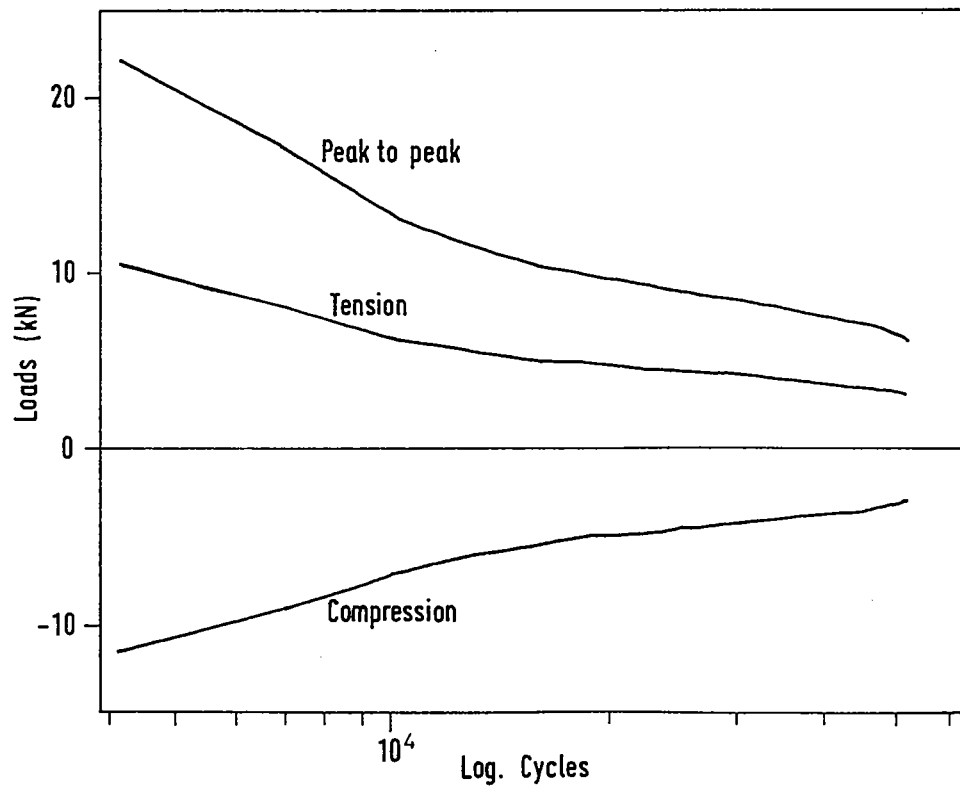


FIG. 7.14 (b) SPECIMEN NO. 75/10T

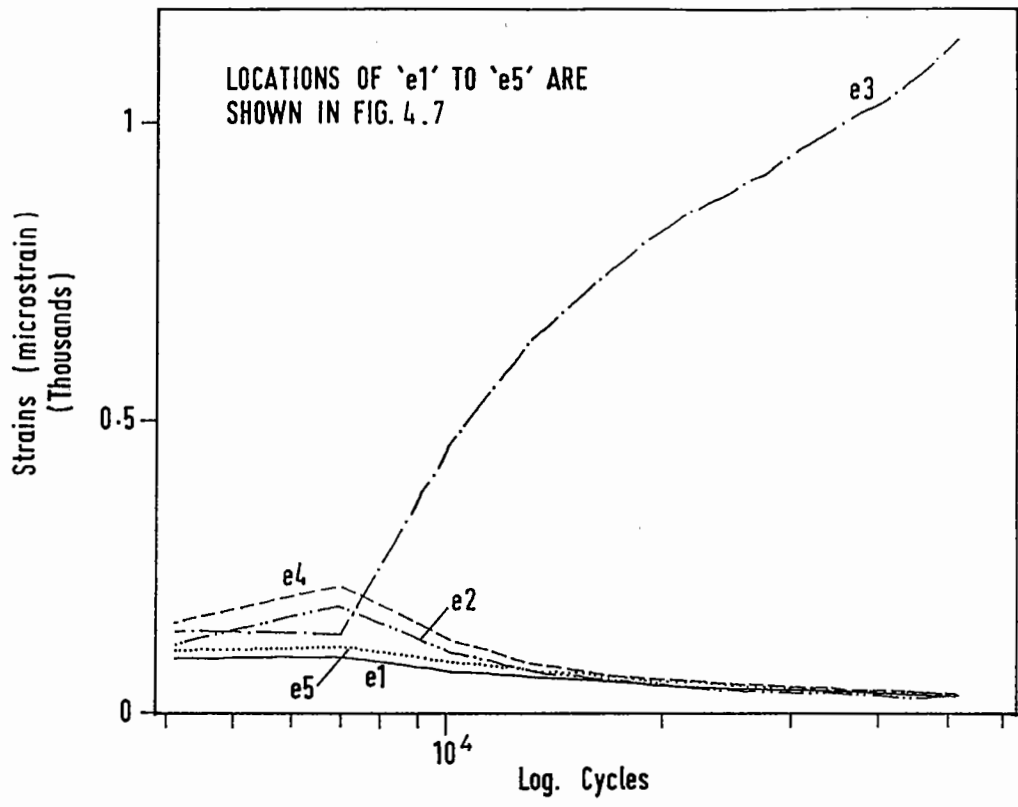


FIG. 7.14 (c) SPECIMEN NO. 75/10T



performance in the tests is given in section 7.3.3.

#### 7.3.1 Test Observations on Group 1 Specimens.

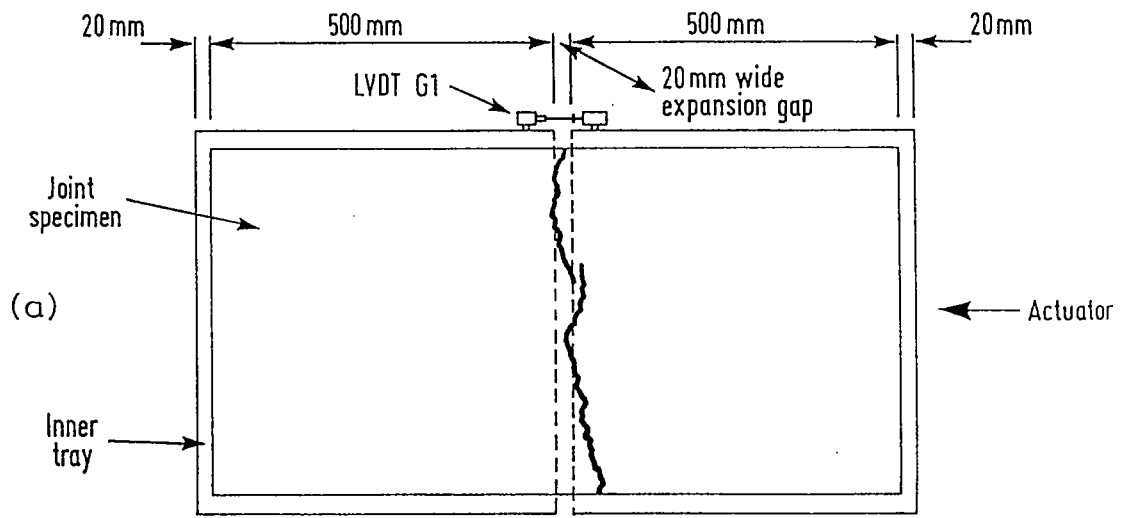
##### (a) Specimen No. 25/20C.

This was the first specimen in this series to be compacted using the 500 t MAN machine and the details of the compaction process are described in section 6.4.1. Pre-compression of the specimen was carried out at 20 °C with a computer controlled applied stress of about 100 kPa. Surprisingly, it took four days (96 hours) to complete, compared with about 8 hrs for specimen no. 1. Higher resistance to creep may indicate that a higher degree of compaction had been achieved by using the new compaction method.

Test on specimen no. 25/20C started with a gap movement of  $\pm 25$  microns and no crack was found up to 4,000,000 cycles. Since this took nearly three weeks, it was decided to increase the gap movement to  $\pm 50$  microns, and after a further 940,000 cycles, the specimen failed. In these tests, the recorded compressive load was relatively higher than the tensile load as shown in Fig. 7.3 (b). Fig. 7.15 (a) shows that the crack again occurred close to the joint gap.

##### (b) Specimen No. 50/20C

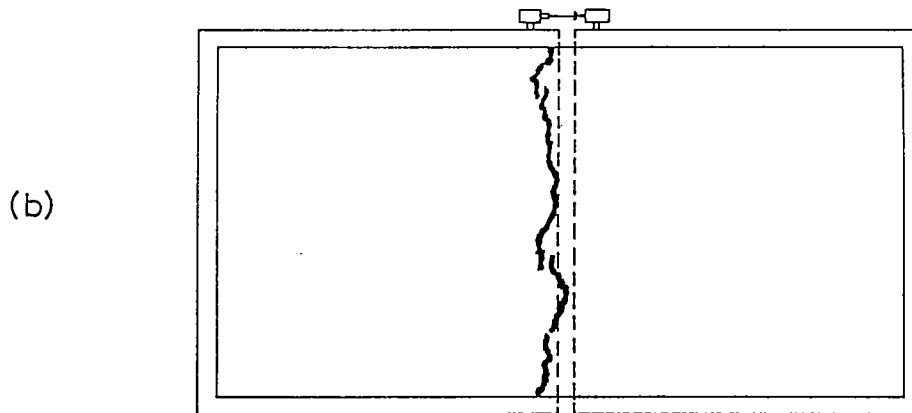
In order to reduce the time spent on pre-compression, while not



(a)

SPECIMEN NO. 25/20C

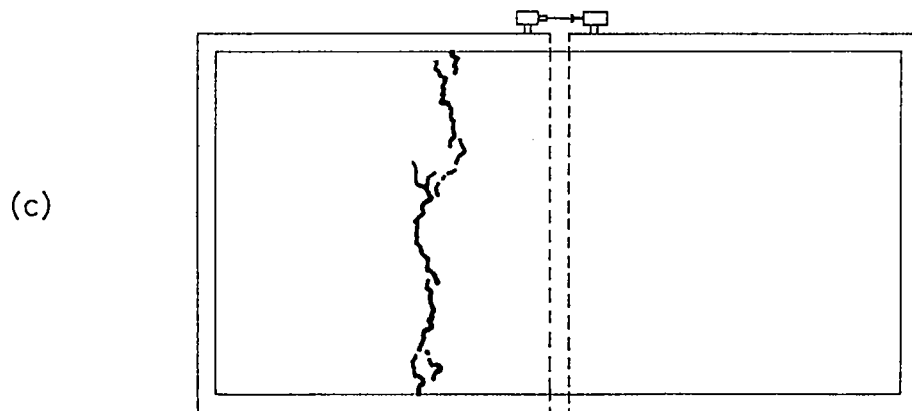
- a) PRECOMPRESSED
- b) MOVEMENT =  $\pm 25$  microns  
 $\pm 50$  microns



(b)

SPECIMEN NO. 50/20C

- a) PRESTRETCHED
- b) MOVEMENT =  $\pm 50$  microns



(c)

SPECIMEN NO. 100/20C

- a) PRECOMPRESSED
- b) MOVEMENT =  $\pm 100$  microns

**FIG.7.15** CRACKS INDUCED AT EXPANSION JOINT AFTER FAILURE (SPECIMENS NO. 25/20C, 50/20C & 100/20C)

damaging the specimen, it was decided to increase the temperature to 40 °C before pre-compression was started. The specimen reached the 3 mm gap reduction within an hour under a constant pressure of about 100 kPa. This resembles the temperature and pressure used in a standard creep test for cylindrical samples of asphalt mixes. The temperature of 40 °C is within the range which can occur for pavements in the U.K. during the summer. However, prestretching of a specimen was still performed at 20 °C and with an applied stress not greater than 35 kPa. This temperature was required to maintain a sufficient tensile strength in the specimen to resist the tensile force and distribute it without causing undesirable local cracking. When the pre-compression was completed, the specimen was allowed to cool down to 20 °C before starting the cyclic test.

The applied cyclic gap movement was  $\pm 50$  microns (Fig. 7.4 (a)) and a single continuous crack was developed after 2,015,000 test cycles. It cracked near the joint gap as shown in Figs. 7.15 (b) & 7.16. The compressive load was higher than the tensile load as expected for a pre-compressed specimen (Fig. 7.4 (b)).

(c) Specimen No. 100/20C

Since the results obtained from the previous two tests were encouraging, it was decided to test specimen no. 100/20C without further alteration to the test method and instrumentation. This would complete a set of three successful tests. The magnitude of

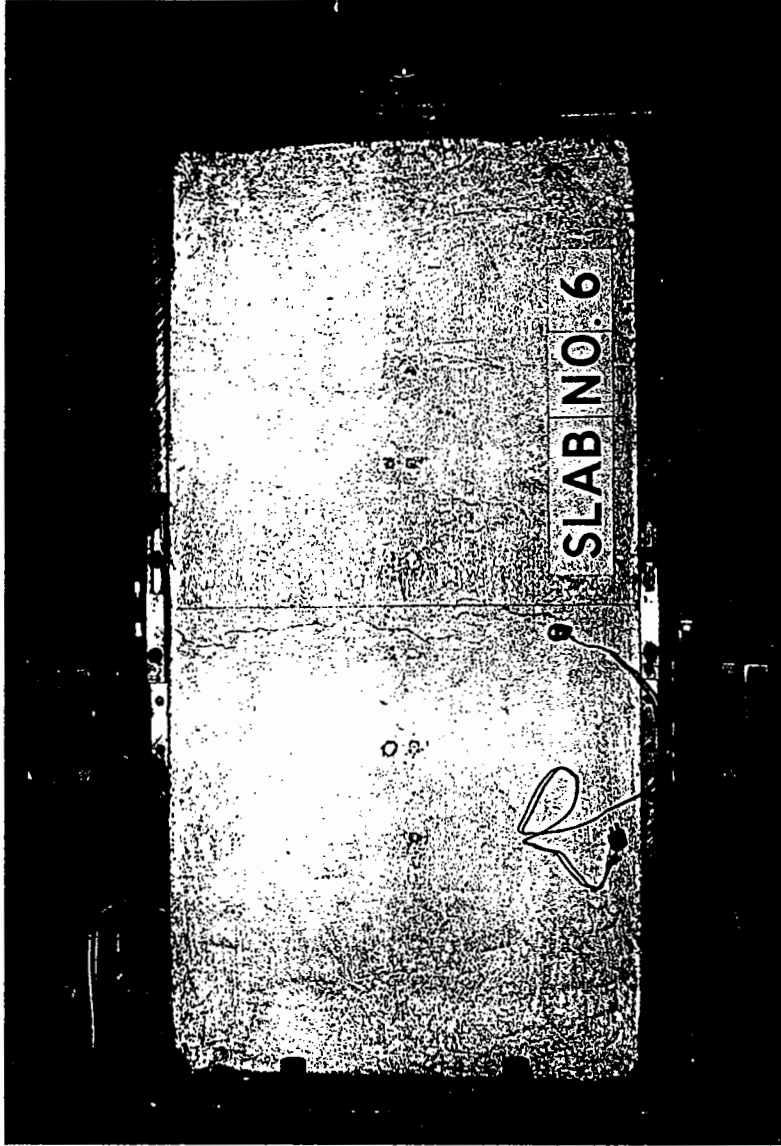


FIG. 7.16 SPECIMEN NO. 50/20C AFTER FAILURE.  
(SLAB NO. 6)

the cyclic gap movement was  $\pm 100$  microns which was the largest in this group of test (Fig. 7.5 (a)). The specimen fractured after 69,500 cycles and cracked at a location which was about 200 mm from the joint gap, ie, near the end of the debonding region (Fig. 7.15(c) & 7.17). The reason for this different crack pattern was not apparent. Since no similar failure pattern was observed in the later tests, further investigation was not considered. The recorded compressive load was slightly higher than the tensile load as in the other pre-compressed specimens (Fig. 7.5 (b)).

### 7.3.2 Discussion of Test Data.

#### a) Joint Gap Movement Controls.

As discussed in section 6.4.2, the gap movement control could be improved by changing the scaling factor of the Dartec system. Some alterations on the standard Dartec software (appendix B) were required to make this change possible. Modification to the software was finished just in time for the group 2 tests. As a result, an obvious improvement in the gap movement control was achieved and this was reflected in the test results as shown in the Figs. 7.6(a) to 7.14(a).

The accuracy of the gap movement control was further improved by using two gap control LVDT's, G1 and G2 as shown in Fig. 4.7. Through a special wiring arrangement, the summation of the output

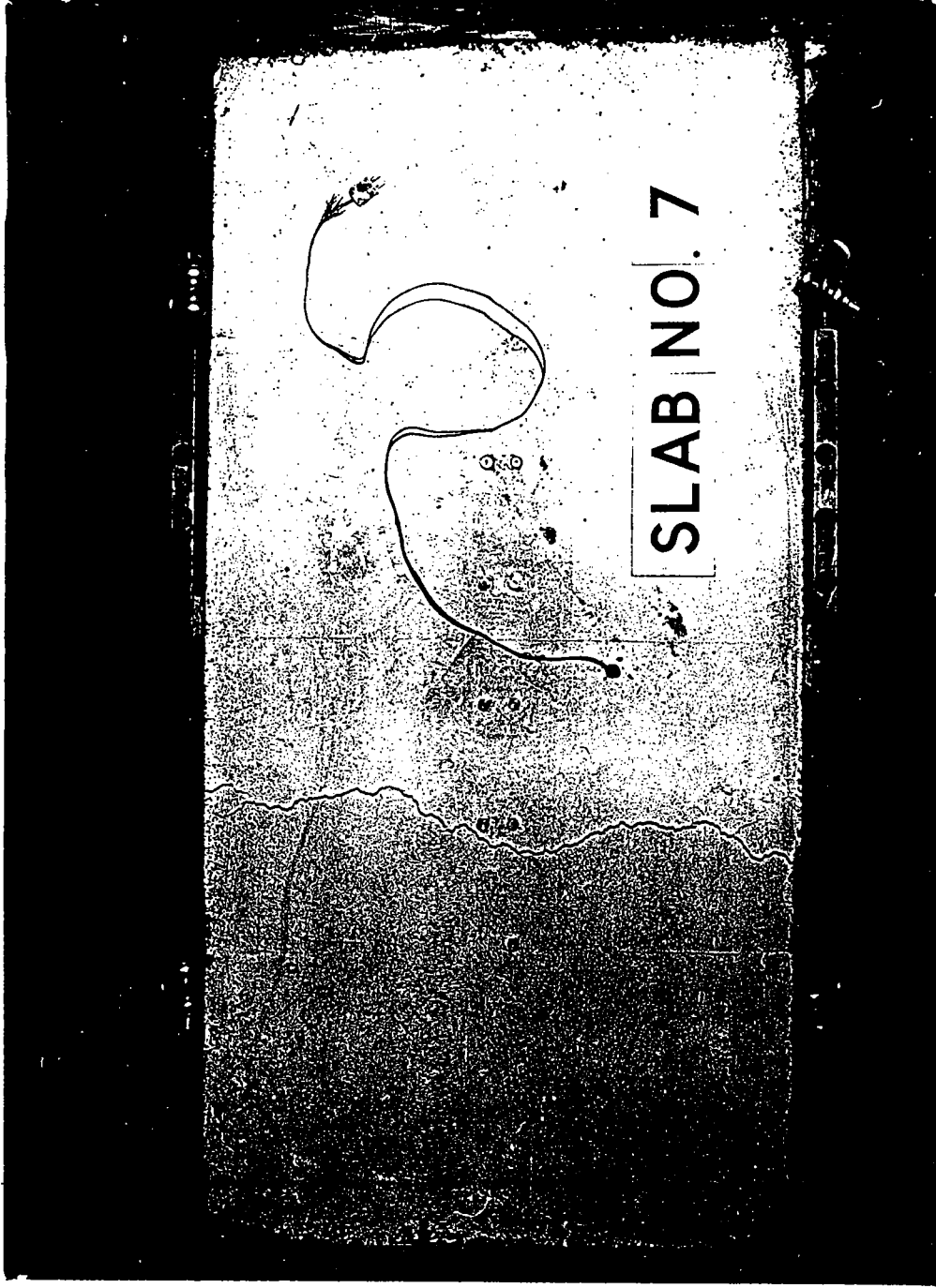


FIG. 7.17 SPECIMEN NO. 100/20C AFTER FAILURE.  
(SLAB NO. 7)

signals from these LVDT's was obtained and input into a single signal conditioning unit. By setting the scaling switches of this unit, an effective average of the LVDT signals was obtained and fed into the Dartec system for gap movement control purpose. This new gap controlling method also solved the problem which caused an excessive strain in the material as described in section 6.3.3.

b) Load Reactions of The Specimens.

Test results, as presented in Figs. 7.3 (b) to 7.14 (b), show that the ratio of the initial tensile and compressive load reactions of a specimen varied with the type of initial stress applied to the specimen before a test started. The ratio was slightly greater than 1 for prestretched specimen tests and less than 1 when precompressed specimens were used. This ratio tended to decrease further when precompressed specimens were tested at a lower temperature. In prestretched specimen tests, both tensile and compressive loads decreased faster than those observed in precompressed specimen tests. In both cases, the load readings dropped rapidly when the specimen started to fail.

c) Effects of Rest Periods.

During the tests of precompressed specimens no. 30/10C & 75/10C, substantial increases in stiffness were observed (Figs. 7.9(b) & 7.11 (b)) after long rest periods were allowed (4 & 11 days respectively). However, the effects of long rest periods were not

observed on prestretched specimen tests except for test no. 2 as described in section 6.3.2. This might be partly due to the relatively short test duration of this type of specimen test and stoppage was not often introduced. Because of the time scale of the present research project, further investigation of the effects of long rest periods on expansion joint performance was not planned.

d) Material Strains.

On the top surface of each specimen, five LVDT's, e1, e2, e3, e4 & e5 were located as shown in Fig. 4.7, These were used to measure the material strains at different positions. Figs. 7.3 (c) to 7.14 (c) shows how these strains varied with the number of completed load cycles. Initially, the values of these strains were relatively constant. As the test continued, the strains, except e3 (over the gap), increased rapidly until they reached their maximum values and started to decrease sharply when the specimen began to fail. Similar observations were reported by Van Dijk (1975) during his wheel tracking tests on slab samples. The shape of the graphical plots of these strain readings (e.g. Figs. 7.3(c) & 7.5(c)) was very similar to those presented by Van Dijk (Fig. 2.6). This might indicate that a realistic failure mode, similar to that of the wheel tracking tests, had been reproduced in the EJS tests. The curves of the strain e3 readings were slightly different from those described above. The e3 reading often started with a low value. In the final stage of a



test, the values of e3 increased sharply when the other four started to fall. This provided a clear indication when and where a specimen failure occurred.

In precompressed specimen tests the initial e1 and e5 values were often higher than the others, while in prestretched specimen tests e2 and e4 were generally the highest two. This indicated that prestretched specimens were less capable of distributing strains over wider areas on either side of the joint gap. This caused a relatively higher strain concentration and resulted in an earlier failure of this type of test.

e) Definition of Specimen Failure.

Based on the information provided in section 7.3.2 b) & d), failure of a specimen was defined as the number of cycles completed when the reactive tensile load on the specimen dropped to 35 % of its initial value. This normally occurred when a crack with a length of over 70% of the total length of the joint was observed at the top surface of the specimen and, at the same time, the material strain measured near the joint gap increased rapidly while, at other positions, it showed a sudden decrease.

It was always the intention to establish a method to identify when and where a specimen failure occurred, not by direct observation but based on the information extracted from the test data collected. The definition of failure given above provided a

useful means to achieve this aim. The success of this approach also allows a test to be run continuously overnight without concern about missing the record of when a failure exactly happened.

### 7.3.3 Fatigue Lives of the Joint Specimens.

Using the definition given in section 7.3.2 e), the calculated fatigue lives of each specimen are listed in Table 7.3. Specimen no. 25/20C was tested in 2 stages. In the first stage, a gap movement of  $\pm 25$  microns was used for 4,000,000 cycles. This was followed by the second stage, in which the gap movement was increased to  $\pm 50$  microns and a further 940,000 cycles were applied before the specimen failed. Results from the test of specimen no. 50/20C showed that the total number of cycles to failure, with a gap movement of  $\pm 50$  microns, was 1,994,099 (Table 7.3). The number of cycles required to fail the specimen no. 25/20C with a constant gap movement of  $\pm 25$  microns can be found using Miner's rule:-

No. of cycles applied with gap movement  
of  $\pm 25$  microns  $(n)_{25} = 4,000,000$

No. of cycles to failure with a constant  
gap movement of  $\pm 25$  microns  $= N_{25}$

Table 7.3 Test Results. (All tests at 5 Hz.)

Group No.	Specimen No.	Stress condition before cycling	Horizontal transient movement (microns)	Test temperature (°C)	Fatigue life (cycles)
1	25/20C	Compression	±25	20	7,567,027
	50/20C	Compression	±50	20	1,994,099
	100/20C	Compression	±100	20	54,357
2	30/20T	Tension	±30	20	1,005,780
	50/20T	Tension	±50	20	41,472
	100/20T	Tension	±100	20	10,500
3	30/10C	Compression	±30	10	2,021,539
	50/10C	Compression	±50	10	712,223
	75/10C	Compression	±75	10	140,396
4	25/10T	Tension	±25	10	840,975
	50/10T	Tension	±50	10	129,934
	75/10T	Tension	±75	10	40,281

No. of cycles applied with gap movement

of  $\pm$  50 microns

$$(n_{50}) = 940,000$$

From the test results of specimen no. 50/20C

No. of cycles to failure with a constant

gap movement of  $\pm$  50 microns

$$(N_{50}) = 1,994,099$$

Using Miner's rule

$$\frac{n_{25}}{N_{25}} + \frac{n_{50}}{N_{50}} = 1$$

therefore:-

$$N_{25} = 7,567,027 \text{ (cycles)}$$

It was originally planned to plot all the test results in curves of initial strain against the number of cycles to failure (fatigue life) on a log-log scale but the test results showed that the distribution of strains, measured on the top surface of the specimens, varied as the test progressed and the crack positions did not correspond to the location of the largest strains ( $\epsilon_3$ ). However, when gap movements and initial tensile

loads were plotted separately against fatigue life on a log-log scale, curves were obtained as shown in Figs. 7.18 & 7.19. Fig. 7.20 shows the result when initial tensile loads on the natural scale are plotted against log fatigue life. Figs. 7.21 to 7.23 show the same curves after linear regression analysis.

Fig. 7.21 shows that the life curves for specimens tested at the same temperature have a similar slope irrespective of the initial stress conditions before the test started. However, prestretched specimens gave much shorter lives. In the case of precompressed specimens, longer lives came with higher test temperature. But in prestretched specimen tests, longer lives were generally obtained at lower test temperature (Fig. 7.21, results shown in dotted line).

From the life curves shown in Fig. 7.22, it was noticed that when specimens were tested at the same temperatures, relatively lower initial tensile reactions were recorded from prestretched specimens. A logical explanation for this was that slight damage to these specimens might have occurred during the prestretching process. Until the reasons for this were fully established, it was decided not to include the prestretched specimen test results in the final analysis. However, the potential use of the prestretch effects should not be overlooked. Under a precisely controlled test procedure, as in the case of EJS tests, prestretching could be used as an alternative method to accelerate the test rate.

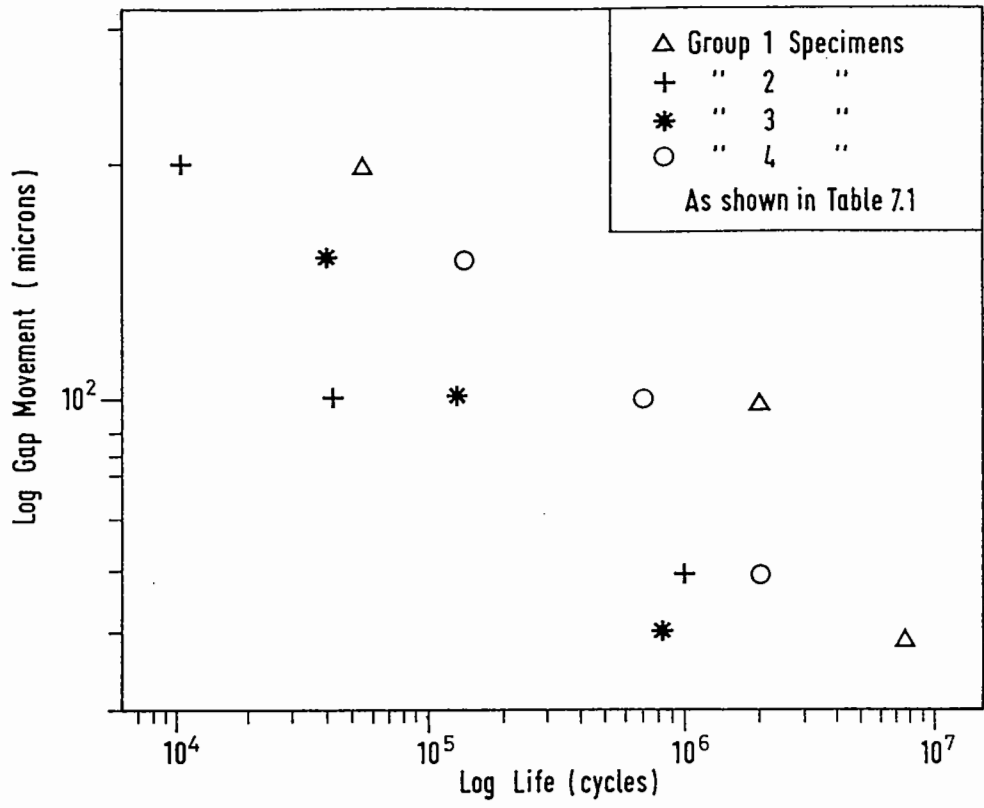


FIG. 7.18 TEST RESULTS

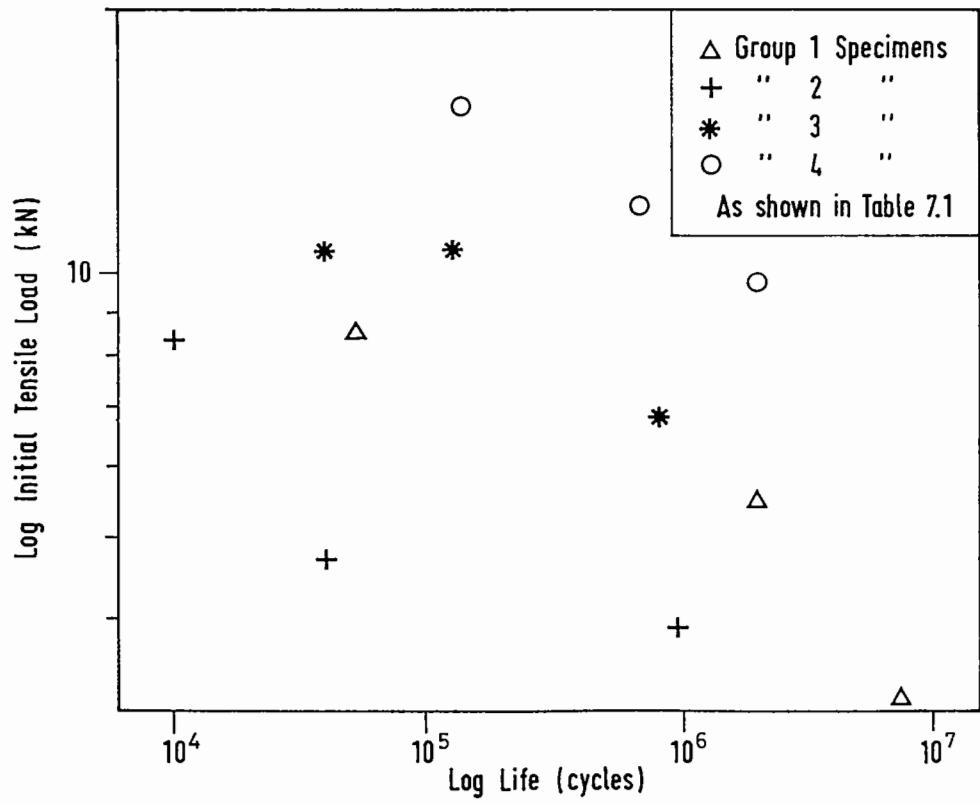


FIG. 7.19 TEST RESULTS

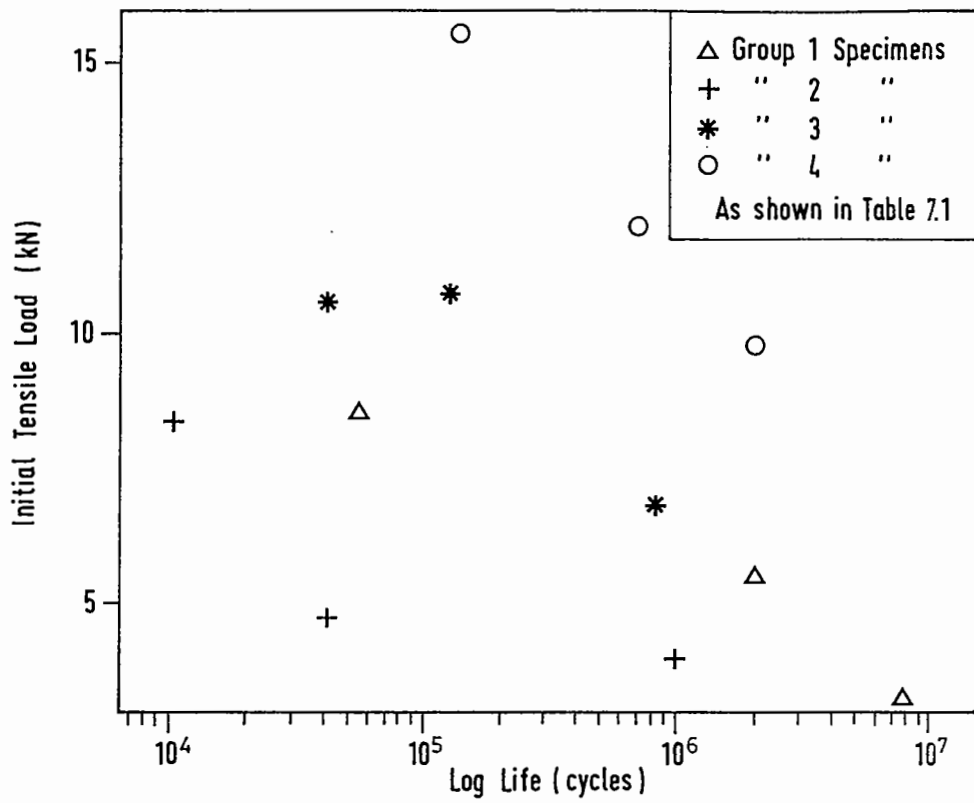


FIG. 7.20 TEST RESULTS

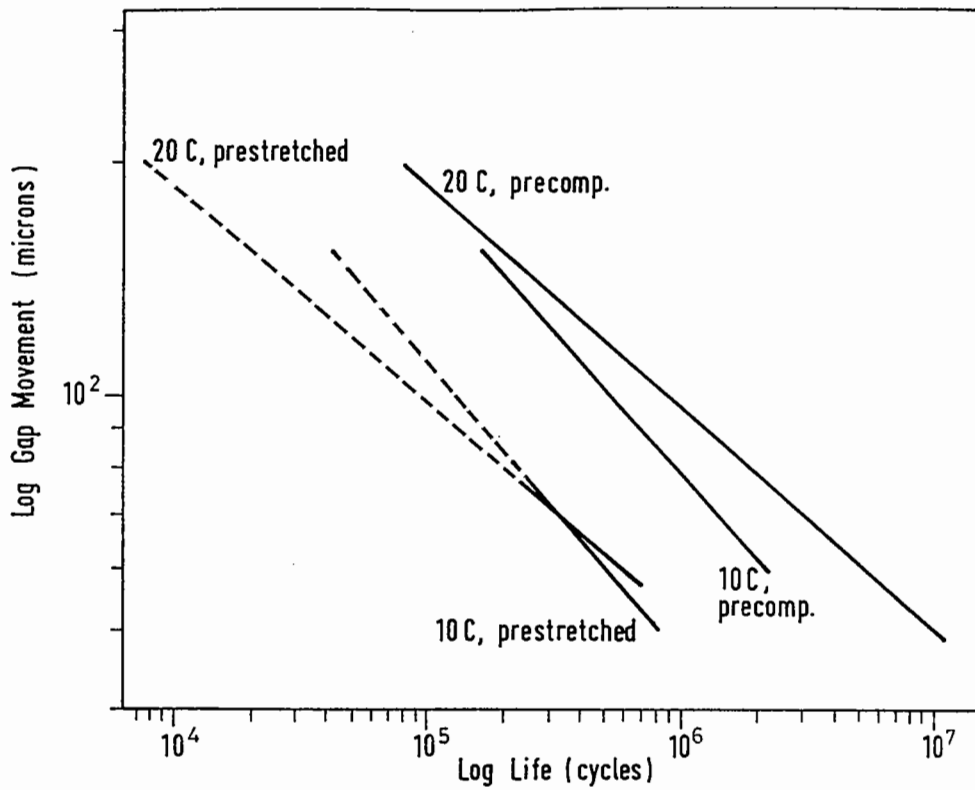


FIG. 7.21 TEST RESULTS  
(Linear regression lines)

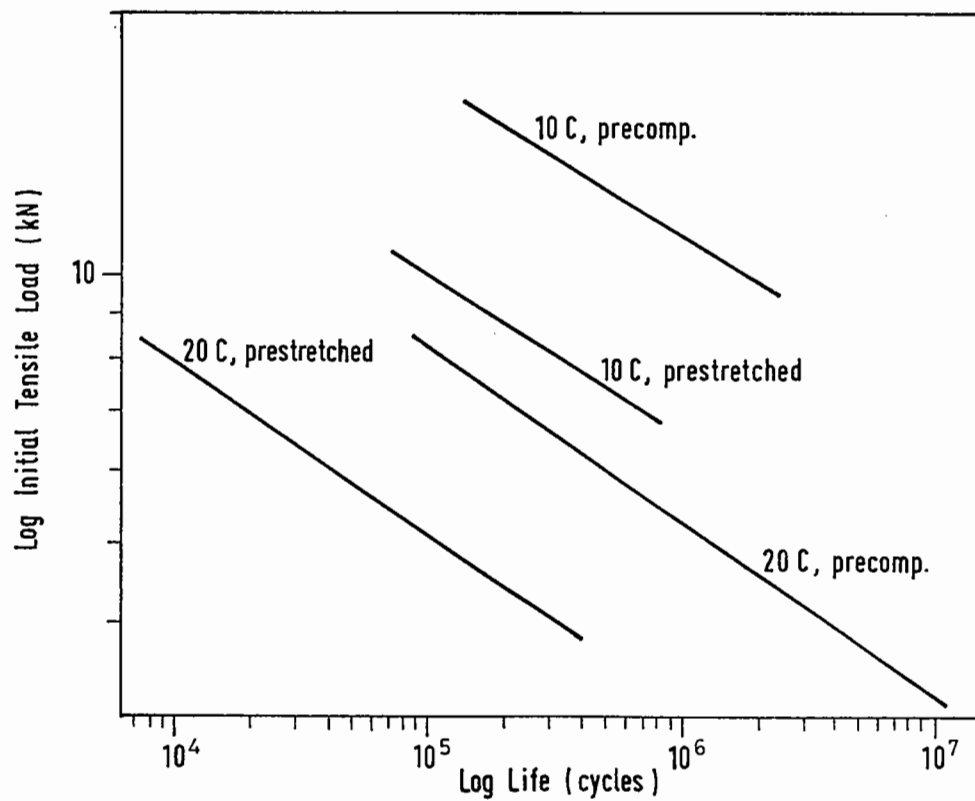


FIG. 7.22 TEST RESULTS  
(Linear regression lines)



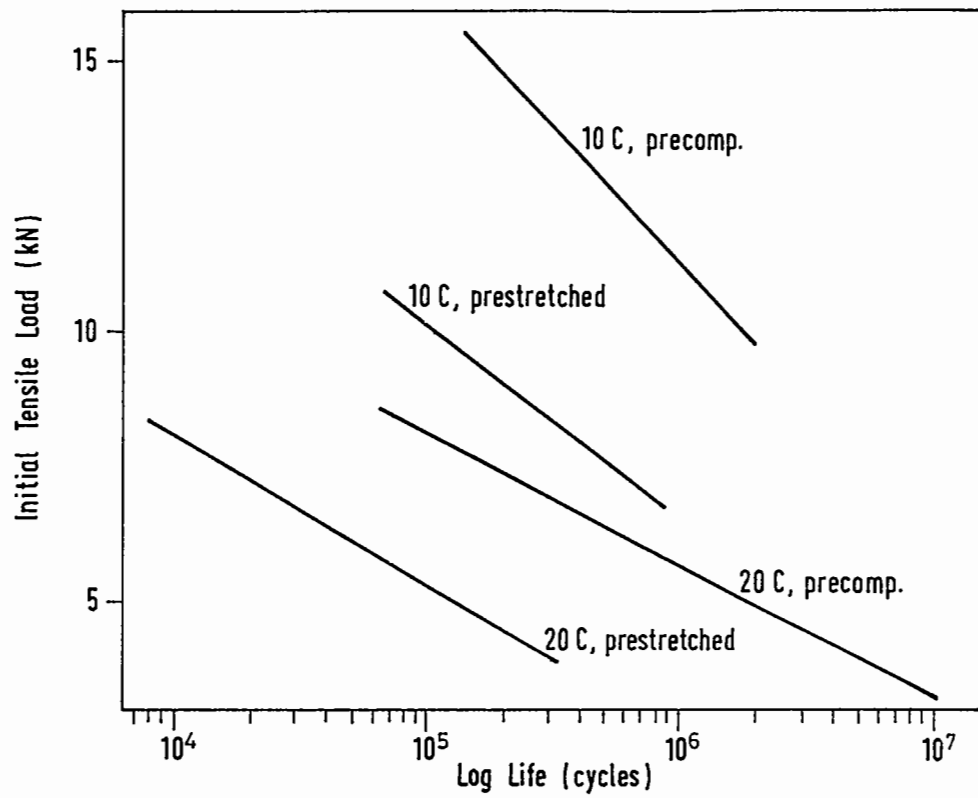


FIG. 7.23 TEST RESULTS  
(Linear regression lines)

Although the life curves in Fig. 7.22 show there is a good correlation between the log initial tensile loads and log life cycles, use of these life curves are not recommended. This is mainly because the position of each curve is highly dependent on the test temperature. Specimen tests must be carried out at different temperatures before a complete set of curves could be produced. This will increase the number of specimens required considerably. In addition, the value of tensile load changed rapidly once a test started and this apparently caused difficulty in the capture of the initial value of the tensile load. In contrast, the life curves produced by plotting log gap movements against log life cycles were free of these troubles.

Since the two life curves of precompressed specimens were so close to each other, it was reasonable to assume that their separation was mainly caused by the natural scatter of fatigue test results. When the precompressed specimen test results were combined, a new life curve, after linear regression analysis, was produced as shown in Fig. 7.24 (dotted line). To compensate the error caused by the omission of rest periods between load cycles, a multiplying factor of 20 was used, as suggested by Raithby and Stirling (1972), to convert this life curve to a new life prediction line (Fig. 7.24 solid line) which could be used for in-service joints. Equations for the regression lines used in Figs. 7.21 & 7.24 are listed in Table 7.4.

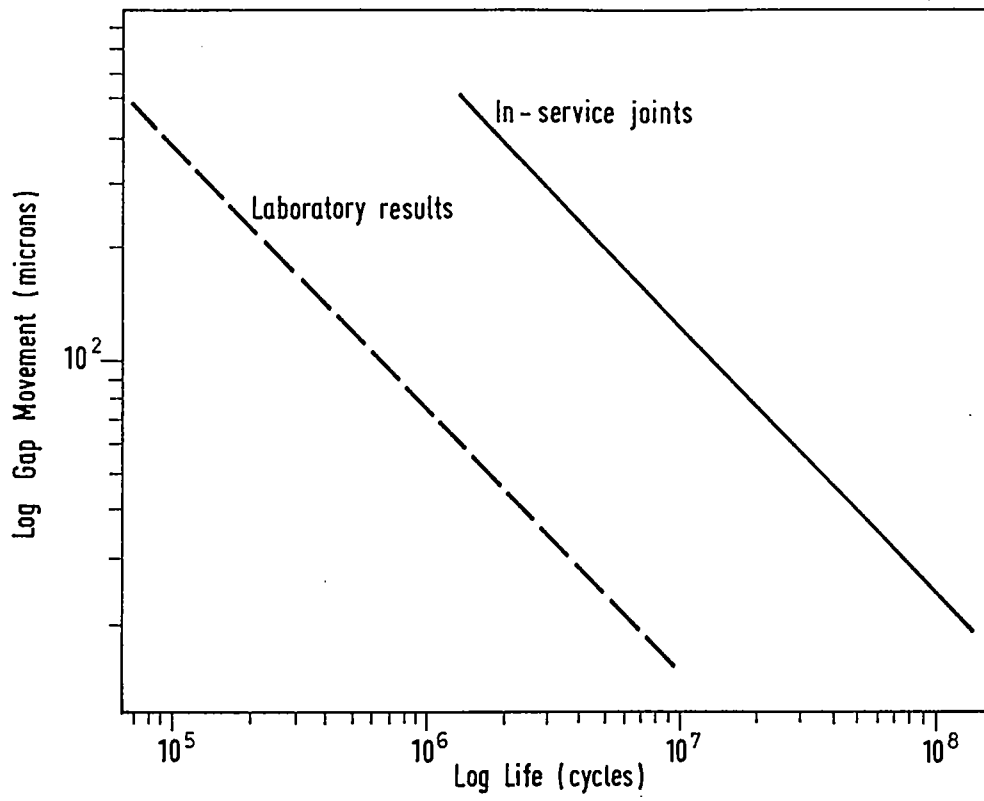


FIG. 7.24 JOINT LIFE CURVES  
( Linear regression lines )

Table. 7.4 Equations for the regression lines in Figs. 7.21 & 7.24.

Test Data Used (Specimens)	Test conditions	Equations	R
Group 1	Precomp. 20 °C	$x = 13.09 - 3.56y$	0.93
Group 2	Preten. 20 °C	$x = 12.35 - 3.68y$	0.91
Group 3	Precomp. 10 °C	$x = 11.47 - 2.87y$	0.96
Group 4	Preten. 10 °C	$x = 10.62 - 2.76y$	1.00
Group 1+3	Precomp. 20 °C & 10 °C	$x = 12.50 - 3.33y$	0.90
In-service Joints	Precomp. 20 °C & 10 °C	$x = 13.80 - 3.33y$	0.90

- N.B.
1.  $x = \text{Log life (estimated)}$ .
  2.  $y = \text{Log gap movement}$ .
  3.  $R = \text{Sample correlation coefficient}$ .

#### 7.4 LONG-TERM (THERMAL) HORIZONTAL MOVEMENT TESTS.

The EJS was designed to generate low frequency gap movements up to 50 mm. This covers the movement range of most joint types including the asphaltic plug joints. Since the working stroke range of the actuators is 100 mm, with some minor modification of the machine components, tests on joint systems with a design movement range up to 100 mm would be possible. However, the maximum design movement of buried joints seldom exceeds 15 mm which is well within the capacity of the EJS.

Four specimens were tested with long-term horizontal movements which simulated the joint movements due to changes of temperature. Special software was written, and integrated into the original Dartec package, for the EJS control. During testing, the specimens were extended and compressed about their original gap position at a constant temperature. Strain rate control at about 0.7 mm/hr was used for all specimens.

##### 7.4.1 Details of the Tests.

As shown in Table 7.1. Specimen no. H/2/20C was tested with a cyclic gap movement of  $\pm 2$  mm and started with the gap closing first. After 17 completed test cycles, randomly spaced minor cracks were developed as shown in Fig. 7.25. A short major crack was also observed above the joint gap near the edge of the specimen. Since no drastic crack development was observed in the

last few test cycles, it was decided to increase the gap movement range to  $\pm 3$  mm to accelerate the test. After four more cycles, a continuous major crack was developed along the joint gap as shown in Fig. 7.26.

It is generally understood that the resistance to cracking of bituminous materials is highly dependent on their tensile strength at a particular strain rate. In order to measure the genuine tensile strength of the specimens, at the strain rate used in the tests, it was decided that subsequent tests should start with the joint gap opened first.

Specimen no. H/2/20T was subjected to the same amount of gap movement as the previous specimen but initially under tension. Fig. 7.27 shows that cracks developed in the specimen after nineteen completed cycles. The specimen was then subjected to a one way extension, i.e. pulled open by 6 mm from its initial gap position. As a result, a major crack was formed as shown in Fig. 7.28.

The applied gap movement for specimen no. H/4/20T was  $\pm 4$  mm. After one completed cycle, two short cracks developed on both ends of the joint gap. The test was then stopped, still under tension, for two days. After the stoppage, the cracks doubled their lengths and some freshly formed short hairline cracks appeared on either side of the joint gap. The test was then resumed and a continuous crack was observed when the specimen was fully extended in the third test cycle. Fig. 7.29 shows the final

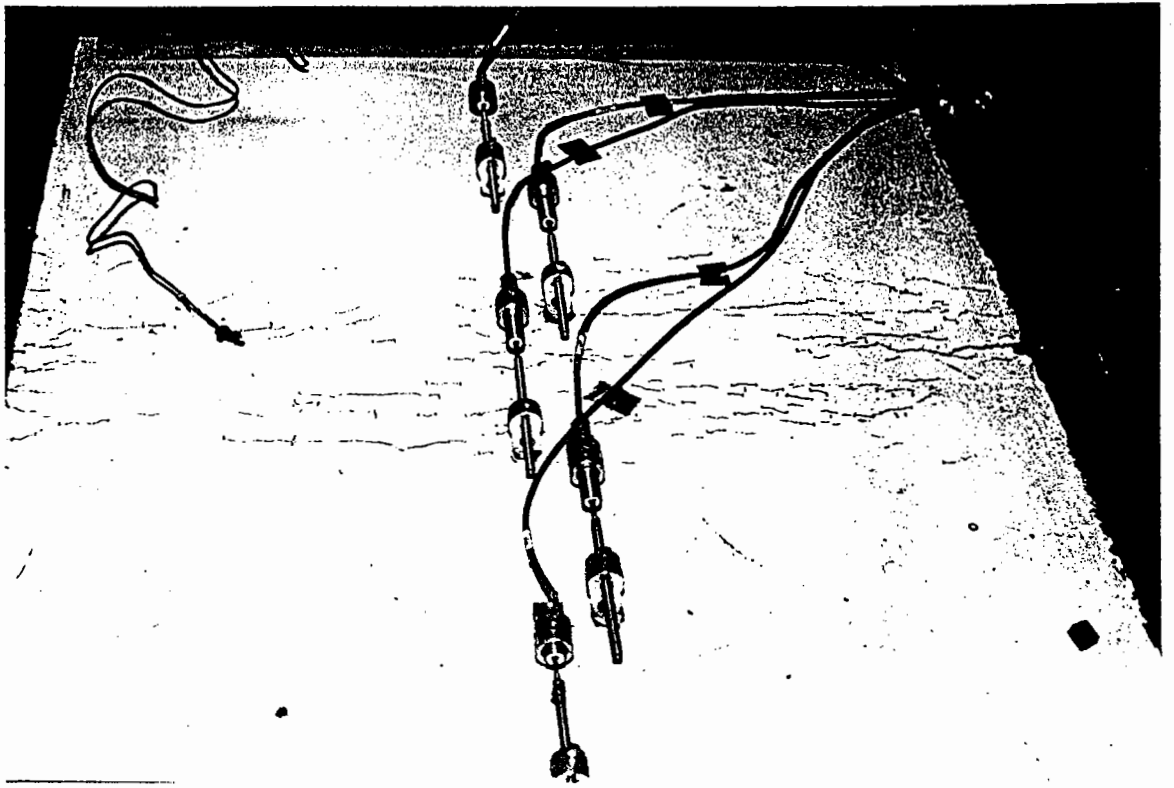


FIG. 7.25 SPECIMEN NO. H/2/20C AFTER 17 TEST CYCLES.

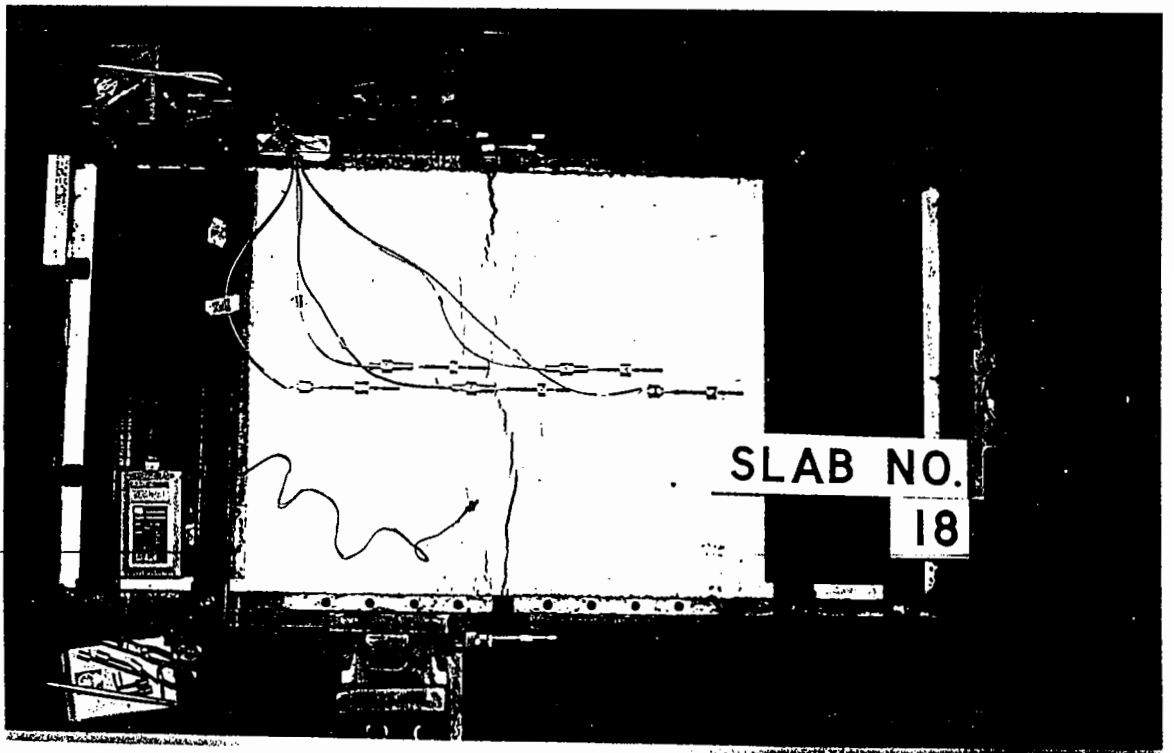


FIG. 7.26 SPECIMEN NO. H/2/20C AFTER 21 TEST CYCLES (SLAB NO. 18).

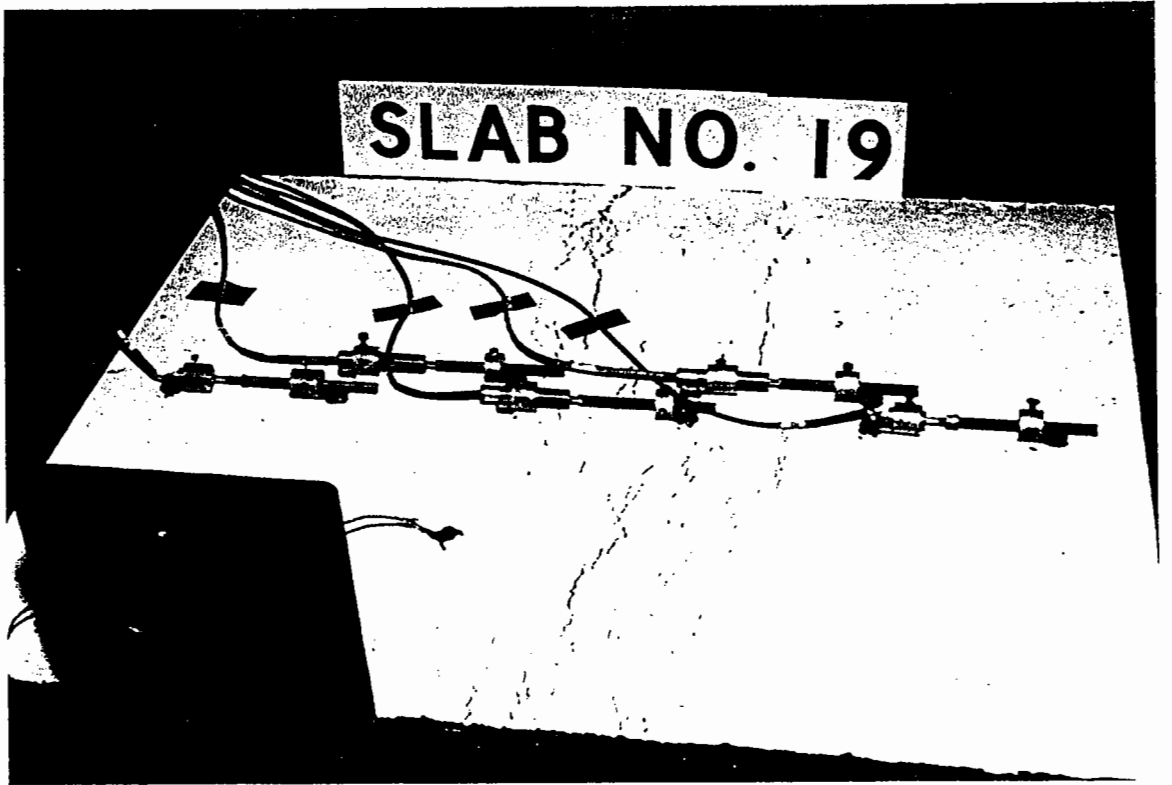


FIG. 7.27 SPECIMEN NO. H/2/20T AFTER 19  
TEST CYCLES (SLAB NO. 19).

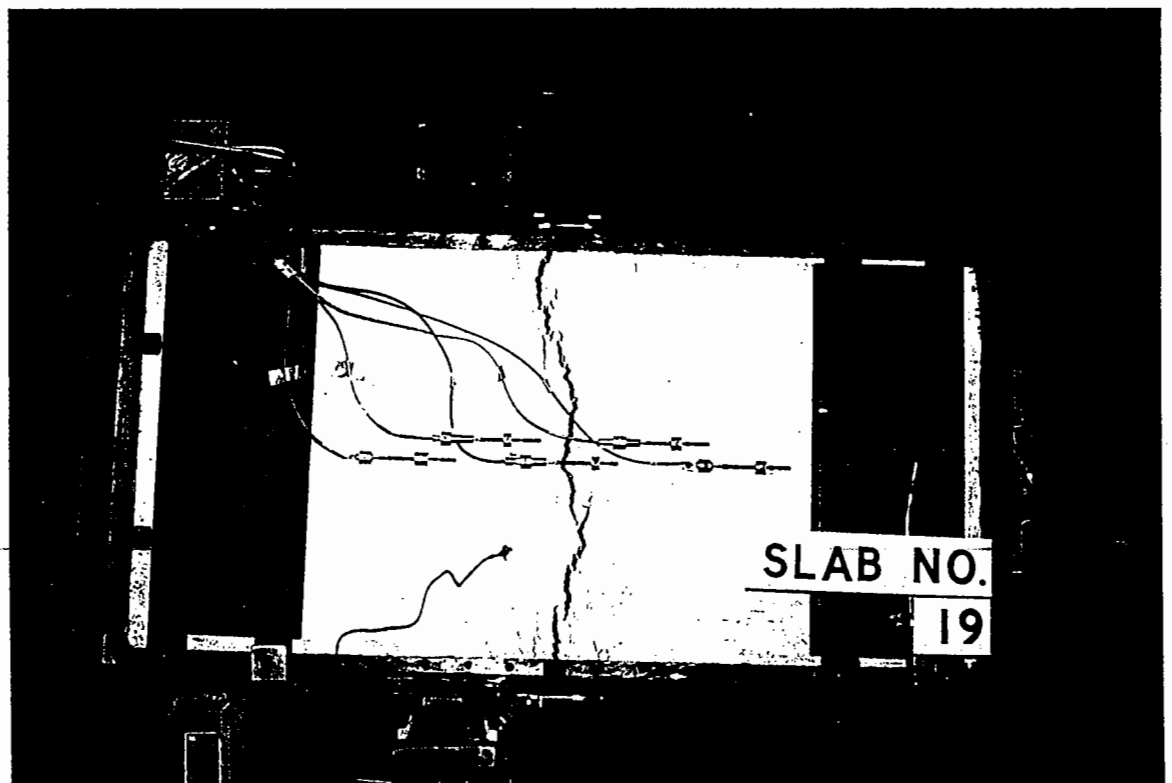


FIG. 7.28 SPECIMEN NO. H/2/20T AFTER EXTENDED  
BY 6 mm (SLAB NO. 19).



state of the specimen after six completed test cycles.

The fourth specimen, no. H/1.25/20T was tested with a gap movement of  $\pm 1.25$  mm. After 18 test cycles, only short hairline cracks were observed as pictured in Fig. 7.30. No other obvious sign of failure was detected.

In the earlier stage of all tests, minor cracks developed in a region which was about 100 mm wide on both sides of the joint gap while a major crack started at the underside of the specimens. For specimens subjected to a gap movement greater than 6 mm, the major crack propagated rapidly towards the top of the specimens and the minor cracks closed. Although these cracks became hardly visible, their existence could be significant since it might explain why, on site, a new crack was often observed alongside the major crack soon after the latter was sealed. This explanation could be verified in the future with laboratory resealing tests using the EJS.

#### 7.4.2 Load Histories of the Specimen Tests.

Fig. 7.31 shows the load history of specimen no. H/2/20C. It indicated that the highest tensile reaction occurred in the second half of the first test cycle. The peak value of the reaction dropped gradually in the first three cycles and then stayed more or less constant. No rise in tensile reaction was observed even after the gap movement was increased to  $\pm 3$ mm. Much

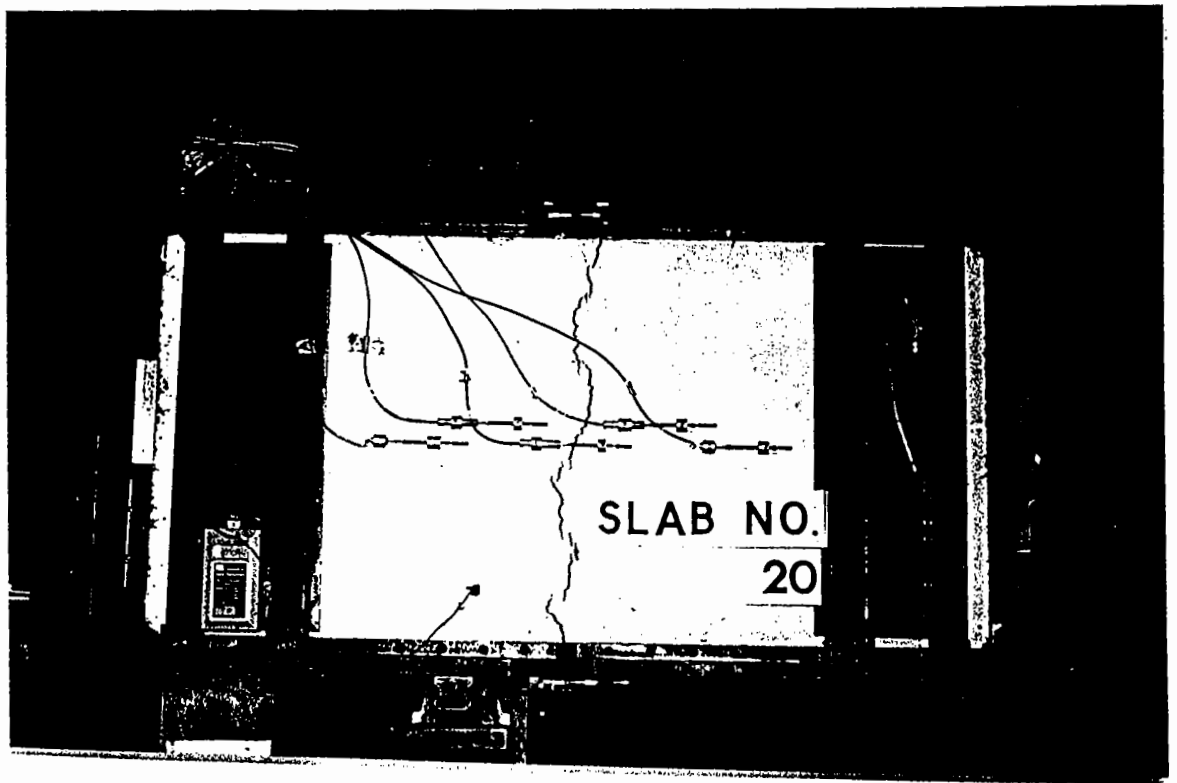


FIG. 7.29 SPECIMEN NO. H/4/20T AFTER 6  
TEST CYCLES (SLAB NO. 20).



FIG. 7.30 SPECIMEN NO. H/1.25/20T AFTER 18  
TEST CYCLES (SLAB NO. 21).

higher compressive reaction was recorded in the first cycle of the test. This reaction dropped rapidly in the first four cycles and remained roughly constant after that. The same process repeated when the gap movement was increased in the second stage of the test as shown in Fig. 7.31. Similar phenomena were recorded in the specimen test no. H/2/20T, except the tensile reaction was considerably higher in the first cycle of the test which was started with initial tension. Figs. 7.32, 7.33 & 7.34 show the different load records of the tests on specimens no. H/2/20T, H/4/20T AND H/1.25/20T respectively.

At the end of the second test, the LVDT's mounted on the top surface of specimens were replaced by those with a wider working range. This overcame the problem of frequent resetting of the LVDT's required during the first two tests. The quality of the data collected was also greatly improved.

#### 7.4.3 Definition of Specimen Failure.

In a long-term movement test, it is obvious that the failure of a specimen could not be defined by the percentage decrease of the tensile reaction of the specimen. However, the curves of the LVDT readings provided some helpful information.

Figs. 7.35 to 7.38 are the graphical plots of the LVDT readings, B1 and e1 to e5, of specimens no. H/4/20T and H/1.25/20T. The positions of these LVDT's are shown in Fig. 4.7. For specimen no.

LOADS (kN)

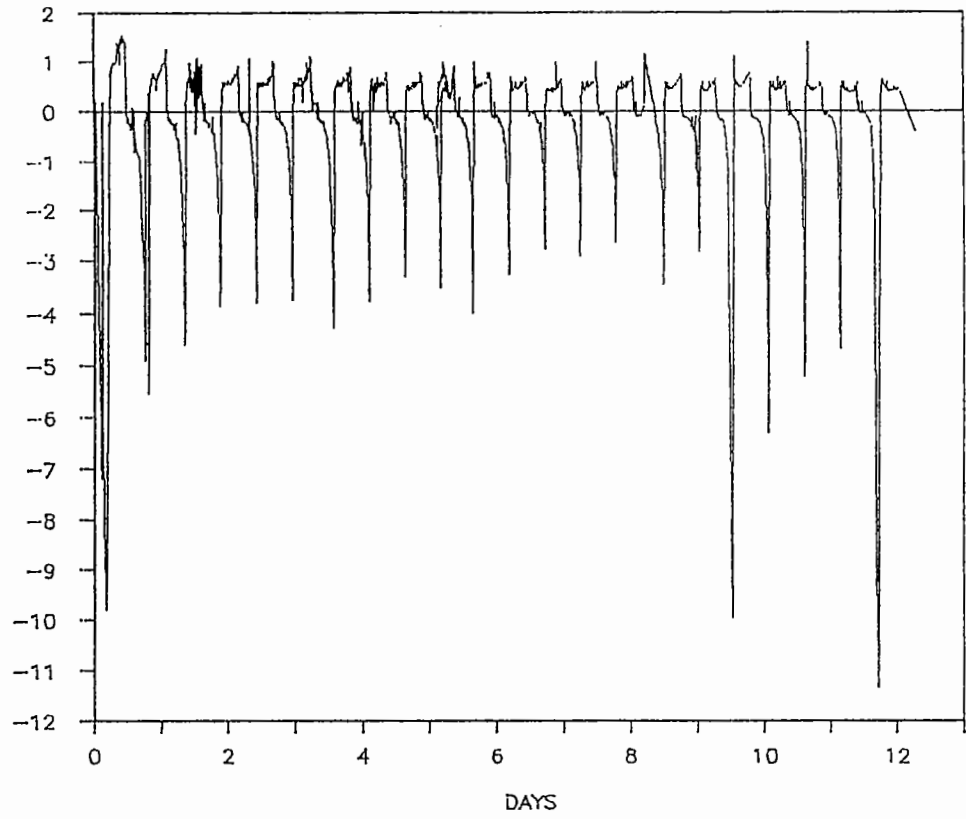


FIG. 7.31 SPECIMEN NO. H/2/20C (SLAB NO. 18).

LOADS (kN)

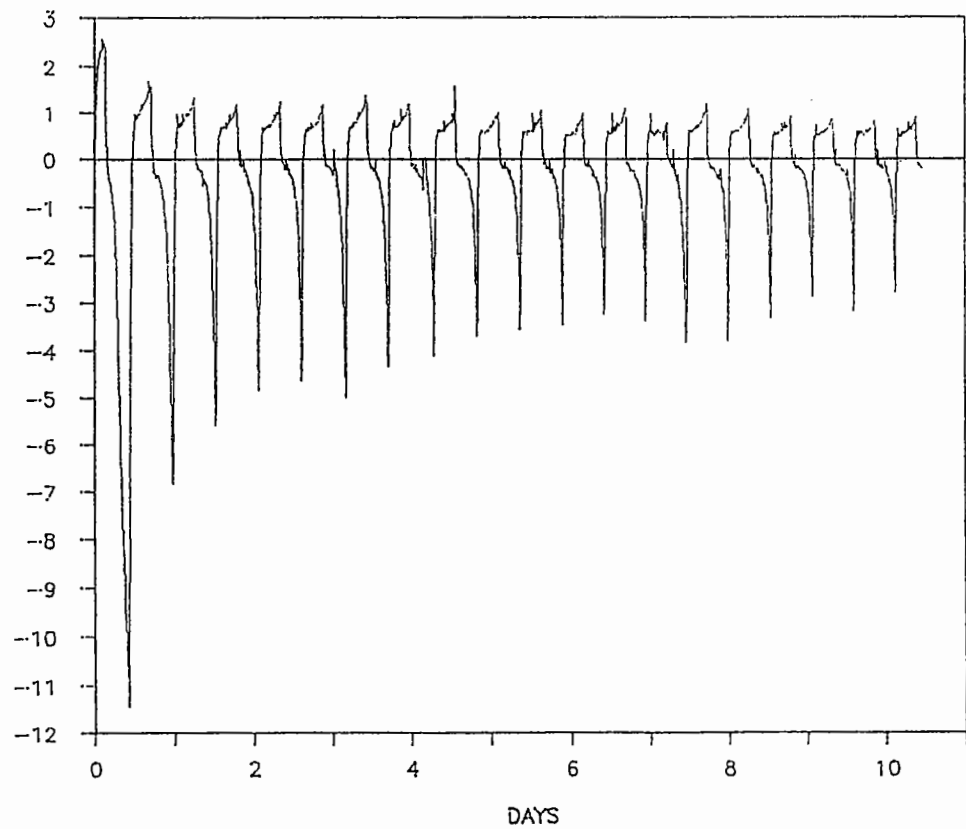


FIG. 7.32 SPECIMEN NO. H/2/20T (SLAB NO. 19).

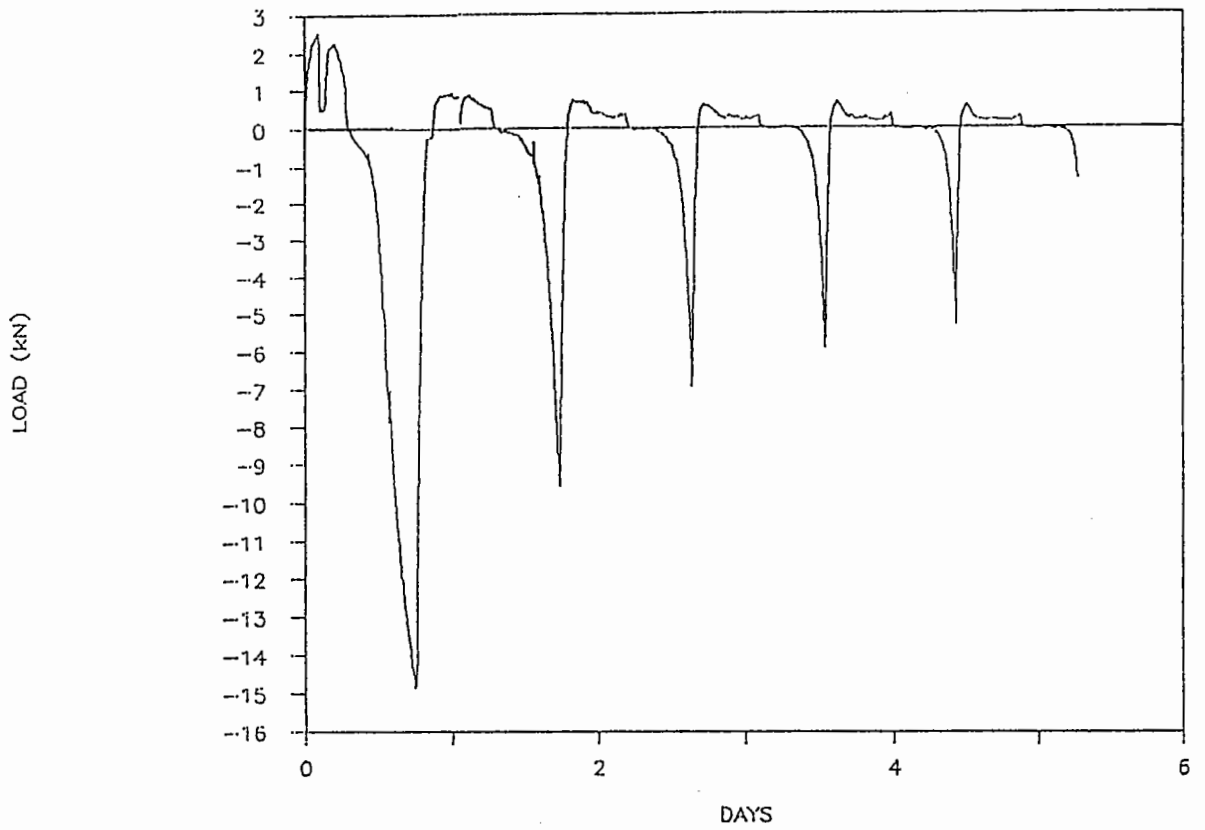


FIG. 7.33 SPECIMEN NO. H/4/20T  
(SLAB NO. 20).

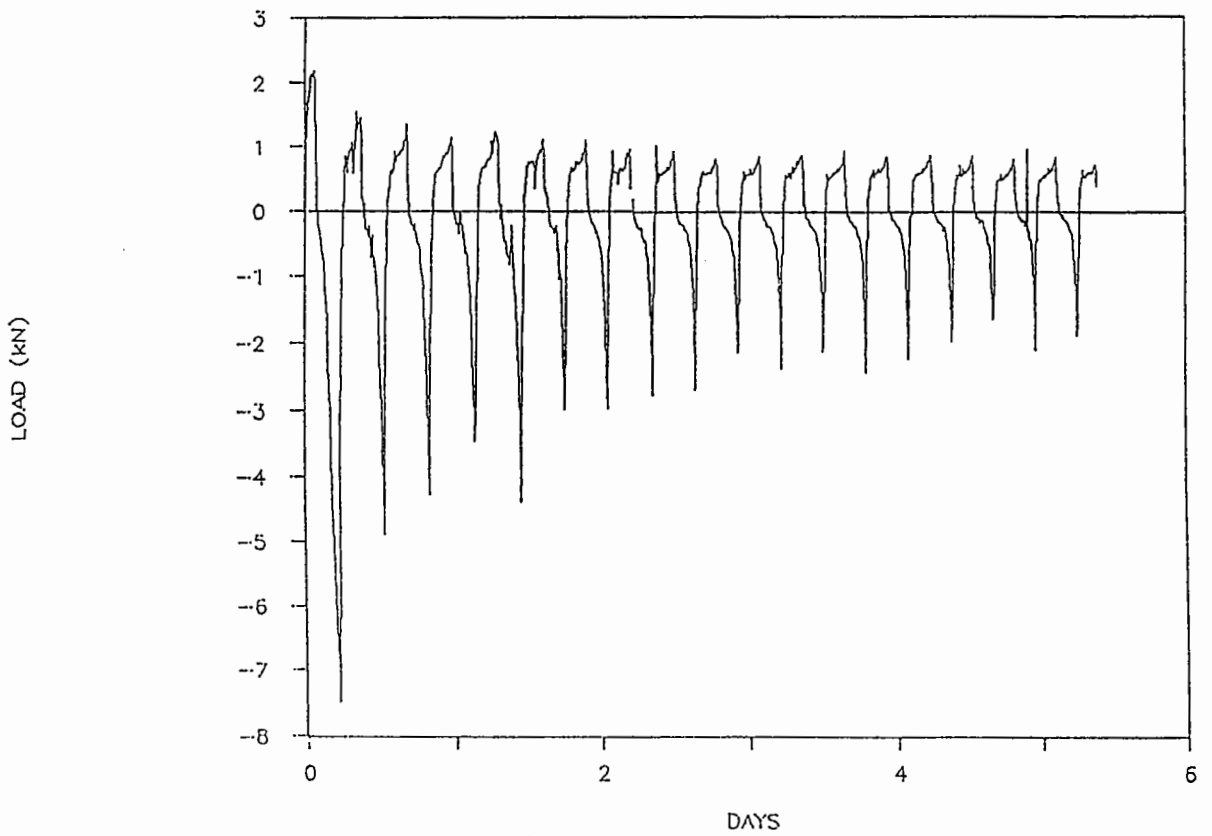


FIG. 7.34 SPECIMEN NO. H/1.25/20T  
(SLAB NO. 21).

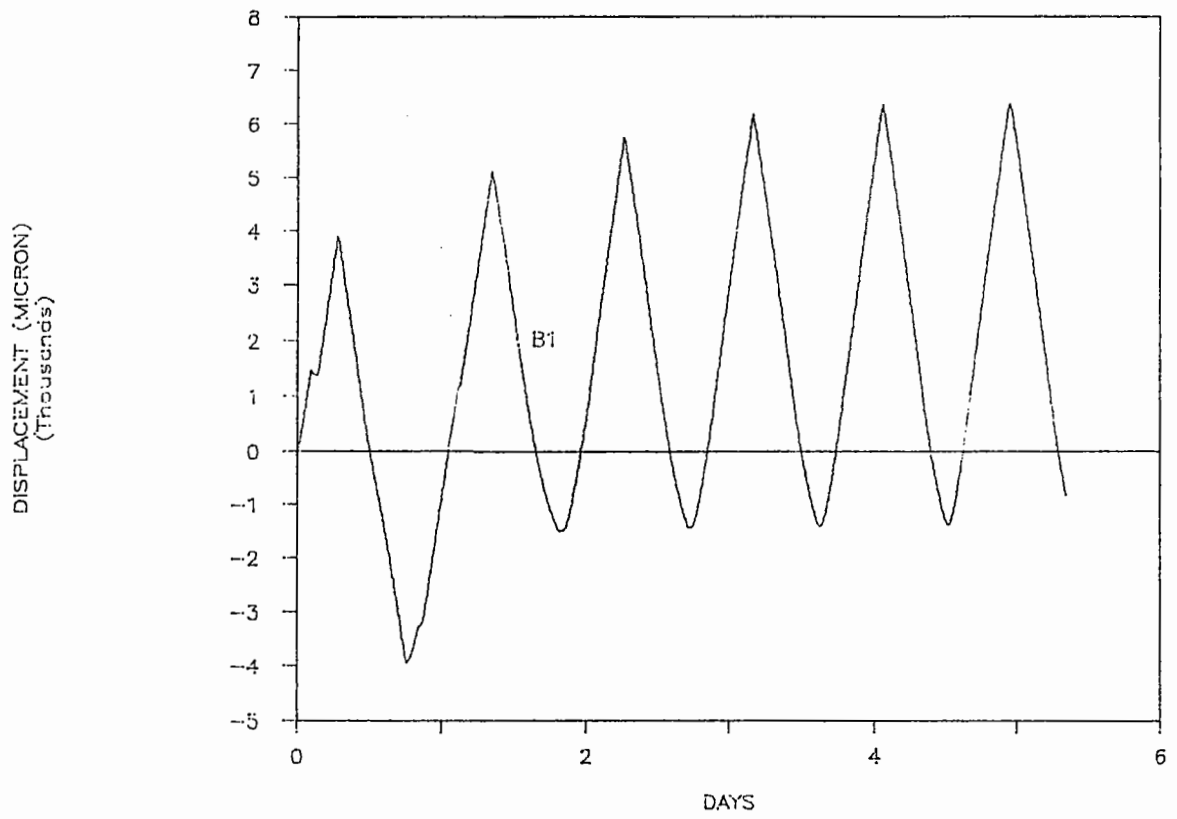


FIG. 7.35(a) SPECIMEN NO. H/4/20T  
(SLAB NO. 20).

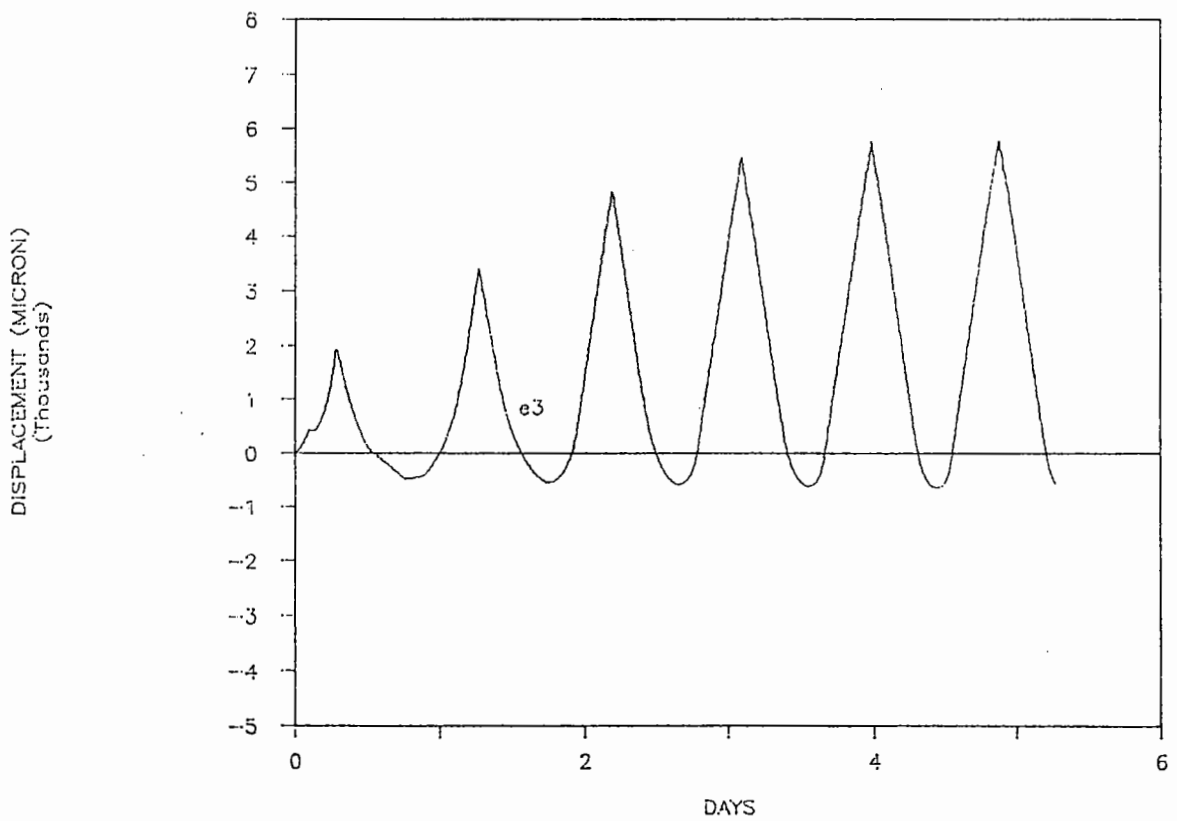


FIG. 7.35(b) SPECIMEN NO. H/4/20T  
(SLAB NO. 20).

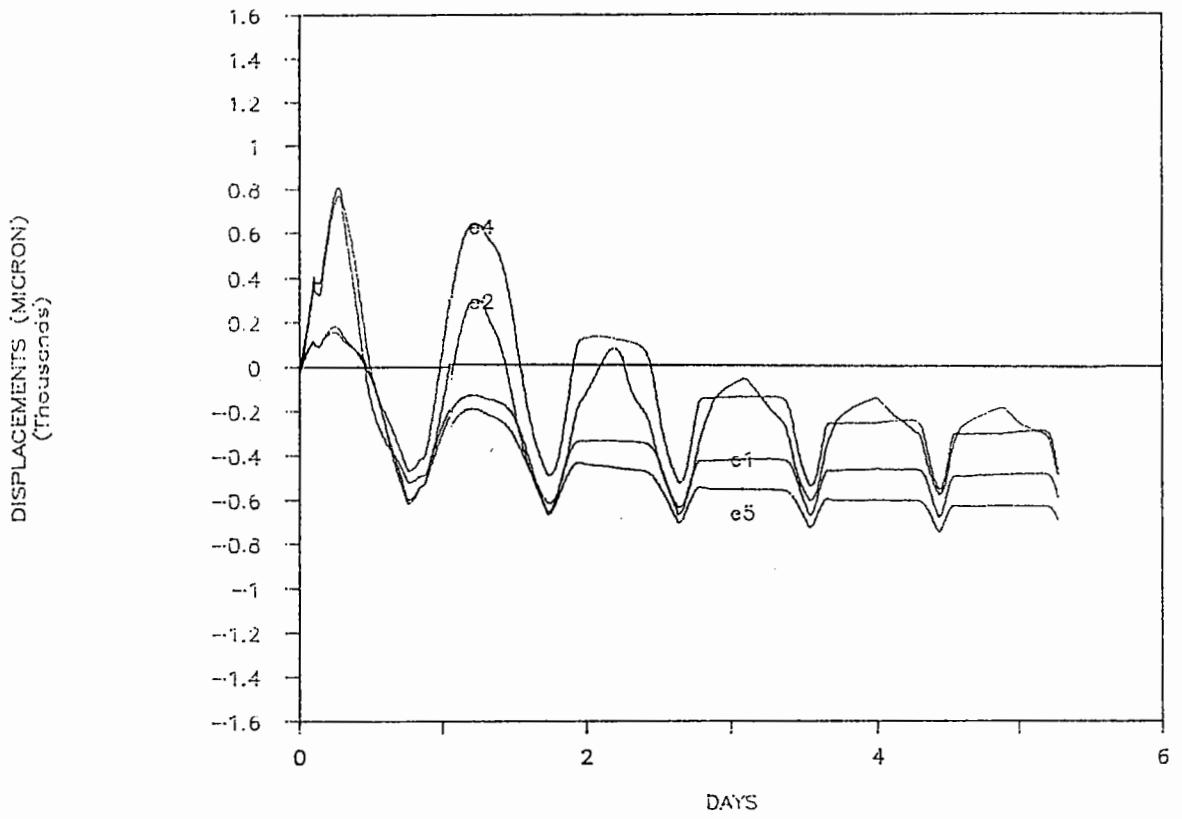


FIG. 7.36 SPECIMEN NO. H/4/20T  
(SLAB NO. 20).

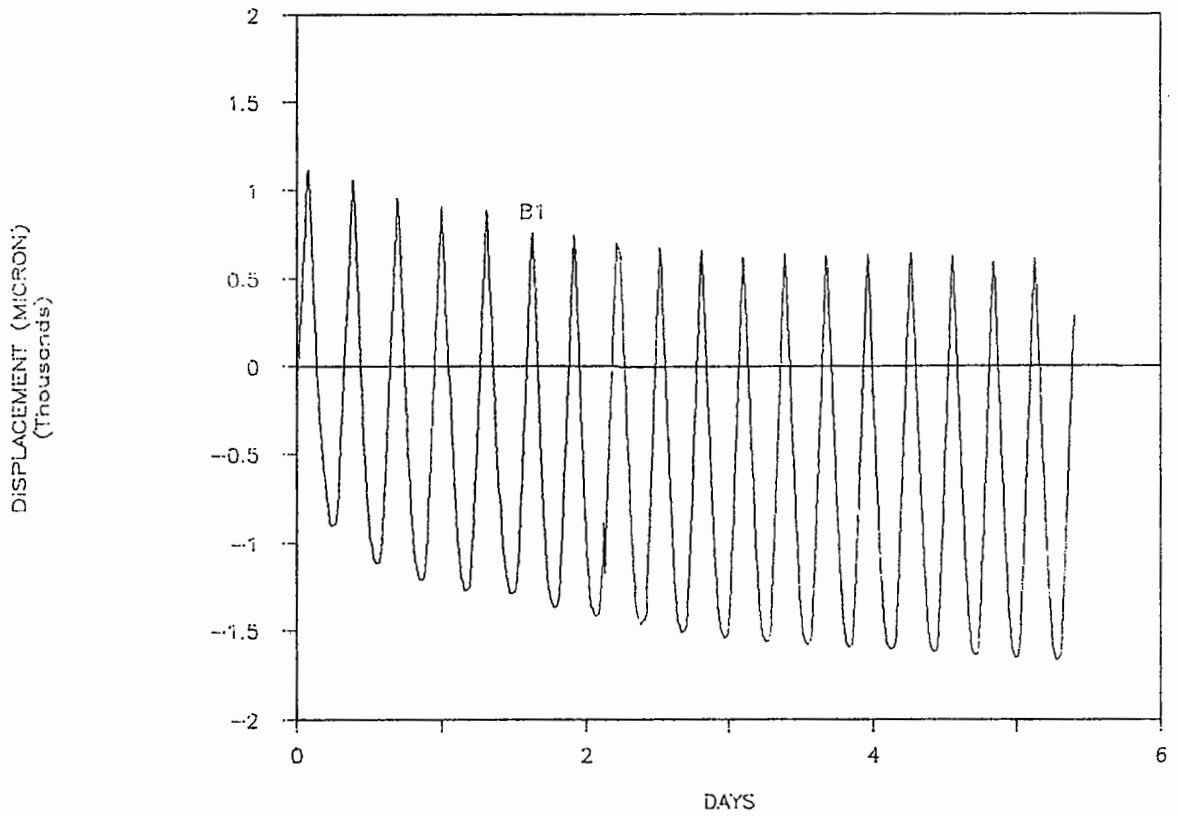


FIG. 7.37(a) SPECIMEN NO. H/1.25/20T  
(SLAB NO. 21).

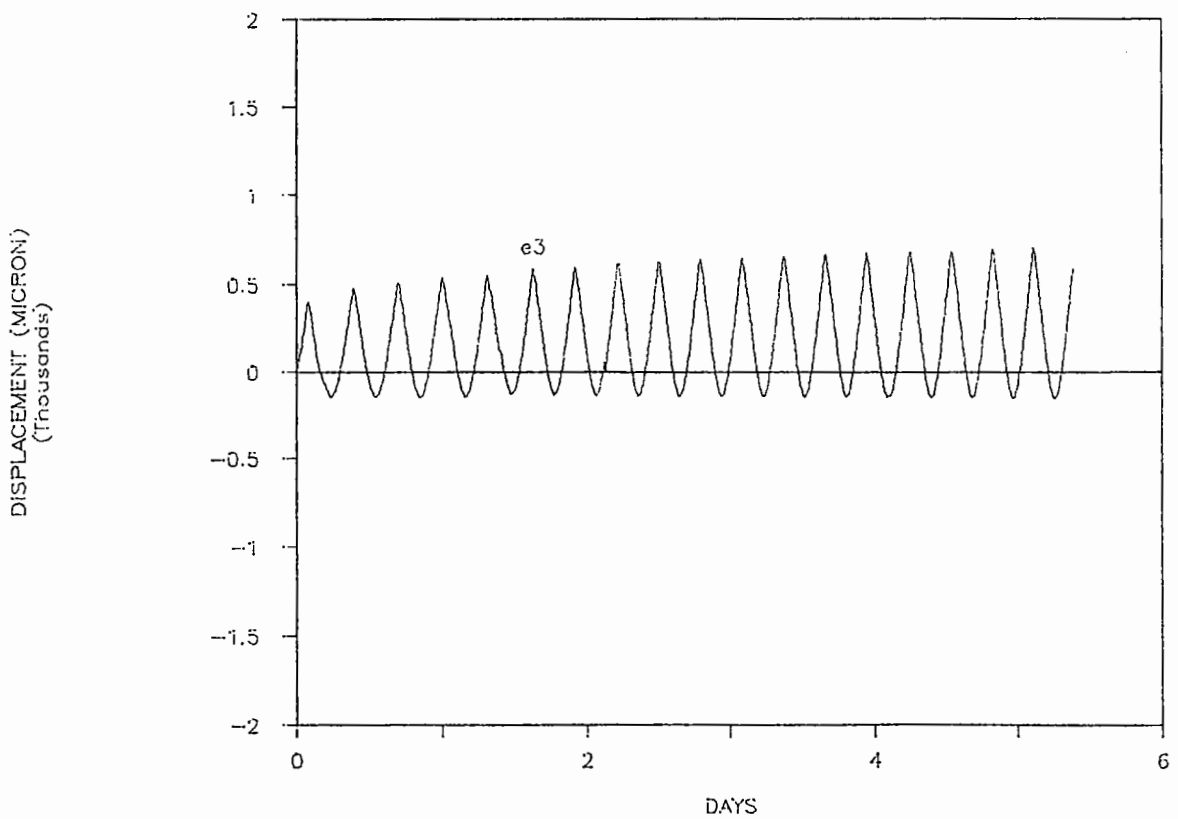


FIG. 7.37(b) SPECIMEN NO. H/1.25/20T  
(SLAB NO. 21).



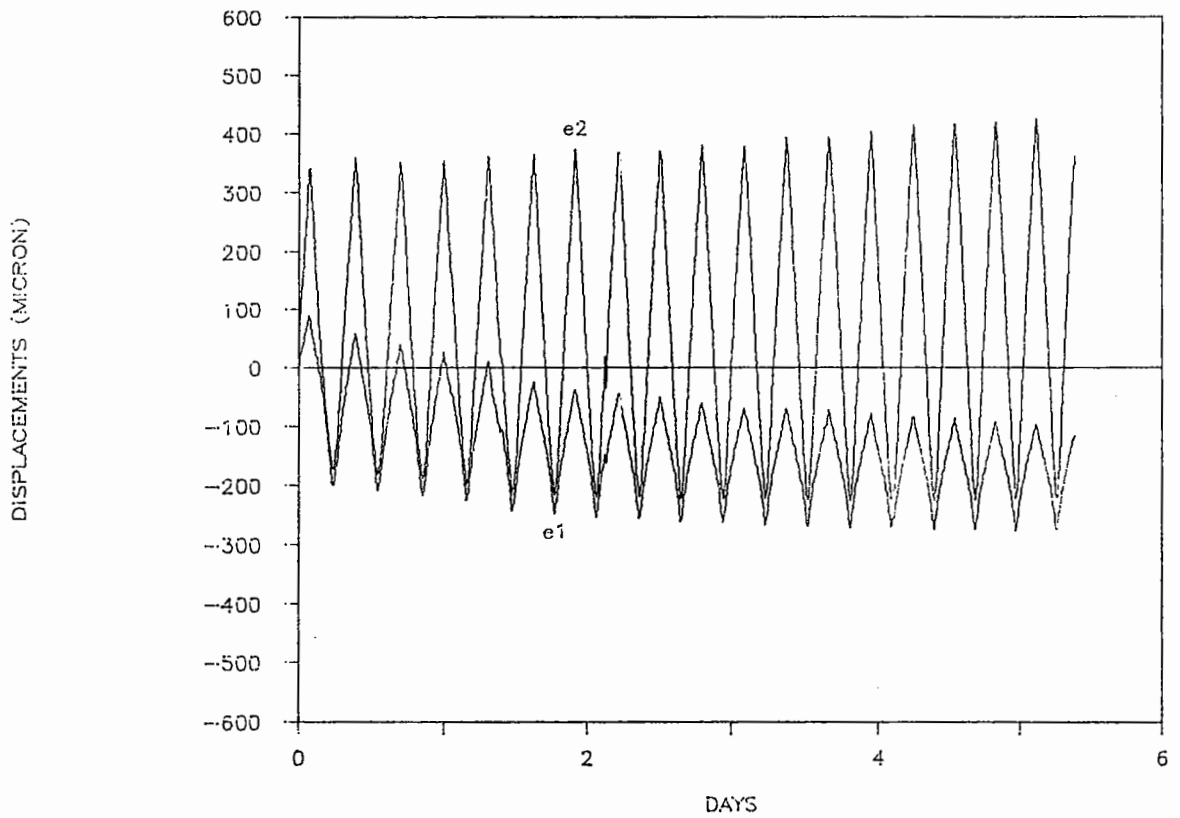


FIG. 7.38(a) SPECIMEN NO. H/1.25/20T  
(SLAB NO. 21).

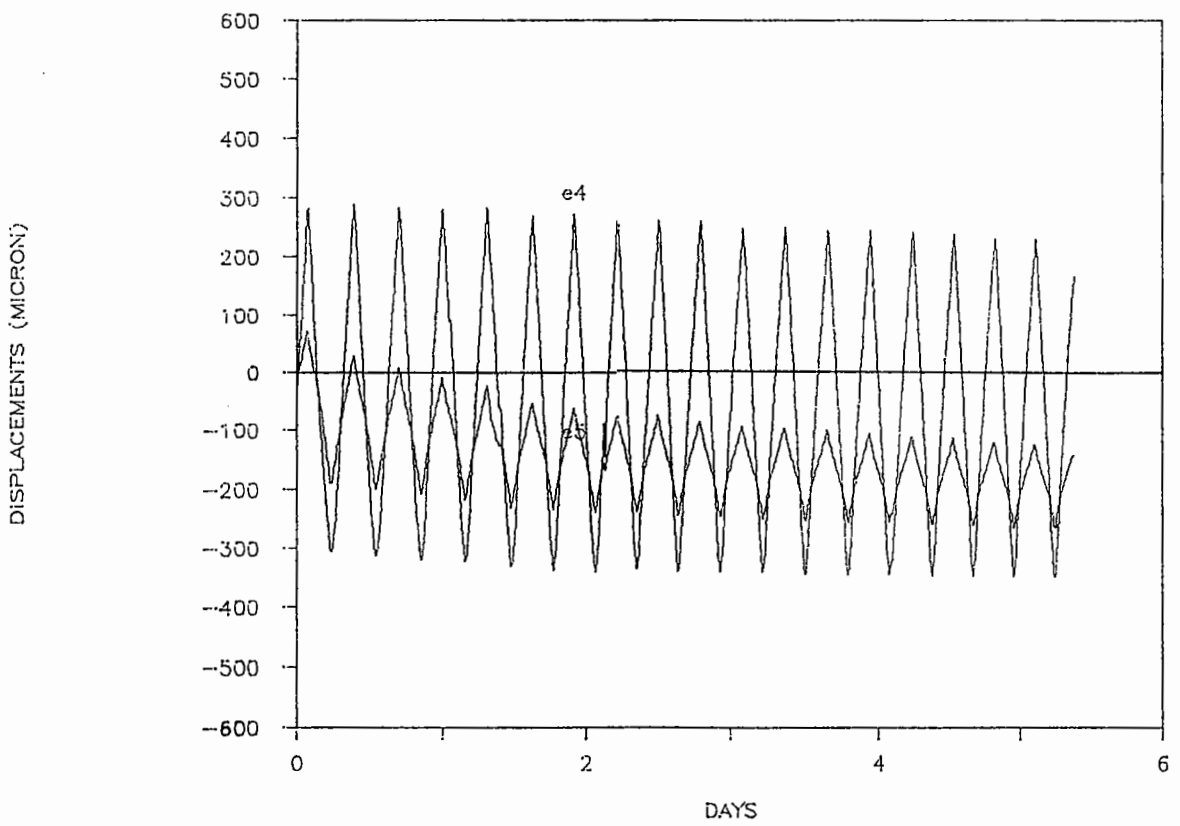


FIG. 7.38(b) SPECIMEN NO. H/1.25/20T  
(SLAB NO. 21).

H/4/20T, at the peak of the third tension cycle during the test, the peak to peak reading of LVDT e3 had become twice its initial value. At the same instance, the smallest LVDT peak to peak reading (e5) dropped more than half of its original value. The drastic shape change of the e1, e2 & e5 curves at this stage of the test should also be noted. This showed that a discontinuity occurred somewhere in the specimen and the LVDT e3 readings indicate a major crack developed near the joint gap. All these were confirmed by test observations.

Based on the findings described above, it is suggested that the time of failure of a specimen in this type of testing could be defined as 'when the peak to peak value of the e3 LVDT is increased to twice its initial value and one of the remaining LVDT's drops to its original value.' This definition could be generalised by replacing the words "the e3 LVDT" above with the words "any one of the LVDT's". This definition is only true when there is no change of gap movement during a test because, once the test is started, it would be impossible to measure the initial values of these defined parameters corresponding to the subsequent gap movement. When this definition is applied to the specimens used in this test programme, the results are as follows:

H/2/20C

Close to failure at the end of the first stage of the test.

H/2/20T	Same as above.
H/4/20T	Specimen failed at the tension peak of the third test cycle.
H/1.25/20T	Far from failure at the end of the test.

Although the definition of failure has been proposed, there is no intention to put it into application until verified by further test results.

It was noticed that the specimens used in these tests would fail to withstand the maximum design thermal movement of a working joint. This is believed to be partly caused by using an accelerated strain rate during the testing and, partly, due to the relatively high test temperature adopted. It is true that in a conventional strain controlled fatigue test, the fatigue life of a specimen will increase with test temperature but, in the EJS test, the specimen would behave differently due to the boundary conditions at the underside of the specimen. In fact, the debonding layer does not provide 100% debonding to the specimen. Inevitably, a certain amount of friction is generated at the interface between the specimen and the debonding layer during a cyclic test. When the temperature is low, the stiffness and tensile strength of the material will be relatively high. When the specimen is being pulled under these conditions, the tensile strength is great enough to overcome the frictional force and cause the specimen to slide. This results in a distribution of

strains along the specimen and helps to extend its fatigue life. Under high temperatures, this would not be possible so more concentrated strains result. Under working conditions, joint materials are always under the maximum tension when the temperature is lowest. Therefore, in future, thermal movement tests should be carried out at a lower temperature to provide more realistic conditions.

## CHAPTER EIGHT

### APPLICATION OF THE TEST RESULTS.

#### 8.1. INTRODUCTION.

Since the present project was only designed to form a part of a long-term research plan as discussed in section 5.1, there was no intention to put a limit on how the test results obtained from this research should be used. However, some possible applications are suggested. Based on the results of the laboratory tests and site studies, a simple mathematical model is established and used to estimate the service lives of buried joints.

#### 8.2 APPLICATION OF TEST RESULTS.

##### 8.2.1 Grading and Selection of Joint Systems.

It was suggested (Eyre et al 1984) that joints could be divided into different grades according to their application as follows:

Grade A: Low traffic, low traffic induced movement.

Grade B: Low traffic, high traffic induced movement.

Grade C: High traffic, low traffic induced movement.

Grade D: High traffic, high traffic induced movement.

This grading can be represented in a graphical form as shown in Fig. 8.1.

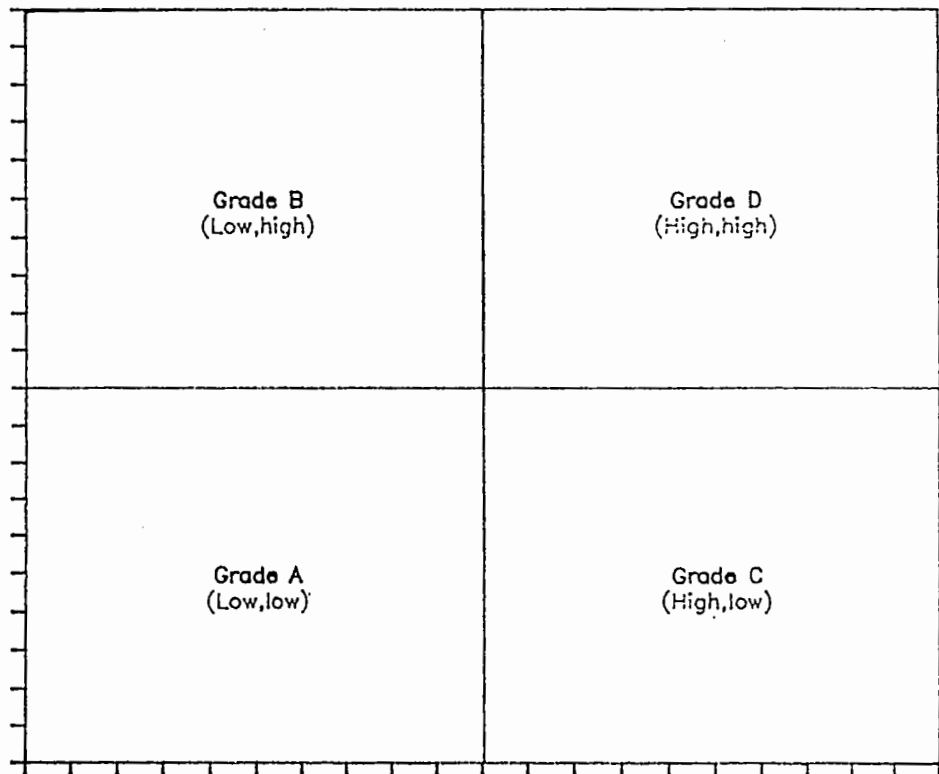
As the research continues, a sufficient number of joint types would be tested. The life prediction curves of each of these joint systems could be added to Fig. 8.1 to form a joint selection graph as shown in Fig. 8.2. In this figure, joint types I & III could be classified as grades A & D respectively, while joint type II could be classified as grade B or C.

In practice, the amount of traffic induced deck movement and traffic flow for a bridge deck could be estimated during its design period. Using these estimated values as co-ordinates, a point could be located on the joint selection graph and a suitable joint system could then be chosen with a much higher degree of confidence.

#### 8.2.2 Comparative Testing.

It is unlikely that a joint selection graph, similar to that of Fig. 8.2, would be completed in the very near future. In order to provide engineers and manufacturers with the most urgently needed information on selection of joints, comparative tests on different joint systems could be carried out with some well

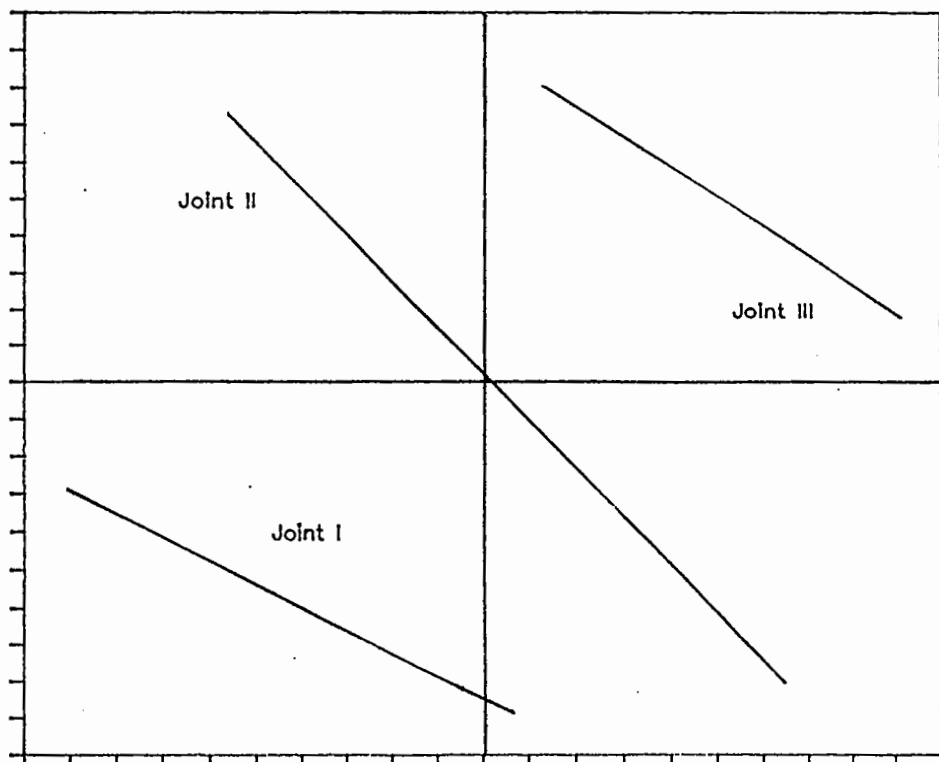
Traffic Induced movement (gap movement)



Traffic flow (cycles)

FIG. 8.1 GRADING OF JOINTS.

Traffic induced movement (gap movement)



Traffic flow (cycles)

FIG. 8.2 GRADING OF JOINTS.

defined procedures. The performance of these tested joints could then be compared with a standard joint system (a control joint), the performance of which has been verified in the road. As a result, the potential in-service performance of these tested joints could be estimated with a reasonable degree of accuracy. Although a comparative test is only regarded as a short-term solution for joint life prediction, it provides a useful means to measure the relative performance of different joint systems in an objective way.

### 8.2.3 Use of Test Results to Improve Joint Design.

The results from long-term (thermal) movement tests (Figs. 7.35 & 7.37) showed that the largest initial strains (all LVDT's have a gauge length of 100 mm) occurred at the underside of the specimens near the joint gap (LVDT B1 readings). At the top of the slabs (Figs. 7.35 to 7.38), maximum initial strains occurred in a region which is about 300 mm wide with the joint gap as its centre line (LVDT's e2, e3 & e4). As the crack propagated rapidly from the underside of the specimen, asphalt strain started to concentrate in the position just above the joint gap (e3). A similar strain distribution was observed in traffic induced horizontal movement tests, except, when precompressed specimens were used, the maximum initial strain could be in the positions where LVDT's e1 and e5 were mounted. Identification of these weak points of a buried joint allows engineers and manufacturers to take appropriate measures when designing a new joint system.



An alternative buried joint design which might provide an improved performance is suggested in Fig. 8.3 in the form of a test specimen for the EJS. The lower layer of reinforcement provided in the new design helps to initiate the effect of the debonding layer and prevents development of reflection cracking while the upper reinforcement increases the overall tensile strength of the surfacing layer to resist fatigue failure. These reinforcement layers could be added easily when a new bridge deck surfacing is installed. Improved performance of this new joint design can be assessed by laboratory tests using the EJS and computer modelling technique, as used by Huband and Wood (1986), may also be adopted.

#### 8.2.4 Direct Prediction of Joint Life.

The spectrum of deck movements for a particular bridge could be measured by means of site instrumentation. These deck movements could be divided into groups according to their ranges and the frequency of occurrence of each group could be calculated. Using this information, the working lives of the expansion joints in the bridge could be estimated with the joint life curve shown in Fig. 7.24 (solid line).

Some examples of calculated joint lives, based on the results of specimen testing and site investigation available to date, are presented in the following sections.



### 8.3 USE OF LABORATORY TEST AND SITE INVESTIGATION RESULTS TO ESTIMATE THE LIVES OF WORKING BURIED JOINTS.

#### 8.3.1 Introduction.

The service performance of fifty buried-type bridge expansion joints were investigated by Price (1982 (a)) over a period of seven years. An attempt has been made to estimate the service lives of buried joints based on the laboratory test results obtained in this research and the site information presented in Price's report.

Three groups of joints have been selected from Price's report and the relevant information on these joints is listed in Table 8.1. The joint numbers used in this table are the same as those shown in the report.

#### 8.3.2. Use of Experimental Results.

The in-service life curve for buried joints as shown in Fig. 7.24 is reproduced in Fig. 8.4. If the magnitude of traffic induced horizontal movement at a buried joint is known, the in-service life of the joint (in cycles), based on laboratory test results, can be estimated from Fig. 8.4.

$$\log L_{\text{cyc}} = 13.8 - 3.33 \times \log D_{\text{gap}} \quad (1)$$

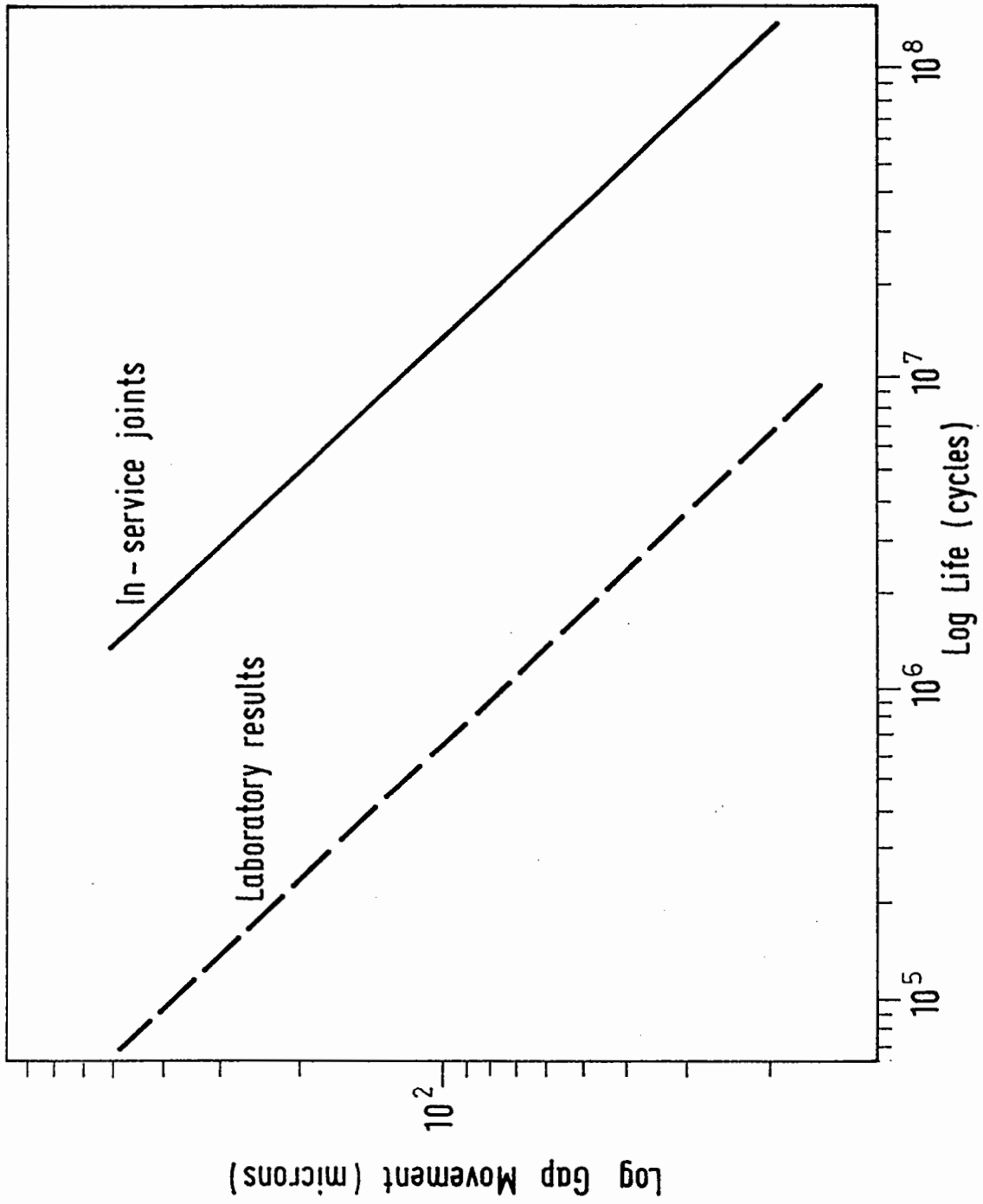


FIG. 8.4 JOINT LIFE CURVES. (Linear regression lines)

Table 8.1 Details of Joints.

Group	Joint no.	Traffic induced horizontal movement (mm)	Estimated no. of commercial vehicle/year	Estimated long. thermal movement at joint (mm)	Reinforcement	Estimated life (year)
1	7-8	0.195	1,570,000	9.9	nil	0.72
	9-10	0.195	1,570,000	9.9	Expanded metal	0.84
2	21	0.01	-	10.5	Fibre matt	3.0
	22	0.01	-	10.5	Fibre matt	3.0
	24	0.005	-	10.2	Fibre matt	3.3
	25	0.005	-	10.2	Fibre matt	3.3
3	26	0.005 to	-	7.0	Fibre matt	5.0
	27	0.01	-	2.0	Fibre matt	5.0

- = Insignificant

where  $L_{cyc}$  = estimated service life (in cycles) of a working joint when subjected to traffic induced horizontal movements only.

$D_{gap}$  = traffic induced horizontal joint gap movement (microns).

When a joint is subjected to traffic induced horizontal movement only, its service life (in years) could be estimated using the following equation:

$$L_t = L_{cyc} / V_{est} \quad (2)$$

where  $L_t$  = Estimated service life (in years) of the joint when subjected to traffic induced horizontal movement only.

$V_{est}$  = Estimated no. of commercial vehicles passing the joint per year.

This assumes that each vehicle is responsible for the application of one cycle of loading on the joint.

### 8.3.3 Estimated Joint Damage Caused by Thermal Movements.

Price (1982 (a)) reported that on bridge structures which were subjected to little or no traffic induced deck movements, all the buried joints with thermal movements up to 10 mm were free of cracks within the seven year observation period. Thermal

movements between 10 and 12 mm caused a single continuous crack after several years service, while for thermal movements greater than 14 mm a single continuous crack was developed within the first 12 to 18 months. It was suggested by Jones (1982) that a properly installed buried joint can be expected to have a working life between 10 and 14 years. Based on this information, it may be concluded that buried joints installed in this type of bridge would last at least 10 years when the thermal movement is less than 10 mm. For the purposes of predicting joint life, it is assumed that movements of 9 mm or less cause minimum damage. Therefore, the minimum joint damage caused by thermal movements alone is presently estimated to be about 10% of the total service life of the joint per year. This is based on the principle of one thermal cycle per year. The change in temperature, between Summer and Winter is regarded as the one principally causing thermal cracking.

The damage to buried joints caused by thermal movements varies with the magnitude of the thermal movement and the type of reinforcement which is used. The effects of these two variables could be included by introducing two factors,  $T$  and  $R$  which are called thermal damage and reinforcement factors respectively. The estimated values of  $R$  are shown in Table 8.2. The joint life curve shown in Fig. 8.4 has a slope of 3.33 which indicates that a power law of 3.33 is applicable to the joint damage effects caused by different transient gap movements. It is suggested that the same power law could be used to account for the damaging

Table 8.2 Values of Reinforcement Factor (R).

	R
Expanded Metal	1
Fibre Mat	2
No Reinforcement	2.5



effects on buried joints due to thermal movements.

$$\text{i.e. } T_m \propto (\text{Thermal movements})^{3.33}$$

It is assumed that  $T_m$  has a minimum value of 1, which is relevant to thermal movements up to 9 mm, and increase to its maximum when the thermal movement is 15 mm or more. Therefore  $T_m$  could be represented by the following equation.

$$T_m = \left[ \frac{\text{Thermal movement (mm)}}{9} \right]^{3.33} \quad (3)$$

where  $1 < T_m < 5.5$

Fig. 8.5 shows the curve of the  $T_m$  values.

Hence, the percentage of damage to a buried joint due to thermal movements per year can be estimated as:  $10 T_m R \%$ .

For example, if expanded metal reinforcement is present in two buried joints with 15 and 10 mm of thermal movements, the

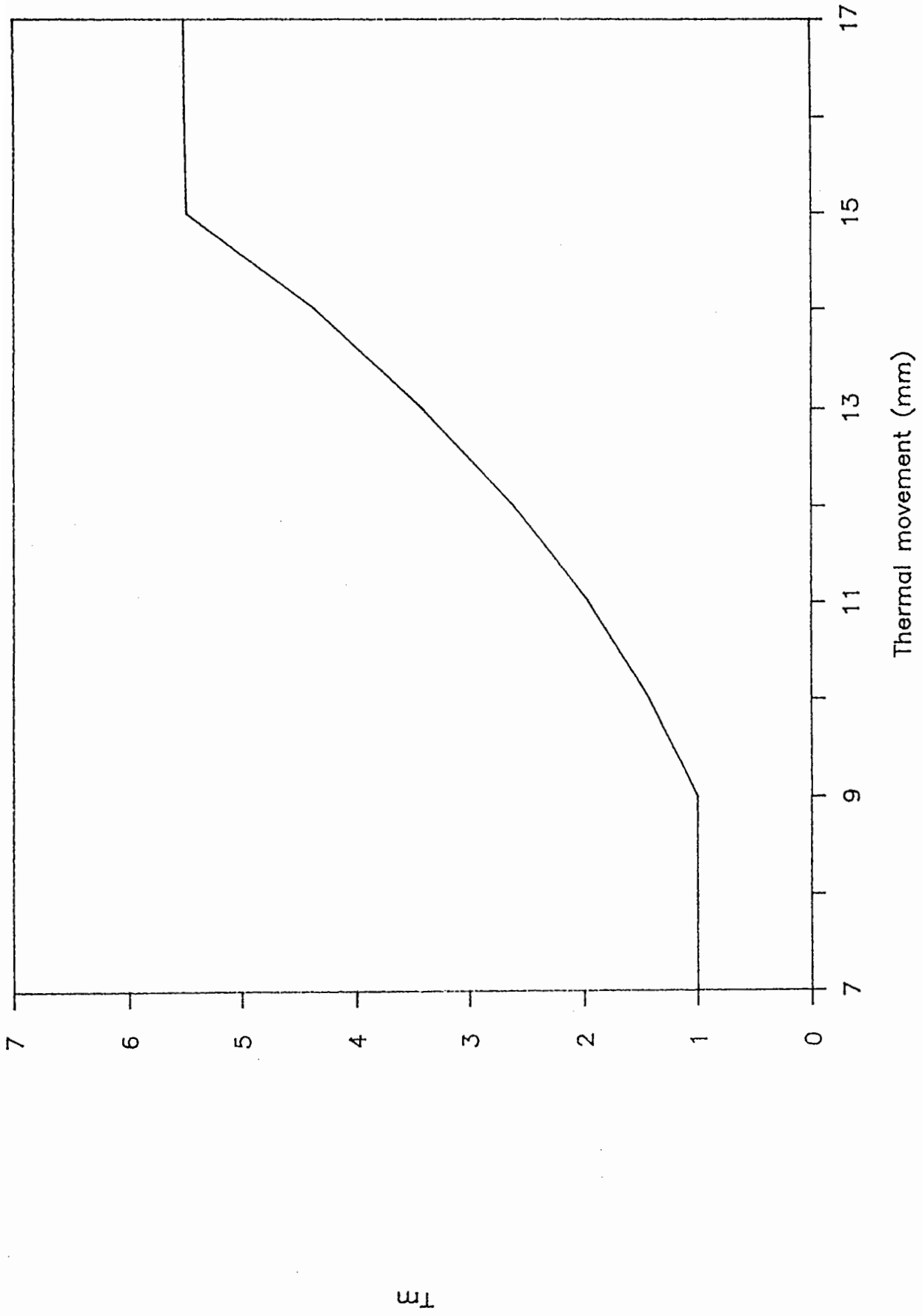


FIG. 8.5  $T_m$  VALUES.

percentage of damage due to these movements per year would be

$$54.8\% \quad (\text{i.e. } 10\% \times \left[ \frac{15}{9} \right]^{3.33} \times 1.0) \text{ and } 14.2\% \text{ respectively.}$$

This represents working lives of 22 months for the first joint and 7 years for the second. These results match closely to those observed by Price.

#### 8.3.4 Life Estimation of Working Joints.

When a buried joint is only subjected to thermal movements, its service life (in years) could be estimated using the following equation:

$$L_{\text{therm}} = 1 / (0.1 T_m R) \quad (4)$$

where  $L_{\text{therm}}$  = Estimated service life (in years) of the joint when subjected to thermal movement only.

The service life of a working joint, when subjected to thermal and traffic induced horizontal movements, could be estimated using the following equation:

$$L = \frac{L_{\text{cyc}}}{V_{\text{est}}} (1 - 0.1 T_m R L) \quad (5)$$

where  $L$  = the estimated service life (in years) of the joint when subjected to thermal and traffic induced horizontal movements.

### 8.3.5. Examples.

Estimated service life of:

A) Joint group 1. (no. 7 to 10)

Estimated service life of the joints (in cycles) when subjected to traffic induced horizontal movements only.

Horizontal movement = 0.195 mm (Table 8.1)

$$L_{\text{cyc}} = 1,493,340 \text{ (say } 1,500,000\text{)}$$

(Equation 1)

Thermal damage and reinforcement factors:

Horizontal thermal movement = 9.9 mm (Table 8.1)

$$T_m = 1.37$$

(Fig. 8.5)

Reinforcement used:	Nil	(Joints 7 & 8)
	Expanded metal	(Joints 9 & 10)
		(Table 8.1)
R:	2.5	(Joints 7 & 8)
	1	(Joints 9 & 10)
		(Table. 8.2.)

Estimated no. of commercial vehicles passing per year:

$$V_{\text{est}} = 1,570,000 \quad (\text{Table 8.1})$$

Therefore, the estimated service life (in years) of joints 7 and 8 is:

$$L = \frac{1,500,000}{1,570,000} (1 - 0.34 L)$$

$$= 0.72 \text{ years} \quad (\text{Equation 5})$$

The estimated service life (in years) of joints 9 and 10 is:

$$L = \frac{1,500,000}{1,570,000} (1 - 0.14 L)$$

$$= 0.84 \text{ years} \quad (\text{Equation 5})$$

B) Joint group 2 (no. 21, 22, 24 & 25).

Due to the small amount of traffic induced horizontal movement involved, its effects could be ignored in this calculation.

Thermal damage and reinforcement factors:

Thermal movements = 10.5 & 10.2 (Joints 21, 22 & 24,25)

(Table 8.1)

$T_m = 1.67 \text{ \& } 1.52$  (Fig. 8.5)

Reinforcement used: Fibre matt

$R = 2$  (Table 8.2)

Therefore, the estimated life of joints 21 & 22:

$$\begin{aligned} L_{\text{therm}} &= 1/(0.1 \times 1.67 \times 2) \\ &= 3 \text{ years} \end{aligned} \quad \text{(Equation 4)}$$

and the estimated life of joints 24 & 25:

$$\begin{aligned} L_{\text{therm}} &= 1/(0.1 \times 1.52 \times 2) \\ &= 3.3 \text{ years} \end{aligned} \quad \text{(Equation 4)}$$

C) Joint group 3 (no. 26 & 27).

Similar to joint group 2,

Thermal damage and reinforcement factors:

Thermal movements = 9.0 and 2.0 mm

$T_m = 1.0$  (Fig. 8.5)

Reinforcement used : Fibre matt

$R = 2$  (Table 8.2)

Therefore, the estimated life of the joints:

$$\begin{aligned} L_{\text{therm}} &= 1/(0.1 \times 1.0 \times 2) && \text{(Equation 4)} \\ &= 5 \text{ years} \end{aligned}$$

Fig. 2.11 shows the in-service condition of the fifty joints as observed by Price (1982 (a)). The service lives of joints 7, 8, 9, 10, 21, 22, 24, 25, 26 & 27, as estimated above, are listed in Table 8.1.

The deterioration of an in-service joint generally started with the formation of short hairline cracks along the joint gap. As these cracks propagated and joined, they formed a continuous single crack across the joint. Multiple cracks and spalling then followed. At this stage, the joint needed replacement. In the laboratory tests, joint failures usually occurred when a continuous single crack was observed. Therefore, the lower and upper life limits of an in-service joint can be defined as the times at which a continuous single crack and multiple cracks are first observed (or the joint is replaced) respectively. These limits are compared with the estimated lives of the joints considered here in Fig. 8.6. Fig. 8.7 shows the results in terms of the average figures for each joint group.

It is reasonable to assume the actual failure point of a joint lies between the upper and lower life limits and its location could be defined as the mid-point of the duration between these life limits. When the average value of these defined points and the corresponding estimated life of the joints in each group are compared, the result will be as shown in Fig. 8.8. This indicates a very close agreement between the estimated and observed service lives and gives some confidence to the tentative procedure outlined here.

#### 8.3.6 Discussion.

In the above examples, only joint movements caused by commercial



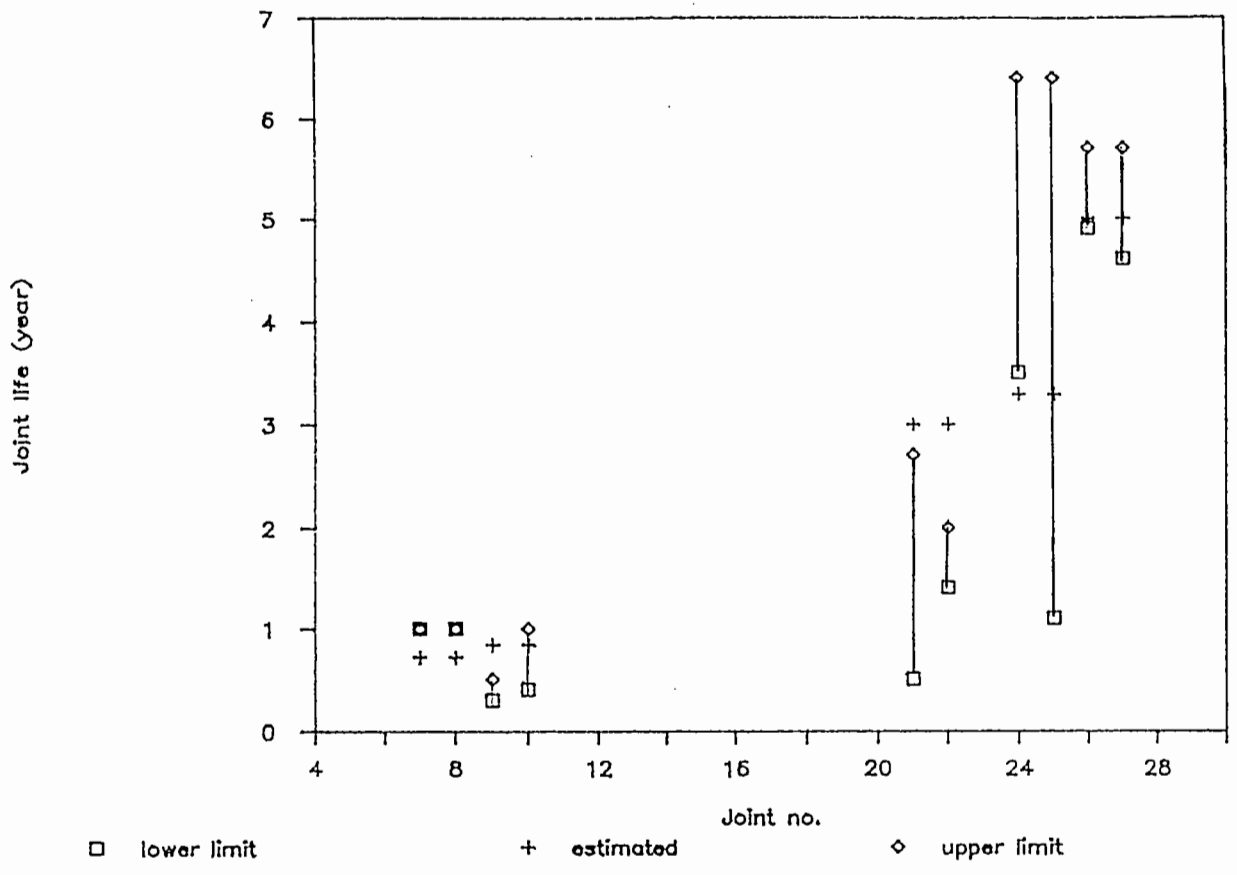


FIG. 8.6 ESTIMATED JOINT LIVES AND DEFINED LIFE LIMITS.

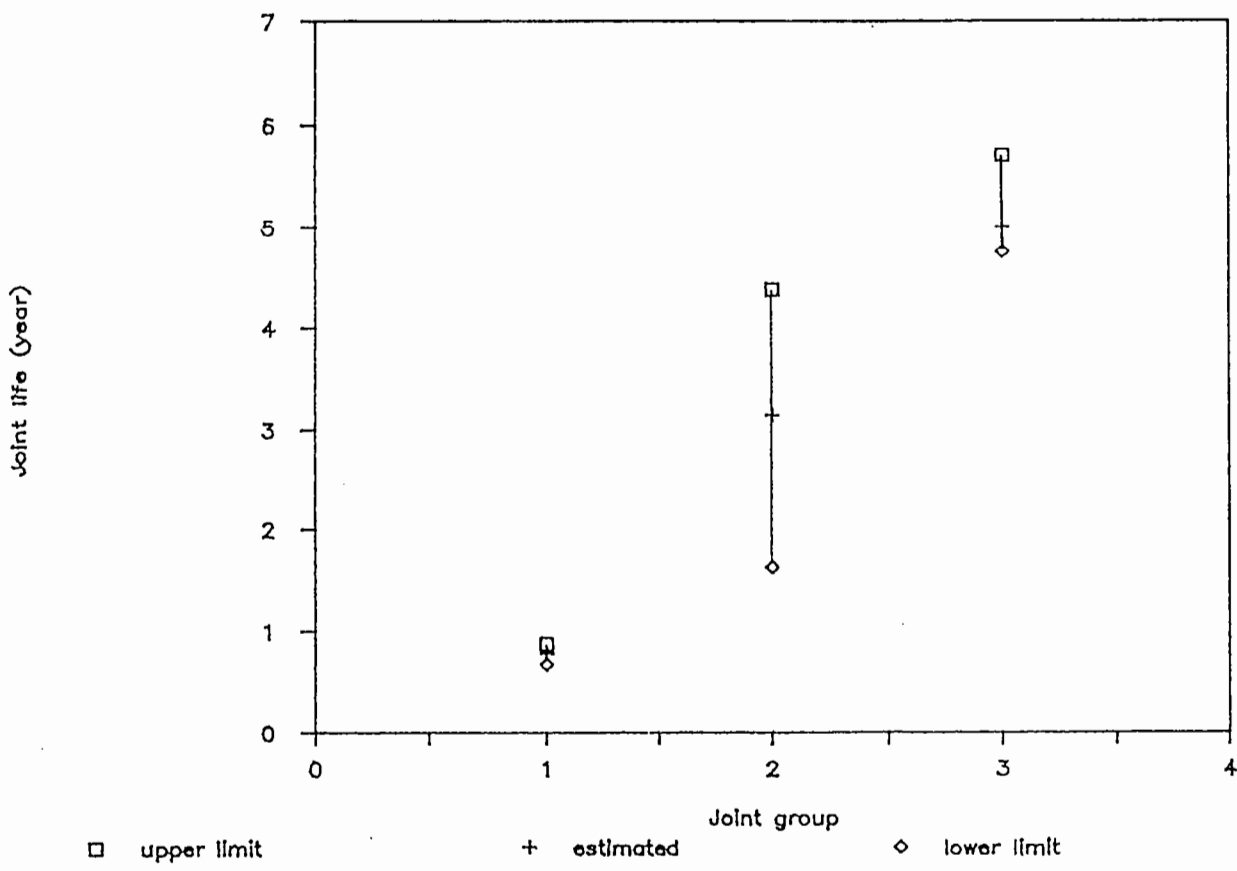


FIG. 8.7 AVERAGE VALUES OF THE ESTIMATED JOINT LIVES AND DEFINED LIFE LIMITS OF THE JOINT GROUPS.

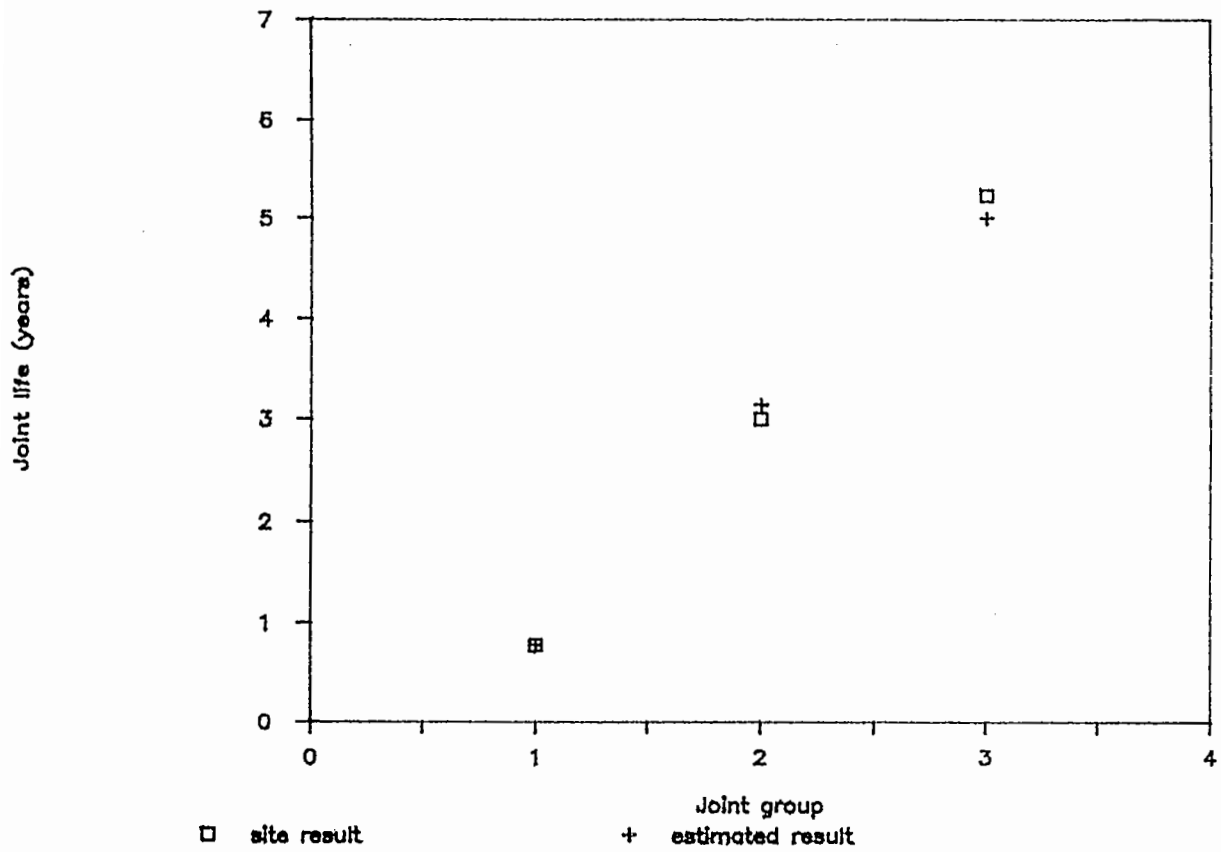


FIG. 8.8 COMPARISON OF THE AVERAGE VALUE OF THE ESTIMATED AND DEFINED LIVES OF THE JOINT GROUPS.

vehicles were considered. However, the effects of other light vehicles could be included when required. If the horizontal joint movements caused by these light vehicles are known, the joint life (in cycles), when subjected to these movements alone, could be estimated using Fig. 8.4. The combined effects of different types of vehicles could be accounted for using Miner's rule. The total effects of seasonal and diurnal thermal movements could also be estimated in a similar way.

Although wheel loads have some damaging and healing effects on joint materials, by means of tracking and compaction respectively, they are considered to be less important than joint movements. The areas covered by wheel tracks consist of a small proportion of the whole joint, and most of the gap movements occur when the wheel loads are away from the joint.

The life estimation technique used herein works reasonably well. However, more information, both from site and laboratory, must be made available before the method could be finalised and used with confidence.



## CHAPTER NINE

### FURTHER JOINT SPECIMEN TESTING.

#### 9.1 INTRODUCTION.

The magnitude of traffic induced vertical and rotational deck movements are normally small in bridges which use buried joints. Therefore, the damaging effects of these deck movements on buried joints are often less significant than those caused by horizontal movements. Table 9.1 shows the typical values of vertical and rotational deck movements measured on site and reported by Price (1982 (a)). Price suggested that the damaging effects of vertical and rotational deck movements are negligible when their magnitudes are less than 2 mm and  $100 \times 10^{-6}$  radian respectively. However, as far as the present project is concerned, it was considered to be important that the behaviour of buried joints when subjected to these deck movements could be studied in the laboratory using the EJS.

In total, four joint specimens were used in the present test series to investigate the effects of these deck movements on the performance of buried expansion joints. The codes used to

Table 9.1 Comparison of Test Data and In-service Conditions.

○  
(All tests are at 3 Hz and 20 C)

Sample	Deck End Rotation <sup>-6</sup> (Radians x 10 )	Vertical Displacement ( mm )	Load Cycles
* In-situ conc. on steel beam bridge.	210	0.17	-
* In-situ conc. bridge.	60	0.04	-
Specimen no. V/0.3/20	-	<u>±</u> 0.30 <u>±</u> 0.70	2,233,000 329,000
Specimen no. V/0.7/20	-	<u>±</u> 0.70	600,000
Specimen no. B/2300/20	2300 3300	-	1,089,500 69,200
Specimen no. B/3300/20	3300	-	213,100

\* = Extract from TRRL report SR 740, Table 3.

specify the test conditions for each specimen are explained as follows:

a) Vertical movement tests:

V	/	0.7	/	20
Vertical movement tests		Movement range in mm.		Test temperature in °C

b) Rotational movement tests:

B	/	2300	/	20
Bending test		Movement range in radian (x 10 <sup>-6</sup> )		Test temperature in °C

To ensure that tests could be finished within a reasonably short time, over-sized movements were used to accelerate the test rate. All tests were carried out at a frequency of 3 Hz and a temperature of 20 °C. Details of the test parameters used for each test are shown in Table 9.1.

## 9.2 VERTICAL MOVEMENT TESTS.

### 9.2.1 Coupling of the Vertical Actuator.

A connection between the vertical actuator and tray carrier 1 (Fig. 3.1) was required before vertical movement tests could be carried out. A coupling with a design similar to that for the horizontal actuator (section 4.1.2) was fixed to the vertical actuator load cell. On top of this coupling, a 40 mm thick steel plate was fixed. This plate could then be coupled with the tray carrier 1 by bolts located at the ends of the plate as shown in Figs. 9.1 & 9.2. During testing, the tray carrier 1 was unlocked from its support, connected to the 40 mm thick steel plate and became free to move up and down under the control of the vertical actuator.

The vertical movement near the joint gap was monitored by two LVDT's which were mounted at the positions shown in Figs. 9.2 & 9.3. The movement of the vertical actuator was controlled by the Dartec system in a similar manner to the gap movement control for horizontal movement tests. Details of this control method are described in section 6.2.3.

### 9.2.2 Instrumentation.

Five LVDT's were used to measure the vertical movements at



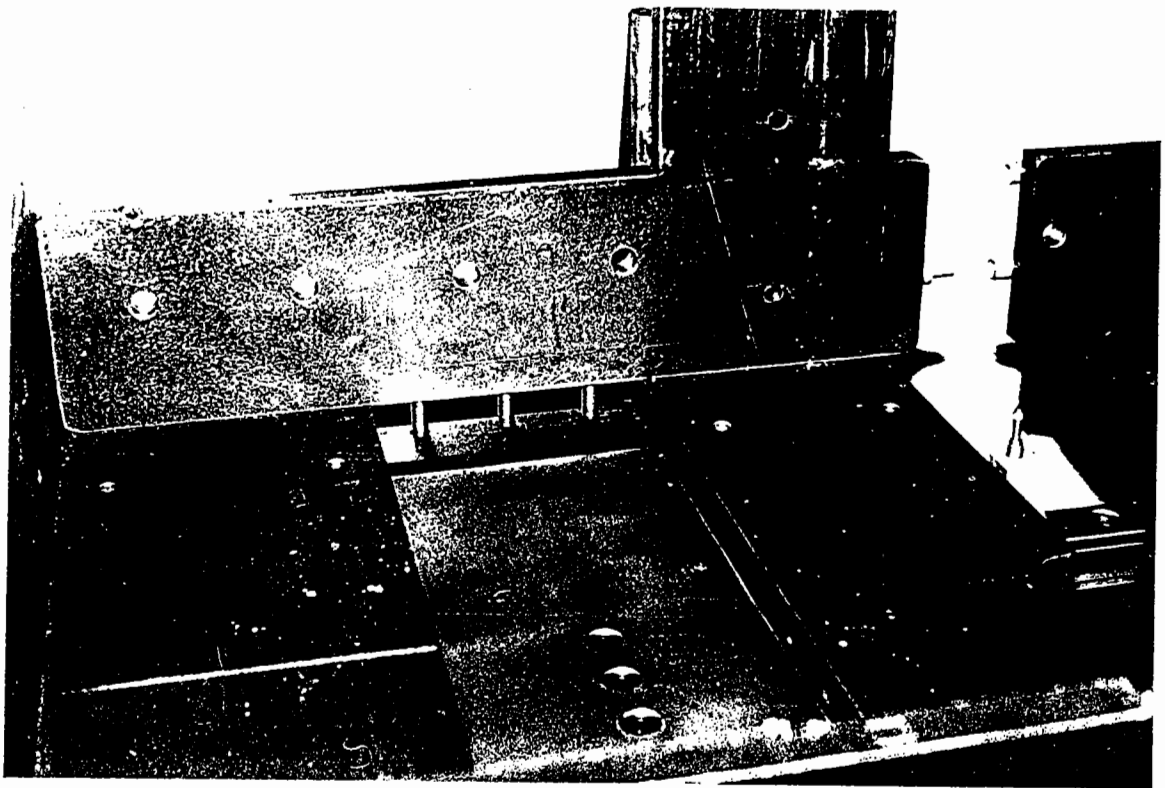


FIG. 9.1 COUPLING PLATE OF THE VERTICAL ACTUATOR.

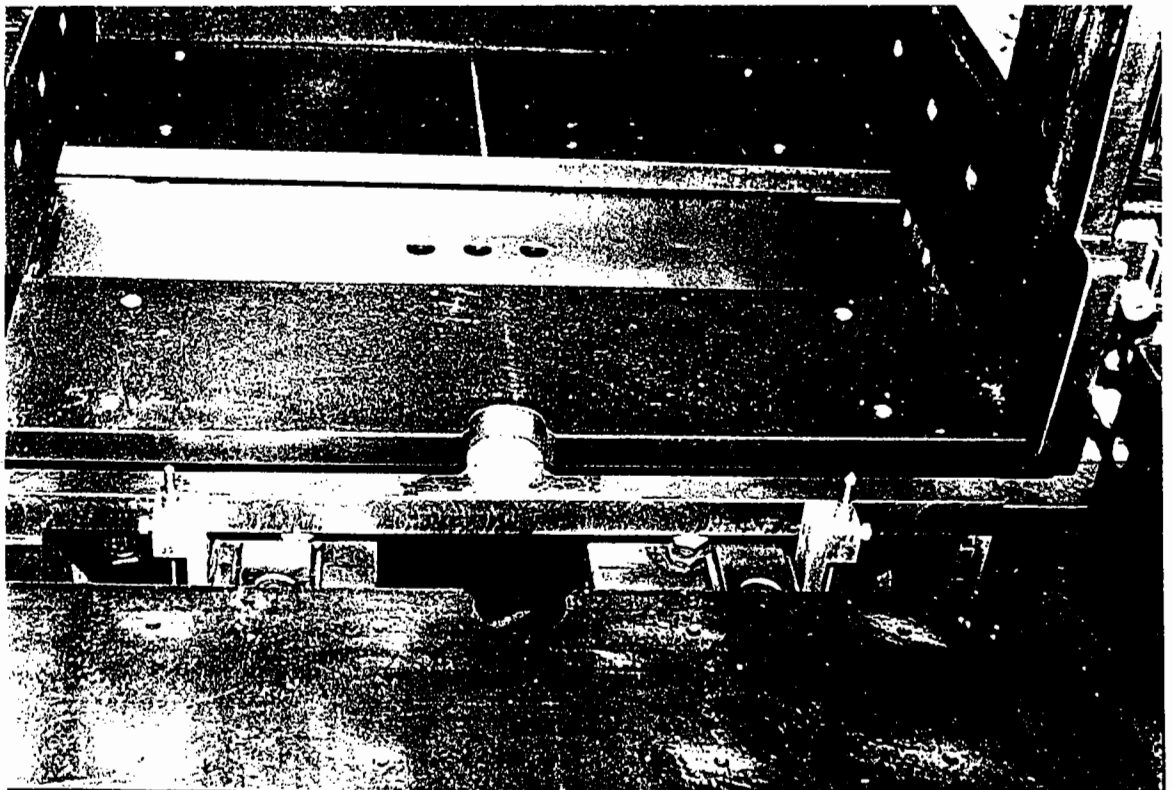


FIG. 9.2 LOCATIONS OF THE VERTICAL MOVEMENT  
CONTROL LVDT'S.



FIG. 9.3 MOUNTING DETAILS OF THE VERTICAL  
MOVEMENT CONTROL LVDT.

different positions on the top surface of the test specimen. These LVDT's were mounted on a steel frame, as shown in Figs. 9.4 & 9.5. The LVDT's were placed at 100 mm centres with the middle LVDT located at the centre point the joint gap. Other measuring devices included the built-in LVDT and load cell of the vertical actuator, two movement control LVDT's and a thermocouple used to measure the temperature of the specimen. The method of data acquisition was the same as that described in section 4.6. Similar instrumentation and data collection methods were used for bending tests.

### 9.2.3 Test Details and Results.

Specimen no. V/0.3/20 was tested in 2 stages. In the first stage, a vertical movement of  $\pm 0.3$  mm was introduced. The test was stopped after 2,233,000 load cycles and no obvious damage to the specimen was observed. In the 2nd stage of the test, the vertical movement was increased to  $\pm 0.7$  mm. After a further 329,000 load cycles, two lines of minor cracks developed about 180 mm on each side of the joint gap. These cracks were very fine and could hardly be seen when the cyclic action was stopped.

The second specimen, no. V/0.7/20, was tested with a vertical movement of  $\pm 0.7$  mm. After 600,000 load cycles. Cracks similar to those observed on specimen no. V/0.3/20 were developed. The locations of these cracks are shown in Fig. 9.6. To make the line of these cracks more obvious, they have been thickened by coloured pens before the photograph was taken.

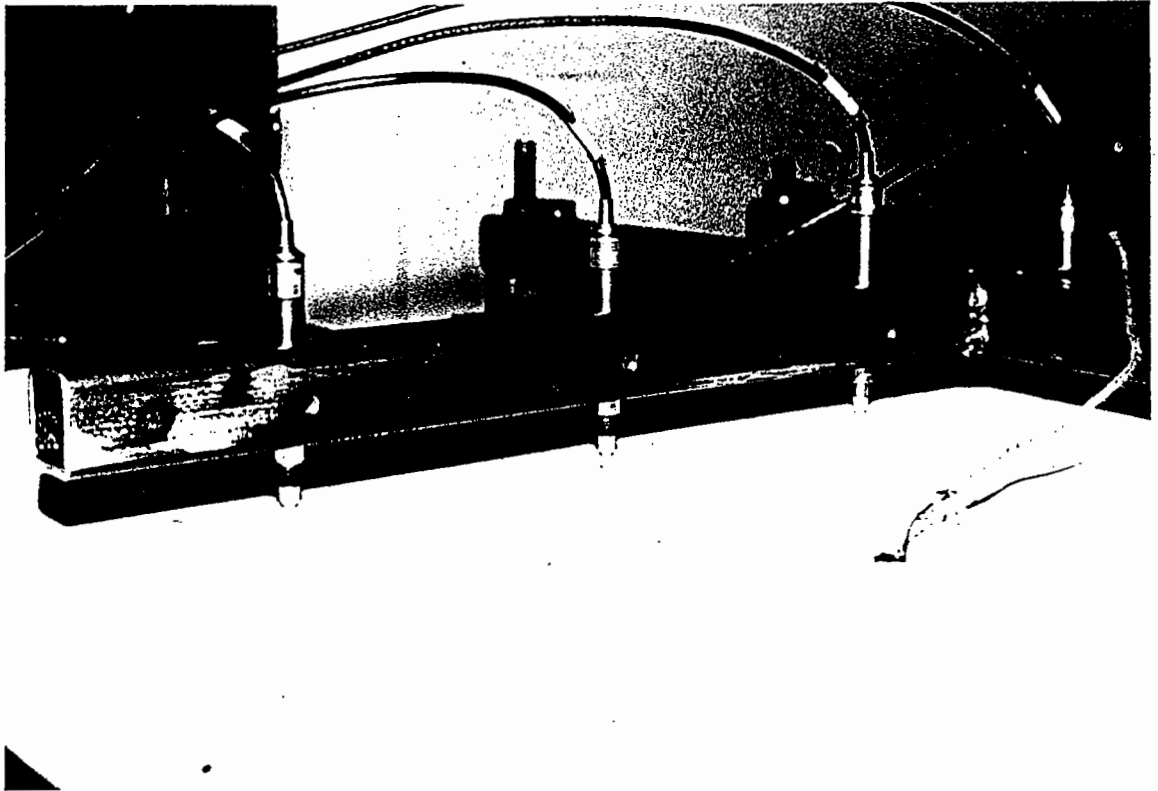


FIG. 9.4 INSTRUMENTATION OF TEST SPECIMEN.

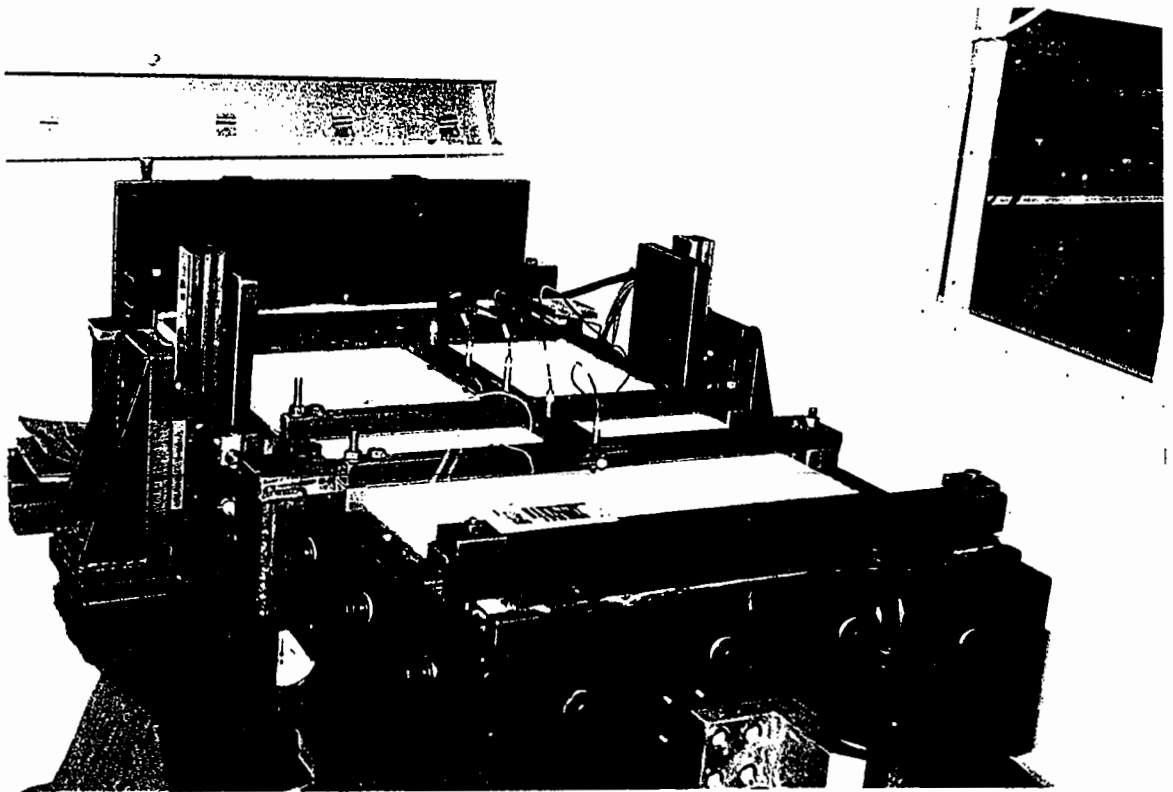


FIG. 9.5 LVDT'S MOUNTING FRAME.

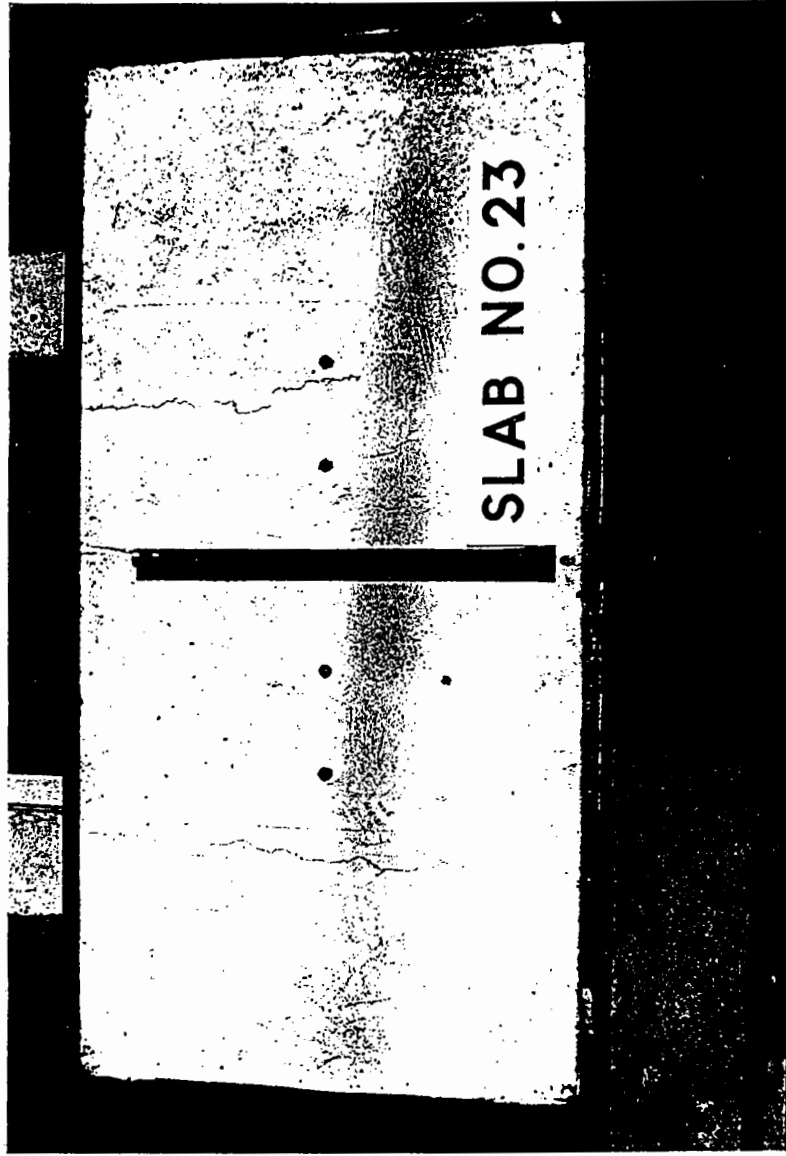


FIG. 9.6 SPECIMEN NO. V/0.7/20 AFTER TEST.  
(SLAB NO. 23).

The load histories of the tests are presented in Figs. 9.7 & 9.8. In Fig. 9.7, the sudden load increase near the end of the plot indicates the start of the 2nd stage of the specimen test. The plots of the tensile loading provide certain indications on how the specimens behaved during the test. As shown in Figs. 9.7 & 9.8, the tensile load reactions dropped quickly in the first couple of thousand load cycles. This might have been due to the break-down of the adhesive force between the joint material and the debonding layer. The loads were then levelled off and varied little for a considerable period. Near the end of the tests, the rate of change of the tensile loads suddenly increased. This might be an indication of when the specimens started to fail.

The smallest vertical movement used in the tests was  $\pm 0.3\text{mm}$ , (Table 9.1) which is over 3.5 times larger than the maximum value recorded in Price's report. If the damaging effects of vertical deck movements follow a power law of 2.5, the actual joint damaging effects introduced in the tests would be increased by 23 times, i. e.  $3.5^{2.5}$ . In fact, no joint damage was observed after 2,233,000 load cycles when such vertical test movement was used. Therefore, it would be reasonable to conclude that the vertical deck movement contributes little to the deterioration of a buried joint unless its magnitude is much higher than normal.

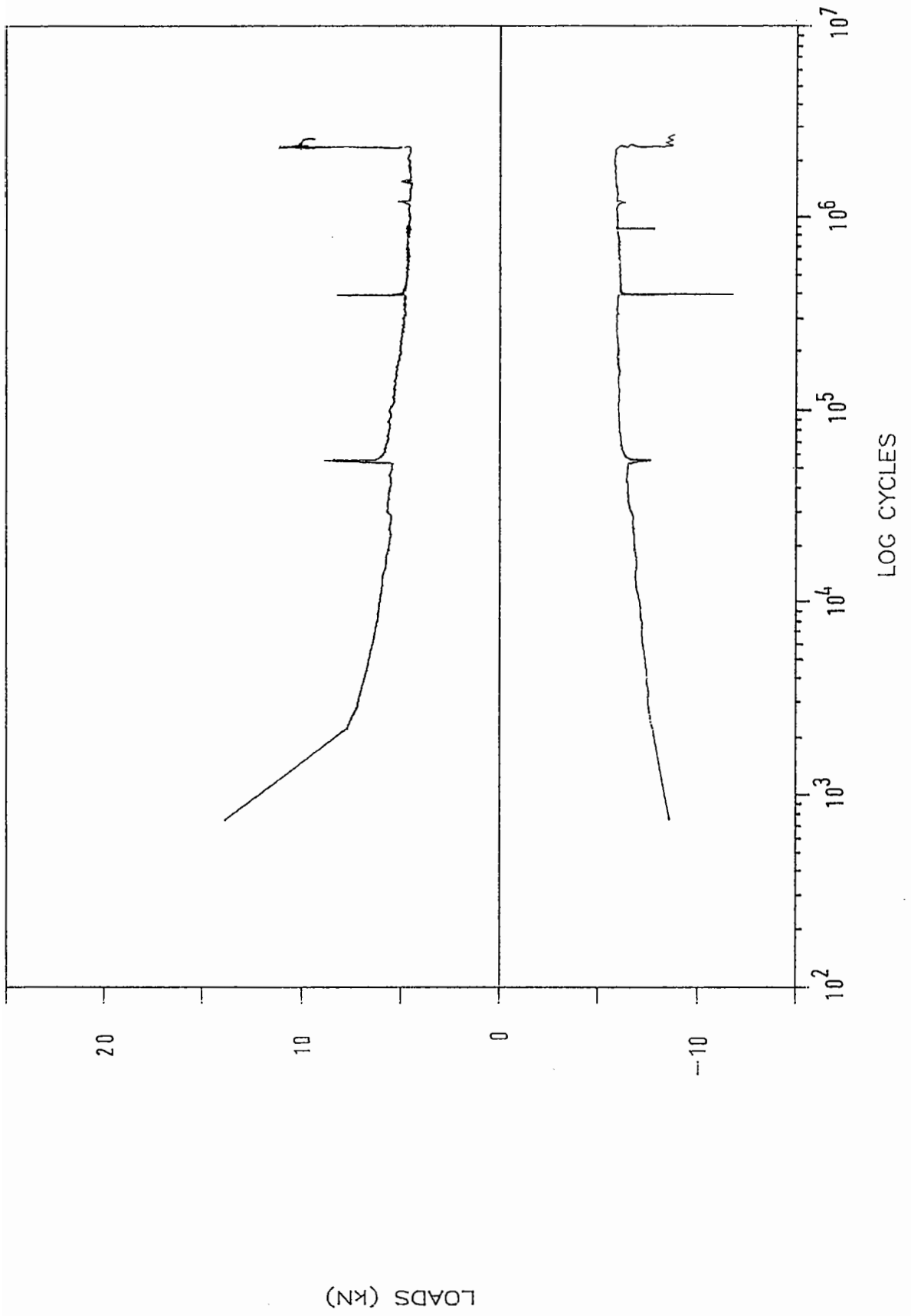


FIG. 9.7 SPECIMEN NO. V/0.3/20.

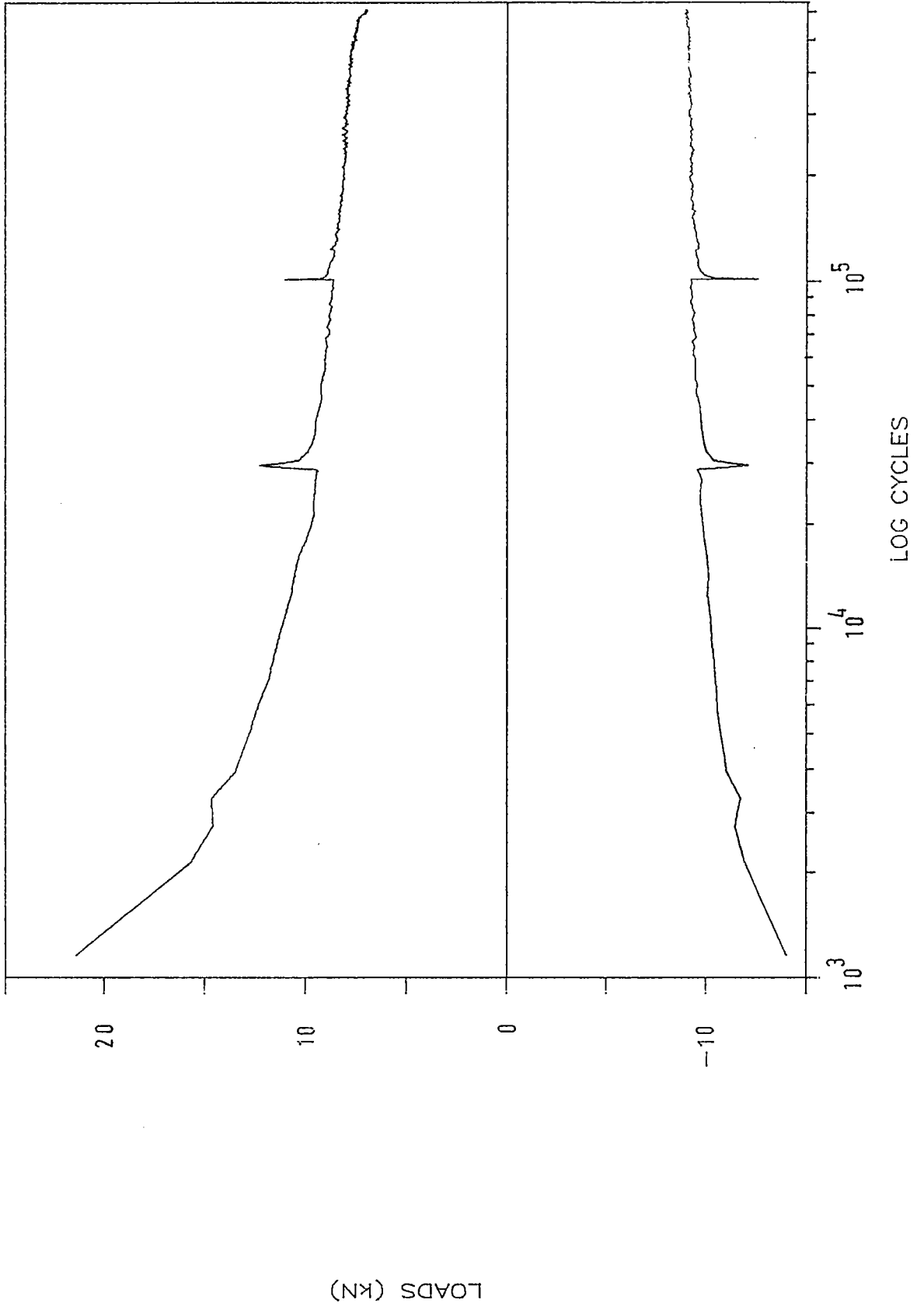


FIG. 9.8 SPECIMEN NO. V/0.7/20.



### 9.3 ROTATIONAL MOVEMENT TESTS.

#### 9.3.1 Modification to the Expansion Joint Simulator (EJS)

The method of generating "bending" in a test specimen with the EJS was described in section 3.2. It was originally planned to relocate the vertical actuator to position 2 (Fig. 3.1) to produce the thrust required for bending. However, by using a pair of newly designed links to join the tray carriers together, bending of the specimen could be generated by the horizontal actuator working in its original position. As shown in Fig. 9.9, each link consisted of two bearings fixed in a steel metal housing. Two "sliding fit" bolts were used to fix the links to the sides of the tray carriers across the joint gap. During testing, the horizontal actuator was connected to tray carrier 2 which was pushed and pulled along its horizontal bearing guides. The links were so designed that they allowed the thrust from the horizontal actuator to be transferred from tray 1 to tray 2 and left the latter free to tilt up and down (rotate) together with the triangular support system about the pivot (Fig. 3.1).

The amount of rotation was monitored by two LVDT's which measured the horizontal displacement of the triangular support system at a position just beneath the tray carriers and near the joint gap. The signals from these LVDT's were then fed into the Dartec system for movement control purposes.

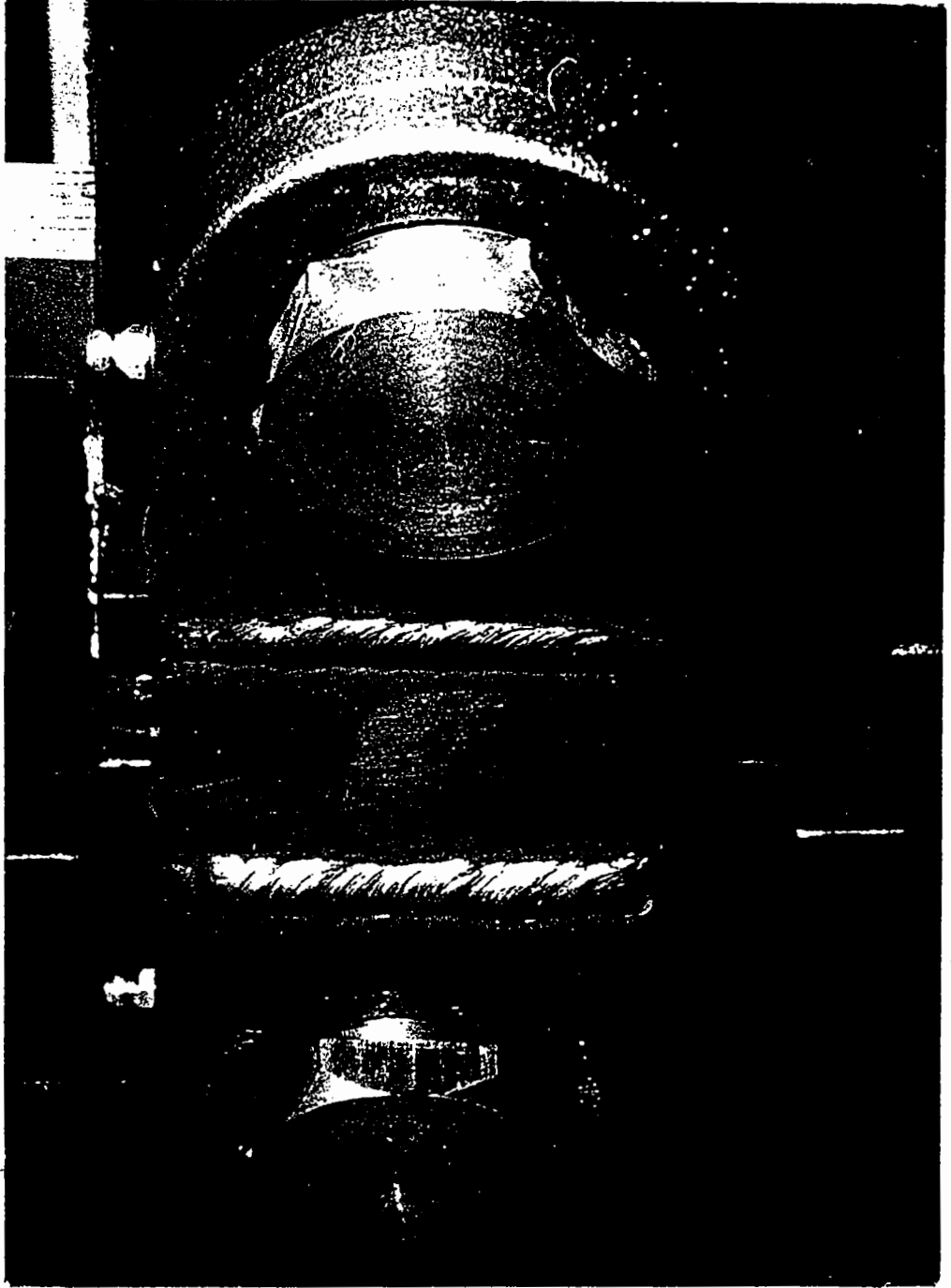


FIG. 9.9 DETAILS OF THE LINK.

### 9.3.2 Test Details and Results.

Initially, specimen no. B/2300/20 was tested with a rotational movement of  $2300 \times 10^{-6}$  radian. After 1,089,500 load cycles, no crack was observed on the surface of the specimen. The rotational movement was then increased to  $3300 \times 10^{-6}$  radian and the test allowed to continue. After a further 69,200 load cycles, a very fine but continuous crack was detected along the joint gap.

The second specimen, no. B/3300/20, was tested with a rotational movement of  $3300 \times 10^{-6}$  radian. After 213,100 load cycles, a continuous crack, similar to that of specimen no. B/2300/20, was observed.

Although the minimum rotational movement used in these tests,  $2300 \times 10^{-6}$  radian, was 11 times greater than the largest rotational movement recorded on site as reported by Price (1982 (a)), specimen B/2300/20 showed no sign of failure after over a million load cycles. The amount of this rotational movement is much greater than any possible design rotational movement for bridges with buried joints.

Figs. 9.10 & 9.11 show the peak to peak values of the vertical displacements measured by the LVDT's mounted on the fixed half of the specimen (tray 2, Fig. 3.1). The readings of the central LVDT in these figures show a sudden change after about 316,000 & 31,600 load cycles respectively. These sudden changes might

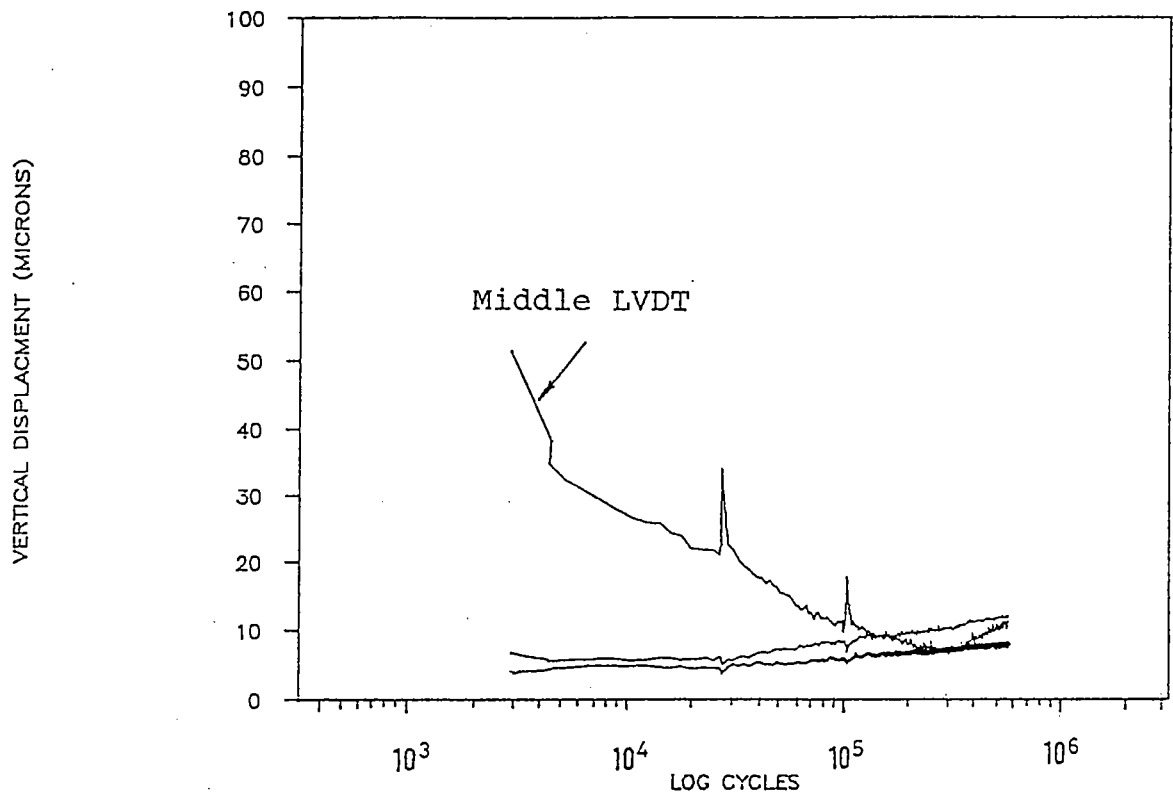


FIG. 9.10 SPECIMEN NO. B/2300/20.

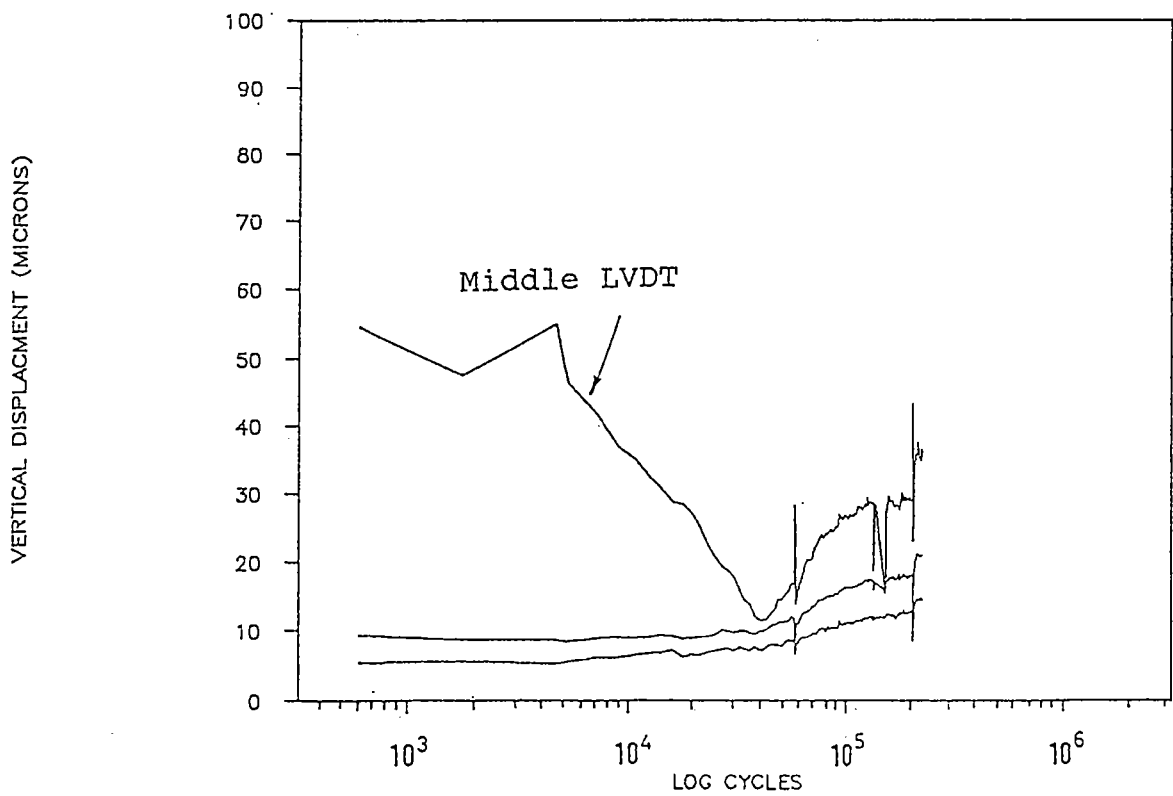


FIG. 9.11 SPECIMEN NO. B/3300/20.

indicate the points of failure of the specimens. However, further information would be required to confirm this.

## CHAPTER TEN

### CONCLUSIONS AND RECOMMENDATIONS FOR FUTURE WORK.

#### 10.1 CONCLUSIONS.

1. An expansion joint simulator (EJS) has been developed at the University of Nottingham. This equipment allows bridge deck expansion joints with a thermal movement up to 50 mm to be tested at an accelerated rate. The overall performance of the EJS was found to be satisfactory.
2. In order to isolate the effects of various deck movements on bridge expansion joints, different movements were introduced independently during testing. However, it is considered that these movements should be combined in future tests if required. This will involve some modifications to the EJS.
3. A technique to conduct accelerated joint tests has been evolved. It involves increased frequency of applied loads and use of continuous cyclic loading. A series of tests on buried joint specimens has been carried out to verify the possibility of testing bridge expansion joints in the laboratory.

4. The performance of the Dartec control system for the EJS was greatly improved after updating by the manufacturer at one stage of the research. A similar operation will be useful in the future as new and more advanced electronic components become available.

5. The computerised data acquisition system developed during the period of this research project performed satisfactorily and justified the considerable amount of time spent on its development. Development of new software should be carried out to meet future testing requirements.

6. A method of making test specimens in the laboratory has been developed. This involved using a large compression testing machine to provide the level of compaction required. The consistency of the specimen quality was confirmed by density measurements using cores from specimens after testing.

If the width of the existing mould is increased by 50 mm, compaction could be carried out by using a small vibrating roller which is readily available. This might facilitate expansion joint manufacturers to produce their own test specimens when required.

7. Specimens tested with horizontal and rotational deck movements failed with a crack along the expansion gap. This matches the failure pattern of in-service joints.

8. Results of specimens tested with transient horizontal movements indicate that the method of grading traffic induced horizontal deck movements used by Price (1982 (a)) is applicable for grading the similar movements simulated in laboratory tests.

9. Based on the results of a five year research project, Clauwaert concluded that horizontal deck movements induced by traffic and temperature changes cause most damage to buried joints. In some cases, when the bridge structures are extremely flexible, the traffic induced vertical movements may also be a significant factor due to their large magnitudes. The results of the present research support this finding.

10. An attempt has been made to estimate service lives of buried joints using laboratory test results. The estimated results compare well with those obtained from site investigation records. However, further development of the method requires detailed analysis of the test data together with the collection of additional site performance data.

11. A multiplying factor of 20 was used, as suggested by Raithby and Sterling (1972), to convert the joint life obtained from the



laboratory tests to an estimated life of the joint when in service. This compensates for the error caused by the omission of rest periods between load cycles.

12. The life curves presented in Fig. 7.21 show the effects of test temperature on joint life. The slopes of the life curves are  $-0.34$  and  $-0.26$  for specimens tested at  $10^{\circ}\text{C}$  and  $20^{\circ}\text{C}$  respectively. This indicates that a power law of 3 to 4 could be applied to the joint damage effects caused by different gap movements.

13. Although prestretched specimens gave much shorter lives, as shown in Fig. 7.21, the slopes of the life curves were not changed. Prestretching specimens before testing could be used as a technique to further reduce testing time.

14. Comparative tests on different types of closed joint systems could be carried out using the expansion joint simulator. Service lives of these joint systems could be estimated by comparing the test results with those of a standard joint whose performance has been verified in the road.

15. Long-term (thermal) tests are extremely time consuming, a test could last up to 30 days. But they should be accommodated in the future research programme. Because of the limited time available in the present project, the results obtained from the long-term (thermal) movement tests to date were limited. However,

they provided important information to identify the critical regions where stress concentrations exist. This may help to improve the design of buried joints in the future. Improved performance of new joint designs could also be verified by laboratory tests using the EJS.

16. In order to capitalise on the present research findings and the initial investment in equipment, it is strongly recommended that research should be continued along the lines explored in the present project and routine testing on bridge deck expansion joints should be started in the near future.

#### 10.2. PROPOSALS FOR FUTURE WORK AND RECOMMENDATIONS.

##### A) Joint Simulator

Although special attention had been given to the design of the simulator for stability, excessive deflections on some components were observed during specimen testing. These components were strengthened during the research. However, it is considered that further improvements could be made as follows:

- i) Modify the existing machine to improve its stability.

ii) Build a new machine based on the existing design but to a larger scale.

The first method would be suitable for a research project of the type carried out to date, since it is less expensive and would not cause major interruption to the progress of the overall research plan. The second method should be adopted when the research reaches a stage where the requirements of the final version of the machine can be clearly specified.

#### B) Control System.

In order to build the joint simulator to the performance specifications and within the original budget, the configuration of the Dartec control system was compromised and some electronic boards were omitted. This greatly reduced the flexibility of the system and prevented full use of the standard Dartec software (appendix B), which is updated periodically and supplied to the existing users by the manufacturer free of charge.

These electronic boards should be purchased for use in future work.

#### C) Temperature controlled room.

The joint simulator is placed in a thermally insulated room. The temperature inside can be varied between 5 °C and 40 °C by using

a combined heating and cooling system controlled through four programmable electronic relays.

When a specimen was tested at a temperature of 5 °C, the room temperature was lowered to a value which allowed the specimen to be cooled down to this temperature. However, during a trial, once the cyclic test was started, the specimen temperature began to rise and stayed at about 8 °C, even though the room temperature remained below 5 °C. This was probably caused by the internal heat generated in the material during cyclic loading. Consequently, a cooling system with twice the capacity of the original machine was installed towards the end of the project. A test trial should be carried out to see if the specimen temperature can be held at 5 °C.

#### D) Data acquisition system.

The data acquisition system which was used has been developed over the period of the present contract. Additional units have been added to the system as necessary. These units are linked together by external wiring. When the final configuration of the system is decided, all units should be accommodated in a purpose built chassis and linked together by internal cables. This would improve the appearance of the system and facilitate its use.

E) Computer software.

Some software was included in the Dartec package (appendix B) for actuator control purposes but, as noted above, modification to these programs and development of new ones are necessary. This process would need to continue as the research develops, especially, when new types of joint specimens are tested.

Software for data acquisition purposes was developed alongside the test control programs. These also need to be continually updated.

F) Specimen testing.

On completion of the existing test programme, more specimens should be tested with traffic induced vertical and bending movements. Buried joints with improved structural details should be investigated to study the possibility of extending the joint life by using an improved design.

Due to the increasing popularity of plug joints, an intensive test programme, which involves different types of plug joints, should be planned for a future research project.

Different joint systems could be tested using the EJS and their performance could be compared with that of a control specimen. Although a comparative test contributes little to the development

of a long-term joint life prediction method, it helps to rank joint systems into different grades according to their relative performance and, hence, provides some urgently needed information for engineers in choosing appropriate joints. It may also encourage manufacturers to improve their products based on the findings of this research.

G) Site investigation.

Specially designed site investigations on bridge deck expansion joints should also be started as soon as possible to collect the information necessary to correlate laboratory test results with the service performance of expansion joints. This type of site investigation should form part of the overall research. Very little time has been devoted to this topic to date because of other priorities. As shown in appendix C. A proposal on this topic was submitted to TRRL in May, 1988.

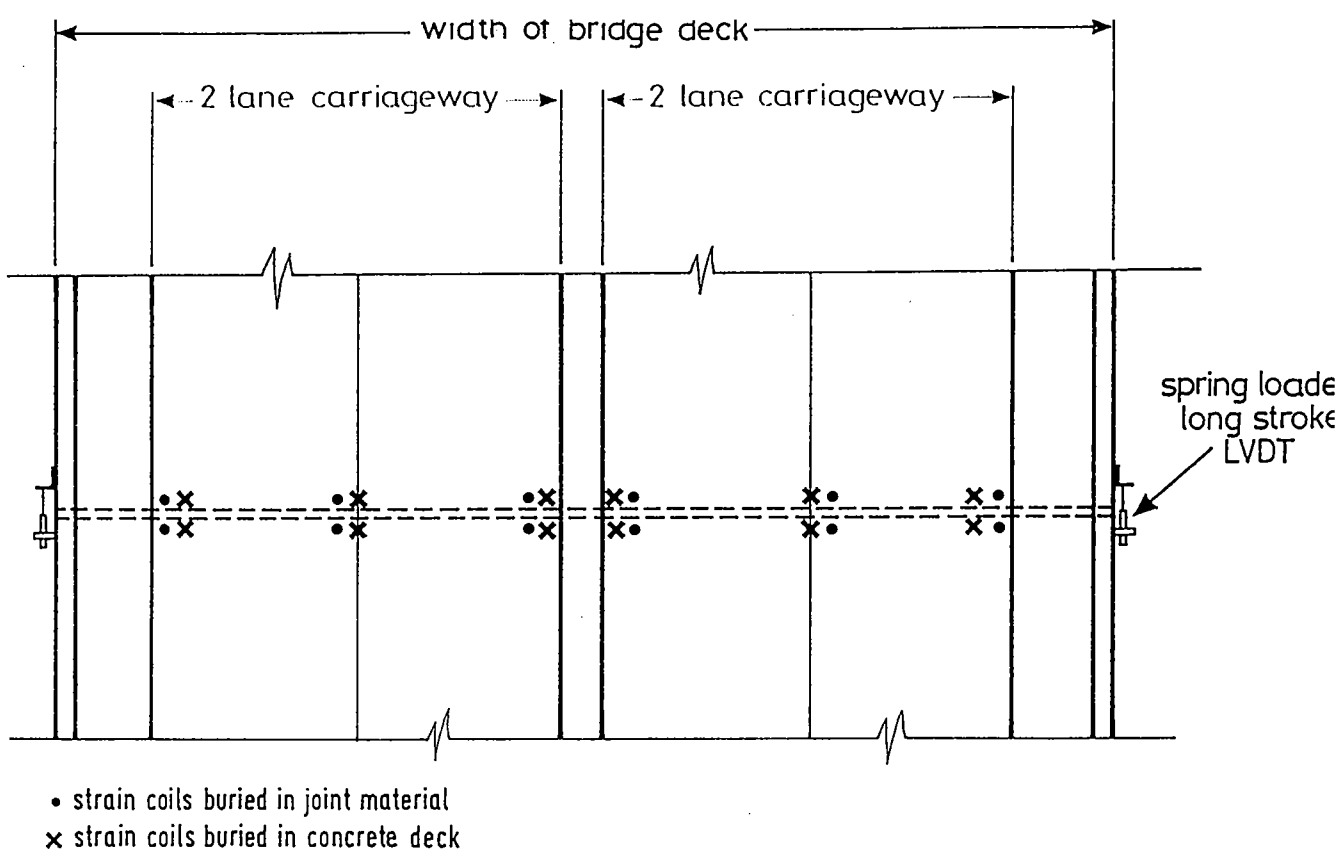


FIG. C.3 INSTRUMENTATION FOR MEASURING LONG-TERM BRIDGE DECK MOVEMENTS

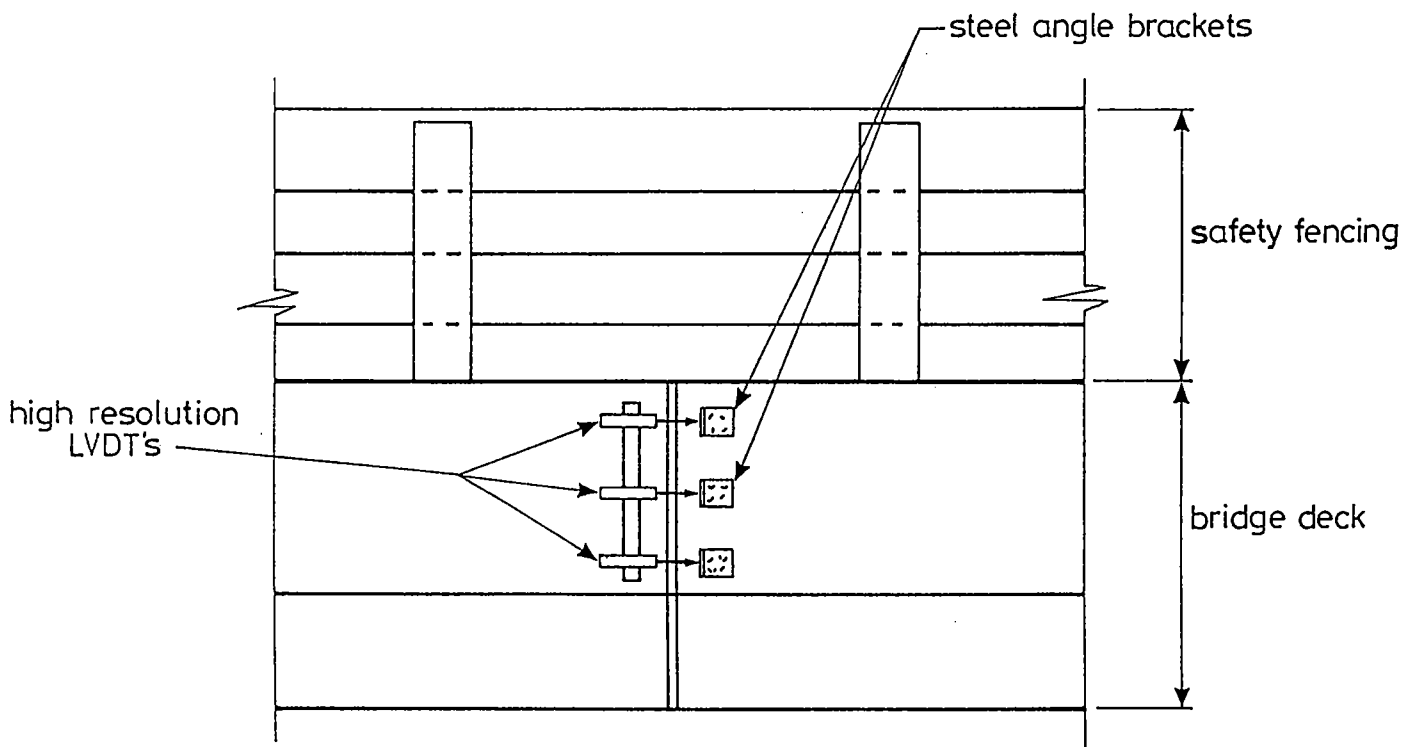


FIG. C.4 INSTRUMENTATION FOR MEASURING SHORT-TERM HORIZONTAL & ROTATIONAL BRIDGE DECK MOVEMENT (SIDE ELEVATION)

## REFERENCES

BISON INSTRUMENT INC. "Instruction Manual, Bison Instrument, Soil Strain Gage Model 410A.

BLACK W, MOSS, D S and EMERSON, MARY. (1976), "Bridge Temperatures Derived from Measurement of Movement", Department of Environment, Department of Transport, TRRL Report LR 748 Crowthorne.

BONNAURE F, GEST G, GRAVOIS A and UGE P (1977), "A New Method of Predicting The Stiffness of Asphalt Paving Mixtures", Proc. Assn. Asphalt Paving Tech. Vol. 46, pp. 64-104.

BRITISH STANDARD INSTITUTION (1980), "Steel, Concrete and Composite Bridges, Part 9, Code of Practice for Bearings", BS 5400 Part 9.

BRITISH STANDARD INSTITUTION (1985), "Hot Rolled Asphalt for Roads and Other Paved Areas, Part 1, Specification for Constituent Material and Asphalt Mixtures", BS 594 Part 1.

BRODRICK B V, SHAM K C and BROWN S F (1986), "Endurance Testing of Bridge Deck Expansion Joints", Interim Report, Submitted to Transport and Road Research Laboratory, University of Nottingham, December.



BROWN S F (1978), (a) "State-of-the-art on Field Instrumentation for Pavement Experiments", Transport Research Record No. 640, pp. 13-28.

BROWN S F (1978 (b)), "Stiffness and Fatigue Requirement for Structural Performance of Asphalt Mixes", Proc. Eurobitume Seminar, London, pp. 141-145.

BROWN S F and BRODRICK B V (1973), "The Performance of Stress and Strain Transducers for use in Pavement Research", Science Research Council Report No. SFB/BVB/593.13, Department of Civil Engineering, University of Nottingham.

BROWN S F and BRODRICK B V (1981 (a)), "Instrumentation for the Nottingham Pavement Test Facility", Transportation Research Record 810, pp 73-79.

BROWN S F and BRODRICK B V (1981 (b)) "Nottingham Pavement Test Facility", Transportation Research Record 810, pp 67-72.

BROWN S F, HUGHES D A B, BRODRICK B V (1985), "Grid Reinforcement for Asphalt Pavements", Report No. 3, Submitted to Nelton/SERC, June.

BROWN S F, HUGHES D A B, BRODRICK B V (1986), "Grid Reinforcement for Asphalt Pavements", Report No. 4, Submitted to Nelton/SERC, February.

CLAUWAERT C (1986), "A Study of Expansion Joints and Buried Joints for Bridges in Belgium", Proc. Second World Congress on Joint Sealing and Bearing Systems for Concrete Structures, San Antonio, Texas, ACI Publication SP-94, pp613-642.

COOPER K E (1976), "The Effect of Mix and Testing Variables on the Fatigue Strength of Bituminous Mixes", M.Phil. Thesis, University of Nottingham.

DAY H G (1981), "Concrete Bridge Articulation", Proc. First World Congress on Joint Sealing and Bearing Systems on Concrete Structures, New York, ACI Publication SP- 70, pp. 55-76.

DEACON J A (1965), "Fatigue of Asphalt Concrete", University of California, D Eng. dissertation.

DEACON J A (1973), "Fatigue Life Prediction", Special Report 140, Highway Research Board, pp. 78-91.

DEACON J A and MONISMITH C L (1967), "Laboratory Flexural Fatigue Testing of Asphalt Concrete with Emphasis on Compound Loading Tests", Highway Research Record 158, pp. 1-31.

EPPS J A and MONISMITH C L (1970), "Influence of Mixture Variables on the Flexural Fatigue Properties of Asphalt Concrete", Proc. Assn. Asphalt Paving Techs, Vol. 38, pp. 423-464.

EYRE R, CULLINGTON D W and PRETLOVE A J (1984), "Durability Testing of Bridge Deck Expansion Joints: A Discussion", Department of Transport, TRRL Report WP/B/77/84, Crowthorne.

EYRE R (1987), "Research on Expansion Joints in Austria", Department of Transport, TRRL Working Paper WP/B/129/87, Crowthorne, February.

HEUKELOM W and KLOMP A J G (1964), "Road Design and Dynamic Loading", Proc. Assn. Asphalt Paving Tech. Vol. 33, pp. 92-125.

HOBBS R E (1982), "Fatigue Test on the Thorma-Jointing System", A Report for Thormack Ltd, CESLIC TJ1.

HUBAND M R AND WOOD T L (1986), "The Durability of Bridge Expansion Joints", B.Eng. Thesis, Department of Civil Engineering, Bristol University, June.

JONES H C (1982), "Survey of Bridge Expansion Joints", General Report (unpublished), Department of Transport, February.

KOZLOV G S (1981), "Field Performance Simulation and Laboratory Tests for Sealants", Proc. First World Congress on Joint Sealing and Bearing Systems on Concrete Structures, New York, ACI Publication SP- 70, pp335-351.

MANNING D G and WITECKI A A (1981), "Requirement for Deck Joints in Highway Structures", Proc. First World Congress on Joint Sealing and Bearing Systems on Concrete Structures, New York, ACI Publication SP- 70, pp. 291-309.

McELVANEY J (1972), "Fatigue of A Bituminous Mixture Under Compound Loading", University of Nottingham, Ph.D. Thesis.

McELVANEY J and PELL P S (1973), "Fatigue Damage of Asphalt: Effect of Rest Periods", Highways and Road Construction, Vol. 41, No. 1766, October, pp. 16-20.

MONISMITH C L and DEACON J A (1969), "Fatigue of Asphalt Paving Mixtures", Jour. Transp. Eng. Div., ASCE, No. TE2, pp. 317-346.

MORTLOCK J D (1974), "The Instrumentation of Bridges for The Measurement of Temperature and Movement". Department of The Environment, TRRL Report LR 641 Crowthorne.

O'NEIL M J (1970), "A Review of Some Cumulative Damage Theories", Australian Def. Sci. Serv. Aeronaut. Res. Lab., Struct. and Material Report 326, June.

PATERSON W D O (1972), "Measurement of Pavement Deformation Using Inductance Coils", RRU Bulletin, No. 13, National Roads Board, New Zealand.

PELL P S (1967), "Fatigue of Asphalt Pavement Mixes", Proc. 2nd Int. Conf. on the Struct. Design of Asphalt Pavements, Ann Arbor, pp. 557-593.

PELL P S (1973), "Characterization of Fatigue Behaviour", Special Report 140, Highway Research Board, Jan., pp. 49-64.

PRETLOVE A J AND SMITH I H (1988), "Rolling Load Testing of Bridge Expansion Joints, A Feasibility Study", TRRL 842/519 (unpublished), Department of Engineering, University of Reading, March.

PRICE A R (1988 (a)), "The Service Performance of Fifty Buried-type Bridge Expansion Joints", Department of Environment, Department of Transport, TRRL Report SR 740 Crowthorne.

PRICE A R (1988 (b)), "Trials of Buried Joints and Surfacing on A Composite Motorway Viaduct", Department of Environment, Department of Transport, TRRL Report LR 1023 Crowthorne.

PRICE A R (1983), "The Performance of Nosing Type Bridge Deck Expansion Joints", Department of Environment, Department of Transport, TRRL Report LR 1071 Crowthorne.

PRICE A R (1984), "The Performance in Service of Bridge Deck Expansion Joints", Department of Environment, Department of Transport, TRRL Report LR 1104 Crowthorne.

PUCCIO G S (1981), "Extruded Seals for Bridges and Structures", Proc. First World Congress on Joint Sealing and Bearing Systems on Concrete Structures, New York, ACI Publication SP-70, pp1957-981.

PURVIS R L and BERGER R H (1983), "Bridge Joint Maintenance", Transportation Research Record 899, pp.1-10.

RAITHBY K D and STERLING A B (1970), "The Effect of Rest Period on the Fatigue Performance of A Rolled Asphalt Under Reversed Loading" , Proc. Assn. Asphalt Paving Techs., Vol. 39, pp. 134-147.

RAITHBY K D and STERLING A B (1972), "Some Effects of Loading History on the Fatigue Performance of Rolled Asphalt", Department of Environment, Department of Transport, TRRL Report LR 496 Crowthorne.

SCHUTZ R J (1981), "Genesis of Modern Sealant Technology", Proc. First World Congress on Joint Sealing and Bearing Systems on Concrete Structures, New York, ACI Publication SP-70, ppl-14.

SELIG E T (1972), "Soil Strain Measurement Using Inductance Coil Method, ASTM Symp. on Performance Criteria and Monitoring for Geotechnical Construction, June, Revised October, 1974.

SHAM K C, BRODRICK B V and BROWN S F (1988), "Endurance Testing of Bridge Deck Expansion Joints", Report No. KCS/1, Submitted to Transport and Road Research Laboratory, University of Nottingham, January.

SHAM K C and BROWN S F (1989), "Endurance Testing of Bridge Deck Expansion Joints", Report on Behaviour of Buried Joints, Submitted to Transport and Road Research Laboratory, University of Nottingham, March.

STEVENSON E J (1976), "Test Rig for Bridge Expansion Joint", Agreement Board, October.

TAYLOR I F (1968), "Asphalt Road Materials in Fatigue", Ph.D. thesis, University of Nottingham.

TONS E (1986), "Field Moulded Joint Seals in Tension and Compression", Proc. Second World Congress on Joint Sealing and Bearing Systems for Concrete Structures, San Antonio, Texas, ACI Publication SP-94, pp.31-47.

TRRL (1983), "Road Pavement Testing", TRRL leaflet LF 968.

VAN DER POEL C (1954), "A General System Describing The Visco-Elastic Properties of Bitumens and its Relation to Routine Test Data", Journ. App. Chem., 4, pp. 221-236.

VAN DIJK W (1975), "Practical Fatigue Characterization of Bituminous Mixes", Proc. Assn. Asphalt Paving Techs. Vol. 44, pp. 39-72.

VAN DIJK W, MOREAUD H, QUEDEVILLE A and UGE P (1972), "The Fatigue of Bitumen and Bituminous Mixes", Proc. 3rd Int. Conf. on the Struct. Design of Asphalt Pavements, London, pp. 354-366.

VAN DRAAT W E F and SOMMER P (1955), "An Apparatus for Determining The Dynamic Elastic Modulus of Asphalt" (in German), Strasse und Autobahn, 6, pp. 206-211.

YURKOWSKY WILLIAM et al (1967 (a)), "Accelerated Testing Technology", RADC Technical Report 67-420, Vol. I, (AD 824449) Rome Air Development Centre, Griffiss Air Force Base, New York, November.

YURKOWSKY WILLIAM et al (1967 (a)), "Handbook of Accelerated Life Testing Methods", RADC Technical Report 67-420, Vol. 2, (AD 824451) Rome Air Development Centre, Griffiss Air Force Base, New York, November.



YURKOWSKY WILLIAM and FULTON D W (1972), "An Assessment of Accelerated Testing", Testing for Prediction of Material Performance in Structure and Components, ASTM STP 515, America Society for Testing and Materials, pp 75-88.



## APPENDIX A

### ELECTRONIC BOARDS OF THE DARTEC 9500 SYSTEM

#### A1. Details of The Dartec 9500'S Circuit Boards.

The functions of each electronic circuit board are described briefly as follows:-

##### (i) A-D board 9500-a1

Basically, this consists of an A-D (Analogue to Digital) converter and a D-A (Digital to Analogue) converter. The A-D unit converts the analogue signals from the built-in load cell, built-in stroke transducer, extension and external inputs into digital values. Extension and external are two optional inputs (Fig. 3.3) for any compatible external devices, such as transducers attached to the specimen. Different names are given for clarity only. The digital signals are then passed on to the appropriate boards through an Information Bus (I-Bus). The D-A unit converts digital error signals into + 10V analogue voltages to drive the servo-valve amplifiers. Both converters have a 15-bit resolution.

(ii) Controller board 9500-b1

The controller board performs a closed loop control for the Dartec system. It takes a selected feedback signal from the A-D board and makes calculations to derive an adjusted command signal for compensation purposes. The feedback signal can be chosen from Load, Stroke, Set Up, Extension and External.

In Load and Stroke control modes, the feedback signal is obtained from the built-in actuator load cell and LVDT respectively. This signal is compared with the corresponding command values. The error between the feedback and command is reduced by a compensation command signal, generated by the controller board, which is sent to the servo-valve amplifier. This in turn operates the servo valve which accurately controls the movement of the actuator.

Set Up is a special stroke control mode which provides a load limit equivalent to about 1% of the machine load capacity. If this limit is exceeded, the controller will instruct the actuator to "back off" in order to keep the load below the allowable limit.

External and extension control modes allow compatible signals generated from any two external devices to be connected and used for controlling purposes.

The controller also allows a bumpless transfer during changes of

control mode by ensuring that all commands follow the feedback signals, even though they are not the control mode used at that time. The board has an interface to pump control and allows software commands to stop pump or dump pressure in case of an emergency. Instructions can be communicated to the board by using the supervising computer.

(iii) Data Processing board 9500-el

This board collects data from the A-D board through the I-bus, then calculates the maximum and minimum values of each feedback channel and stores them in the memory. From this basic data, peak to peak and mean values can be calculated. The board is an essential element when changes of scalings of load, stroke and extension are required. However, it can be omitted if the scaling is fixed by computer software as is the case with the expansion joint simulator.

(iv) Function Generation board 9500-pl

This function generator can produce sine, square and ramp waveforms between programmed levels chosen by the operator. It produces a command value and feeds it to the loop controller which, in turn, instructs the actuators to move accordingly. The levels, the frequency, the number of cycles and the control mode can be fed into the board by using the supervisory computer keyboard.

The function generator calculates a transition from the current loop controller command value to turning point level A, and then continues to produce a cycle from level A to the next turning point level B and back to level A according to the input level values. Turning points refer to the peak or trough of a waveform. The function generator will stop after a programmed number of cycles has been finished. With appropriate computer software, complex dynamic test routines can be set up and then run under the Dartec 9500's control.

(v) Computer Interface 9500-g2

This is an interface between the Dartec 9500 Interboard Communication Bus (C-bus) and the standard RS232C format. The board allows the computer to instruct and get information from any one of the boards in the 9500 system. This allows the Dartec system to be controlled by using external computer programs. Instructions from the supervisory computer are sent to the Dartec system through the g2 board by using 4-digit codes which are over 500 in number.

(vi) Trip Board 9500 -v1

This board provides trip facilities in 39 trip conditions. An immediate or delayed action can be chosen for each of these conditions. It also provides 8 external input ports to allow trip actions to be controlled by external input signals. The

trips are set up through the supervisory computer. Each type of trip can be switched on (enabled) and off (disabled) as required.

During a cyclic load test, System A (vertical actuator control) works as a master. The function generator in System A produces a traffic frequency waveform signal instructing the vertical actuator to cycle between the signal limits. At the same time, the waveform signals are channelled through an additional A-D board (a2) into an external unit which was built at the University. The slave, System B, receives the waveform signals from the external unit and instructs the horizontal actuator to start cycling accordingly. Two "summers" were added to the a2 board and the external unit respectively to allow inversion and scaling of the slave commands. The trip facilities in System A are also shared by System B. If an overload occurs in System B, the overload signal from System B will be fed back to System A as an external command to trip both systems and stop the test.





## APPENDIX B

### STANDARD SOFTWARE OF THE DARTEC 9500 SYSTEM

#### B1. Standard Software Supplied by Dartec.

A software package is included in the Dartec 9500 system purchased for this research project. The software comprises six programs. The main program is called "Menu", through which other programs can be accessed. The functions of these programs are described briefly as following:

##### 1. MENU

This program displays a menu of all the software available in a particular Dartec system on the visual display unit (VDU) and allows other programs to be accessed by simple numeric selection through the computer keyboard.

##### 2. SET UP

This program allows the user to set up different machine parameters, such as the scaling factors of load, stroke and extension signals, the control loop gain values and the command

source. The currently set values are displayed on the screen and adjustment can be made through the computer keyboard. The existing setting can be saved into a file for future reference.

### 3. STATUS

This displays the current state of all the electronic circuit boards in the system. The program provides an on/off control of the function generator and the trip facilities. Machine control mode can also be selected when this program is running.

### 4. DYNAMIC

This program provides a constant amplitude cyclic testing facility to the Dartec system. Once the dynamic control mode, waveform together with the upper and lower limit values, frequency and the number of cycles to finish are set, a cyclic test can be conducted under the supervision of the control system. The control units continuously monitor all the feedback signals and adjust the corresponding command values to ensure that all fixed test parameters are met.

### 5. TRIP

This program allows the 39 trip conditions provided by the trip (v1) board to be set and activated. There are three types of trip

test routines available, i.e. Bounds Test, Error Test and External Test. Bounds Test allows the upper and lower limits to be set on command and all feedback signals. Exceeding any of these limits will set off a trip. Error Test enables errors on the servo-valve and control signals to be monitored and trip will be activated whenever an error limit is exceeded. External Test provides logical tests to be made on eight external switch inputs. The signals from these inputs can trigger a trip. A variety of actions on trip operation can be selected through the TRIP program, ranging from set off an alarm and stop function generator to a complete system shutdown. Resetting and identifying the cause of the trip can be carried out through this program routine.

## 6. INDICATOR

INDICATOR is a cut down version of the standard program called "MONITOR". INDICATOR continually reads the current load, stroke and command signals and displays their values on the VDU. The program has been improved by the author to include a display of the current amount of joint gap movements in mm.



## APPENDIX C

### PROPOSAL FOR FIELD MEASUREMENTS ON BRIDGE DECK EXPANSION JOINTS.

(PREPARED FOR TRRL BRIDGE DIVISION: MAY 1988)

#### Cl. Introduction.

This proposal arises from discussions between TRRL (Transport and Road Research Laboratory) and the University of Nottingham on 11th February 1988 . It was agreed that site monitoring of bridge deck movements at expansion joints, either on existing bridges or new constructions, was desirable as part of the overall research effort on joint performance. The results could then be compared with the laboratory test results obtained from the present project at Nottingham and assist in the planning of the future work.

Bridge deck movements can be divided into two types, the long-term movements due to changes of ambient temperature and the short-term movements induced by traffic loading. In order to understand the individual effects of these movements on joint performance, they should be measured and studied separately.

Since bituminous materials are highly temperature susceptible, it will be important to know the temperature of the joint material

at the time when the movements are measured. Consequently it is suggested that the material temperature, the movements across the joint gap and the ambient temperature will be the main parameters to be monitored.

## C2. Proposed Site Instrumentation.

### i) Measurement of joint material temperature.

Thermocouples would be used to measure the temperature of the joint material and the concrete deck near the joint. A proposed arrangement is shown in Figs. C1 & C2.

### ii) Measurement of ambient temperature.

The shade air temperature would be measured by two pairs of thermocouples suspended beneath the underside of bridge deck in order to shelter them from direct sunlight and weather.

### iii) Measurement of long-term horizontal movements

There are different types of expansion joints used in the U. K. However, as far as this project is concerned, only joints with a maximum expansion joint movement of 50 mm will be investigated.

A pair of spring loaded, long stroke LVDT's would be mounted on both sides of the bridge deck across the joint gap as shown in Fig. C3. The working range of these LVDT's will depend on the

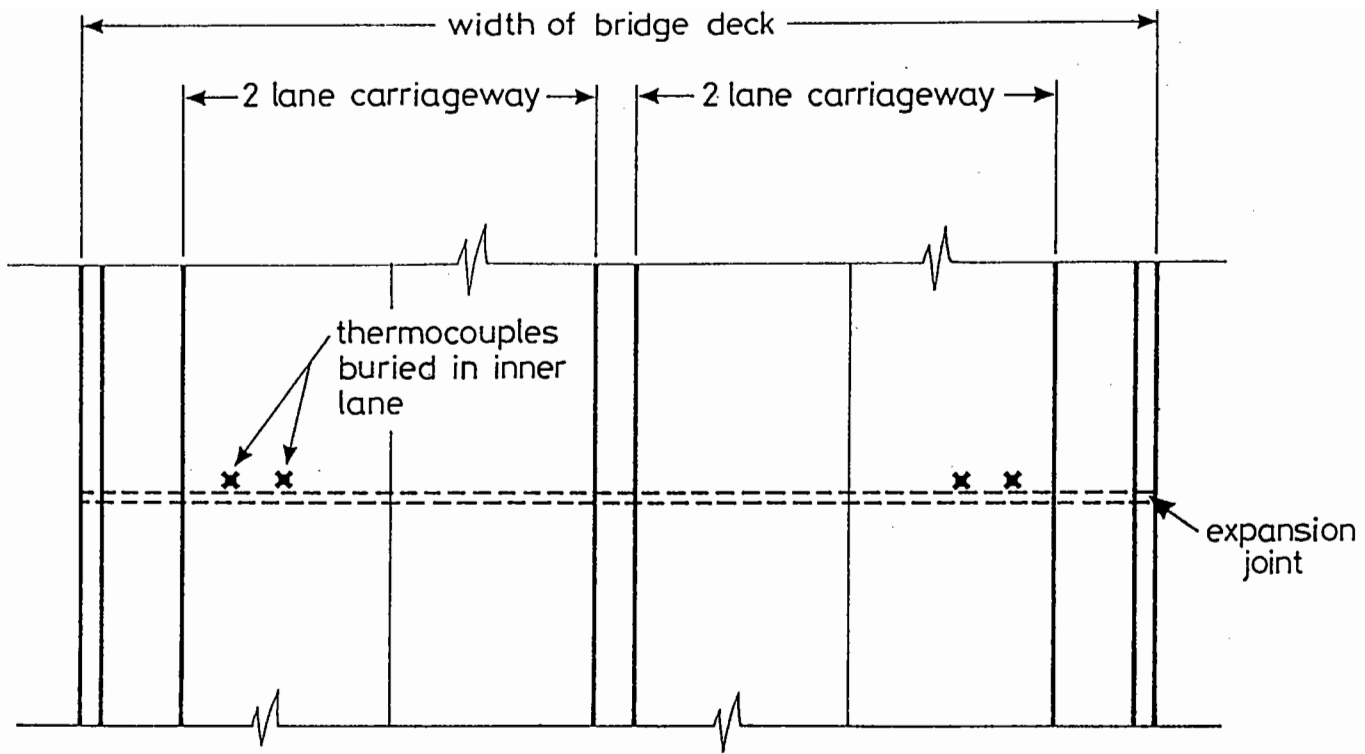


FIG.C.1 ARRANGEMENT OF THERMOCOUPLES

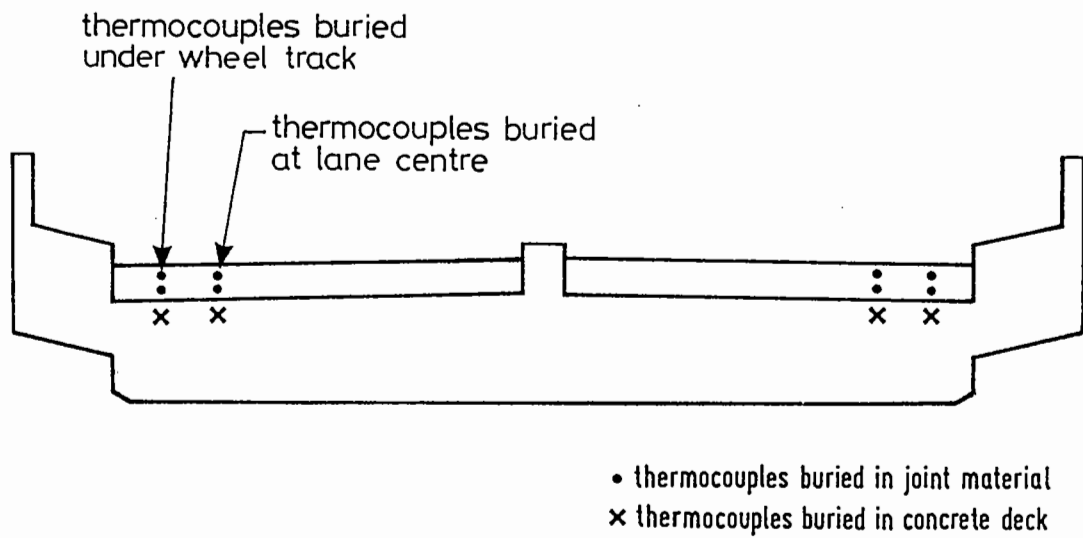


FIG.C.2 CROSS-SECTION OF BRIDGE DECK

amount of deck movement expected. Since the LVDT's will be used to measure long-term deck movement, due to temperature changes, they will stay in their positions for a considerable period of time, so it is important that these LVDT's are weatherproof and protected from vandalism.

In addition to the LVDT's, inductance strain coils would be buried in the concrete deck and the joint material to measure the gap movement. These strain coils would be monitored in turn using a single Bison instrument and a multi-channel scanner. The possibility of using strain coils depends on the arrangement of steel reinforcement inside the deck. There must be sufficient spacing between the coils and the steel to avoid interference with the electromagnetic field about the coils.

iv) Measurement of short-term movements.

Three high resolution LVDT's would be mounted on each side of the bridge deck as shown in Fig. C4. By measuring the horizontal deck movements at three different levels, any rotational movement of the deck can also be detected.

The transient vertical movement would be measured by another pair of high resolution LVDT's as shown in Fig. C5.

It is suggested that it should be possible for all LVDT's used for short-term measurement to be removed from the site on completion of the day's readings.



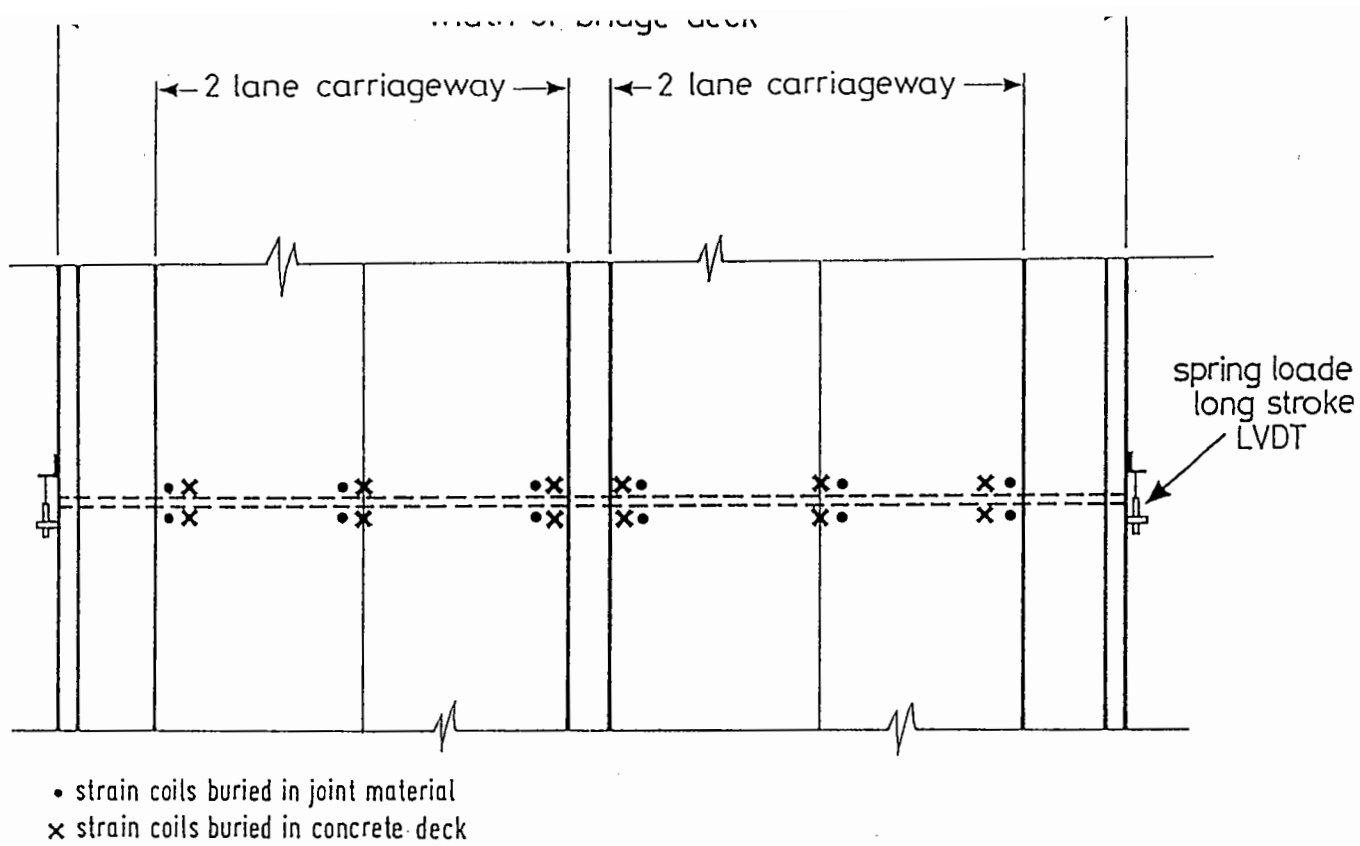


FIG. C.3 INSTRUMENTATION FOR MEASURING LONG-TERM BRIDGE DECK MOVEMENTS

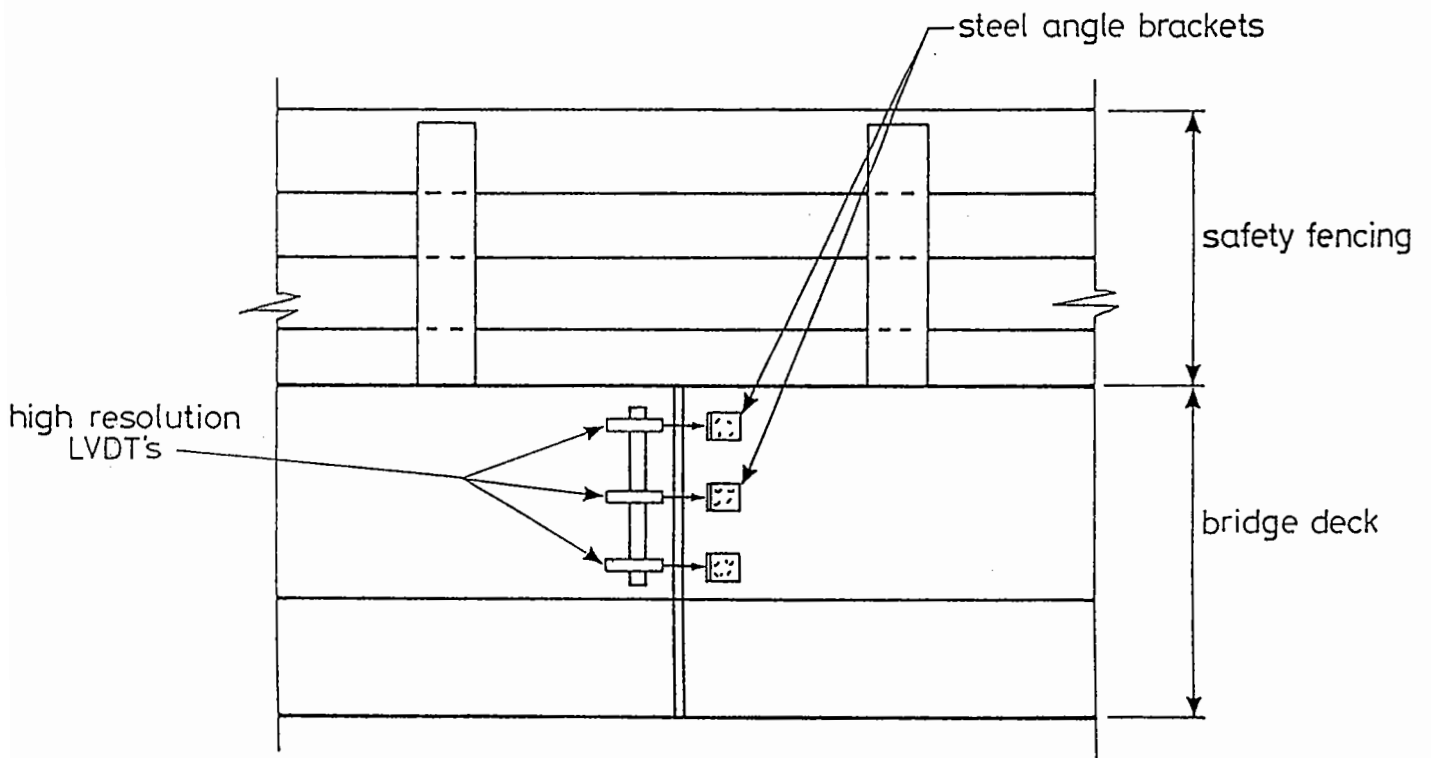


FIG. C.4 INSTRUMENTATION FOR MEASURING SHORT-TERM HORIZONTAL & ROTATIONAL BRIDGE DECK MOVEMENT (SIDE ELEVATION)

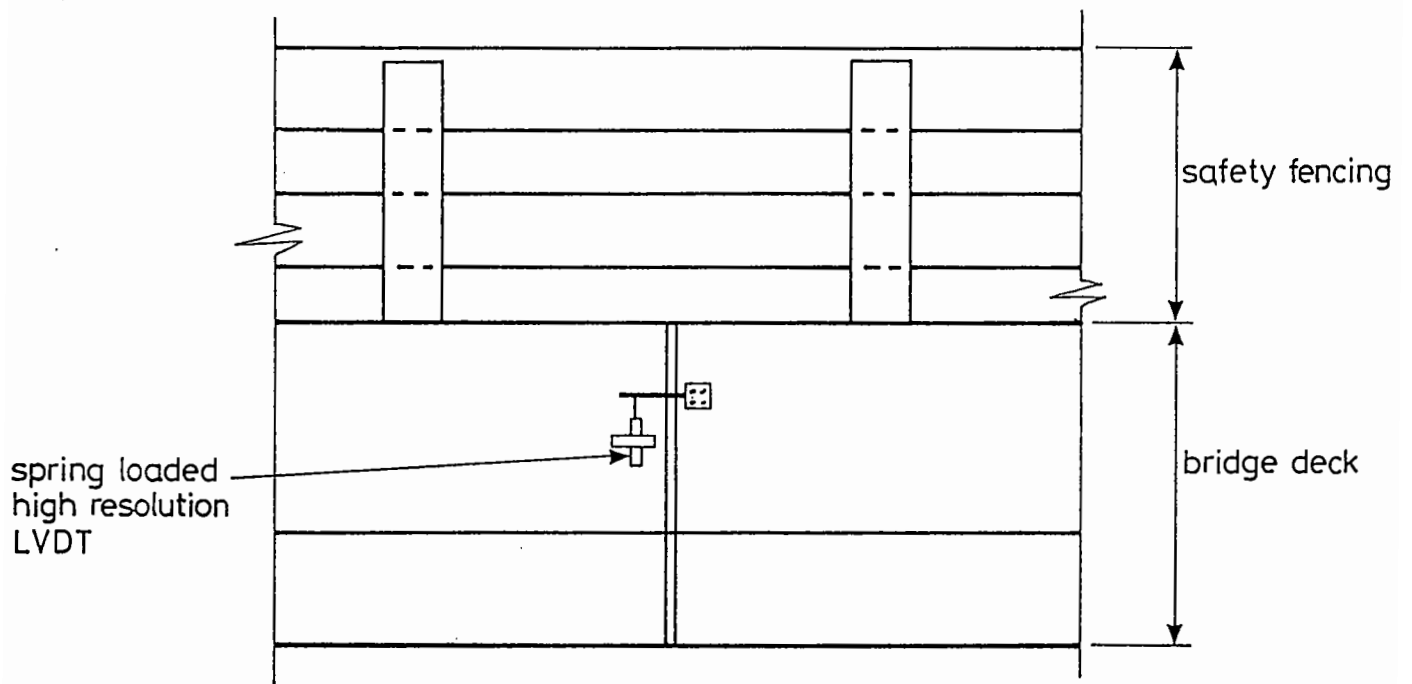


FIG. C.5 INSTRUMENTATION FOR MEASURING  
SHORT-TERM VERTICAL BRIDGE DECK  
MOVEMENT (SIDE ELEVATION)

Strain coils mentioned in the previous section could also be used to measure the transient movements of the deck due to traffic loading. Movements measured by the strain coils could be compared with those obtained by using the LVDT's.

### C3. Data Acquisition.

i) For long-term measurements

These include measurements of:

- a) Ambient temperatures (2 no. of thermocouples.)
- b) Joint material and concrete deck temperatures (12 no. of thermocouples.)
- c) Thermal movement of bridge deck (2 no. LVDT's and 12 pairs of strain coils)

It is proposed that a microprocessor unit with built-in Analogue to Digital (A to D) converter and disk drive should be used. The Walton Digilogger Data Acquisition System could be appropriate..

The technical details of this unit are as follows:

Analogue inputs:	32 differential input channels
Analogue ranges:	$\pm 10$ volts
Digital inputs:	16 bit digital input
Command input:	Through RS232 interface

Disk capacity: 320 K or 640 K  
Power: 110/240 V AC  
Working temperature: 5 C to 50 C ambient  
Humidity: 20-90% non-condensing.  
Compatibility: Most HP computers and an IBM PC version  
is available as an option.

Configuration information, such as scan intervals, number of channels to be logged, date/time etc., can be input to the digilogger with a computer keyboard through an RS232 interface. Once the logger has been set up, data logging can be carried out independently, i.e. without the computer. Battery support allows the configuration information to be maintained in the system during transit. However, mains electricity supply is required during the data logging process. The digilogger has a 3.5 in. disk driver built in. With this driver, both analogue and digital data can be logged, recorded and then transferred to other computer systems for further analysis. The unit has 32 analogue input channels and is capable of collecting data at a speed of 4 signals for each channel per second. This speed is sufficient for long-term data collection purposes. Signals from LVDT's and thermocouples could be measured whenever required while strain coils could be monitored in turn by using a single Bison control unit with automatic balancing and multi-channel scanning facilities.

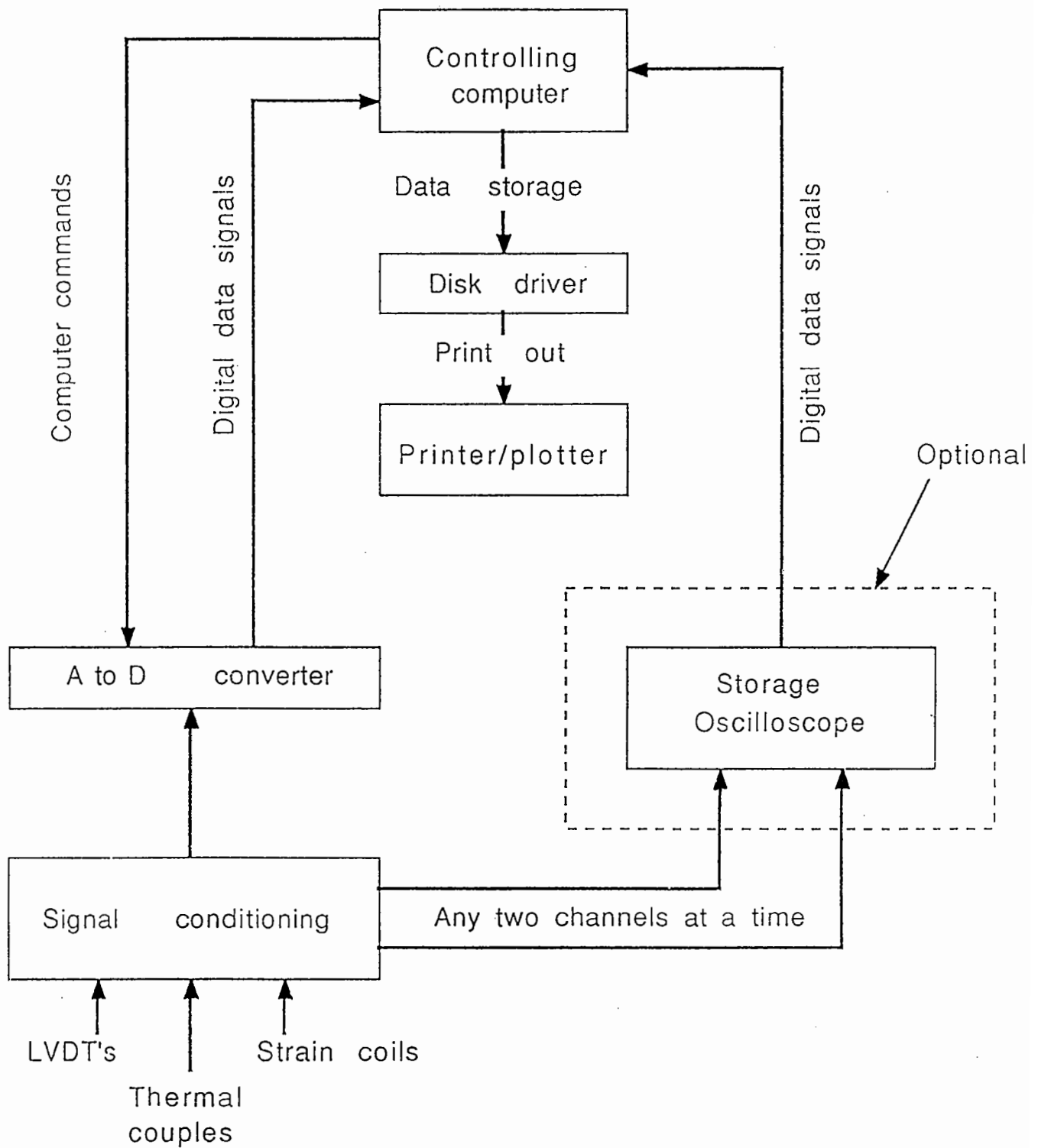
ii) For short-term measurements

These include measurements of:

- a) Traffic induced horizontal and rotational movements (6 LVDT's and 12 pairs of strain coils). The strain coils could be monitored one pair at a time by using a single Bison unit.
- b) Traffic induced vertical movements (2 LVDT's)

Fig. C6 shows a proposed data acquisition system for short-term measurements. The system consists of an IBM compatible computer and a high speed, large storage A to D converter. The computer recommended is the Amstrad PC1512 with twin floppy disk drives and a monochrome monitor. The CIL DTR 1580 which has 16 input channels with 128 Kbyte memory as standard would be a suitable choice of A to D converter. The large internal memory of the converter is sufficient for the high speed data conversion, of 20 us per signal, to be stored. Analogue input signals can range from 1 V to 10V with a  $\pm$  15 bit resolution. Communication between the A to D converter and the computer is provided by either an IEEE 488 parallel bus or an RS232 serial port. Collection of data can be triggered by instructions from software or hardware.

A storage oscilloscope is recommended as an add-on option. The unit can display any two channels of data signals on the screen for instantaneous monitoring purposes. This gives an immediate indication of whether the transducers are working satisfactorily. The oscilloscope also provides other facilities, such as holding the display on the screen, expanding the signal for detail



(Signals from measuring instrument )

Fig.C.6 Schematic diagram of data acquisition system for short-term measurements

analysis, automatic triggering of data collection, data storage etc. Data can be transferred from the oscilloscope to a computer and vice-versa. On site, it provides two extra data capture channels and an effective monitoring facility for displaying stored data on return to the laboratory.

C4. Estimated Costs. (exclusive of VAT and delivery)

i) Measuring instruments

a) 2 no. long stroke LVDT's (RDP DCT/2000A with water resistance option)	£ -
b) 8 no. high resolution LVDT's (RDP D5/200AG)	£ -
c) 14 no. thermocouples	£ -
d) 12 pairs of strain coils	£ -
e) Automatic Bison control unit & multi-channel scanner.	£ -
f) 2 no. power supply unit with indicator (RDP Dataspan 2035)	£ -
g) 16 no. LVDT's amplifier (RDP Dataspan 2021)	£ -
h) 1 no. panel mouting case and wiring.	£ -
j) miscellaneous (cables, fittings etc.)	£ -

---

Sub-total: £ -

ii) Data Acquisition

a) Walton digilogger system	£ -
b) 1 no. IBM compatible computer (Amstrad PC1512 mono with twin drive)	£ -
c) 1 no. IEEE 488 interface card (CIL PC-IEEE + 32K)	£ -
d) 1 no. connection cable	£ -
e) 1 no. analogue to digital converter with large storage (CIL DTR1580)	£ -
f) 1 no. storage oscilloscope	£ -

---

Sub-total: £ -

iii) Others

a) Contingency	£ -
----------------	-----

Total: £ -

---

Note that labour costs for installation will be extra.